## ABSTRACT

Title of Dissertation:          A PETROLOGIC, GEOCHEMICAL AND OSMIUM ISOTOPIC STUDY OF SELECTED PRECAMBRIAN KOMATIITES

Amitava Gangopadhyay, Ph. D., 2004

Dissertation Directed By:       Professor Richard J. Walker, Department of Geology

The major and trace elements, and Re-Os isotope systematics of the ca. 2.7-Ga komatiites from the Alexo and Dundonald Beach areas in the Abitibi greenstone belt, Canada, and ca. 2.0-Ga komatiites from Jeesiörova, Finnish Lapland were examined in order to constrain the long-term Os isotopic evolution of their mantle sources and also to evaluate different petrogenetic models for their generation.

The Re-Os isotope results for whole-rock komatiites and chromite separates from Alexo, Dundonald Beach and the Jeesiörova areas, all yield precisely chondritic intial Os isotopic compositions of their mantle sources ($\gamma_{Os}$ = -0.1± 1.0, 0.0 ± 0.6 and 0.1± 0.5, respectively), consistent with that for the projected primitive upper mantle. The uniform chondritic initial Os isotopic compositions of these komatiites suggest their derivation from mantle sources that had undergone neither long-term Re-depletion nor enrichments in radiogenic $^{187}$Os. The uniform chondritic initial Os isotopic compositions of the Ti-rich Finnish komatiites also suggest that the processes responsible for high Ti concentrations in the Finnish rocks must have either been coeval with the generation of the rocks or Re and Os were not significantly fractionated during the processes.

The uniform Os isotopic compositions of the Precambrian mantle source regions for these komatiites are in contrast to the variably radiogenic Os isotopic compositions, commonly reported for the present-day ocean island basalts and modern arc-related rocks. This suggests that the Precambrian mantle was significantly more homogeneous than the present-day mantle. Finally, the high-precision Os isotopic results of this study, combined with those previously published for Precambrian ultramafic rocks suggest that although Os isotopic heterogeneities began to appear in the terrestrial mantle as early as ~2.8 Ga, large portions of the Precambrian mantle were evidently not affected by the processes responsible for long-term Os isotopic heterogeneities.

A PETROLOGIC, GEOCHEMICAL AND OSMIUM ISOTOPIC STUDY OF
SELECTED PRECAMBRIAN KOMATIITES

By

Amitava Gangopadhyay

Dissertation submitted to the Faculty of the Graduate School of the
University of Maryland, College Park, in partial fulfillment
of the requirements for the degree of
Doctor of Philosophy
2004

Advisory Committee:
Professor Richarad J. Walker, Chair
Professor Roberta L. Rudnick
Associate Professor William F. McDonough
Dr. Harry Becker, Assistant Research Scientist

# Dedication

To my parents and my wife

# Acknowledgements

During this work, I have benefited from direct and indirect help and encouragement from a large number of people, too numerous to mention here; I am grateful to all of them. First and foremost, I am immensely grateful to Prof. Richard J. Walker for giving me an opportunity to work on such an interesting project. His usual high expectations, while giving me complete freedom on selecting a scientific problem and deciding on how to address it, has enriched my intellectual upbringing, which will definitely leave an imprint on the way I will do science in the future. His inimitably precise and accurate professional guidance, tall personality, respectable parsimony of speech, combined with sporadic humorous outbursts, all will go into shaping my own professionalism and gesture in scientific career for the coming years. Rich is my advisor.

I am indebted to Dr. Harry Becker for his generous help with chemical processing of samples and instrumental methods of analyses at the early stage of my learning of the Re-Os isotope systematics. I also owe a great deal of gratitude to him for helpful discussions on many occasions, and his prompt comments and feedback on my research proposal and an early version of the dissertation. Finally, I am thankful to him for serving as one of my dissertation committee members.

I had the honor of having Prof. Roberta L. Rudnick as one of my dissertation committee members. Her meticulous comments and suggestions on issues of primary importance have improved this dissertation both substantially and stylistically. I had the privilege to get valuable comments and suggestions from Prof. William (Bill) F. McDonough that prompted me to modify some of the manuscripts presented here.

# Table of Contents

# List of Tables

# List of Figures

**CHAPTER 3**

**CHAPTER 5**

**CHAPTER 6**

# Chapter 1: INTRODUCTION

## 1. 1. Komatiites: Nomenclature and classification

This study covers two different aspects of komatiite petrogenesis: [1] examination of petrologic and geochemical characteristics of selected komatiites and evaluation of different petrogenetic models for their generation; and [2] determination of initial Os isotopic compositions of the selected suite of komatiites in order to further constrain the nature and extents of Os isotopic heterogeneity in the Precambrian mantle. Accordingly, in the following sections, a broad overview is presented describing the different types of komatiites and existing models for their generation. Finally, at the end of this chapter, the objectives of this study and a broad outlay of the dissertation are presented.

The term "komatiite" was introduced by Viljoen and Viljoen (1969 a, b) after their discovery of a suite of highly magnesian extrusive rocks in the Komati River valley in the Barberton Mountainland, South Africa. Detailed discussions on the global distribution, compositional varieties, petrographic characteristics and petrologic aspects of generation of komatiites may be found in Arndt and Nisbet (1982a). In brief, komatiitic lavas have erupted mostly during ~3.3-2.7 Ga during the Archean and less commonly at ~2 Ga during the Proterozoic. There are, however, notable exceptions, such as the Mesozoic komatiites from Gorgona Island (Echeverria, 1980) and those from the Permo-Triassic Emeishan greenstone belt in NW Vietnam (Hanski et al., 2004). Komatiites were originally defined as a distinct class of ultramafic rocks based on their high MgO contents (> 18 wt.%) in the inferred parental magmas, distinctive field occurrences, such as chilled flow tops and

pillow-like structures, and unique "spinifex" texture (Arndt and Nisbet, 1982b). Spinifex texture refers to random or parallel orientation of large plates, needles or complex skeletal grains of olivine or clinopyroxene in a matrix typically of fine skeletal grains of olivine, clinopyroxene and commonly devtrified glass (Arndt et al., 1977a, 1977b; see Fig. 1.1). This texture forms as a result of large thermal gradients in the erupted lavas due to rapid quenching, commonly in seawater (Shore and Fowler, 1999). Spinefex textures are, however, not a diagnostic characteristic of komatiites, as some picritic rocks also show this texture (Hanski and Smolkin, 1995). Moreover, recent studies suggest that, although komatiites are commonly extrusive, some Archean komatiites are likely to have been emplaced as shallow intrusives (Houlé et al., 2002; Cas et al., 2003; Arndt et al., in press) or at mid-crustal levels (Parman et al., 1997; Grove et al., 1999). The less magnesian rocks (<18 wt.%) that are often volumetrically dominant and ubiquitously associated with komatiites are commonly called komatiitic basalts. The relationship between komatiites and komatiitic basalts in a given outcrop is not always clear. These two rock types in a single volcanic assemblage often exhibit vastly different rare earth element (REE) patterns and isotopic characteristics, suggesting a different nature of their mantle sources and/or petrogenetic processes for their generation (e.g., Hanski et al., 2001 ).

The chemical compositions (particularly MgO, FeO, $SiO_2$, and $Al_2O_3$) of komatiites vary within wide limits from one suite of rocks to another and reflect a 'series' of rocks derived from variable ranges of compositions for parental magmas (Arndt et al., 1998). Two broad chemical types of komatiites, however, have long
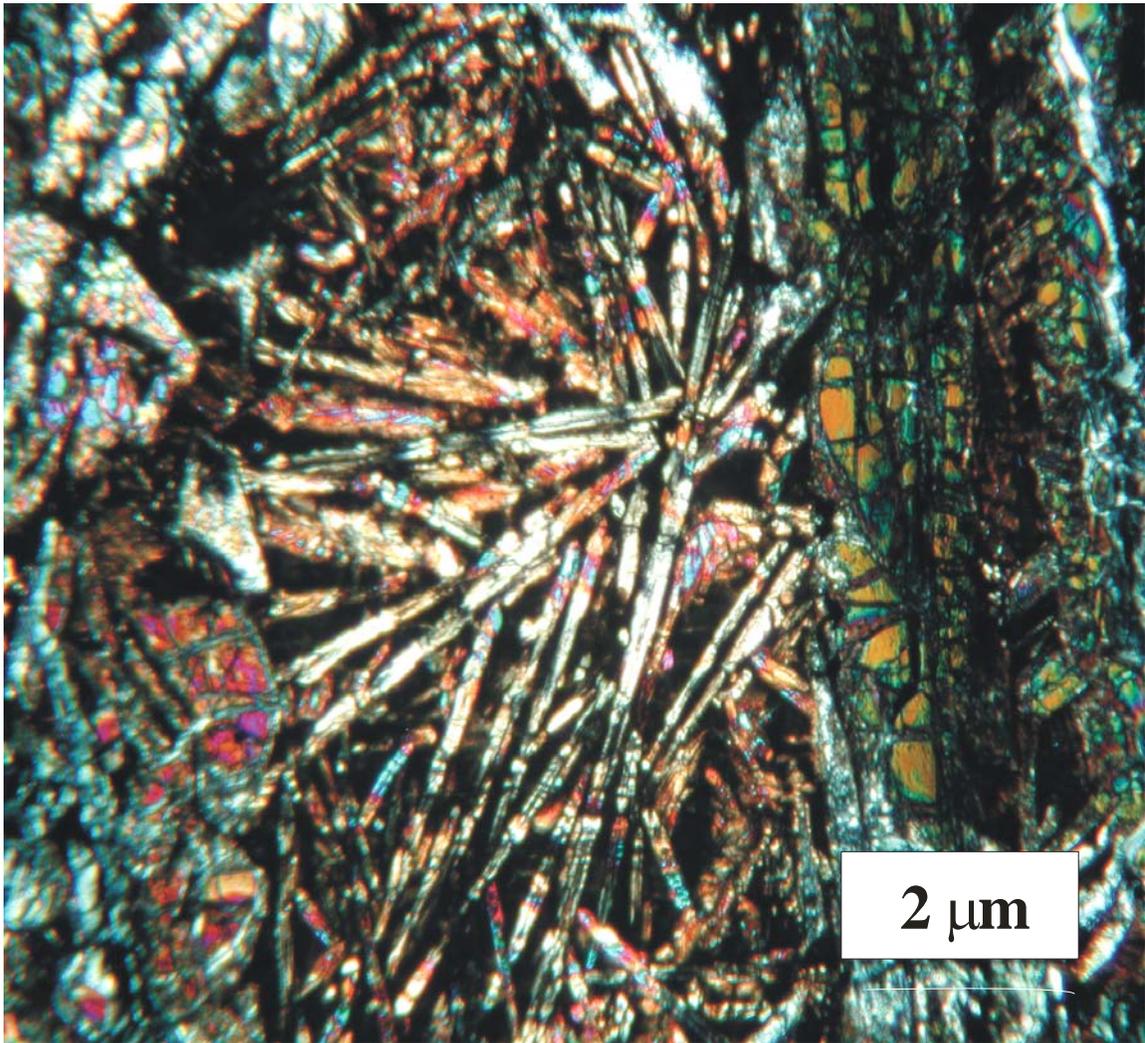
**Fig. 1.1.** Photomicrograph of a spinifex-textured komatiitc basalt under crossed nicols. Long needles of olivine and clinopyroxene is set in a mostly devitrified glass. The sample was collected from Alexo Township, Ontario, Canada.

been recognized (e.g., Nesbitt et al., 1979): [1] Al-undepleted or "Munro-type" and [2] Al-depleted or "Barberton-type" komatiites (Fig. 1.2). Komatiites with nearly chondritic $Al_2O_3/TiO_2$ ratios (~20; McDonough and Sun, 1995) are referred to as Al-undepleted komatiites. Examples include komatiites from Alexo and Munro Townships in the Abitibi greenstone belt, Canada. They also typically have $CaO/Al_2O_3 < 1$ and flat chondrite-normalized (CN) heavy rare earth element (HREE) pattern (e.g., $Gd/Yb_{CN} \sim 1$). Al-depleted komatiites, on the other hand, have subchondritic $Al_2O_3/TiO_2$ (typically 6-12) and characteristic HREE-depletion ($Gd/Yb_{CN} > 1$). The komatiites from the Komati Formation in the Barberton Mountainland are typical examples of the Al-depleted type. In chapter 2, the major element concentrations and Os isotopic characteristics of the Al-undepleted Alexo komatiites are discussed.

As more major and trace element data for komatiitic rocks from both Precambrian and Phanerozoic greenstone belts have become available, it is now recognized that geochemical characteristics of some komatiites are not entirely consistent with either of the types in the simple two-fold classification. For example, the komatiitic rocks recently reported from the Commondale area in the Kaapvaal craton, S. Africa have extremely low REE concentrations, yet significantly higher silica contents than that at a given MgO level for other types of komatiites (Wilson, 2003). Also, the komatiitic rocks from the Jeesiörova area in the ca. 2 Ga Central Lapland Greenstone Belt, northern Finland have subchondritic $Al_2O_3/TiO_2$ ratios (10-13) similar to those in Al-depleted rocks, yet they have similar aluminum contents at given MgO levels of the Al-undepleted komatiites (Fig. 1.2). The subchondritic
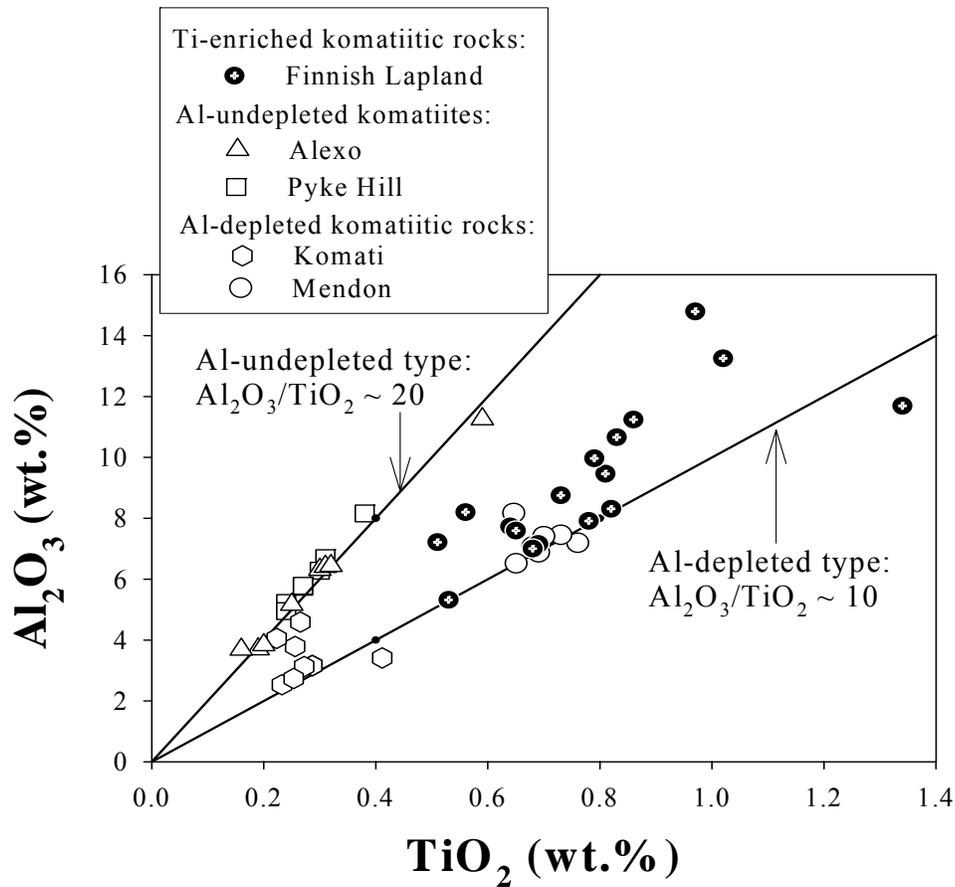
**Fig. 1.2.** Plot of $Al_2O_3$ vs. $TiO_2$ for high-MgO komatiites and komatiitic basalts of different chemical types: [1] Ti-enriched komatiitic rocks from Finnish Lapland (Hanski et al., 2001); [2] Al-undepleted komatiites from Alexo (Gangopahyay and Walker, 2003) and Pyke Hill (unpubl. data) in the Abitibi greenstone belt, Canada; and [3] Al-depleted komatiitic rocks from Mendon (Lahaye et al., 1995) and Komati Formations (Parman et al., 2002) in the Barberton Mountainland, S. Africa. Note that most of the Finnish rocks have $Al_2O_3/TiO_2$ ratios that fall between those of the Al-depleted and Al-undepleted types.

$Al_2O_3/TiO_2$ ratio in the Jessiörova komatiites is a result of higher $TiO_2$ content than that at a specific MgO level in both Al-undepleted and Al-depleted komatiites. These distinctive chemical characteristic of Jessiörova komatiites led Hanski et al. (2001) to construct a new scheme of classification for komatiites based on olivine-projected molecular $Al_2O_3$-$TiO_2$ relations. The Jessiörova komatiites, according to this scheme, plot in the distinct field of "Ti-enriched" komatiites. It is shown in chapter 3, that the Jessiörova komatiites, in addition to Ti, are also enriched in similarly incompatible elements relative to both Al-depleted and Al-undepleted types. It is now also apparent that the nearly contemporaneous komatiitic rocks from the Karasjok greenstone belt in Northern Norway (Barnes and Often, 1990) and from the Onega plateau, Russia (Puchtel et al., 1998) also belong to this "Ti-enriched" category. More examples of this distinct chemical type of komatiite have recently been reported from the Abitibi greenstone belt (e.g., see Sproule et al., 2002). Contrary to the traditional view of komatiite occurrences (e.g., Sun, 1984), it is now also recognized that Al-undepleted, Al-depleted and/or Ti-enriched komatiites can coexist in a single greenstone belt and, in some cases, within a single volcanic assemblage (e.g., Kidd-Munro assemblage in the Abitibi greenstone belt, Canada; Sproule et al., 2002). It is important to determine, therefore, whether relatively high abundances of Ti are a primary feature of the mantle sources for these rocks, or a result of: [1] lower degrees of melting; [2] higher degrees of differentiation; [3] lithospheric contamination; or [4] different conditions of melting (P-T-$fO_2$) relative to the more common Munro- or Barberton-type komatiites. In chapter 3, the petrologic, geochemical and combined Nd-Os isotopic

characteristics of the Jessiörova komatiites are discussed in relation to these considerations.

## 1.2. Petrogenetic models for komatiites

A comprehensive historical view of different petrogenetic models for the generation of komatiites may be found in Grove and Parman (2004). In brief, there are currently two classes of competing petrogenetic models: plume-based models of anhydrous melting in intraplate settings (e.g., Herzberg, 1992; Nisbet et al., 1993; McDonough and Ireland, 1993) and subduction-related hydrous melting in supra-subduction zone settings (e.g., Allègre, 1982; Parman et al., 1997; Grove et al., 1999). Neither of these two models alone explains the complete spectrum of petrologic, geochemical and isotopic characteristics of different chemical types of komatiites. It is possible that different komatiite types were generated under these two contrasting geodynamic settings (e.g., see Arndt et al., 1998; Grove and Parman, 2004).

The most widely accepted model for komatiite petrogenesis, so far, is the plume-based model, which suggests that ultramafic magamas, such as komatiites and picrites, are products of high degrees (up to ~50%) of partial melting of ascending mantle plumes. This model is based mainly on high liquidus temperatures (> 1600ºC) of komatiites inferred from the results of anhydrous melting experiments of peridotites (e.g., Green et al, 1975; Herzberg, 1992). The plume model suggests that the Al-depleted and Al-undepleted komatiites that may coexist in a single greenstone belt (e.g., in the Abitibi greenstone belt) are derived from different parts of a single plume (e.g., Xie et al., 1993; Sproule et al., 2002). The subchondritic $Al_2O_3/TiO_2$ and HREE-depletion ($Gd/Yb_{CN} > 1$) in Al-depleted komatiites have been suggested to

reflect a mantle source with residual majoritic garnet (Lahaye et al., 1995; Herzberg, 1995; McDonough et al., 1997), or separation of garnet from the magma during differentiation in the deep (>400 km) mantle (Gruau et al., 1990; Blichert-Toft and Arndt, 1999). Some geochemical characteristics, such as negative Nb, Zr and Hf anomalies in the Al-depleted komatiites have been used to support this model (e.g., Lahaye et al., 1995). However, it is now recognized that the analyses of high field strength elements (HFSE) are commonly fraught with uncertainties due to incomplete dissolution of HFSE-rich phases in mafic-ultramafic rocks (e.g., Blichert-Toft et al., 2004). Thus, some of the negative HFSE anomalies (particularly Zr and Hf) may be analytical artifacts. Nevertheless, recent experimentally determined partition coefficients for REE and other trace elements between majorite garnet and silicate melt have been used to support the model of garnet fractionation for the generation of Al-depleted komatiites (Corgne and Wood, 2004). On the contrary, the Al-undepleted komatiites, according to this model, were derived from shallower parts of the mantle plume (< 400 km) where garnet was not a fractionating phase. In chapter 2, the combined Nd-Os isotopic characteristics of Al-undepleted Alexo komatiites have been used to suggest their generation from convective upper mantle.

The high liquidus temperatures (Green et al, 1975) for komatiites that are inferred based on assumed anhydrous melting of their mantle sources have long been challenged, and as an alternative, some komatiites have been argued to be products of subduction-related hydrous melting (e.g., Allègre, 1982; Parman et al., 1997; Grove et al., 1999). Furthermore, the presence of magmatic water in some komatiites has been documented in previous studies. For example, Stone et al. (1997) estimated $H_2O$

contents of 1.2% from magmatic amphiboles of Boston Creek ultramafic flows. A relatively smaller amount of water (~0.2 wt.%) was documented in melt inclusions in komatiites from the late-Archean Reliance formation of Belingwe (McDonough and Danyuschevsky, 1995). More recently, ion probe analyses of melt inclusions in early fractionating Cr-spinels suggest a hydrous (0.8-0.9% $H_2O$ corresponding to ~24% MgO) parental liquid for Belingwe komatiites (Shimizu et al., 2001). It is likely that the estimates obtained from melt inclusions place lower limits on the $H_2O$ contents of undegassed parental magmas prior to entrapment as inclusions. Recent experimental studies (Asahara et al., 1998), however, suggest that addition of 0.5% $H_2O$ to mantle peridotite does not significantly depress the volatile-free komatiite liquidus. Accordingly, Shimizu et al. (2001) suggested a hydrous, yet high-temperature plume origin for Belingwe komatiites. Moreover, relatively high contents of $H_2O$ in a plume source may be derived from dehydrating oceanic crust during subduction and, therefore, have an important bearing on the Os isotopic composition of plume-derived magmas. For example, the mantle source for the Belingwe komatiites had a suprachondritic initial Os isotopic composition (Walker and Nisbet, 2002). It is not clear, however, whether the high abundance of $H_2O$ is derived from: [1] primordial $H_2O$ in the Archean mantle; [2] dewatering of subducted oceanic lithosphere; or [3] non-magmatic $H_2O$ (e.g., meteoric) introduced during emplacement of the lavas at near-surface levels. In chapter 4, the two contrasting models are evaluated for the new class of HREE-depleted, yet Ti-enriched komatiites from the Finnish Lapland.

Attempts have also been made to reconcile the two contrasting petrogenetic models and to integrate them into a single model of impingement of mantle plume

upon subducting oceanic lithosphere (Kerrich et al., 1998; Sproule et al., 2002). This hybrid model is based on the observation that boninite series rocks, that are typically formed in modern arc settings, are intercalated with komatiites in several localities in the Abitibi greenstone belt (Kerrich et al., 1998). The "interfingering" of plume-derived rocks of komatiite-tholeiite association and the subduction-related boninite series rocks, according to this model, suggests interaction of a mantle plume with a subducting slab. Although such an argument is intuitively opportunistic and "unappealing" (Grove and Parman, 2004), the possibility of interaction between mantle plume and subducted slab cannot be categorically ruled out. However, some relatively recent komatiites form part of lithologic associations that do not include typical arc-related lavas. For example, the Mesozoic Gorgona komatiites are part of the Carribean oceanic plateau, and their lithologic associations do not include arc-related lavas, such as boninites (e.g., Echeverra, 1980; Arndt et al., 1997).

## 1.3. Secondary processes: Pitfalls and possible remedies

Petrologic, geochemical and isotopic studies suggest that Precambrian komatiites, in general, were affected by secondary processes to varying degrees, such as [i] surficial weathering; [ii] post-crystallization hydrothermal alteration; [iii] greenschist to amphibolite facies metamorphism; [iv] seawater interaction; and [v] assimilation of lithospheric components (e.g., Beswick, 1982; Jolly, 1982; Arndt et al., 1989; Arndt and Lesher, 1992; Lesher and Arndt, 1995; Lahaye and Arndt, 1996; Rollinson, 1999; Hanski et al., 2001). The degrees to which these secondary processes have obliterated the characteristics of the mantle sources for komatiites vary greatly from one suite of rocks to another. Also, the choice of samples is largely

guided by the nature and objective of a particular petrologic, geochemical or isotopic study. The present study is mostly focused on the use of Re-Os systematics of komatiites, and, accordingly, this section (section 1.3) is devoted to addressing the issues relating to careful selection of samples for Os isotopic study.

Deep drill core samples, if available, are preferred in order to minimize the effects of surface weathering-related element mobility in the emplaced lavas (e.g., Puchtel et al., 2004a, 2004b). The vast majority of geochemical and isotopic studies of komatiites, however, have utilized samples from surface flows of komatiitic lavas. All of the komatiite samples used in the present study were collected from surface outcrops. It is demonstrated in chapter 2 that carefully selected, least-altered komatiite samples from surface flows can preserve the primary Re-Os elemental and isotope systematics of emplaced lavas. Conversely, drill core samples used in the Os isotopic study of komatites from Belingwe, Zimbabwe, have shown large-scale open-system behavior, most likely due to hydrothermal alteration (Walker and Nisbet, 2002).

For the study of primary magmatic major and trace element characteristics, the most commonly applied technique to evaluate secondary mobility of elements in komatiites involves the use of olivine fractionation and accumulation trends for a given suite of rocks (Arndt 1977a; Arndt, 1986). This method utilizes the fact that olivine is the dominant fractionating mineral in most komatiitic magmas and, accordingly, on plots of MgO versus least-mobile incompatible major element oxides and trace elements (e.g., $Al_2O_3$, $TiO_2$, Zr, Sm), linear trends with negative slopes are normally observed. The linear trends, when projected back to the field for olivine

compositions determined in the same suite of rocks, provides evidence for limited mobility of the respective elements. Deviations from such olivine-control trends, on the other hand, are commonly ascribed to post-magmatic mobility of a given element due primarily to hydrothermal alteration and metamorphism. This criterion has been used to evaluate the post-crystallization mobility of elements in rocks from Alexo and Dundonald Beach in the Abitibi greenstone belt, Canada (chapters 2 and 3).

In a recent ion microprobe study of fresh clinopyroxene from the Barberton komatites, a new approach was applied to evaluate the mobility of trace elements in the whole rocks due to metamorphism (Parman et al., 2003). This method involves determination of trace element concentrations of fresh clinopyroxene and calculation of those in a projected clinopyroxene composition in equilibrium with the whole-rock sample. The differences between the calculated and measured trace element concentrations, according to this scheme, yield the percentage loss or gain of each element. The study of Parman et al. (2003) suggested that REE were not significantly mobile during the greenschist facies metamorphism of Barberton rocks. Similarly, the komatiites from the Abitibi greenstone belt studied here (chapters 2 and 4) and also those from the Jeesiörova area in the Finnish Lapland (chapter 3) were metamor-phosed to greenschist facies. In each case, the relatively immobile behavior of REE has been noted either in the present study or in previously published work on the flows (e.g., Lahaye and Arndt, 1996; Hanski et al., 2001). The possible effects of metamorphism on the Re-Os systematics of the Abitibi rocks are discussed in chapter 5.

A previous oxygen isotope study of Pyke Hill komatiites (stratigraphically-equivalent to the Alexo rocks studied here) suggests their interaction with ambient seawater (Beaty and Taylor, 1982). The effects of hydrothermal alteration (induced by seawater) on the major and trace element characteristics of komatiites may be significant, and, as described above, can be evaluated using the olivine-control criteria. However, seawater interaction might not have significantly modified the initial Os isotopic compositions of komatiites, because ambient seawater most likely had more than 3 orders of magnitude lower Os concentrations than those of the erupted lavas (Sharma et al. 1997).

Evidence for crustal contamination in komatiites is provided by combinations of lithophile element distributions (e.g., negative Nb anomalies; Perring et al., 1996), LREE-enrichment (e.g., Lesher and Arndt, 1995), unradiogenic Nd isotopes and radiogenic Pb isotopic compositions (Puchtel et al., 1996). The komatite flows from the Alexo and Jeesiörova areas are well-characterized in terms of major and trace elements, and lithophile element isotope systematics, and were suggested to have undergone limited or no crustal contamination (e.g., Lahaye and Arndt, 1996). In the absence of Nd and Pb isotopic composition of the Dundonald rocks, their key trace element characteristics have been compared with some Precambrian komatiites for which trace elements and lithophile element isotopic characteristics suggest significant crustal contamination (chapter 4). Also, typical continental crust has about 2 orders of magnitude lower Os concentrations than in komatiitic parental magmas, and, accordingly, the Os isotopic compositons of the komatiitic magmas may not

necessarily be significantly modified even after relatively large degrees of crustal contamination.

The interaction of the subcontinental lithospheric mantle (SCLM) and presumably hotter asthenospheric melt is another process that can potentially modify the Os isotopic composition of primary komatiitic melt derived from the asthenosphere. This is because the SCLM is commonly observed to have subchondritic $^{187}Os/^{188}Os$ as a result of prior Re depletion (e.g., Walker et al., 1989; Rudnick and Lee, 2002). For example, the subchondritic initial Os isotopic composition of the Al-depleted ultramafic flows from Boston Creek, Canada may suggest their derivation dominantly from a SCLM-like mantle source that had undergone prior melt depletion. In chapter 4, a combination of Os and Nd isotopic characteristics is used to monitor the interaction between SCLM and asthenospheric melts for the generation of Jeesiörova komatiites from the Finnish Lapland.

## 1.4. The application of the Re-Os system to the study of Precambrian komatiites

A comprehensive review of the Re-Os isotope system and its application to high temperature geochemistry may be found in Shirey and Walker (1998). Only a brief overview is presented here detailing the context in which the present Os isotopic work of Precambrian komatiites was carried out.

The importance of Os isotopes ($^{187}Re \rightarrow {}^{187}Os + \beta^-$; $\lambda = 1.666 \times 10^{-11} yr^{-1}$, Smoliar et al., 1996) as petrogenetic tracers has long been recognized (Allègre and Luck, 1980). The potential of the $^{187}Re\text{-}^{187}Os$ isotope system as a tracer of processes in planetary mantle stems primarily from a combination of the chalcophilic and highly siderophilic nature of both Re and Os and their different compatibilities during

mantle melting. Rhenium is preferentially partitioned into magmatic liquids, whereas Os mostly resides in mantle minerals during low to moderate degrees of partial melting of mantle sources. Because both Re and Os are highly siderophile elements, it follows that these two elements partitioned nearly quantitatively into the metallic core during its segregation in the early earth. Accordingly, it is now widely believed that the Re and Os present in modern and ancient mantle-derived rocks were originally derived from a 'late veneer' of chondritic materials added to the mantle following the completion of core formation (e.g. Kimura et al., 1974; Chou, 1978; Sun, 1982; Morgan, 1985; Meisel et al., 1996; but also see Jones and Drake, 1986; Brett, 1984 and McDonough, 1995 for alternative hypotheses). Thus, Os isotopic studies of mantle-derived rocks, such as komatiites can provide insights into the nature of late accreted materials, their distribution in different mantle reservoirs and the rate at which they were added to terrestrial and possibly other planetary bodies.

Despite a generally chondritic relative abundance of all eight highly siderophile elements [HSE: Re, Au and 6 platinum group of elements (PGE: Ir, Os, Ru, Pt, Rh, Pd)], significant portions of the modern terrestrial mantle are heterogeneous in terms of Os isotopic compositions. For example, the initial Os isotopic compositions of present-day ocean island basalts (e.g., Reisberg et al., 1993, Hauri and Hart 1993, Roy-Barman and Allègre, 1995) show large-scale variation ($\gamma_{Os}$ is as high as +25; where $\gamma_{Os}$ is the percent deviation of $^{187}Os/^{188}Os$ of a sample from the chondritic ratio at a given time). Also, the initial Os isotopic compostions of different mantle domains, as sampled by abyssal peridotites (Martin, 1991; Snow and Reisberg, 1995), ophiolites  (Luck and Allègre, 1991; Walker et al., 1996; 2002),

mantle xenoliths (Morgan, 1986; Walker et al., 1989; Chesley et al., 1999; Miesel et al., 1996, 2001), ultramafic and related rocks (e.g., Walker et al., 1988; Hattori and Hart, 1991; Foster et al., 1996; Walker and Stone, 2001; Puchtel et al., 2001a, 2001b), and flood basalts (Horan et al., 1995; Allègre et al., 1999) collectively show either chondritic Os isotopic composition or large range of positive deviations from the chondritic Os isotopic evolution trajectory. The estimated Os isotopic composition of the mantle sources for mid-oceanic ridge basalts (MORB), on the other hand, is essentially chondritic (Walker et al., 1996; Brandon et al., 2000) or only slightly subchondritic (Snow and Reisberg, 1995). Moreover, it is now clear that the primitive upper mantle (PUM) has $^{187}Os/^{188}Os$ ratios ($0.1296 \pm 0.0008$) similar to the ranges observed in ordinary and enstatite chondrites (Meisel et al., 1996, 2001). It is important to determine, therefore, how and when the different portions of the earth's mantle developed the Os isotopic heterogeneities.

Different mechanisms have been proposed to explain the enrichments in $^{187}Os$ of mantle sources relative to projected chondritic compositions. For example, suprachondritic initial $^{187}Os/^{188}Os$ for younger volcanic rocks, such as modern ocean island basalts (OIBs) may reflect incorporation of recycled radiogenic oceanic crust into their mantle source (Hauri and Hart, 1993; Reisberg et al., 1993; Fig. 1.3). Alternatively, a core-mantle interaction model has been proposed to explain the coupled $^{187}Os$-$^{186}Os$ enrichments in Siberian flood basalts, Hawaiian picritic rocks (Walker et al., 1995; Brandon et al., 1998, 1999) and also in komatiitic rocks from Gorgona island (Brandon et al., 2003). This model, based on empirical estimates of higher liquid-metal/solid-metal partition coefficients of Re and Pt than that for Os
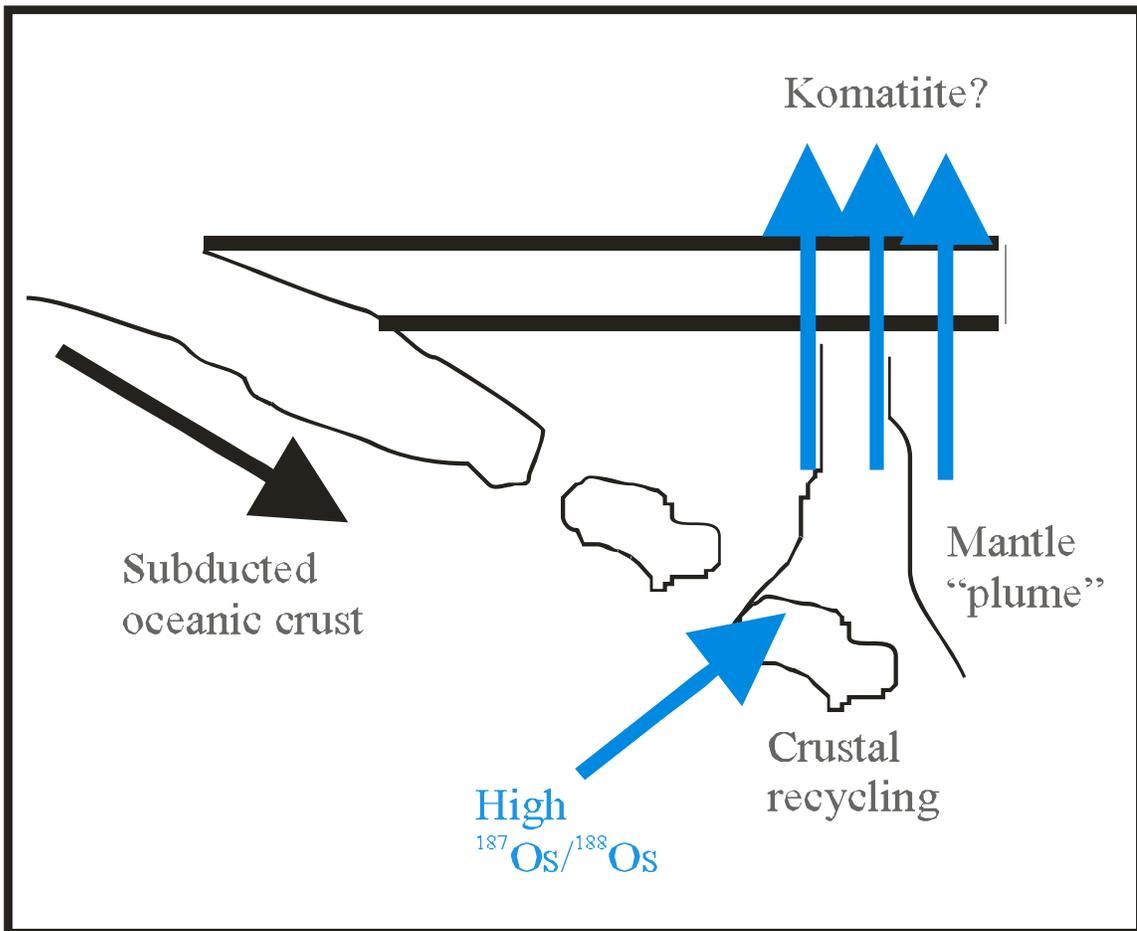
**Fig. 1. 3.** A schematic diagram to illustrate the role of radiogenic oceanic crust in the origin of high $^{187}Os/^{188}Os$ ratios of ocean island basalts.
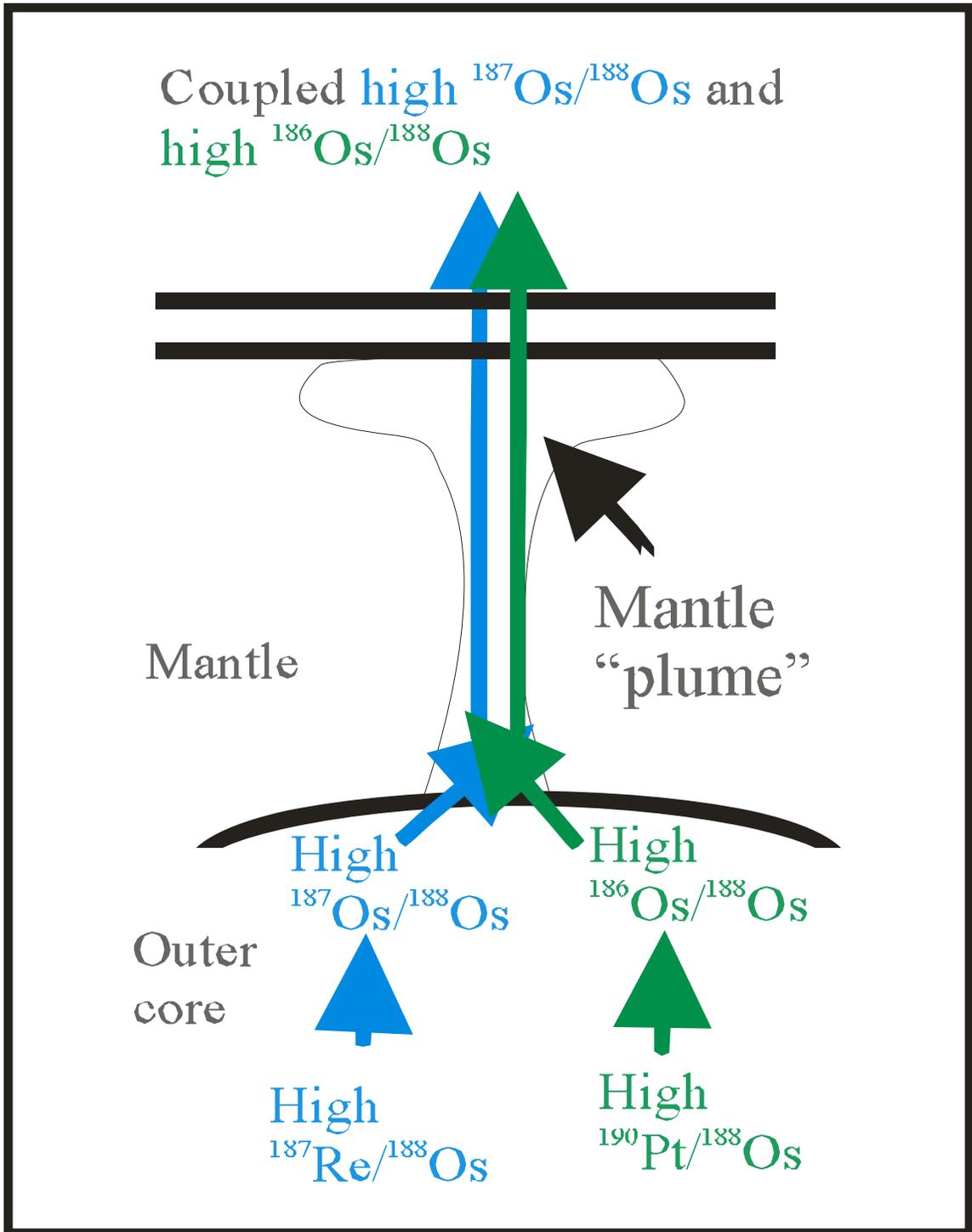
**Fig. 1.4.** A schematic diagram to illustrate the role of core-mantle interaction in the origin of radiogenic Os isotopic component in komatiitic and picritic rocks from Hawaiian and Gorgona islands.

derived from magmatic iron meteorites, suggests that the separation of liquid outer core from the solid inner core involved fractionation of Re/Os and Pt/Os ratios (Fig. 1.4). The putative suprachondritic Re/Os and Pt/Os ratios in the outer core, therefore, would have led to radiogenic ingrowth of both $^{187}Os$ and $^{186}Os$ through geologic time. The coupled enrichments in $^{187}Os$ and $^{186}Os$ in plume-derived lavas, according to this model, suggest that the putative radiogenic outer core materials were entrained in their mantle sources through physical admixture and/or isotopic equilibration at the core-mantle boundary. Puchtel et al. (2001a) have suggested a similar possibility for $^{187}Os$-enriched komatiites from the 2.8 Ga Kostomuksha greenstone belt.

Previous studies have also suggested that addition of lower mantle material with a presumably enriched $^{187}Os$ and $^{186}Os$ (e.g., as a result of early differentiation in a magma ocean) in a plume source can potentially produce isotopic enrichments observed in some mantle derived rocks (Walker et al., 1997). Additionally, several researchers (e.g., Morgan et al., 2001) suggested that the regional scale variations of HSE compositions in different mantle domains may represent the original spatial heterogeneity in the late veneer materials.

While the mechanisms discussed above can account for enrichment or depletion in $^{187}Os$ isotopes observed in different mantle domains, the evolution of these compositions through geologic time is, so far, poorly constrained. Understanding the origin, age and evolution of these heterogeneities requires systematic studies of both ancient and modern mantle-derived rocks. Precambrian komatiites are good candidates to this end, primarily for the following reasons: First, komatiites have high Os abundance and low Re/Os ratios that result in minimal

correction for measured $^{187}Os/^{188}Os$ ratios to obtain the initial Os isotopic composition of their mantle sources. Second, komatiitic lavas commonly have high modal abundances of chromites that are relatively resistant to weathering and alteration and have 2-3 orders of magnitude higher Os concentrations than whole rocks. This, combined with typically low Re/Os ratios in chromites provides direct means of determination of initial Os isotopic composition for the mantle sources for host lavas. Third, komatiites are high degree partial melts from their mantle sources and hence, the melting processes likely averaged local small-scale inhomogeneities. Thus, unlike mantle xenoliths, komatiitic lavas are likely to have sampled relatively large mantle reservoirs. Fourth, although komatiite melts are susceptible to crustal contamination due to their high liquidus temperatures, their Os isotope systematics, unlike basalts, remains relatively immune to relatively large degrees of crustal contamination by typical low-Os crustal materials because most komatiite magmas have up to 2 orders of magnitude higher Os concentrations than typical crustal materials (Walker and Nisbet, 2001). Finally, most Archean and Proterozoic komatiites are well characterized in terms of major and trace elements and lithophile element isotope systems (e.g., Sm-Nd, Pb-Pb) and, therefore, a careful selection of least-altered whole-rock samples from different flows prior to Os isotopic analyses is possible.

## 1.5. Scope of the present work

The primary objective of this work was to examine the petrologic and geochemical characteristics of selected suites of Precambrian komatiites and to determine the initial Os isotopic compositions of their mantle sources in order to (a)

characterize the Os isotopic heterogeneity in the Precambrian mantle and (b) constrain petrogenetic processes for the generation of komatiites. To this end, the following work was carried out for three suites of komatiites:

[1] ca. 2.7-Ga komatiites from the Alexo area in the Abitibi greenstone belt, Canada. The chemical composition (major element oxides) and Re-Os isotopic systematics of the Alexo flows were determined in this study (Chapter 2).

[2] ca. 2.0-Ga komatiitic rocks from Jeesiörova area in the Kittiliä greenstone Complex, Finland. The Re-Os systematics of these flows were examined and integrated to a model for the generation of the rocks (Chapter 3).

[3] ca. 2.7-Ga komatiitites and komatiitic basalts from Dundonald Beach area in the Abitibi greenstone belt, Ontario, Canada. The geochemical characteristics of two separate flows were examined in relation to the existing models for the generation of komatiites (Chapter 4).

[4] The Re-Os systematics of komatiites and  komatiitic basalt units were examined in order to determine the initial Os isotopic composition of the mantle sources for these rocks (Chapter 5).

[5] Finally, based on the results obtained in this study and those from previous studies, a comprehensive discussion is presented (Chapter 6).

# CHAPTER 2: Re-Os SYSTEMATICS OF THE ca. 2.7 Ga KOMATIITES FROM ALEXO, ONTARIO, CANADA

## Abstract

The Re-Os isotope systematics of a suite of komatiitic flows from Alexo Township, in the Abitibi greenstone belt, Ontario were examined in order to characterize the partitioning behaviors of Re and Os during the generation and subsequent differentiation of komatiitic magma, and also to determine the initial Os isotopic composition of the late-Archean mantle source of these rocks. This suite of komatiites was suitable for these objectives because of their high Os concentrations, $\geq \sim 1$ ppb, and low $^{187}Re/^{188}Os$ ratios (ranging between 0.4 and 2.4). The Re-Os isotope results for whole rock komatiites and chromite separates yield a model 3 isochron age of $2762 \pm 76$ Ma. This age is in general agreement with previously determined U-Pb ages of zircons from associated felsic units and also with Sm-Nd and Pb-Pb isochron ages of these flows. This suite of Alexo komatiites, thus, demonstrate relatively limited mobility of Re and Os at the whole-rock scale, even after large-scale alteration and ambient lower greenschist facies metamorphism. The initial Os isotopic composition ($^{187}Os/^{188}Os_{(I)} = 0.1080 \pm 0.0012$) obtained from the regression is essentially chondritic ($\gamma_{Os} = -0.1 \pm 1.0$). Our results, therefore, suggest an absence of any large-scale deviation in initial Os isotopic composition of the mantle source of these komatiites relative to the putative chondritic composition of the contemporaneous convective upper mantle.

For these komatiites, Os was moderately compatible with the mantle residue ($D_{Os}^{mantle-melt} \sim 2.1$), whereas Re was incompatible ($D_{Re} \sim 0.20$). These D's are consistent with those previously estimated for other Archean komatiites (e.g. Walker et al., 1988). The apparent $D_{Os}^{olivine/liquid}$ and $D_{Re}^{olivine/liquid}$ in Alexo komatiites are 1.7 and 0.66, respectively. Our results, therefore, suggest that Os is slightly compatible whereas Re is moderately incompatible in olivine or a coprecipitating phase during magmatic differentiation of komatiitic liquids. The concentrations of Re and Os in Alexo komatiites are also comparable to those reported for komatiites from other greenstone belts. The apparent magmatic behaviors of both Re and Os in the whole-rock komatiites indicate that the Re-Os elemental systematics are primary features of these rocks.

The Os isotopic results obtained for the Alexo komatiites, combined with those from the spatially associated Munro Township komatiites (e.g. Walker et al., 1988; Shirey, 1997), suggest a source for komatiites in the southern volcanic zone of the Abitibi greenstone belt that was dominated by Os with a chondritic isotopic composition. Also, the Os isotopic results, combined with previous Nd and Pb isotopic results, are consistent with derivation of the komatiites from either the contemporaneous convective upper mantle or a deep mantle source with isotopically similar characteristics. These results imply that, if the chondritic Os isotopic composition of the mantle sources for the komatiites were set by a chondritic "late veneer", most late accretion and subsequent homogenization within the mantle must have occurred prior to their eruption at ~2.7 Ga.

## 2.1. INTRODUCTION

The $^{187}$Re-$^{187}$Os isotope systematics ($^{187}$Re $\rightarrow$ $^{187}$Os + $\beta^-$; $\lambda$ =1.666 x 10$^{-11}$yr$^{-1}$; Smoliar et al., 1996) of materials derived from young mantle plumes show that plumes tap mantle reservoirs with significant heterogeneity in terms of Os isotopic compositions. For example, modern ocean island basalts (Reisberg et al., 1993, Hauri and Hart 1993, Roy-Barman and Allegre, 1995), Phanerozoic flood basalts (Horan et al., 1995; Allegre et al., 1999) and ultramafic rocks (Walker et al., 1999) show a large variability in initial Os isotopic compositions with $\gamma_{Os}$ ranging between 0 and ~ +25 (where $\gamma_{Os}$ is the percentage deviation in $^{187}$Os/$^{188}$Os from the projected chondritic composition at a given time). In contrast, the Os isotopic composition of the modern convecting upper mantle is within the range of chondritic meteorites ($\gamma_{Os}$ ranging between about –3 and +1; Snow and Reisberg, 1995; Brandon et al., 2000; Walker et al., 2002). Thus, many young plume sources are considerably more radiogenic than the modern convecting upper mantle. One important question, therefore, is how and when the plume sources developed the observed Os isotopic enrichments.

Os isotopic heterogeneities in the terrestrial mantle, indeed, can be traced as far back as late Archean. For example, some Archean ultramafic systems, e.g., Munro Township komatiites in the 2.7 Ga Abitibi greenstone belt (Walker et al., 1988; Shirey, 1997) and ore-bearing sulfides from Kambalda in Western Australia (Foster et al., 1996) show broadly chondritic initial Os isotopic compositions. In contrast, there are significant deviations from projected chondritic compositions for other late Archean mantle sources. For example, the Boston Creek komatiites of the Abitibi greenstone belt were derived from a source with subchondritic $^{187}$Os/$^{188}$Os (Walker

and Stone, 2001), whereas the sources of the komatiites from Kostomuksha, Russia (Puchtel et al., 2001a) and Belingwe, Zimbabwe (Walker and Nisbet, 2002) were suprachondritic.

Understanding the origin, age and evolution of the Os isotopic heterogeneities in the terrestrial mantle requires systematic studies of both ancient and modern mantle-derived rocks. Precambrian komatiites are good candidates to study the development of Os isotopic heterogeneities in plume sources because of their high Os abundance, low Re/Os ratios and relatively robust preservation of initial Os isotopic composition during alteration and low-grade metamorphism (e.g. Walker et al., 1988). Furthermore, at least some komatiites are believed to be derived from mantle plumes (Herzberg, 1992; Nisbet et al., 1993; McDonough and Ireland, 1993) and represent high-degree partial melts of their mantle sources. Hence, the melting processes likely removed local small-scale isotopic inhomogeneities in the source during their generation. Although the high eruption temperatures of komatiitic melts make them susceptible to crustal contamination, the high Os abundances in most komatiite magmas can preserve the original Os isotopic composition of the mantle sources, even after a relatively large degree of contamination by typical low-Os crustal materials (e.g. Walker and Nisbet, 2002). Furthermore, crustal contamination for these rocks can be monitored by other isotope systems, such as Sm-Nd and Pb-Pb, which are much more sensitive to crustal assimilation (e.g., Puchtel et al., 2001b). Additionally, there are many Archean and Proterozoic komatiites that are well characterized in terms of major and trace elements and other lithophile element

isotope systems and, therefore, a careful selection of least altered whole-rock samples from different flows prior to their isotopic analyses is possible.

Here we present the Re-Os isotope systematics and major and selected trace element characteristics of a suite of ca. 2.7 Ga komatiite flows from Alexo Township in the Superior Province, Ontario, Canada. Two factors guided the choice of our samples: [1] The Alexo flows are precisely dated at 2700-2727 Ma (e.g. Nunes and Pyke, 1980). Therefore, a comparison between these ages and those obtained from Re-Os isochron is possible; and [2] Some of these rocks have abundant chromites that allow a precise determination of the initial Os isotopic composition of the flows.

## 2.2. SAMPLES AND ANALYTICAL METHODS

Eight whole-rock samples and three chromite separates from the komatiite flows were analyzed. The textural characteristics of these rocks include both spinifex and massive (textural types are detailed in Table 2.1). Olivine occurs mainly in two different modes: [1] relatively large subhedral to euhedral cumulate crystals; and [2] long plates or laths (± clinopyroxene needles) defining spinifex texture. Minor secondary opaque oxides (magnetite) are also present along fracture planes of olivine crystals. Olivine is partially chloritized in some samples with spinifex texture. Samples with high modal abundances of cumulate olivine are typically mostly serpentinized. The cumulate olivines in these samples are mostly subhedral. The glassy matrix is generally devitrified.

All whole rock samples were collected from outcrops. The samples were first crushed into mm-sized pieces and cleaned with Milli-Q™ water repeatedly under ultrasonic bath for at least one hour. The freshest unaltered pieces were handpicked

**Table 2. 1:** Whole rock major element oxides (recalculated on anhydrous basis) and selected trace element data for the Alexo komatiites.

| Sample | Alx-1 | Alx-2 | Alx-3 | Alx-4 | Alx-5H | Alx-5W | Alx-6 | Alx-26 |
|---|---|---|---|---|---|---|---|---|
| Texture | Cumulate | Random spinifex | Plate spinifex | Basal cumulate | Cpx-spinifex | Komatitic basalt | Cumulate | Chevron spinifex |
| $SiO_2$ (wt%) | 45.43 | 45.66 | 45.64 | 44.63 | 44.63 | 47.73 | 43.77 | 45.47 |
| $TiO_2$ | 0.19 | 0.30 | 0.31 | 0.20 | 0.16 | 0.59 | 0.25 | 0.32 |
| $Al_2O_3$ | 3.70 | 6.31 | 6.41 | 3.84 | 3.69 | 11.26 | 5.17 | 6.44 |
| $Fe_2O_3$* | 8.30 | 11.09 | 10.93 | 8.72 | 9.17 | 11.75 | 13.24 | 11.13 |
| MnO | 0.14 | 0.18 | 0.18 | 0.14 | 0.17 | 0.19 | 0.22 | 0.16 |
| MgO | 40.20 | 30.21 | 29.86 | 39.54 | 39.83 | 11.62 | 31.37 | 30.16 |
| CaO | 1.66 | 5.57 | 5.70 | 2.65 | 1.39 | 17.04 | 5.40 | 5.99 |
| $Na_2O$ | 0.00 | 0.47 | 0.27 | 0.00 | 0.00 | 0.09 | 0.11 | 0.24 |
| $K_2O$ | 0.01 | 0.11 | 0.08 | 0.00 | 0.00 | 0.01 | 0.02 | 0.06 |
| $P_2O_5$ | 0.01 | 0.02 | 0.02 | 0.01 | 0.01 | 0.04 | 0.02 | 0.02 |
| Total | 99.64 | 99.92 | 99.40 | 99.73 | 99.05 | 100.32 | 99.57 | 99.99 |
| | | | | | | | | |
| Mg#$^\Psi$ | 0.91 | 0.84 | 0.84 | 0.90 | 0.90 | 0.66 | 0.82 | 0.84 |
| $CaO/Al_2O_3$ | 0.45 | 0.88 | 0.89 | 0.69 | 0.38 | 1.51 | 1.04 | 0.93 |
| $CaO/$ $(CaO+Al_2O_3)$ | 0.31 | 0.47 | 0.47 | 0.41 | 0.27 | 0.60 | 0.51 | 0.48 |
| $Al_2O_3/TiO_2$ | 19.5 | 21.0 | 20.7 | 19.2 | 23.1 | 19.1 | 20.7 | 20.1 |
| $TiO_2/P_2O_5$ | 19 | 15 | 15.5 | 20 | 16 | 14.75 | 12.5 | 16 |
| | | | | | | | | |
| Trace elements (ppm) | | | | | | | | |
| Cr | 1703 | 2456 | 2383 | 1757 | 3671 | 840 | 2679 | 2280 |
| Ni | 2218 | 1650 | 1680 | 2268 | 1957 | 199 | 1068 | 1557 |

*$Fe_2O_3$ as total Fe;

$^\Psi$Calculated as mole% MgO/(MgO + FeO) with 90% of total iron as FeO.

and dried in an oven at approximately 60°C for about an hour. These pieces were then ground with an agate mill. The powders were carefully mixed and homogenized. Different aliquots of the same whole-rock powder were used in major and trace element, and isotopic analyses of each sample. The chromite separates were obtained from Eero Hanski (Geol. Surv. of Finland) and Igor Puchtel (Univ. of Chicago; also the whole rock sample, Alx-26). X-ray fluorescence (XRF) analyses of major and trace elements of the komatiites reported here were performed with a Siemens MRS-400 multi-channel simultaneous X-ray spectrometer at the University of Massachusetts.

The chemical separation techniques for Re-Os analyses employed in this study have followed previously published work (Shirey and Walker, 1995; Cohen and Waters, 1996). In brief, approximately 2-3 g of whole-rock powders were added to ~ 3g of concentrated HCl and 6g of concentrated $HNO_3$ and frozen into Pyrex™ Carius tubes. Unlike the whole-rock powders, relatively smaller amounts of chromites (Table 2.2) were used due to their limited available quantities. Appropriate amounts of separate $^{190}Os$ and $^{185}Re$ spikes were added and the tube was subsequently sealed and heated at 240°C for at least 12 hours. Sample digestion for chromites lasted at least 24 hours to ensure complete dissolution. Unlike the whole-rock powders, mixed $^{190}Os$-$^{185}Re$ spikes were used for the chromite separates. Osmium was separated by solvent extraction into carbon tetrachloride and subsequently transferred into high-purity concentrated HBr (Cohen and Waters, 1996). The final purification and pre-concentration for Os was accomplished via microdistillation in a conical Teflon™ vial. Rhenium was recovered from aqua regia via anion exchange techniques (Morgan

**Table 2.2:** Rhenium and Os isotopic and compositional data[1] for the whole-rock Alexo komatiites and primary chromite separates. Total analytical uncertainties, except where noted in parentheses, are ±0.3% for $^{187}Re/^{188}Os$ and ±0.1% for $^{187}Os/^{188}Os$ (2σ%) for both whole rocks (WR) and chromites (CMT.).

| Samples | Sample[2] types | Sample weight (g) | Re (ppb) | Os (ppb) | $^{192}Os$ (ppb) | $^{187}Os/^{188}Os$ | $^{187}Re/^{188}Os$ | $\gamma_{Os}$[3] |
|---|---|---|---|---|---|---|---|---|
| Alx-1 | WR | 2.00 | 0.2519 | 2.572 | 1.05 | 0.13138 | 0.4722 | +1.0±0.2 |
| Repl.[4] | WR | 3.00 | 0.2391 | 2.597 | 1.06 | 0.13041 | 0.4438 | +1.3±0.2 |
| Alx-2 | WR | 2.00 | 0.4136 | 1.911 | 0.78 | 0.1561(3) | 1.047 | -1.2±0.4 |
| Alx-3 | WR | 3.01 | 0.4834 | 1.609 | 0.65 | 0.17521 | 1.456 | -1.3±0.4 |
| Alx-4 | WR | 2.00 | 0.2892 | 3.315 | 1.36 | 0.1261(2) | 0.4203 | -1.6±0.2 |
| Repl . | WR | 3.00 | 0.2479 | 3.390 | 1.39 | 0.1252(5) | 0.3522 | +0.5±0.5 |
| Alx-5H | WR | 3.01 | 0.2256 | 1.055 | 0.43 | 0.15601 | 1.034 | -0.7±0.3 |
| Cm-A5c | CMT. | 0.074 | 0.9355 | 13.39 | 5.48 | 0.12135 | 0.336(20) | -2.4±1.0 |
| Repl. | CMT. | 0.107 | 0.8502 | 11.58 | 4.74 | 0.12640 | 0.354(15) | +1.5±0.8 |
| Cm-A5b | CMT. | 0.408 | 0.6312 | 9.048 | 3.70 | 0.1254(2) | 0.336(12) | +1.4±0.8 |
| Alx-5W[5] | WR | 2.00 | 0.7275 | 0.451 | 0.18 | 0.4992(2)* | 8.148(32) | +7.1±2.8 |
| Repl. | WR | 3.01 | 0.7510 | 0.405 | 0.16 | 0.5550(6) | 9.442 | +2.4±1.8 |
| Alx-6 | WR | 2.00 | 0.3508 | 0.704 | 0.28 | 0.2232(4) | 2.433 | +0.6±0.7 |
| Repl. | WR | 3.01 | 0.3478 | 0.727 | 0.29 | 0.21865 | 2.332 | +0.8±0.5 |
| Alx-26 | WR | 3.01 | 0.4143 | 1.877 | 0.77 | 0.1615(5)* | 1.068 | +2.9±0.6 |
| Alx-26c | CMT. | 0.122 | 0.5204 | 27.42 | 11.2 | 0.1131(3)* | 0.0913(56) | +0.6±0.6 |

[1]All Os analyses (except where marked with asterisks) were accomplished using a Faraday cup, whereas Re analyses were performed with an electron multiplier.

[2]WR = whole rock; CMT. = chromite.

[3]Calculated values at the Re-Os regression age of 2.76 Ga. The chondritic $^{187}Os/^{188}Os$ at 2.76 Ga is calculated to be 0.10810, based on average $^{187}Re/^{188}Os$ ratio of chondrites and initial $^{187}Os/^{188}Os$ (T = 4.558 Ga) for early Solar System materials (IIIA irons) of 0.40186 and 0.09531, respectively (Shirey and Walker, 1998). λ =1.666 x $10^{-11}yr^{-1}$ (Smoliar et al., 1996).

[4]Repl. = replicate analyses of different aliquots from separate powder splits.

[5]Komatiitic basalt; the rest of the whole-rock samples are high-MgO komatiites.

and Walker, 1989). The analytical blanks for Re and Os were $7.6 \pm 1.7$ pg and $2.5 \pm 1.0$ pg (n = 4), respectively, and are negligible compared to their concentrations in most samples. The blank contribution, however, was substantial (>6%) for some of the Re analyses of chromites. The isotopic compositions of the blanks were natural for Re and had $^{187}Os/^{188}Os$ of $0.3130 \pm 0367$ (n = 4). All data were corrected for blanks and the isotopic and concentration data in Table 2.2 reflect the corrected values. The uncertainties in blanks are reflected in respective uncertainties for isotopic and concentration data in Table 2.2. The external reproducibilities for Os analyses, as determined from multiple analyses of comparable amounts of standard, were better than $\pm0.2\%$ on the electron multiplier and $\pm0.1\%$ on the Faraday cup. The Re analyses of all samples were performed with an electron multiplier and the reproducibilities of standard analyses were typically better than $\pm0.2\%$.

The isotopic compositions of Re and Os were obtained using negative thermal ionization mass spectrometry (Creaser et al., 1991; Völkening et al., 1991). The mass spectrometric procedures followed in this study have been discussed in Walker et al. (1994) and Morgan et al. (1995). Samples with high Os abundances were analyzed with Faraday cups under static mode (using a Sector 54 mass spectrometer), whereas those with relatively low abundances of Os and/or Re were analyzed with electron multiplier using a 12" NBS mass spectrometer.

## 2. 3. RESULTS

Detailed discussions of the geochemical characteristics of the Alexo flows may be found in Arndt (1986), Lahaye et al. (1995) and Lahaye and Arndt (1996). In brief, the komatiites are highly magnesian (MgO up to 40.2 wt%, Table 2.1) and

typically have $CaO/Al_2O_3 \leq 1$ (with the exception of a komatiitic basalt, Alx-5W). The rocks show uniform $Al_2O_3/TiO_2$, $TiO_2/P_2O_5$ (and also Sr/Y and Zr/Y ratios, not reported here) ratios, suggesting apparently unaltered whole-rock compositions. All of the whole rocks have chondritic $Al_2O_3/TiO_2$ ratios of 19 to 23, similar to Al-undepleted komatiites from Tisdale Township (Fan and Kerrich, 1997) and Munro Township (Arndt, 1977; 1986), also of the Abitibi belt.

The Re and Os concentrations and isotopic data are given in Table 2.2. Whole-rock Re and Os concentrations vary between 0.239 to 0.751 ppb and 0.405 to 3.390 ppb, respectively. The highest concentration of Re and the lowest concentration of Os are found in the komatiitic basalt (Alx-5W). The concentrations of Os in the chromite separates, on the other hand, are much higher (9 to 27 ppb) with typically low $^{187}Re/^{188}Os$ ratios (0.09 to 0.35).

Based on a comparative study of different komatiite terrains, Nisbet et al. (1993) concluded that random spinifex komatiites most closely represent parental liquid compositions. If true for the Alexo flows, then parental magmas (represented by Alx-2 random spinifex) had ca. 30 wt% MgO (Mg# 0.84) and Os and Re concentrations of approximately 1.9 and 0.4 ppb, respectively. The major and trace element characteristics of our sample Alx-2 are in good agreement with the assumed Alexo parental liquid composition, represented by sample M666 obtained from a larger dataset of Arndt (1986). Major element characteristics (Table 2.1), consistent with 30 wt% MgO, including 6 wt% $Al_2O_3$, 45 wt% $SiO_2$ and a $CaO/(CaO+Al_2O_3)$ ratio of 0.41-0.47 for Alexo komatiites, all correspond to about 50% partial melting at a pressure of ~5 GPa or ~160 km (Herzberg, 1992).

The Re-Os data for whole-rock komatiite samples, excluding the two data points for komatiitic basalt Alx-5W, and chromite separates were regressed via a least squares fitting routine (Ludwig, 1998; Fig. 2.1). The model 3 age of 2762 ± 76 Ma is in general agreement with the more precise U-Pb zircon ages of 2725 ± 2 Ma and 2702 ± 2 Ma for the underlying and overlying felsic units, respectively (Nunes and Pyke, 1980; Corfu, 1993). Also, our Re-Os regression age is within uncertainties of Sm-Nd isochron age of 2752 ± 87 Ma and the Pb-Pb isochron age of 2690 ± 15 Ma for these flows (Dupre et al., 1984). However, the MSWD value for our regression is high (112). The possible causes of the high MSWD value are discussed below. The initial $^{187}Os/^{188}Os$ obtained from the regression (0.1080 ± 0.0012) is essentially chondritic ($\gamma_{Os}$ = -0.1 ± 1.0). The two data points for komatiitic basalt, Alx-5W, when included in the regression calculation, result in a relatively more precise, yet significantly older age of 2790 ± 23 Ma with similarly high MSWD value (103). The initial $^{187}Os/^{188}Os$ ratios of the regressions in both cases, however, are identical and chondritic ($\gamma_{Os}$= -0.1 ± 1.0). Note that the duplicate analyses for this sample do not overlap within the analytical uncertainties ($\gamma_{Os}$ = +3.4 ± 2.8 versus –2.0 ± 1.8) suggestive of modest, post-magmatic open-system behavior.

## 2. 4. DISCUSSION

### 2. 4.1. Distribution and magmatic behavior of Re and Os

The importance of isolating secondary processes and demonstrating magmatic behavior of both Re and Os in the study of Os isotopic compositions of ancient komatiite source mantles cannot be over-emphasized. Precambrian komatiites, in general, have undergone different combinations of secondary processes: [i] surficial
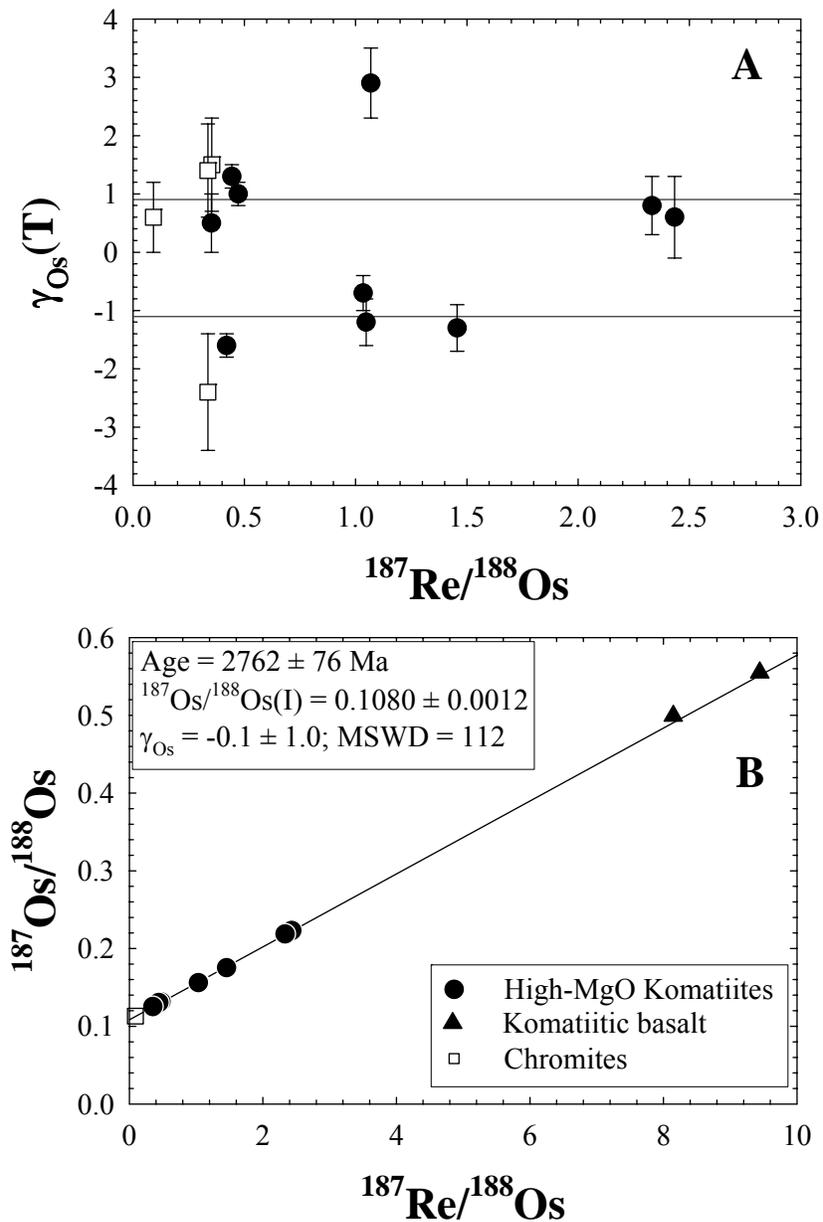
**Fig. 2.1.** Re-Os isotope diagram for whole rock komatiites and chromite separates from Alexo flows: [A] The uncertainties in calculated $\gamma_{Os}$ values of the samples and their replicates, plotted against $^{187}Re/^{188}Os$. The two solid horizontal lines mark the upper and lower limits of calculated $\gamma_{Os}$ values at 2.76 Ga, based on uncertainty in the initial $^{187}Os/^{188}Os$ obtained from the Re-Os regression, as shown in the lower diagram [B].

weathering; [ii] post-crystallization hydrothermal alteration; [iii] low- to medium-grade metamorphism [iv] seawater interaction; [v] assimilation of crustal component (± fractional crystallization); and [vi] contamination by lithospheric mantle. The degrees of these secondary processes vary from one suite to another. In this section, we consider distributions of Re and Os in Alexo komatiites, and compare them with those in komatiites from other greenstone belts in order to evaluate whether or not the distribution patterns were generated via a magmatic origin.

The whole rocks show a primary control of olivine over the abundance of Ni, defined by a straight line, when regressed on a plot of MgO versus Ni (Fig. 2.2). This apparent olivine control line is, however, parallel but shifted towards lower values of Ni relative to that obtained by Arndt (1986). This shift is likely a result of two points on our plot with significantly lower values of Ni concentrations relative to other whole rocks at similar levels of MgO. Although there is a significant scatter about the apparent olivine control line, it projects back to the approximate field of olivine compositions obtained for Alexo flows (Arndt, 1986). Similarly, the field for MgO contents and Cr concentrations of these olivines are also plotted (Fig. 2.2). It is not clear, however, whether Cr concentrations are primarily controlled by late-fractionating Cr-spinels, as there is one sample (Alx-5H) with significantly higher Cr at similar MgO (~40 wt.%, Fig. 2.2). The dashed arrow, on the other hand, shows the effect of olivine accumulation. The apparent straight line (dashed arrow) joining the Alexo parental magma composition and Cr concentrations of olivine in Alexo flows similarly extends back to the approximate MgO–Cr field of olivine in Alexo komatiites (Arndt, 1986). It is likely, therefore, that olivine accumulation in the

34
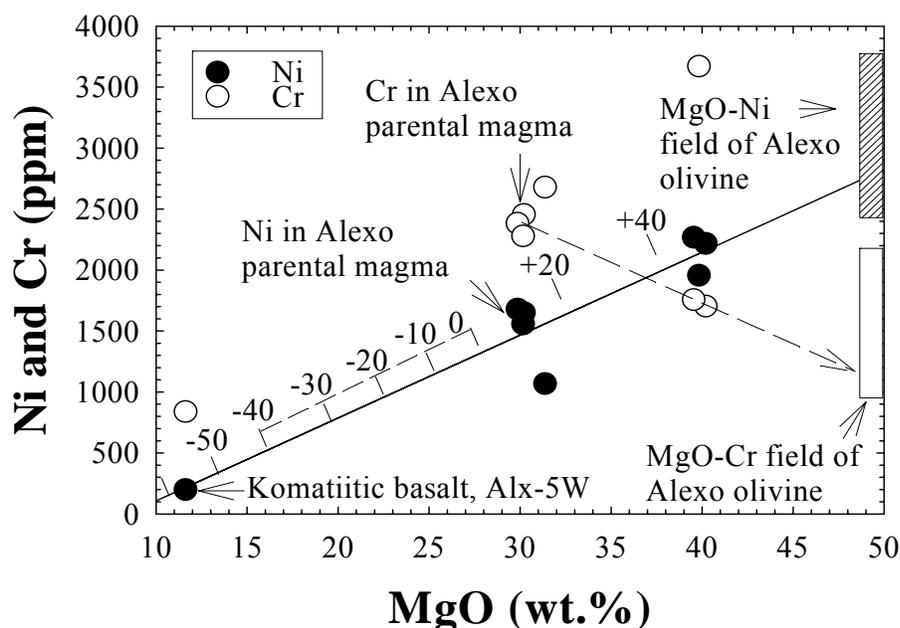
**Fig. 2.2.** A positive correlation between MgO and abundances of Ni in Alexo whole rocks, shown by the solid line, suggests that Ni concentration is primarily controlled by olivine fractionation – accumulation. The shaded rectangular box is the approximate field of olivine in Alexo lavas (Arndt, 1986). Note that the apparent olivine control line projects back to this olivine field. The line with short dashes is the apparent olivine control line in Arndt (1986) and the negative numbers (e.g. −10, -20 etc.) indicate the percentages of olivine fractionation in the Alexo komatiites, and are extrapolated beyond 40%. Similarly, the positive numbers (e.g. +20) are percentages of olivine accumulations (Arndt, 1986). The dashed arrow shows the effect of olivine accumulation, based on the approximate range of MgO and Cr (empty box) in olivine in Alexo flows (Arndt, 1986). Also note that Alx-5H is the only cpx-spinifex komatiite and has the highest concentrations of Cr, consistent with high $D_{Cr}^{cpx/melt}$.

samples with ~40 wt.% MgO was accompanied by an increase in Ni concentrations and a corresponding decrease in Cr concentrations. This interpretation is consistent with olivine being the only major fractionating phase in Alexo flows (Arndt, 1986). Such an apparent olivine control, therefore, suggests a relatively well-preserved nature at the whole–rock scale of our suite of samples. Also plotted on Fig. 2.2 are the calculated proportions of olivine fractionation (Arndt, 1986). The basaltic komatiite (Alx-5W) is likely to have undergone more than 50% of olivine fractionation, whereas the rocks with ~40 wt.% MgO have accumulated approximately 40% olivine. Our suite of Alexo samples, therefore is representative of a large differentiation sequence.

There is a positive correlation between concentrations of Os and Ni for the whole rocks (Fig. 2.3). Nickel is partitioned into olivine during magmatic differentiation and, hence, its covariance with Os suggests that a significant fraction of Os resides either in olivine or in a coprecipitating minor or trace phase. Based on microprobe data of core and rim compositions of olivine in the assumed Alexo parental liquid (sample M666), Arndt (1986) estimated $D_{Ni}^{\text{olivine/liquid}}$ at $2.0 \pm 0.1$. Using this value for $D_{Ni}^{\text{olivine/liquid}}$, gives a calculated $D_{Os}^{\text{olivine/liquid}}$ of $1.7 \pm 0.1$. This $D_{Os}^{\text{olivine/liquid}}$ value is consistent with the one obtained in a previous study of the same komatiites ($D_{Os}^{\text{olivine/melt}}$ ~1.8; Brügmann et al., 1987). This suggests that Os was moderately compatible in olivine during magmatic differentiation of Alexo komaiites. Alternatively, the Os may be highly compatible in sulfide inclusions trapped in olivine, as suggested by Lahaye et al. (2001). The calculated $D_{Re}^{\text{olivine/liquid}}$ (0.6), in
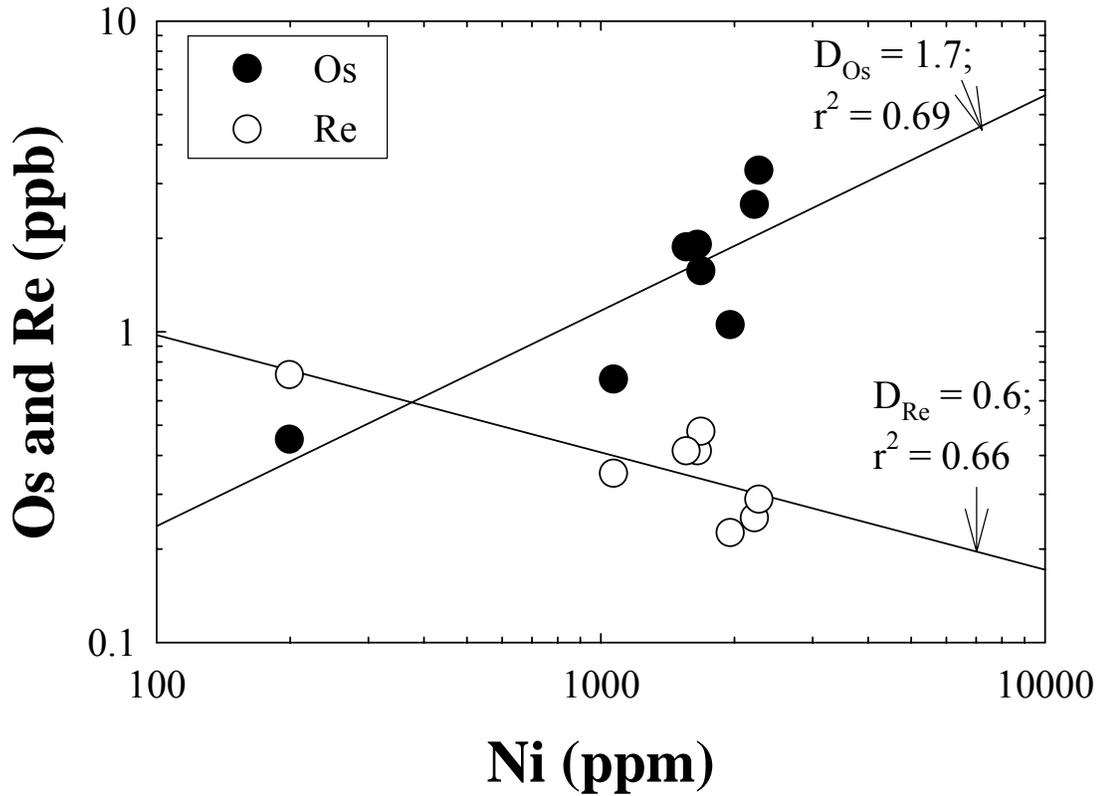
**Fig. 2.3.** The concentrations of Os and Re in Alexo whole rocks are plotted against Ni. The two solid lines are the best-fit linear regressions through the Os and Re concentration data against Ni. The D values for Os and Re, as shown on the plot, are calculated from the slopes of these lines.

contrast, indicates that Re was moderately incompatible during crystal-liquid fractionation.

The concentrations of both Re and Os are considerably higher in the chromite separates relative to their host komatiites (Table 2.2). The concentrations, however, vary significantly even within different aliquots of the chromite splits from the same host rock. In addition, the Re and Os abundances in the present set of samples are not primarily controlled by Cr concentrations (Fig. 2.4). This observation is consistent with a lack of correlation between Os and Cr concentrations in Munro Township komatiites (Walker et al., 1988). Therefore, an uneven distribution of Os in chromites, combined with an inverse relation between the concentrations of Os and Cr in the whole rocks suggests that Os is more likely hosted in sulfide inclusions within Cr-spinels, rather than spinel lattices, as a positive correlation would be likely in the latter case.

For some komatiite suites (e.g., Walker and Nisbet, 2002), Re shows variable degrees of mobilization during weathering, hydrothermal alteration or low-grade metamorphism. For the Alexo rocks, however, a positive linear correlation between Re concentration and alumina content in the whole-rocks is consistent with a constant distribution coefficient during magmatic differentiation (Fig. 2.5). Alumina is normally immobile during alteration and its concentration increases as a function of higher degrees of magmatic differentiation. The positive linear correlation obtained for our Alexo samples, therefore, suggests that Re experienced very limited mobility at the whole-rock scale during post-crystallization alteration. The magmatic behavior
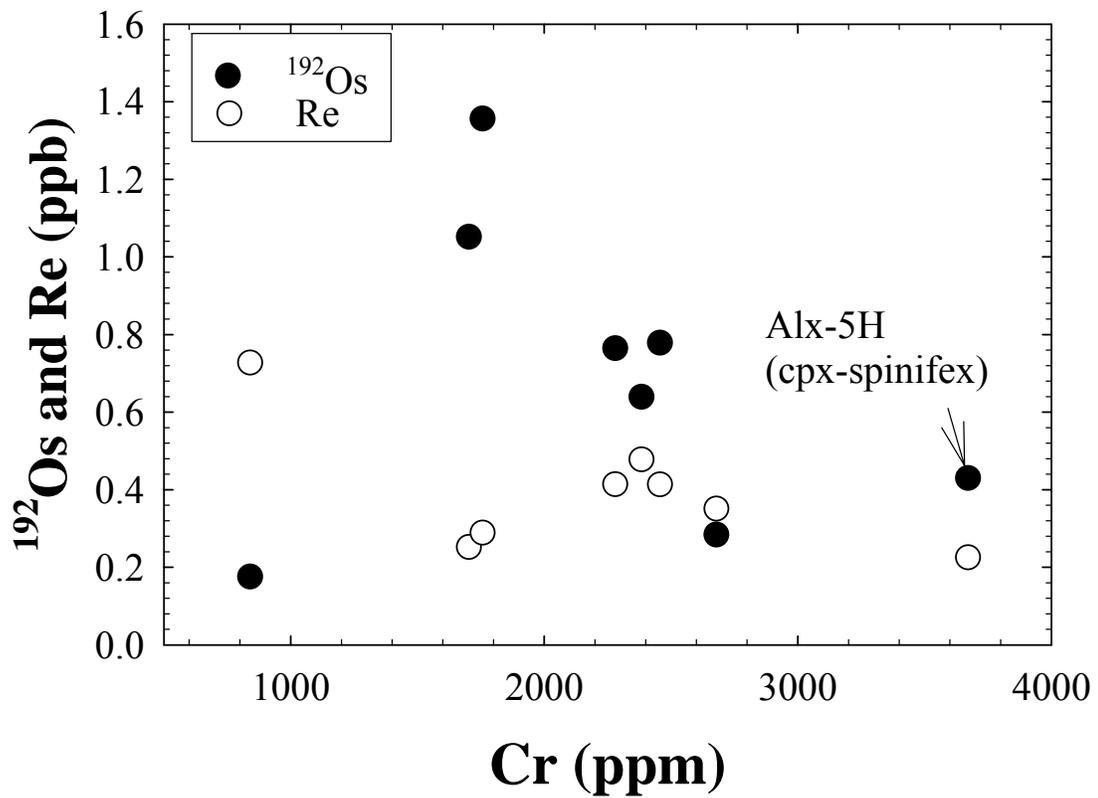
**Fig. 2.4.** Concentrations of Cr and $^{192}$Os show an inverse relation, suggesting that the chromites are not the primary hosts of Os in these rocks. Note that Alx-5H has the highest Cr concentrations and yet its Os concentrations fall towards the low end of the array. Rhenium concentrations slightly decrease with increasing Cr contents.
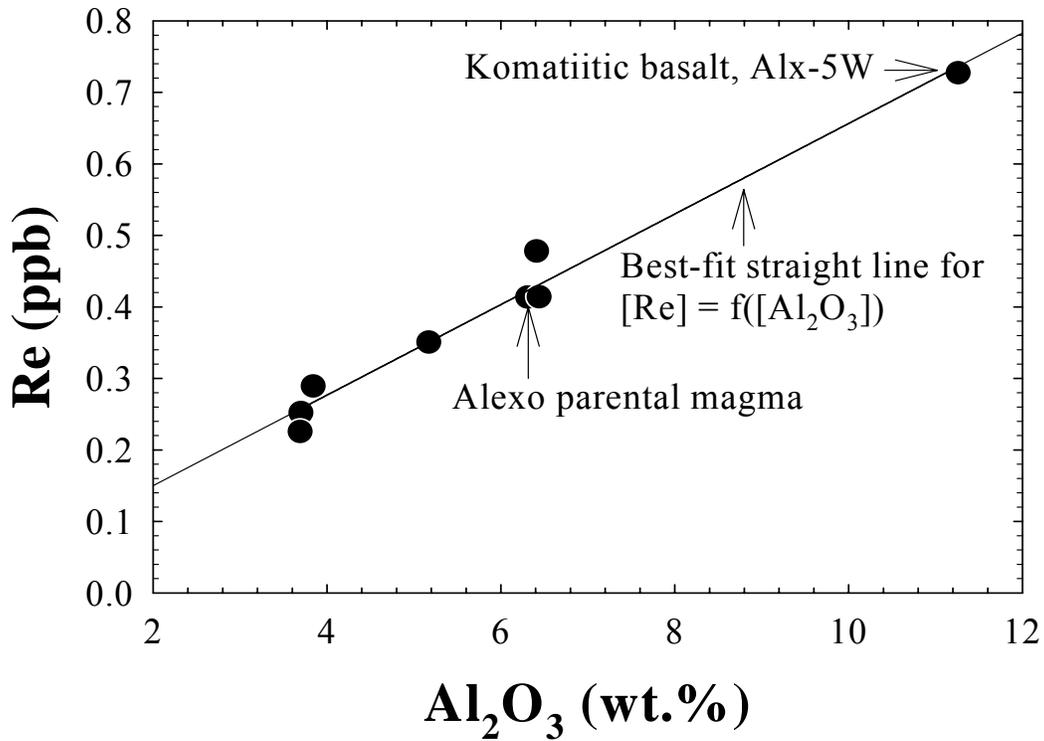
**Fig. 2.5.** Plot of Re concentrations (ppb) and $Al_2O_3$ contents (wt.%) in these whole-rock Alexo komatiites. A positive correlation between Re and $Al_2O_3$ in these komatiites is consistent with their similar incompatibilities in magmatic liquids. Rhenium is susceptible to weathering and alteration whereas, Al is relatively immobile. This plot, therefore, suggests an absence of significant mobility of Re in the Alexo samples.

of both Re and Os in these rocks is, therefore, consistent with several elemental covariation diagrams (Figs. 2.2 – 2.5). It is important to note that the komatiitic basalt (Alx-5W) is highly differentiated yet shows magmatic characteristics cogenetic with other samples in the present suite (e.g., Fig. 2.5). It is likely, therefore, that the komatiites and the highly differentiated komatiitic basalt were derived from the same batch of magma.

The concentrations of MgO and Os in Alexo komatiites, along with those for other komatiite whole rock data have been plotted in Fig. 2.6. The relatively higher concentrations of MgO in three Alexo komatiites are due to high modal abundances of cumulate olivine in those samples. Concentrations of Os in Alexo komatiites are, however, similar to those in other komatiites. In general, there is a positive correlation between the concentrations of Os and MgO (between approximately 25 and 10 wt.%). Similarly, Os concentrations and Re/Os ratios in Alexo komatiites fall within the ranges observed in other komatiites (Fig. 2.7). The mantle source of the Alexo komatiites was, therefore, typical in terms of the above geochemical parameters and comparable with other komatiites.

The bulk distribution coefficients for Re and Os between the komatiite melt and the mantle residue have been calculated based on the assumptions that: [1] Alx-2 random spinifex komatiite (with Os and Re concentrations of 1.9 and 0.4 ppb, respectively) is representative of the Alexo parental magma, and [2] the komatiites were generated by 50% equilibrium batch melting from a fertile mantle source with Re and Os concentrations of 0.3 and 3 ppb, respectively (Morgan et al., 1986). Our estimate of 1.9 ppb for the Os concentrations of Alexo parental magma is in good
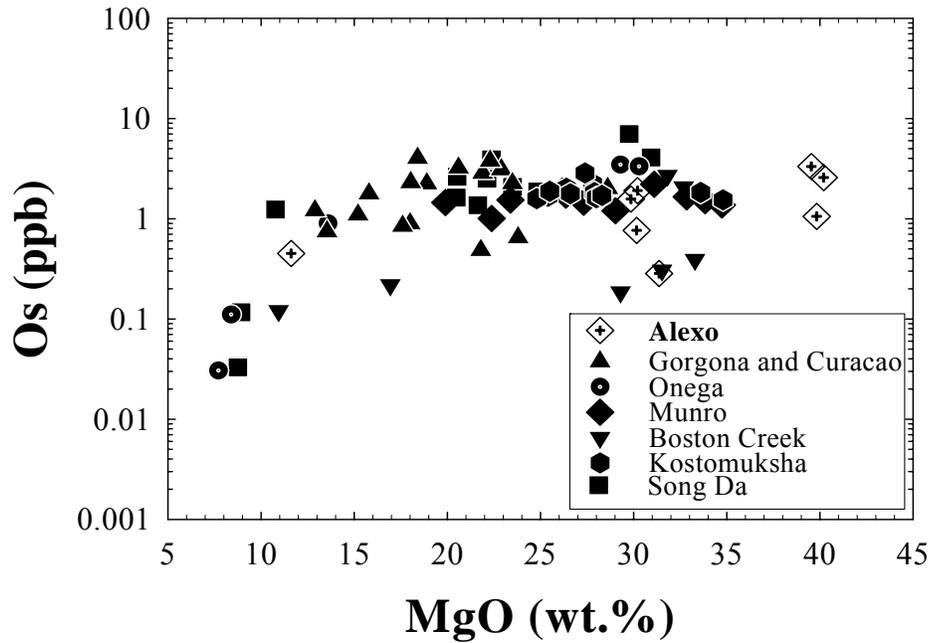
**Fig. 2.6.** The MgO contents (wt%) and Os concentrations in whole rock Alexo komatiites are compared with those from other selected plume-related ultramafic lavas. The three samples of Alexo rocks in our study with ~40 wt% MgO have high modal abundance of cumulate olivine. Data sources: komatiites from Song Da, Vietnam (Hanski et al., 2002); komatiitic and picritic flows from Gorgona island and Curacao, Colombia (Walker et al., 1999); mafic-ultramafic sill from Onega, Russia (Puchtel et al., 1999); Munro komatiites from Abitibi, Canada (Walker et al., 1988); Boston Creek komatiites, Canada (Walker and Stone, 2001); Kostomuksha komatiites, Russia (Puchtel et al., 2001).
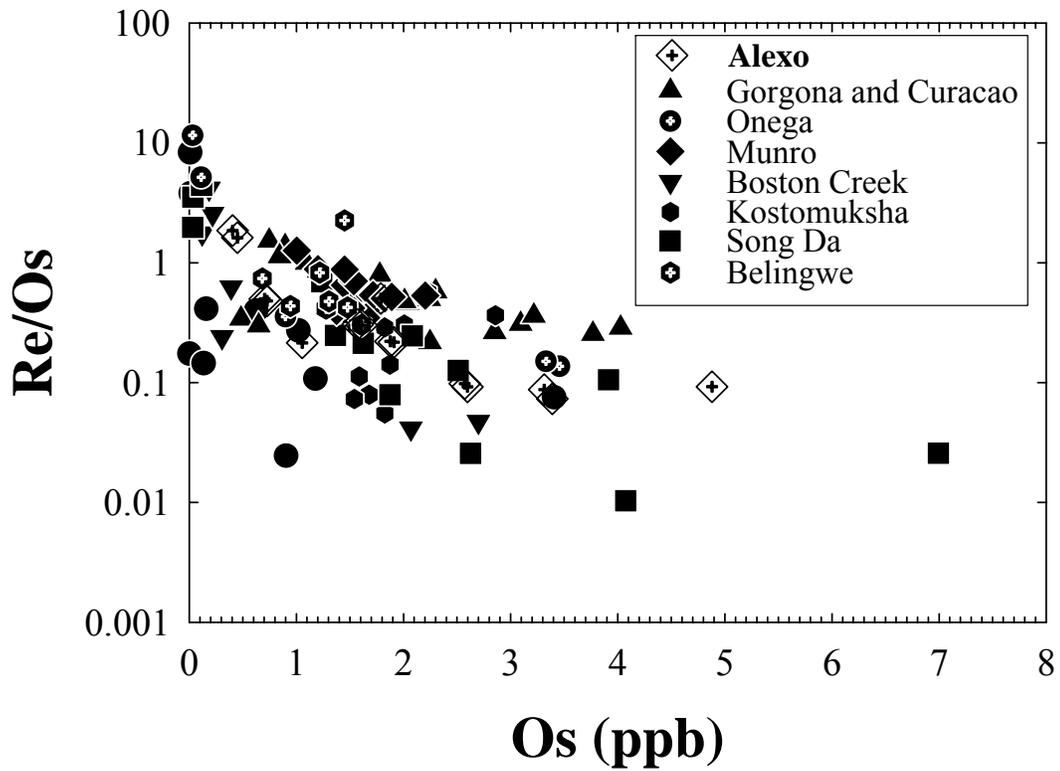
**Fig. 2.7.** Plot of Re/Os versus Os. The range of Re/Os relative to Os in the Alexo komatiite suite is within the ranges observed in other komatiites. Data sources as in Fig. 6 with additional data from Belingwe komatiites, Zimbabwe (Walker and Nisbet, 2002).

agreement with that independently estimated from the KAL-1 standard ($1.8 \pm 0.1$ ppb; Puchtel and Humayun, 2000). The assumed extent of melting is in agreement with separate estimates based on experimental results (Herzberg, 1992) and geochemical considerations (~45% of Arndt, 1986). The calculated D values for Re and Os are 0.2 and 2.1, respectively. The D value of 2.1 for Os is consistent with that obtained by Walker et al. (1988) for Munro Township komatiites ($D_{Os}$ of 1.9 assuming 26% melting). Similarly, the Gorgona komatiites were interpreted to yield a D value of 1.5 with somewhat lower degrees of melting (20%; Walker et al., 1999). Our D values, therefore, suggest that Os was moderately compatible, whereas Re was incompatible in the mantle residue during the generation of Alexo komatiite magma.

### 2.4.2. Preservation of Re-Os isotope system of Alexo komatiites

The present study has important implications for the degree of preservation of Re-Os isotope system at the scale of whole rocks and minerals in komatiite lavas. The high MSWD value (112) obtained for our regression indicates significant scatter outside of estimated analytical uncertainties. Possible causes that might have contributed to the excess scatter about the regression are: (a) differences in the ages of the samples; (b) variation in initial $^{187}Os/^{188}Os$ ratios; (c) the assigned analytical uncertainties have underestimated the actual uncertainties in the corrected isotopic ratios; and (d) limited open-system behavior of Re and/or Os in these rocks.

Although the samples include multiple flows within a small area, the data are consistent with magmatic behavior of both Re and Os in the samples, which, in turn, is indicative of a cogenetic suite. In addition, no large differences in the ages of ultramafic rocks from the Abitibi Greenstone Belt, in general, and Alexo, in

particular, have, so far, been recorded. As mentioned earlier, the age of Alexo flows is precisely known from U-Pb zircon dating of overlying and underlying units, and includes a restricted range between 2700 and 2727 Ma (Nunes and Pyke, 1980). Moreover, new high-resolution U-Pb zircon ages along with compilation of previous geochronological data strongly suggests that the southern Abitibi greenstone belt represents an autochthonous stratigraphy with the dominantly volcanic assemblages ranging in age from 2697-2750 Ma (Ayer et al., 2002). It is, unlikely, therefore, that differences in ages of the rocks have contributed to the high MSWD value.

The actual variations in initial $^{187}Os/^{188}Os$ ratios of the samples are likewise unlikely, but cannot categorically be ruled out. Komatiites, in general, are believed to be generated through high degrees of partial melting from their mantle sources. As a result, it is likely that the high degrees of melting (~50%) that generated the Alexo parental magma would have removed small-scale differences, if any, in initial $^{187}Os/^{188}Os$ ratios of the source. Significant variations in the initial $^{187}Os/^{188}Os$ within a single suite of the Mesozoic Gorgona komatiites, however, were reported by Walker et al. (1999).

The whole rocks as well as the chromites have very high concentrations of Os (Table 2.2) and had minor blank contributions in the total Os analyzed for these samples. Also, most of the Os analyses were performed with Faraday cups with high precision (typically 0.05% 2σ) under static analytical mode. The total analytical blanks for both Re and Os, and also the external reproducibility on Re and Os standards, are well within the ranges we have obtained in our laboratory over the

years. It is unlikely, therefore, that any significant analytical uncertainties have remained unaccounted for in our regression calculation.

The high MSWD value may most likely be a result of minor open-system behavior in the Re-Os isotope systematics in our samples. This is because the Abitibi rocks, in general, are significantly altered and metamorphosed dominantly to greenschist facies that locally reach up to amphibolite facies (Jolly, 1982). The Alexo flows, however, had undergone prehnite-pumpellyite grade of metamorphism (Lahaye et al., 2001 and references therein). The signature of alteration is documented in Lahaye and Arndt (1996) and also in our petrographic study of these rocks. For example, most of our samples have undergone secondary replacement of olivine by serpentine, oxidation of olivine to magnetite and devitrification of glass. There is, however, no apparent correlation between isotopic characteristics of our whole rocks and their degrees of alteration, as suggested by studied petrographic characteristics. Nevertheless, as noted earlier, duplicate analyses of the basaltic komatiite sample (Alx-5W), yield $\gamma_{Os}$ values that are outside of the analytical uncertainties of each other (+7.1 ± 2.8 versus +2.4 ± 1.8; Table 2.2). The scatter may, therefore, be due to limited open-system behavior as a result of low-grade metamorphism and/or hydrothermal alteration. Note, however, that the elimination of the two points slightly increases the MSWD value of the regressions (103 to 112). Nonetheless, there is evidence for minor open-system behavior in Pb-Pb system of these rocks. For example, using the ISOPLOT program (Lugwig, 1998), we have recalculated the $^{207}$Pb-$^{206}$Pb isochron regression of Alexo komatiites, based on the data in Table 2.1 of Dupre et al. (1984). The age we have obtained from the model 2

regression is similar but has slightly larger uncertainty (2692 ± 34 Ma) relative to that of Dupre et al. (1984) (2690 ± 15 Ma). The MSWD value of the isochron, although unspecified in Dupre et al. (1984), is also high (77). As noted by Dupre et al. (1984), the spread in U/Pb, however, was most likely caused by post-magmatic hydrothermal alteration. Therefore, it is possible that the same hydrothermal alteration event has contributed to the minor open-system behavior of the Re-Os isotope system of our samples. Also, similar excess scatters about Re-Os regressions have been documented in previous studies of ancient komatiites. For example, Puchtel et al. (1999) have reported an MSWD value of 108 for their Re-Os regression for Onega plume-related lavas even with relatively larger degrees of analytical uncertainties (± 0.5% for both $^{187}Os/^{188}Os$ and $^{187}Re/^{188}Os$ ratios).

The apparent magmatic behaviors of both Re and Os, and preservation of a reliable isochron for the Alexo rocks suggest that the Re-Os isotope system offers a relatively robust tracer of mantle processes related to this ultramafic magmatic system. This is in contrast to the Rb-Sr system, which is usually compromised due to post-crsytallization secondary processes (e.g., Walker et al., 1988). The apparent resistance of the Re-Os system to the secondary processes, combined with high concentrations of Os in chromites and also moderate compatibility of Os in olivine suggest that these elements were mostly concentrated in trapped inclusions within olivines, chromites and possibly other trace phases, and were relatively immobile during mineral replacements at the whole rock scale.

**2.4.3. Implications of a chondritic initial Os isotopic composition for the Alexo mantle source**

It is now widely believed that the ultimate source of Re and Os in modern and ancient mantle derived rocks was a 'late veneer' of chondritic material added to the mantle following their presumed nearly quantitative removal during core formation (e.g. Kimura et al., 1974; Chou, 1978; Morgan, 1985; Morgan et al., 2001). If true for the Alexo mantle source, the chondritic initial $^{187}Os/^{188}Os$ for these rocks implies that sufficient late accretion and subsequent homogenization of the mantle source of these rocks must have occurred prior to the time of their crystallization at 2.7 Ga and since had not undergone any long-term fractionation of Re/Os or $^{187}Os$ enrichment. Such a chondritic Os isotopic evolution of the mantle source for Alexo komatiites is consistent with chondritic Os isotopic compositions of even older mantle-derived systems, such as 3.8 Ga spinel peidotite from West Greenland and ~3.5 Ga komatiites from the Pilbara region of Western Australia (Bennett et al., 2002). The essentially chondritic initial $^{187}Os/^{188}Os$ for Alexo is also consistent with that previously reported from spatially associated Munro Township komatiites (Walker et al., 1988; Shirey, 1997). Combined, these results may suggest an absence of any large-scale Os isotopic heterogeneity in the southern volcanic zone of the Abitibi greenstone belt. Similar chondritic initial $^{187}Os/^{188}Os$ ratios have also been reported for komatiites from ~2.7 Ga Norseman-Wiluna Belt (Foster et al., 1996) and ~2.8 Ga Ruth Well komatiites in Australia (Miesel et al., 2001a), and komatiitic basalts from ~2.5 Ga Vetreny belt in the Baltic shield (Puchtel et al., 2001b). Collectively, these results indicate the presence of a chondritic mantle source in several areas worldwide at the end of the

Archean. Also, the chondritic initial $^{187}Os/^{188}Os$ for Alexo komatiites is consistent with the generally chondritic evolution of Proterozoic and Phanerozoic upper mantle (e.g., Snow and Reisberg, 1995; Brandon et al., 2000; Walker et al., 1996; 2002).

The chondritic initial Os isotopic composition for Alexo komatiites ($\gamma_{Os}$ = -0.1 ± 1.0), within uncertainties, overlaps with the Os isotopic evolution trajectories for both hypothetical primitive upper mantle (PUM: Meisel et al., 2001b) and convective upper mantle (Snow and Reisberg, 1995; Brandon et al., 2000; Walker et al., 2002), projected back at the eruption age of these lavas at ~2.7 Ga. In other words, the source of Alexo komatites, based on our Os isotopic results, is indistinguishable from the contemporaneous convective upper mantle. The Nd-isotopic compositions of Alexo flows, on the other hand, unequivocally record a long-term depletion in LREE ($\varepsilon_{Nd}$ = +2.4 ± 0.5; Dupre et al., 1984). Also note that this initial Nd isotopic composition, within uncertainties, overlaps with the depleted mantle trajectories of DePaolo (1981) and Goldstein et al. (1984) at 2.7 Ga. The initial Nd isotopic composition of these komatiites is, therefore, consistent with their derivation from a mantle reservoir with a long-term depletion in LREE. A LREE-depleted, relatively shallow mantle source for Al-undepleted komatiites, such as those from Alexo and Munro Townships, is also consistent with a flat HREE pattern, common absence of HFSE anomaly (e.g. Xie et al., 1993; Kerrich and Xie, 2002) and estimated depth of melting at ~160 Km (Herzberg, 1992), all suggesting the absence of either majorite or pyrope garnet signature.

As suggested by our estimated D values, Os is slightly compatible, whereas Re is moderately incompatible during high degrees of mantle melting. Hence, LREE-

depletion as a result of prior extraction of melt could potentially generate a Re/Os ratio in the residue that would be lower than that in the unmelted source mantle. It is, therefore, interesting to note that the depleted Nd isotopic composition is not accompanied by evidence for long-term depletion in Re/Os. Similar decoupling of Os and Nd isotopes may be found in other Archean komatiites. For example, the komatiites from Munro Township record a depleted d isotopic comsposition ($\epsilon_{Nd}$ = +2 to +3) and yet also have chondritic initial Os isotopic composition (Walker et al., 1988). Also, such an isotopic decoupling is found at a much larger scale of crust-mantle differentiation. The convective upper mantle records progressively higher degrees of depletion in terms of Nd isotopic composition through geologic time (DePaolo, 1981; McCulloch and Bennett, 1994) and yet may have evolved through a broadly chondritic Os isotopic trajectory (Snow and Reisberg, 1995; Brandon et al., 2000; Walker et al., 1996; 2001).

The apparent lack of correlation between the Re-Os and Sm-Nd isotope systematics in these Archean komatiites may indicate any combination of the following possibilities: [a] the degree of prior melting was too low to generate resolvable Re depletion and yet sufficient to reflect on Nd isotopic record; [b] a fortuitous change in the partitioning behavior of Re and Os, possibly as a result of different melting conditions and abundance of other phases (such as sulfide) in the Early Archean mantle that did not allow resolvable fractionation of Re from Os; and [c] sufficient late accretion occurred subsequent to the extraction of melts that caused the depletion in Nd/Sm ratio so that the observed chondritic Os isotopic composition of these mantle sources essentially represents that of the late veneer.

## 2. 5. SUMMARY

[1] Alexo komatiites demonstrate apparent magmatic behavior of Re and Os in the whole rocks. The concentrations of Re and Os in these rocks are comparable with those in both Precambrian and Phanerozoic komatiites from elsewhere. Our calculated bulk distribution coefficients for Os and Re between the Alexo parental magma and the mantle residue are 2.1 and 0.2, respectively. These D values, therefore, suggest that Os was slightly compatible in the mantle residue, whereas Re was moderately incompatible during the melting of Alexo mantle source. Similarly, our calculated partition coefficients for Os and Re between olivine and the fractionating liquid are 1.7 and 0.66, respectively. These $K_d$ values, therefore, suggest that Os was slightly compatible, whereas Re was moderately incompatible during the fractionation of Alexo parental magma. The moderate compatibility of Os in olivine may suggest preferential entrapment of Os in sulfide inclusions within olivine and/or incorporation of Os in olivine crystal structures.

[2] Re-Os regression of these rocks yields an age of 2762 ± 76 Ma. This age is in general agreement with the U-Pb zircon ages of associated felsic units (2710-2717 Ma; Nunes and Pyke, 1980; Corfu, 1993). Our Re-Os regression age is also in agreement with Pb-Pb (2690 ± 15 Ma) and Sm-Nd isochron ages (2752 ± 87 Ma) obtained in a previous study of these lavas (Dupre et al., 1984). The high MSWD value (112) obtained for the Re-Os regression suggests modest degrees of mobility of Re and/or Os during post-crystallization alteration and low-grade metamorphism.

[3] The initial $^{187}Os/^{188}Os$ obtained from our regression (0.1080 ± 0.0012) is essentially chondritic ($\gamma_{Os}$ = -0.1 ± 1.0). The chondritic initial Os isotopic composition

for Alexo rocks is consistent with that obtained for spatially associated komatiites from Munro Township (e.g., $\gamma_{Os}$ = +0.1 ± 1.5 for Pyke Hill komatiites; Shirey, 1997). The initial Nd isotopic composition of Alexo ($\varepsilon_{Nd}$ ~ +3.8; Lahaye et al., 1995) and Munro Township ($\varepsilon_{Nd}$ = +2 to +3; Dupre et al., 1984) komatiites, on the other hand, unequivocally reflect LREE-depleted mantle sources for these rocks. Combined, the chondritic initial Os isotopic composition for the source of Alexo komatiites is indistinguishable from the contemporaneous convective upper mantle.

# CHAPTER 3: Origin of Paleoproterozoic Komatiitic Rocks From Jeesiörova, Kittilä Greenstone Complex, Finnish Lapland

[1. Submitted as: Gangopadhyay, A., Walker, R. J., Hanski, E., and Solheid, P., Origin of Paleoproterozoic komatiitic rocks from Jeesiörova, Kittilä Greenstone Complex, Finnish Lapland, J. Petrol. (in revision).

2. This is my original work. However, Fig. 3.2 was provided to me by Eero Hanski (now at the University of Oulu, Finland). The whole rock major and trace element data used here are taken from Hanski et al. (2001). I prepared sections 3.2, 3.3 and part of 3.4 based on my reading of Hanski et al. (2001) and some details that E. Hanski provided to me. I also prepared section 3.4.2 based on the details of analytical techniques for Mössbauer spectra provided to me by P. Solheild.]

**Abstract**

Komatiites from the Jeesiörova area in the ~2 Ga Kittilä Greenstone Complex in Finnish Lapland have subchondritic $Al_2O_3/TiO_2$ ratios, similar to those in Al-depleted komatiites from the Barberton Mountainland, South Africa. The Jeesiörova komatiites, however, are distinct in that their Al abundances are (a) higher than those at given MgO contents of Al-depleted rocks, yet (b) similar to those in the Al-undepleted komatiites from elsewhere. In addition, the Al and Ti contents of chromites in the Jeesiörova komatiites are distinctly higher than in chromites found in Al-depleted komatiites. Consequently, the Jeesiörova komatiites were likely Al-undepleted, but rich in Ti relative to typical Al-undepleted komatiites. Some similarly incompatible elements, including Eu, Gd, Zr and Hf are also enriched to about the same extent in these rocks. Neither majorite fractionation in the source of the komatiites nor hydrous melting in a supra-subduction zone setting is likely to have produced these komatiites. The high concentrations of Ti and similarly incompatible elements in the Jeesiörova rocks may have resulted from contamination of their parental melt via interaction with Ti-rich metasomatic mineral assemblages in the

lithospheric mantle or enrichment of the source in Ti and similarly incompatible elements by addition of basaltic melt to their mantle source. Preferential incorporation of Ti-rich phases would likely have led to a collateral enrichment of Nb that is not observed in these rocks. The Re-Os isotope results for chromite separates from the Jeesiörova rocks yield an average initial $^{187}Os/^{188}Os$ of $0.1131 \pm 0.0006$ ($2\sigma$; $\gamma_{Os} = 0.1 \pm 0.5$). These results, coupled with an initial $\varepsilon_{Nd}$ of ~+4, indicate that melt parental to the komatiite likely had minimal chemical interaction with ancient lithospheric mantle. If the source of the komatiites was enriched in a basaltic component, the combined Os-Nd isotopic results limit the enrichment process to within approximately 200 Ma prior to the formation of the komatiites. The Os-Nd isotopic composition of these rocks is consistent with their derivation dominantly from the contemporaneous convective upper mantle.

KEY WORDS: Komatiites; Re/Os isotopes; chromites; Ti-enrichment; HFSE; mantle geochemistry

## 3.1. INTRODUCTION

Komatiites have been divided into two broad chemical types, Al-undepleted (with near-chondritic $Al_2O_3/TiO_2$ ratios of ~20) and Al-depleted (subchondritic $Al_2O_3/TiO_2$ ratios of typically ~11: Nesbitt et al., 1979). Komatiites from Alexo and Pyke Hill in the Abitibi greenstone belt, Canada, are typical examples of the Al-undepleted type (also termed "Munro-type"), whereas those from the Komati Formation in the Barberton Mountainland, South Africa, are examples of the Al-depleted type (also known as the "Barberton-type"). The komatiitic rocks from the Jeesiörova area in the Central Lapland Greenstone Belt, northern Finland are distinct

from these two types of komatiites in that they have subchondritic $Al_2O_3/TiO_2$ ratios (typically ~10-13) similar to those in Al-depleted rocks, yet compared with the latter, they have significantly higher aluminum contents at given MgO levels (Fig. 3.1A). Moreover, the aluminum contents in the Jeesiörova rocks are similar to those of Al-undepleted komatiites at given MgO contents. However, they have significantly higher $TiO_2$ contents at specific MgO and $Al_2O_3$ levels than either Al-depleted or Al-undepleted komatiites from elsewhere (Fig. 3.1B). This combination of distinctive bulk chemical characteristics of the Jeesiörova rocks prompted construction of a new classification scheme for komatiites using olivine-projected molecular $Al_2O_3$-$TiO_2$ relations (Hanski et al., 2001). The Jeesiörova rocks, according to this scheme, plot in the distinct field of "Ti-enriched" komatiites. Aluminum-depleted, Al-undepleted and/or Ti-enriched rock types can coexist in a single greenstone belt and, in some cases, within a single volcanic assemblage (e.g., Kidd-Munro assemblage in the Abitibi greenstone belt, Canada: Sproule et al., 2002). It is important to determine, therefore, whether the apparent Ti-enrichment is a feature of the mantle source, and if so, what the implications of Ti enrichments are for the nature of the source and petrogenetic processes involved in their genesis.

Here we compare and contrast the petrologic, geochemical and isotopic characteristics of the Jeesiörova komatiites with the well-studied Munro and Barberton type komatiites in order to assess the origin of the Finnish rocks. We present electron microprobe data for chemical compositions of chromites from the Finnish suite of rocks, and use them in conjunction with the $Fe^{3+}/\Sigma Fe$ ratios of

**Fig. 3.1. (A)** Plot of whole-rock MgO versus $Al_2O_3$ contents (wt.%) of the Jeesiörova komatiitic rocks. For comparison, Al-undepleted and Al-depleted komatiites from Canada and South Africa are also plotted. Data sources: Alexo (Gangopadhyay and Walker, 2003) and Pyke Hill (Fan and Kerrich, 1997, combined with new unpublished data (n = 7) in the Abitibi greenstone belt, Canada; Komati (Lahaye et al., 1995; Parman et al., 2003) and Mendon (Lahaye et al., 2003) in the Barberton Mountain Land, S. Africa. All data are volatile-free values. Note that the $Al_2O_3$ contents in the Jeesiörova rocks are significantly higher than in the Al-depleted Barberton rocks and are similar to those at given MgO contents in the Al-undepleted Abitibi rocks. **(B)** Plot of MgO versus $TiO_2$ contents in the same suites of rocks as in (A). This plot shows that the Jeesiörova rocks appear significantly enriched in $TiO_2$ relative to both Al-undepleted and Al-depleted rocks at a given MgO content.
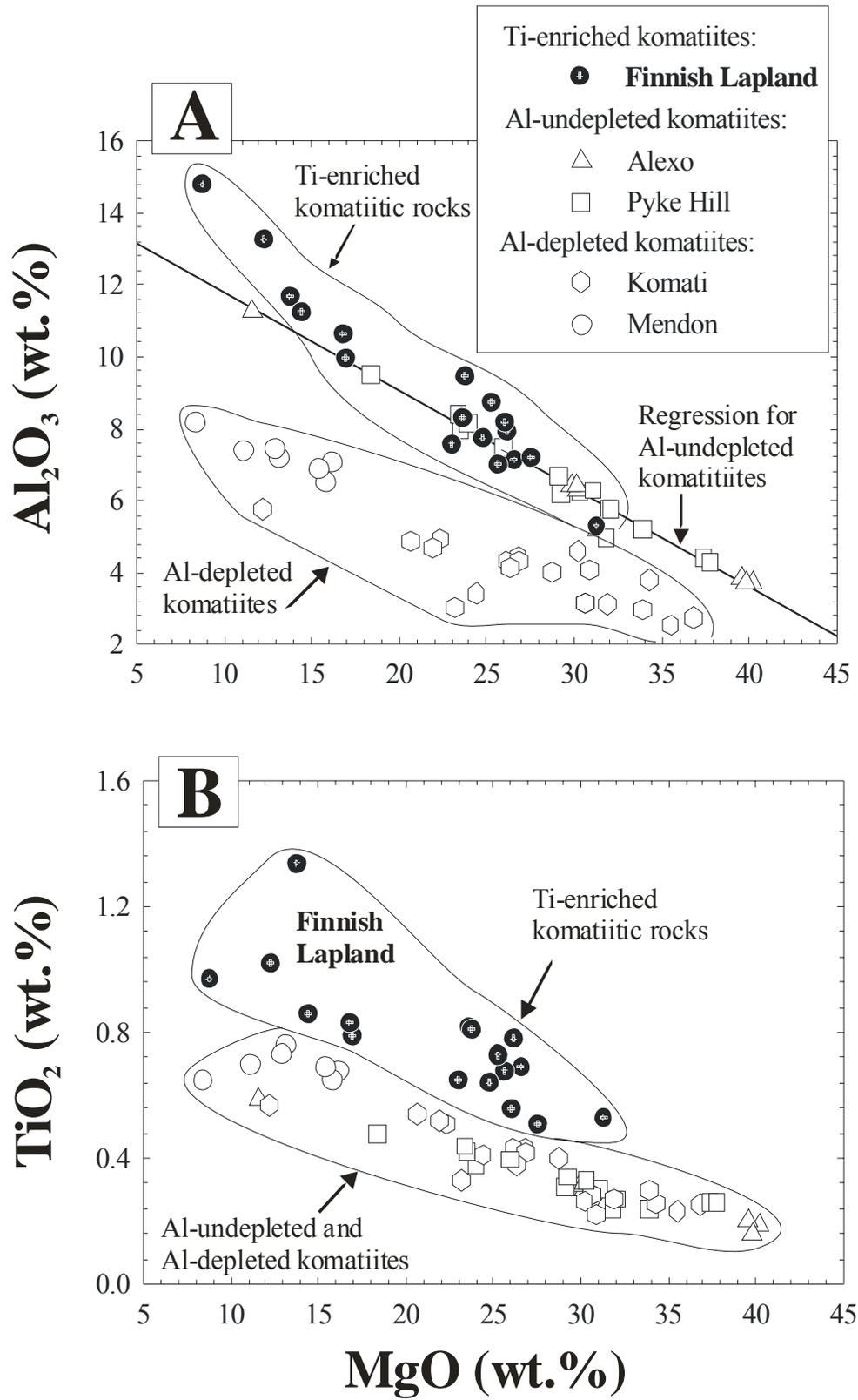
**Fig. 3.1.**

selected chromite separates obtained from Mössbauer spectra in order to constrain the redox state of magmas during the generation of these rocks. Additionally, we present high-precision Re-Os isotope data obtained for chromites in order to determine the initial Os isotopic composition of the mantle source for this chemically distinct type of komatiite. The initial Os isotopic composition, combined with previous determinations of the Nd isotopic composition for the same suite of rocks (Hanski et al., 2001) are used to evaluate the possible roles of contamination by (a) crustal materials, (b) Ti-rich metasomatized lithospheric mineral assemblages  and (c) recycling of oceanic crust in the generation of these rocks. Finally, we use previously published major and trace element data for the same suite of rocks (Hanski et al., 2001) and lay out the pros and cons of several petrogenetic models for the generation of these rocks.

## 3.2. GEOLOGICAL SETTING AND ROCK TYPES

Samples were collected from the Jeesiörova area, located in the southern part of the Kittilä Greenstone Complex, Central Lapland (Fig. 3.2A). Detailed discussions of the stratigraphic subdivisions, major rock types of the Kittilä Greenstone Complex, and their petrologic and geochemical characteristics may be found in Lehtonen et al. (1998) and Hanski et al. (2001). In brief, the Kittilä Greenstone Complex is part of an approximately 400-km-long belt, which runs through Finnish Lapland and extends to the Karasjok greenstone belt in northern Norway (Barnes and Often, 1990). The entire belt contains abundant, highly-magnesian volcanic rocks whose parental magmas varied in chemical composition from LREE-depleted komatiites to LREE-enriched picrites (Hanski et al., 2001). A characteristic feature of the belt is the

58
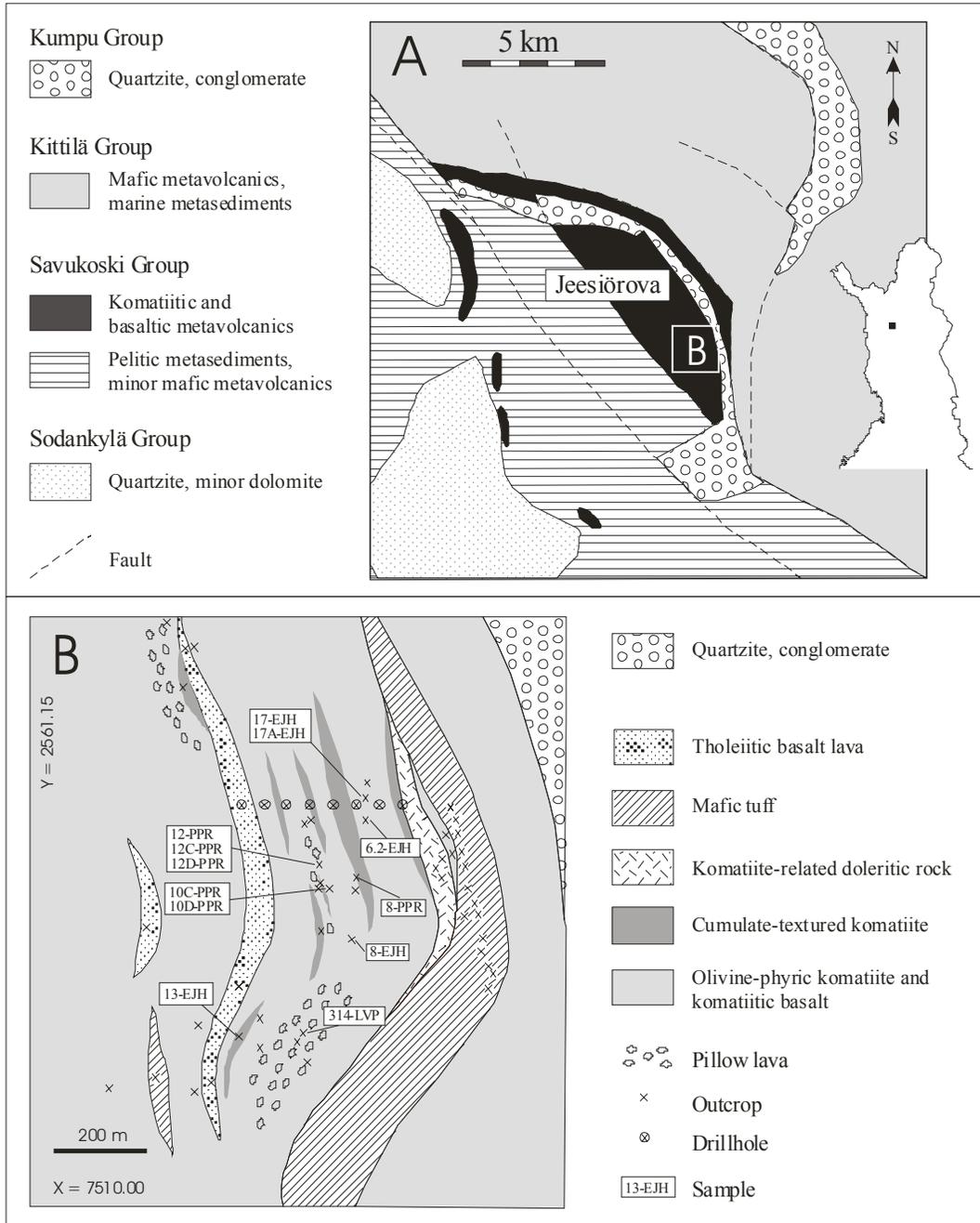
**Fig. 3.2. (A)** Geological map of the Jeesiörova area, central Finnish Lapland; **(B)** Detailed map from the Jeesiörova area showing sampling locations of the present study.

presence of ultramafic volcaniclastic rocks that vary from agglomerate-like deposits to fine-grained, laminated tuffs (Saverikko, 1985; Barnes and Often, 1990).Komatiitic rocks also occur as massive lavas, pillow lavas, and associated pillow breccias.

The Jeesiörova komatiites are found in a zone which is ~15 km long and 4 km wide (Fig. 3.2A). These rocks belong to the Savukoski Group together with the underlying pelitic metasedimentary rocks. A fault zone, called the "Sirkka line", separates the Savukoski Group rocks from younger (~2.0 Ga) basaltic metavolcanic rocks and metasedimentary rocks of the Kittilä Group that crop out on the NE side of the Jeesiörova area. The clastic metasedimentary rocks of the Sodankylä Group are the oldest (2.3 Ga) rocks in the area, whereas the youngest supracrustal rocks are represented by the quartzites and conglomerates of the ~1.88 Ga Kumpu Group, which lie unconformably on the rocks of the Savukoski and Kittilä Groups.

Drill cores through the lower contact of the komatiite-bearing lava succession in the Jeesiörova area show that the volcanic sequence was deposited on a 20-m-thick unit of cherts and carbonate rocks that are underlain by black schists. The volcanism started with 20 m of tholeiitic lavas that were followed by volcaniclastic komatiites (50 m) and finally overlain by massive komatiitic lavas (>100 m). The total thickness of the volcanic rocks is difficult to estimate but may reach several hundreds of meters.

The bedrock in the part of the Jeesiörova area (Fig. 3.2B) is dominated by olivine-phyric komatiitic rocks. Due to limited outcrops, individual lava flows cannot be delineated. There are, however, zones of cumulate-textured komatiites that likely represent lower parts of thick lava flows. Komatiitic rocks also occur as pillow lavas

with the pillow size varying from 0.2 to 1 m. Various mafic rocks are interbedded with ultramafic rocks (Fig. 3.2B). The mafic rocks include LREE-depleted tuffs and dolerites. There are also mafic amygdaloidal lava flows, marked as tholeiites in Fig. 3.2A, which are moderately LREE-enriched and probably not genetically related to the associated komatiites.

## 3.3. SAMPLES

The samples examined in this study are all komatiites collected from outcrops (Fig. 3.2B), and are well-characterized in terms of major and trace elements, and Sm-Nd isotopes (Hanski et al., 2001).

Whole-rock samples were first crushed into mm-sized pieces. The freshest unaltered pieces were ground with a steel pan. Different aliquots of the same whole-rock powder were used in major and trace element, and isotopic analyses of each sample.

The mineral separates (chromite, clinopyroxene, and sulfide) were obtained using standard crushing, milling, concentration table, and heavy liquid techniques. Separation of large quantities of chromites was possible due to their relatively large grain size and well-preserved nature (low magnetic susceptibility). After removing the most magnetic fraction with a hand magnet, the chromite separates were divided into different fractions, depending on the alteration of chromite (presence of magnetite rim) and using different current settings in a Frantz™ magnetic separator. Likewise, for sulfide separates, we obtained a fraction dominated by pentlandite, whereas the other fractions were mixtures containing pyrrhotite, pentlandite, and chalcopyrite.

### 3.4. ANALYTICAL TECHNIQUES

Details of whole-rock chemical analyses of the komatiites have been reported elsewhere (Hanski et al., 2001). In brief, whole-rock XRF data for major and minor element abundances were obtained using a Phillip PW 1480 spectrometer at the Geological Survey of Finland (GSF) and a Phillips PW 1410 spectrometer at the University of Tasmania (UT). The concentrations of rare earth elements and other trace elements were determined by inductively coupled plasma mass spectrometry (ICP-MS) using a Perkin-Elmer Sciex Elan 5000 instrument at the GSF and an HP 4500 instrument at the UT. The whole-rock major and trace element data of Hanski et al. (2001) are supplemented by two additional samples (10C-PPR-97 and 314-LVP-86) and are all presented here as an appendix (Appendix 3.1).

*3.4.1. Electron Microprobe*

The chemical compositions of chromites (Table 3.1) from selected samples were determined using a Cameca Camebax SX50 microprobe at the Geological Survey of Finland. The analytical conditions included an accelerating potential of 25 kV, a sample current of 47 nA, and a beam diameter of 1 μm. Representative microprobe analyses of chromites are presented in Table 3.1.

*3.4.2. Mössbauer Analyses*

Mössbauer spectra were collected for 5 selected chromite separates at the Institute for Rock Magnetism at the University of Minesota, Minneapolis. The chromite separates were crushed and approximately 20-30 mg of powder was dispersed in powdered sugar in a 12-mm-diameter sample holder. The spectra were collected at room temperature using a constant acceleration transmission spectrometer

**Table 3.1:** Representative microprobe analyses of chromites from the Lapland komatiites. All analyses were obtained from the core of equant grains.

| Sample: | 13-EJH-97 | 6.2-EJH-97 | 12C-PPR-97 | 17-EJH-97 | 10C-PPR-97 | 12D-PPR-97 | 8-PPR-97 | 10D-PPR-97 | 12-PPR-97 |
|---|---|---|---|---|---|---|---|---|---|
| $SiO_2$ | 0.11 | 0.14 | 0.06 | 0.07 | 0.05 | 0.05 | 0.06 | 0.08 | 0.10 |
| $TiO_2$ | 0.40 | 0.44 | 0.58 | 0.47 | 0.60 | 0.69 | 0.75 | 0.51 | 0.55 |
| $Al_2O_3$ | 13.98 | 13.16 | 14.54 | 13.55 | 13.45 | 14.93 | 16.04 | 13.39 | 13.82 |
| $Cr_2O_3$ | 47.43 | 51.13 | 50.90 | 49.67 | 50.96 | 48.92 | 44.92 | 54.23 | 52.33 |
| $V_2O_3$ | n.d. | n.d. | n.d. | n.d. | n.d. | n.d. | 0.24 | 0.11 | 0.17 |
| $Fe_2O_3{}^*$ | 8.53 | 5.58 | 6.01 | 7.03 | 6.38 | 6.75 | 9.23 | 4.70 | 5.43 |
| FeO | 16.06 | 15.93 | 11.57 | 15.86 | 13.31 | 12.12 | 14.78 | 10.19 | 11.18 |
| MnO | 0.14 | 0.12 | 0.07 | 0.12 | 0.00 | 0.06 | 0.25 | 0.09 | 0.21 |
| MgO | 11.64 | 11.78 | 14.91 | 11.89 | 13.66 | 14.50 | 13.00 | 15.73 | 15.05 |
| CaO | 0.10 | 0.02 | 0.00 | 0.03 | 0.01 | 0.01 | 0.02 | 0.00 | 0.01 |
| CoO | 0.03 | 0.03 | 0.03 | 0.03 | 0.03 | 0.02 | 0.00 | 0.02 | 0.00 |
| NiO | 0.16 | 0.15 | 0.22 | 0.18 | 0.19 | 0.22 | 0.23 | 0.23 | 0.23 |
| ZnO | n.d. | n.d. | n.d. | n.d. | n.d. | n.d. | 0.07 | 0.03 | 0.03 |
| Total | 98.57 | 98.48 | 98.90 | 98.89 | 98.64 | 98.26 | 99.59 | 99.31 | 99.11 |
| Cr#[1] | 0.695 | 0.723 | 0.701 | 0.711 | 0.718 | 0.687 | 0.653 | 0.731 | 0.717 |
| Mg#[2] | 0.564 | 0.569 | 0.697 | 0.572 | 0.647 | 0.681 | 0.611 | 0.733 | 0.706 |
| $Fe^{3+}$#[3] | 0.106 | 0.070 | 0.073 | 0.087 | 0.079 | 0.083 | 0.113 | 0.057 | 0.066 |
| $Fe^{3+}/\Sigma Fe$[4] | | 0.27 | | | 0.21 | | | 0.28 | 0.16 | 0.22 |

*$Fe_2O_3$ and FeO were distributed based on calculations assuming stoichiometry.

n.d. = not determined.

Following calculations are in atomic proportions: [1]Cr# = Cr/(Cr+Al); [2]Mg# = Mg/(Mg+$Fe^{2+}$); [3]$Fe^{3+}$# = $Fe^{3+}$/($Fe^{3+}$+Cr+Al).

[4]determined through Mössbauer analyses.

with a $^{57}Co$ in Rh matrix source and an activity of approximately 5mC. The spectra were fit with 4 doublets and 2 sextets using a least squares fitting routine. The hyperfine parameters as well as peak area and width were allowed to float with no bounds enforced. Three of the samples, 12-PPR-97, 10C-PPR-97 and 6.2-EJH-97 have significant amounts of a magnetically ordered phase with the hyperfine parameters consistent with magnetite. Of the 4 doublets that were fit for all of the samples, three can be assigned to $Fe^{2+}$ with isomer shifts above 0.63 mm/s and quadrupole splitting above 1.2 mm/s, and one can be assigned to $Fe^{3+}$ with isomer shift ranging from 0.16-0.45 mm/s and quadrupole splitting between 0.53-0.86 mm/s. Although some ambiguity exists due to the 3 overlapping $Fe^{2+}$ doublets, the overall area assignment to $Fe^{2+}$ is not affected excepting only the relation between the $Fe^{2+}$ doublets. The $Fe^{2+}/Fe^{3+}$ ratios were calculated from the paramagnetic doublets as defined above. In order to calculate the $Fe^{3+}/\Sigma Fe$ ratios of paramagnetic iron, we excluded the iron in the magnetite. Assuming stoichiometry, magnetite can be expressed as $Fe^{3+}[Fe^{2+}Fe^{3+}]O_4$ with the tetrahedral site containing only $Fe^{3+}$ and the octahedral site containing equal contents of $Fe^{2+}$ and $Fe^{3+}$. The ferric/ferrous ratios of selected chromite separates obtained through analyses of Mössbauer spectra are also included in Table 3.1.

*3.4.3. Re-Os Isotope Analyses*

The chemical separation techniques for Re-Os analyses employed in this study have followed previously published work (Shirey and Walker, 1995; Cohen and Waters, 1996). In brief, approximately 3g of whole-rock powder was dissolved in reverse aqua regia, and frozen and equilibrated with spikes in sealed Pyrex™ Carius

tubes. The tubes containing whole-rock powder were heated at 240°C for at least 24 hours, whereas those with mineral separates (chromite, clinopyroxene and sulfide) for at least 48 hours to facilitate complete digestion. Osmium was separated by solvent extraction into carbon tetrachloride and finally transferred into concentrated HBr (Cohen and Waters, 1996). The final purification for Os was accomplished via micro-distillation. Rhenium was recovered from aqua regia via anion exchange column chemistry (Morgan and Walker, 1989). The total ranges in analytical blanks for Re and Os were 1.2-6.4 pg (excluding one outlier with 12.7 pg of Re) and 1.3-6.9 pg (n=6), respectively, and are negligible compared to their concentrations in most of the whole-rock samples. The blank contribution, however, was substantial (typically between 2 and 10%) for some of the Re analyses of chromites. The isotopic compositions of the blanks were natural for Re and $^{187}Os/^{188}Os$ varied between 0.135 and 0.223 (excepting one outlier with 0.319). All data were corrected for blanks and the isotopic and concentration data in Table 3.2 represent the corrected values. The uncertainties in blanks are reflected in respective uncertainties for isotopic and concentration data in Table 3.2. The external reproducibility on standard analyses for Os and Re were typically better than ±0.1 and ±0.3%, respectively.

The isotopic compositions of Re and Os were obtained using negative thermal ionization mass spectrometry (Creaser et al., 1991; Völkening et al., 1991). The mass spectrometric procedures followed in this study have been discussed in Walker et al. (1994) and Morgan et al. (1995). Samples with high Os abundances (whole-rock, chromite and sulfide) were analyzed with Faraday cups in the static mode (using a Sector 54 mass spectrometer), whereas those with relatively low abundances of Os

**Table.3.2:** Re and Os concentrations and isotope data for the whole-rock komatiites and mineral separates

| Samples | Re (ppb) | Os (ppb) | $^{187}$Re/$^{188}$Os | $^{187}$Os/$^{188}$Os | $\gamma_{Os}(T)^*$ | Model ages (Ga) |
|---|---|---|---|---|---|---|
| **Whole-rocks:** | | | | | | |
| 8-PPR-97 | 0.5715 | 2.734 | 1.011 | 0.15978 | +10±0.3 | |
| 10D-PPR-97 | 0.7815 | 4.788 | 0.7885 | 0.14789 | +6.6±0.5 | |
| 12-PPR-97 | 0.5438 | 6.166 | 0.4254 | 0.13638 | +7.6±0.2 | |
| 12C-PPR-97 | 0.8238 | 5.758 | 0.6905 | 0.14001 | +2.6±0.2 | |
| 6.2-EJH-97 | 0.9671 | 3.013 | 1.554 | 0.16351 | -3.2±0.3 | |
| 8-EJH-97 | 0.3341 | 1.284 | 1.266 | 0.20185 | +40±0.5 | |
| 12D-PPR-97 | 0.6362 | 5.135 | 0.5976 | 0.13628 | +2.2±0.2 | |
| 17-EJH-97 | 0.4132 | 2.345 | 0.8527 | 0.16111 | +16±0.3 | |
| 17A-EJH-97 | 0.8862 | 2.696 | 1.591 | 0.16322 | -4.6±0.3 | |
| 313-3203 | 0.0590 | 1.389 | 0.2048 | 0.13190 | +10±0.4 | |
| 10C-PPR-97 | 0.5008 | 3.860 | 0.6256 | 0.13322 | -1.4±0.2 | |
| **Chromites:** | | | | | | |
| 10C-PPR-97 | 0.732 | 102.1 | 0.0345 | 0.11404 | -0.2±0.2 | |
| Dupl$^†$ | 0.790 | 121.0 | 0.0314 | 0.11397 | -0.1±0.1 | |
| Trpl$^Φ$ | 1.18 | 77.41 | 0.0736 | 0.11520 | -0.3±0.1 | |
| 314-LVP-86 | 0.711 | 75.91 | 0.0451 | 0.11569 | +1.0±0.4 | |
| Dupl. | 0.946 | 65.99 | 0.0689 | 0.11645 | +0.9±0.5 | |
| 8-PPR-97 | 0.433 | 84.53 | 0.0246 | 0.11371 | -0.1±0.1 | |
| 8-PPR-97-2 | 0.437 | 70.84 | 0.0296 | 0.11404 | 0.0±0.4 | |
| 12C-PPR-97 | 0.471 | 161.9 | 0.0140 | 0.11342 | -0.1±0.1 | |
| 12D-PPR-97/2 | 0.722 | 223.2 | 0.0156 | 0.11342 | -0.1±0.2 | |
| 10D-PPR-97 | 0.887 | 53.80 | 0.0793 | 0.11556 | -0.2±0.6 | |
| 17A-EJH-97 | 0.901 | 84.46 | 0.0513 | 0.11368 | -1.0±0.6 | |
| **Clinopyroxenes:** | | | | | | |
| 10D-PPR-97 | 1.388 | 1.118 | 6.209 | 0.42027 | +80 | |
| 12-PPR-97$^Ψ$ | 2.178 | 153.4 | 0.0683 | 0.11812 | +2.4 | |
| 12D-PPR-97 | 0.2226 | 0.7118 | 1.520 | 0.19442 | +25 | |
| 17-EJH-97 | 0.6252 | 6.895 | 0.4374 | 0.13525 | +6.2 | |
| 17A-EJH-97 | 0.3711 | 0.9037 | 2.000 | 0.21212 | +26 | |
| Dupl. | 0.2935 | 0.4224 | 3.427 | 0.31007 | +69 | |
| 12C-PPR-97 | 0.9818 | 0.5503 | 9.007 | 0.49843 | +63 | |
| Dupl. | 0.8444 | 0.5233 | 8.134 | 0.48341 | +77 | |
| **Sulfides:** | | | | | | |
| 10C-PPR-97 | 59.56 | 2.942 | 156.5 | 4.8617 | -624 | 1.8 |
| Dupl. | 59.73 | 4.730 | 80.47 | 2.6248 | -258 | 1.8 |
| 10D-PPR-97 | 167.5 | 5.042 | 410.2 | 13.067 | -1186 | 1.9 |
| Dupl. | 195.8 | 5.410 | 503.1 | 14.917 | -2410 | 1.7 |
| 12C-PPR-97$^a$ | 270.1 | 6.176 | 2008 | 67.751 | -2070 | 2.0 |

Note: [1] Total analytical uncertainties are 0.3% for $^{187}$Re/$^{188}$Os and 0.1% for $^{187}$Os/$^{188}$Os (2σ). For clinopyroxenes, the uncertainties on $^{187}$Os/$^{188}$Os ratios are ±0.3% (2σ). [2] All Os analyses, except for clinopyroxenes, were performed on a Faraday cup, whereas all Re analyses were accomplished using an electron multiplier;[3] $^a$ = Pentlandite; $^b$ = chalcopyrite; $^Ψ$ = clinopyroxene + chromite; [4] * = calculated values at the Re-Os regression age of 2.056 Ga. The projected chondritic $^{187}$Os/$^{188}$Os at 2.056 Ga is calculated to be 0.11300, using the average $^{187}$Re/$^{188}$Os ratio of chondrites and initial $^{187}$Os/$^{188}$Os (at T = 4.558 Ga) for early solar system materials (IIIA irons) of 0.40186 and 0.09531, respectively (Shirey and Walker, 1998), and λ ($^{187}$Re→$^{187}$Os + β$^-$) = $1.666×10^{-11}$ year$^{-1}$ (Smoliar et al., 1996); [5] $^†$ Dupl. and $^Φ$Trpl. denote duplicate and triplicate analyses of different aliquots of powder, respectively.

(e.g., clinopyroxene) and/or Re (e.g., chromite) were analyzed with an electron multiplier using a 12" NBS mass spectrometer.

## 3.5. RESULTS

### 3.5.1. Salient whole rock geochemical characteristics

The Jeesiörova komatiites have subchondritic $Al_2O_3/TiO_2$ ratios and characteristic HREE-depletion ($Gd/Yb_{CN} > 1$), similar to those typical of Al-depleted komatiites (Lahaye et al., 1995). However, the Jeesiörova rocks have high abundances of high-field strength elements (HFSE: e.g., Ti, Zr, Hf) relative to those at a given MgO level of both Al-depleted and Al-undepleted komatiites (Fig. 3.1B; also see Hanski et al., 2001). These elements, however, do not appaear as significant positive anomalies in primitive mantle-normalized spidergrams (Figs. 3.3 A-B), suggesting that the Jeesiörova komatiites also have elevated abundances of elements with incompatibilities similar to those of Ti, Zr and Hf, such as the rare-earth elements, Eu, Gd, Nd and Sm. For example, ratios of Ti to similarly incompatible elements (e.g., $Ti/Ti* = Ti/10^{(logSm + 3logGd)/4}$, calculated after McCuaig et al., 1994, where all elements are normalized to primitive mantle) for the Jeesiörova komatiites overlap with those for the Al-undepleted Abitibi komatiites (Lahaye and Arndt, 1996; Fan and Kerrich, 1997) and also some Al-depleted komatiites (Lahaye et al., 1995; Parman et al., 2003; Fig. 3.4). The higher relative abundance of Ti in the Jeesiörova rocks is also accompanied by comparable degrees of relative enrichments in similarly incompatible elements (e.g., Eu, Gd, Zr), as is evidenced by the absence of significant positive Ti anomalies on a primitive mantle-normalized trace element variation
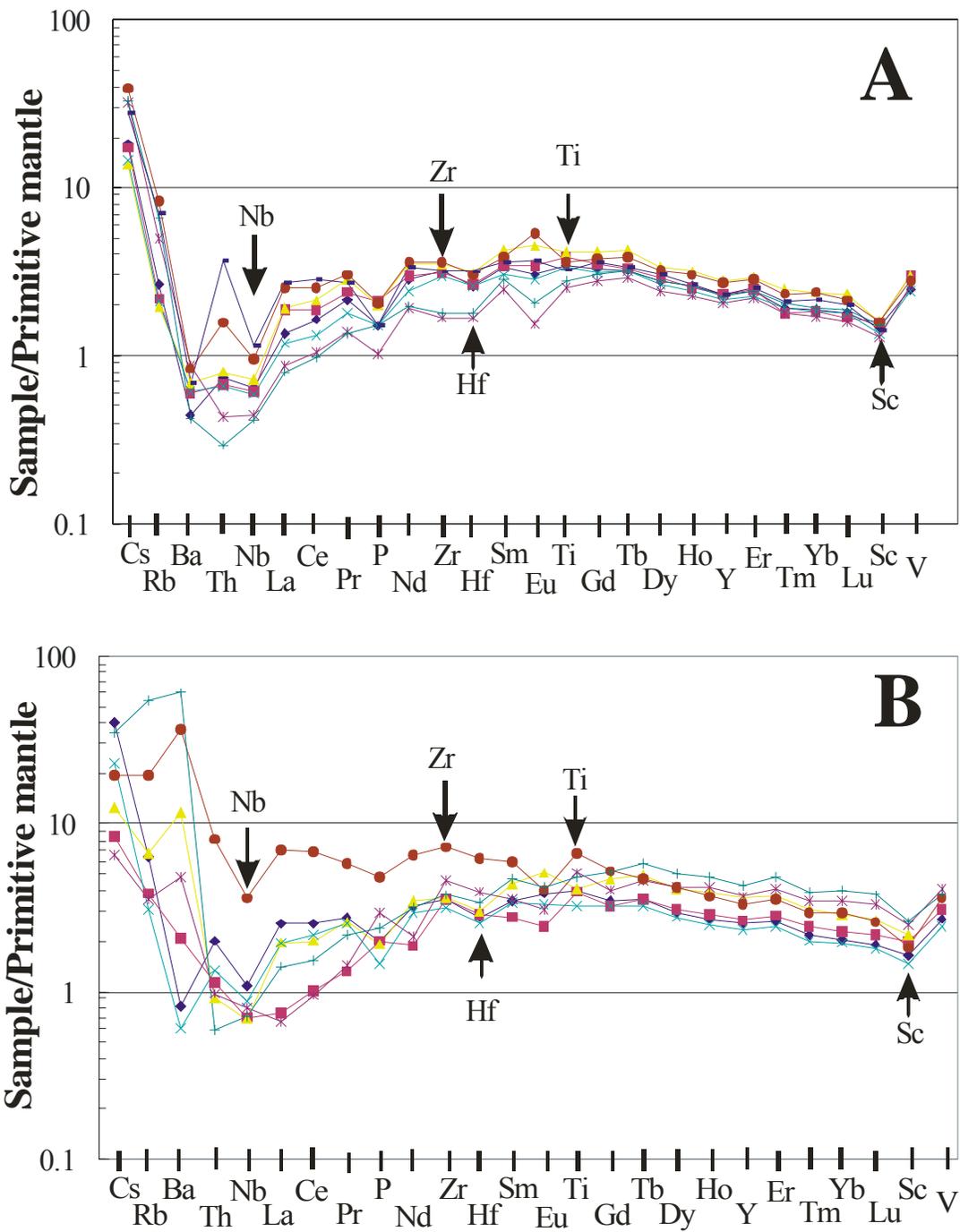
**Fig. 3.3.** Primitive mantle-normalized extended rare-earth element (REE) diagram for the Jeesioröva komatiites. For clarity, the entire set of samples in Hanski et al. (2001) are shown in two separate spidergrams **(A-B).**
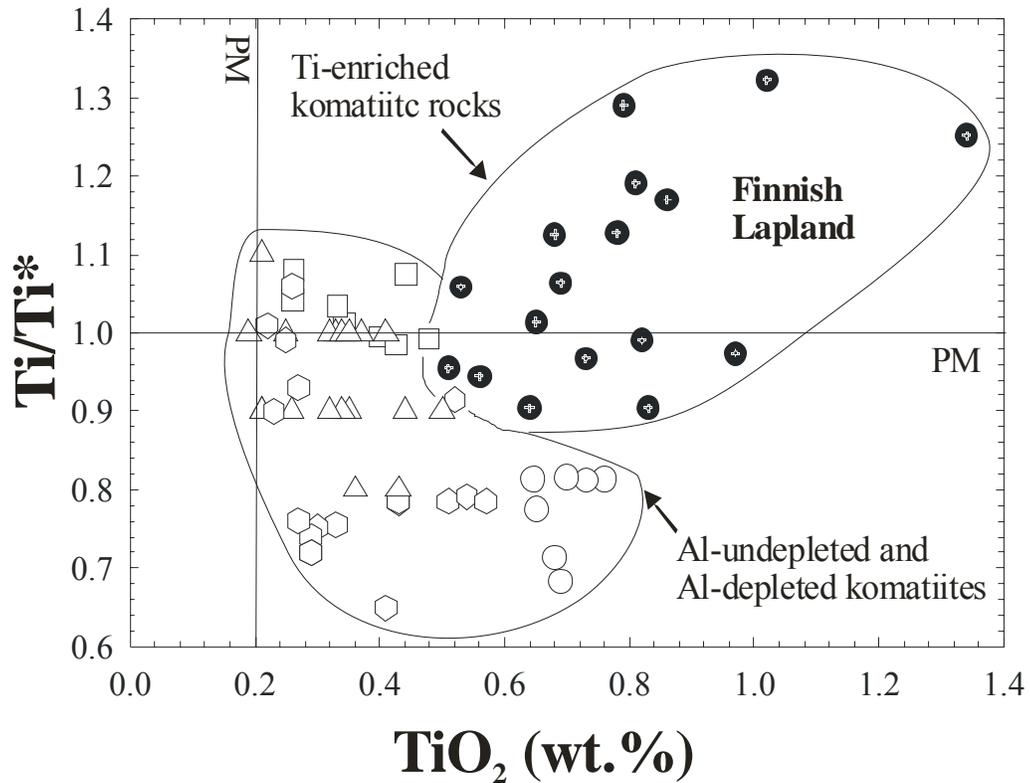
**Fig. 3.4.** Plot of the whole-rock $TiO_2$ contents in the Jeesiörova rocks versus Ti anomalies ($Ti/Ti* = Ti/10^{(logSm + 3logGd)/4}$, calculated after McCuaig et al., 1994, where all the elements are normalized to primitive mantle: McDonough and Sun, 1995). The combined field for Al-undepleted and Al-depleted rocks is drawn based on data of Fig. 1. Note that most of the Finnish rocks show positive Ti anomalies, and there is a broad positive correlation between $TiO_2$ and Ti anomalies in the Finnish rocks.

diagram (Fig. 3.3). In contrast to high concentrations of Ti and Zr, virtually all Jeesiörova samples show negative Nb anomalies (Fig. 3.3).

*3.5.2. Re-Os concentrations and isotopic compositions*

The Re-Os concentrations and isotopic composition data for the whole-rocks and mineral separates (chromite, clinopyroxene and sulfide) are reported in Table 3.2. The concentrations of Re and Os, and Re/Os ratios for all the sample types are plotted in Figs. 3.5A-B. The abundances of both Os and Re vary over two orders of magnitude (Fig. 3.5A). The Os concentrations are highest in chromite and lowest in clinopyroxene separates.

The very high concentrations of Os, coupled with low Re concentrations in chromite result in very low Re/Os ratios (Fig. 3.5B). Because of their low Re/Os ratios and minimal correction of $^{187}Os/^{188}Os$ for age, chromites were used to precisely determine the initial $^{187}Os/^{188}Os$ for these rocks. The weighted average initial ratio, $0.1131 \pm 0.0006$ (2$\sigma$), corresponds to a $\gamma_{Os}$ of $0.1 \pm 0.5$ at the 2.056 Ga age of crystallization (Fig. 3.6A). The Re-Os isotope results for the chromites do not yield a precise isochron due to the very limited spread in their $^{187}Re/^{188}Os$ ratios (~0.01-0.07; Table 3.2) coupled with large uncertainties in Re concentrations.

The concentrations of Os in the whole-rocks are typically high, varying between ~1.3 and 6.2 ppb. Similarly, the whole-rock Re concentrations are also high (mostly above 0.5 ppb) relative to komatiites from elsewhere (e.g., Gangopadhyay and Walker, 2003). The whole-rock samples mostly plot above a chondritic reference isochron (Fig. 3.6B) and display a large variation in their respective calculated initial $\gamma_{Os}$ values (Table 3.2).
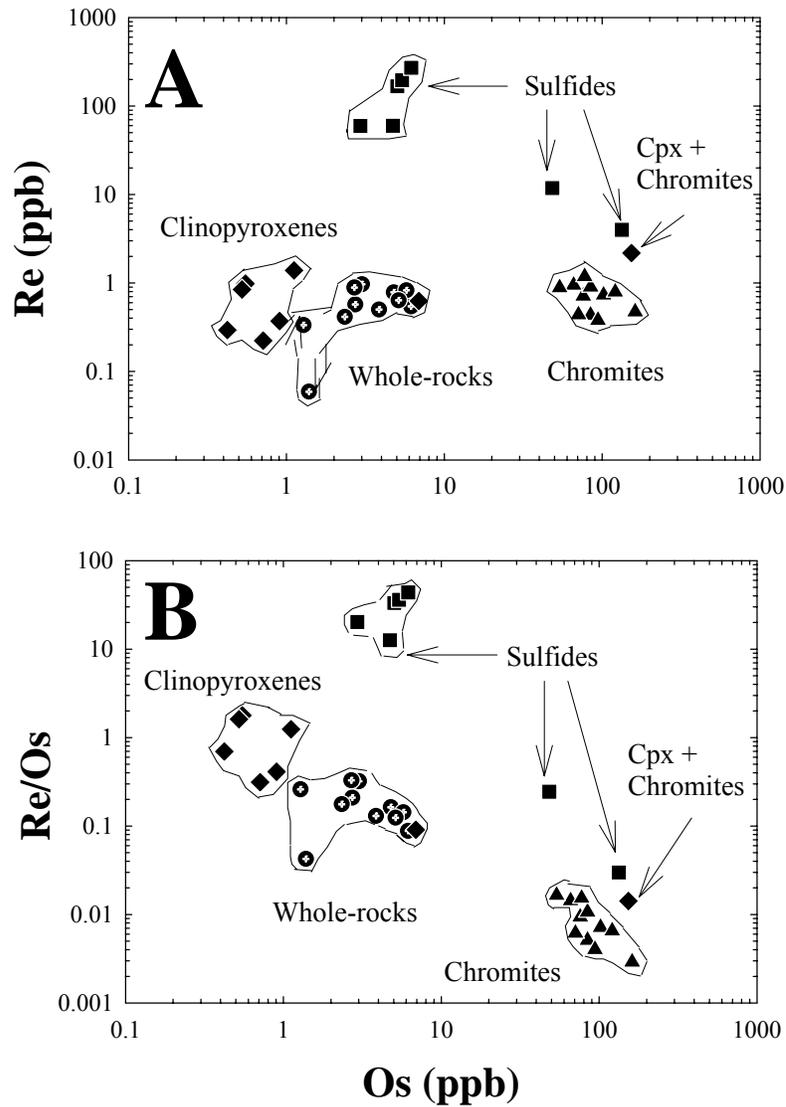
**Fig. 3.5.** Plot of (**A**) concentrations of Re and Os (ppb) in whole rocks and mineral separates (clinopyroxene, sulfide, and chromite) in the Finnish rocks. Note the significantly higher Os concentrations in chromite and sulfide separates than in both whole rocks and clinopyroxene separates. The sulfide separates typically have the highest Re concentrations among all the sample types. (**B**) The Os concentrations of the same samples are plotted against Re/Os ratios. Note the chromites have the lowest Re/Os ratios, whereas the sulfides have the highest values of the ratio.

71
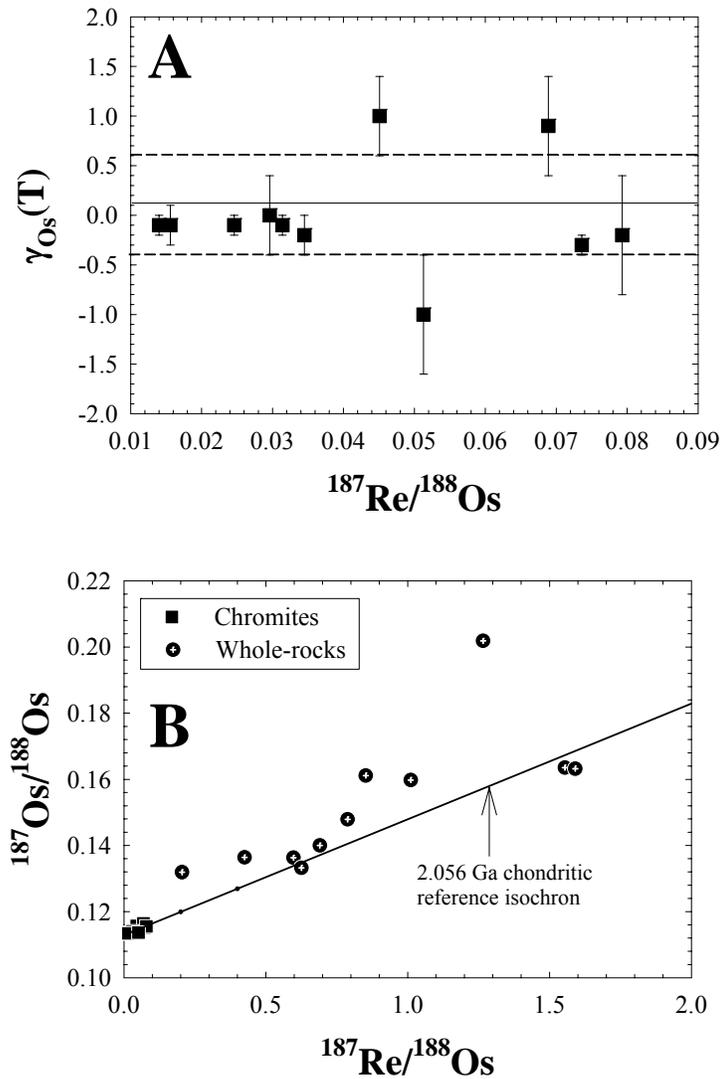
**Fig. 3.6. (A)** Plot of calculated initial $\gamma_{Os}$ (at the crystallization age of 2.056 Ga; Hanski et al., 2001) versus $^{187}Re/^{188}Os$ of chromites from the Finnish rocks. The solid horizon line represents the chondritic reference line, whereas the dashed lines show the upper and lower limits of $\gamma_{Os}$ corresponding to the 2 sigma variations in the calculated weighted average initial $^{187}Os/^{188}Os$ for the chromites. Note that all of the individual chromite data plot within this $2\sigma$ uncertainties. **(B)** The $^{187}Re/^{188}Os$ versus $^{187}Os/^{188}Os$ plot of the whole-rock komatiites and chromites from the Finnish Lapland.

The sulfide separates have the highest Re concentrations and most of them have very high Re/Os ratios (Fig. 3.5B). One pentlandite and one chalcopyrite separate from sample 800-LVP-46 have very high Os concentrations of ~48 and 133 ppb, respectively. The sulfide separates give generally consistent Os model ages of ca. 1.8 Ga. The model age is ~250 Ma younger than the Sm-Nd age of these rocks (2056 ± 50 Ma: Hanski et al., 2001). This suggests that the primary Re-Os elemental systematics of the sulfides were disturbed ~250 Ma after their crystallization due to secondary processes such as hydrothermal alteration and/or metamorphic resetting. As a result, the sulfides give anomalous initial $\gamma_{Os}$ values for the magmatic formation age (Table 3.2). It is not uncommon for the Re-Os system to display open-system behavior in sulfide phases associated with komatiites (e.g., Luck and Allègre, 1984; Walker et al., 1997; Shirey and Walker, 1995).

Clinopyroxene separates have both relatively high Os (> 0.5 ppb up to ~ 1 ppb excepting one separate 17-EJH-97) and Re concentrations (up to ~ 1.4 ppb). Also, clinopyroxene separates give highly variable initial $\gamma_{Os}$ values (ranging between +6 and +84). Most of the whole-rock and clinopyroxene separates in these rocks give generally consistent initial Nd isotopic compositions (Hanski et al., 2001), whereas the Re-Os isotope systematics of the same samples indicate large-scale open-system behavior. This may be due to the presence of secondary sulfide inclusions within clinopyroxene or sulfide impurities in our clinopyroxene separates.

## 3.6. DISCUSSION

### 3.6.1. Are the Jeesiörova komatiites Al-depleted?

The Jeesiörova komatiites have $Al_2O_3/TiO_2$ ratios that are significantly lower (typically between 10 and 13) than the near-chondritic value of ~20 reported for Al-undepleted komatiites from Alexo (~19-23; Arndt, 1986) and Pyke Hill (~17-20; e.g., Pyke et al., 1973; Nesbitt and Sun, 1976) in the Abitibi greenstone belt. This could result from low concentrations of Al or high abundances of Ti in the Jeesiörova komatiites relative to the Al-undepleted Munro-type komatiites. Several aspects of the Jeesiörova rocks, however, suggest that the parental liquids were not Al-depleted. First, the bulk aluminum contents at given MgO levels of the Jeesiörova rocks are significantly higher than in the Al-depleted Barberton rocks, and similar to (or even slightly higher in some samples than) those in Al-undepleted Munro rocks (Fig. 3.1A). Second, the chromites in the Jeesiörova rocks have distinctly higher Al contents than those in the Al-depleted komatiites from elsewhere (Barnes and Roeder, 2001; Fig. 3.7A). The chromites in the Finnish rocks are, on the other hand, chemically similar to chromites from the Al-undepleted komatiites from Gorgona Island (Echeverria, 1980) and Pyke Hill in the Munro Township (Arndt et al., 1977; Fig. 3.7A). The similar Al contents of chromites in both Jeesiörova rocks and those in Al-undepleted komatiites from Pyke Hill, Canada (Arndt et al., 1977), Vetreny, Russia (Puchtel et al., 1996) and Belingwe, Zimbabwe (Zhou and Kerrich, 1992) are also apparent in Fig. 3.7B. Combined, these characteristics suggest that aluminum contents in the magmas parental to the Finnish rocks were more similar to those of Al-undepleted, rather than Al-depleted rocks.

74

**Fig. 3.7. (A)** Plot of trivalent cations (Al-Cr-$Fe^{3+}$) in chromites in Ti-enriched Lapland rocks compared with Al-undepleted Munro (Arndt et al., 1977) and Gorgona (Echeverria, 1980) rocks. The approximate positions of the fields of Al-depleted komatiites (ADK) and boninites are shown after Barnes and Roeder (2001). The field for arc-related picrites is based on data from Eggins (1993). This plot shows that the chromites in the Finnish rocks have very similar cation contents in their M2 sites when compared with the Munro and Gorgona rocks. Also, note that the Finnish chromites have significantly lower $Fe^{3+}$ contents relative to the arc-related picrites and also lower Cr contents compared to Al-depleted komatiites and boninites. **(B)** Plot of $Al_2O_3$ versus $TiO_2$ (mole%) in chromites from Lapland komatiites, compared with those from Al-undepleted komatiites (Gorgona, Pyke Hill, Vetreny, and Belingwe). A sizeable portion of the Lapland chromites have higher $TiO_2$ at a given level of $Al_2O_3$ relative to the other two rock types. Data sources: Gorgona (Echeverria, 1980); Pyke Hill (Arndt et al., 1977); Vetreny (Puchtel et al., 1996); Belingwe (Zhou and Kerrich, 1992).
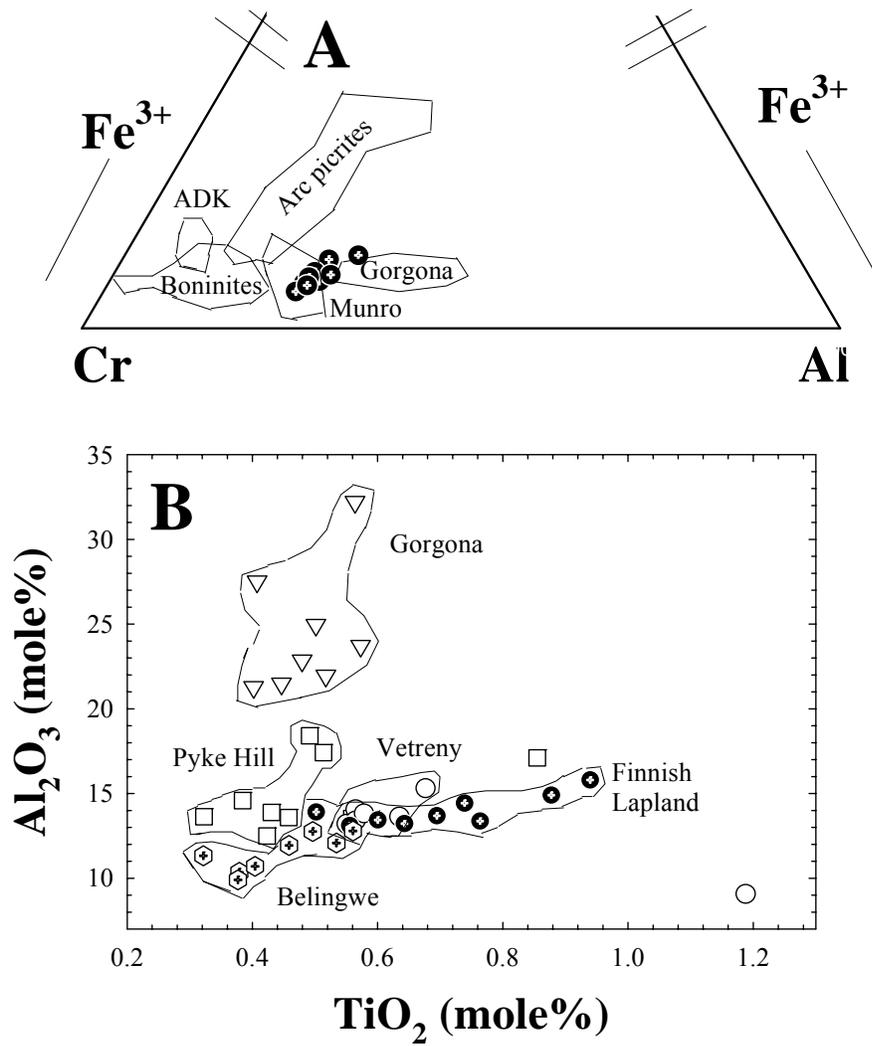
**Fig. 3.7.**

Although the Jeesiörova komatiites have higher relative concentrations of Ti and similarly incompatible elements, they also have subchondritic $Al_2O_3/TiO_2$ ratios and are HREE-depleted (e.g., chondrite-normalized Gd/Yb >1), characteristics that are similar to those commonly observed in Al-depleted komatiites (Lahaye et al., 1995). Consequently, although it seems likely that the parental magmas were Al-undepleted, it is still necessary to consider two models that are often cited for production of Al-depleted komatiites.

Previous studies of Al-depleted Barberton-type komatiites (e.g., Lahaye et al., 1995) have documented negative correlations between HREE depletions and anomalies of some HFSE (e.g., $Zr/Zr^* = Zr/10^{(logSm + logNd)/2}$: McCuaig et al., 1994). These features have been explained to be a result of fractionation of the high-pressure form of garnet (majorite garnet at > 14 GPa) in the deep mantle (Yurimoto and Ohtani, 1992; Xie and Kerrich, 1994; Lahaye et al., 1995). This interpretation was based on the close correspondence between variations in HFSE and HREE concentrations in Al-depleted rocks, consistent with calculated majorite fractionation trends using experimentally determined partition coefficients (Kato et al., 1988; Yurimoto and Ohtani, 1992). The depletions in HREE and variations in HFSE versus REE in the Jeesiörova rocks are plotted in Figs. 3.8 A-B. Calculated majorite fractionation trends using published partition coefficients (Yurimoto and Ohtani, 1992) do not show correspondence with the natural variations of the respective elements in the Jeesiörova rocks.

In addition to the above trace element characteristics, the Re concentrations of the Jeesiörova komatiites are not accompanied by any evidence for majorite

**Fig. 3.8.** Plots of HFSE anomalies (Ti, Zr and Nb) and other key trace elements in the Finnish rocks compared with those for the same suites of Al-undepleted (Alexo and Pyke Hill) and Al-depleted (Komati and Mendon) rocks as in Fig. 3.1. The HFSE anomalies (Ti/Ti* as in Fig. 2; $Zr/Zr* = Zr/10^{(logSm + logNd)/2}$; $Nb/Nb* = Nb/10^{(2\ logLa - logCe)}$) were calculated after McCuaig et al. (1994). Also shown are the calculated majorite fractionation trends (solid line with tick marks showing percentages of majorite fractionation). The numbers next to each tick mark represent percentage fractionation of majorite. The $D^{majorite/liq.}$ values for each element are from Yurimoto and Ohtani (1992). The reference lines for chondrite and PM (primitive mantle) are after McDonough and Sun (1995). **(A)** Note the broad positive correlation between Ti and Zr anomalies in the Finnish rocks. **(B)** Note the pronounced negative Nb anomalies in the Finnish rocks. **(C)** Note that both the Ti/Zr and La/Sm ratios in the Finnish rocks plot within the Munro-type rocks rather than Al-depleted Barberton rocks. **(D)** The field of boninites is from Hickey and Frey (1982). The trace elements ratios for the Finnish rocks plotted in all of these diagrams (A-D) are not consistent with the calculated majorite fractionation trends.
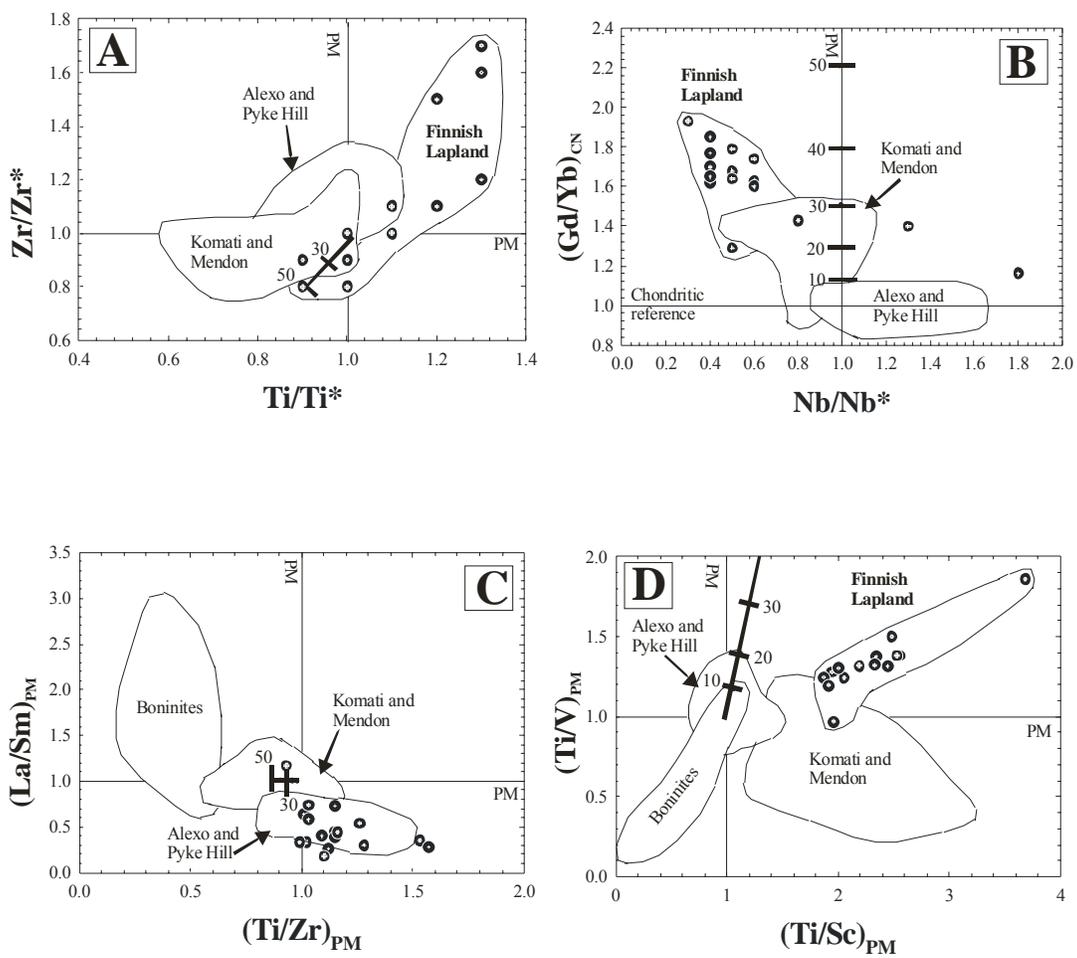
**Fig. 3.8.**

fractionation. Previous experimental study has suggested that Re is compatible in garnet during mantle melting ($D_{Re}^{garnet/silicate\ melt}$ = 2.7: Righter and Hauri, 1998). If generally true for majorite garnet, it is likely that, majorite fractionaton in the mantle source for Jeesiörova komatiites would have led to significant depletion of Re. Instead, the Re concentrations in virtually all the Jeesiörova samples (~500-900 pg/g; Table 3.2) are *higher* than in Al-undepleted komatiites (e.g., ~300-400 pg/g in Alexo komatiites: Gangopadhyay and Walker, 2003).

Collectively, trace element distribution patterns, as discussed above, suggest that either (a) the D values considered for these models are not appropriate for the Finnish rocks, (b) the assumption that the putative primitive mantle composition represents the Jeesiörova mantle composition is not valid, or (c) majorite fractionation was not involved in the generation of these rocks. The first two possibilities cannot be ruled out, but are considered unlikely because the D values and/or model starting mantle parameters would have to be considerably different from those used in previous studies (e.g., Lahaye et al., 1995) in order to account for the abundances of the respective elements in the Jeesiörova komatiites. We conclude that majorite fractionation in the deep mantle was likely not responsible for the combined subchondritic $Al_2O_3/TiO_2$ ratios and HREE-depletions of the Jeesiörova komatiites.

In an alternative petrogenetic model, some of the petrologic and geochemical characteristics of the Al-depleted Barberton komatiites have been explained in terms of their possible origin through hydrous melting in supra-subduction zone settings (e.g., Grove et al., 1999; Parman et al., 2003). For example, the negative correlation between Ti/Zr and La/Sm ratios in komatiite chill margins and komatiitic basalts from

Barberton has been shown to vary in a manner similar to that observed in Phanerozoic boninites (Parman et al., 2003). This feature was interpreted by Parman et al. (2003) to be a result of mixing between a silicate melt with high La/Sm ratio and a hydrous fluid with high Ti/Zr ratio. There is little evidence to support a similar origin for the Jeesiörova komatiites. For example, on a primitive mantle-normalized diagram of La/Sm versus Ti/Zr, the Jeesiörova rocks plot within the field of Al-undepleted Abitibi komatiites, rather than Al-depleted Barberton komatiites (Fig. 3.8C). The trace element ratios do not show any evidence for mixing between hydrous fluids and silicate melts compositionally similar to those that were suggested for the Barberton rocks (Parman et al., 2003). Additionally, as can be seen on a primitive mantle-normalized plot, the Finnish rocks, unlike boninites (Hickey and Frey, 1982), are enriched rather than depleted in Ti relative to other transitional elements, such as V and Sc (Fig. 3.8D).

In addition to whole rock trace element characteristics, the redox state of Jeesiörova rocks is also unlikely to support their generation in what are typically highly oxidized arc environments. The redox state for the Jeesiörova rocks were estimated using $Fe^{3+}$#'s and $Fe^{3+}/\Sigma Fe$ ratios of selected chromites determined through microprobe and Mössbauer analyses, respectively (Table 3.1). The $Fe^{3+}$# for the chromites in the Jeesiörova rocks are compared with those and corresponding $fO_2$ values in 1-atm experimental charges of Murck and Cambell (1986) and Roeder and Reynolds (1991) with natural komatiitic lavas as starting materials (Fig. 3.9). The entire range of $Fe^{3+}$#'s of chromites in the Jeesiörova rocks corresponds approximately to FMQ±1.4. This range in $fO_2$ values for the Jeesiörova rocks is also
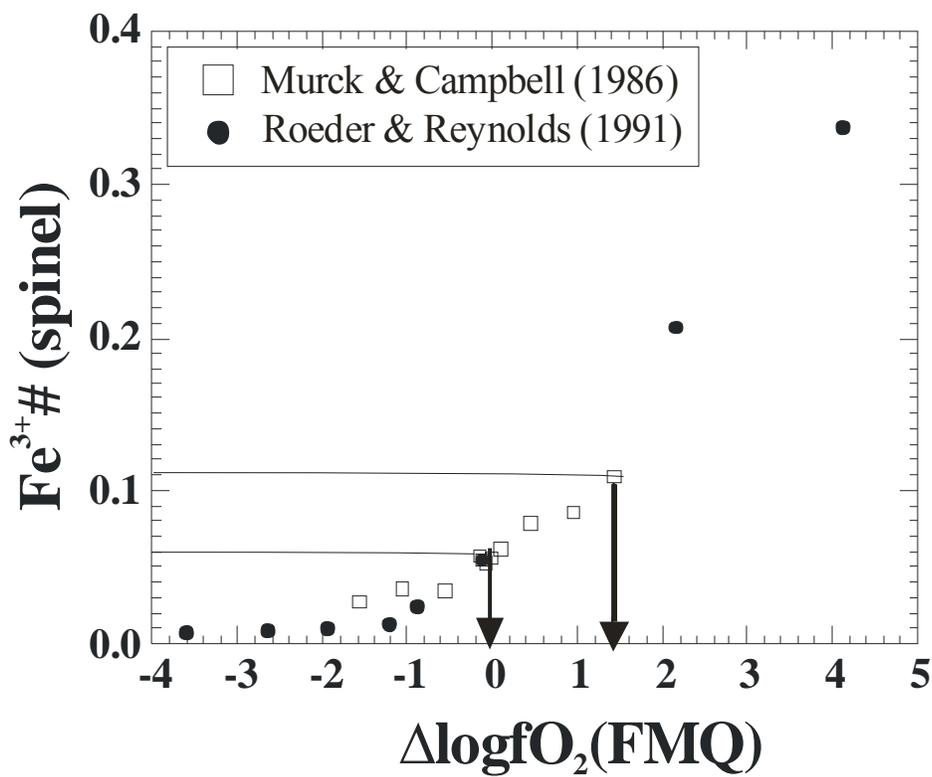
**Fig. 3.9.** Plot of $Fe^{3+}$#s [$Fe^{3+}$/($Fe^{3+}$+Cr+Al)] of chromites in the experimental charges of Murck and Campbell (1986) versus $\Delta logfO_2$ [$logfO_2 - log(FMQ)$] values for the respective experimental runs. Note that the entire range of $Fe^{3+}$#s obtained for chromites in the Finnish rocks, as shown by the two horizontal lines, corresponds approximately to FMQ±1.4.

consistent with that obtained for mafic-ultramafic lavas cited by Fisk and Bence (1980), and Barnes (1986). It is, however, recognized that the conventional microprobe analyses of chromites do not always yield accurate value of $fO_2$, whereas $Fe^{3+}/\Sigma Fe$ ratios of chromites determined through Mössbauer analyses are potentially more accurate for the purpose of oxygen barometry (e.g., Wood and Virgo, 1989). For this reason, the $Fe^{3+}/\Sigma Fe$ ratios of selected chromite separates from the Finnish rocks were determined by Mössbauer analyses. The $Fe^{3+}/\Sigma Fe$ values for five chromite separates vary within a limited range of 0.16-0.28 that corresponds to $fO_2$ of -1.5 < $\Delta FMQ$ < +0.7 (Parkinson and Arculus, 1999 and references therein). Thus, microprobe and Mössbauer analyses of chromites collectively yield an $fO_2$ for the Finnish rocks of -1.5<$\Delta FMQ$<+1.4. For comparison, arc-related lavas typically have redox states that vary from ~FMQ to as high as ~FMQ+6 (as summarized in Lee et al., 2003). In contrast, estimates for the oceanic mantle as sampled by MORB and abyssal peridotites are typically ~FMQ to FMQ-2. Although the entire range of $fO_2$ values obtained for the Jeesiörova rocks overlap with some relatively rare, least oxidized arc rocks, they are lower than most arc-related rocks. Instead, the $fO_2$ estimates for the Jeesiörova rocks are indistinguishable from those for the non-arc oceanic mantle. The range of $fO_2$ values for the Finnish rocks is also indistinguishable from the empirical estimates of $fO_2$ based on the whole-rock V systematics of the Al-undepleted komatiitic basalts from Fred's Flow in the Munro Township (Canil and Fedortchouk, 2001) and, in general, with those for the Archean Al-undepleted komatiites (Canil. 1999). This suggests that the redox states during the partial melting

of sources for both the Al-undepleted Munro rocks and Ti-rich Finnish rocks were not significantly different.

### 3.6.2. Are the Jeesiörova komatiites Ti-enriched?

As noted earlier, the $TiO_2$ contents in the Jeesiörova rocks are significantly higher than those at a given MgO level of both the Al-depleted Barberton rocks and the Al-undepleted Abitibi rocks (Fig. 3.1B). The $TiO_2$ contents of the chromites in the Finnish rocks are also higher than those in chromites from Al-undepleted komatiites with similar aluminum contents reported from Munro Township, Canada (Arndt et al., 1977) and Vetreny, Russia (Puchtel et al., 1996; Fig. 3.7B). Combined, these chemical characteristics suggest that the Jeesiörova rocks, when compared to the Al-undepleted or Al-depleted komatiites, are enriched in Ti relative to Al.

Actual Ti enrichment relative to similarly incompatible elements (Eu, Gd) in komatiites is, however, rare. For example, the entire range of Ti/Ti* in the Al-undepleted and Al-depleted komatiites is 0.6-1.1, and that in the Jeesiörova rocks is 0.9-1.3 (Fig. 3.10). Nevertheless, elevated abundances of Ti, similar to those in Jeesiörova rocks, are also found in komatiites from the presumed extension of the Lapland complex in the Karasjok greenstone belt, northern Norway (Barnes and Often, 1990), mafic-ultramafic lavas and sills (MgO ~14-30 wt.%) from the Onega plateau in the SE Baltic Shield (Puchtel et al., 1998), and picritic rocks from Baffin Bay, West Greenland (Clarke, 1970; Francis, 1985).

### 3.6.3. Higher relative Ti abundance as a feature of the mantle source

Based on consideration of the major and trace element characteristics of the Ti-rich komatiites from the Karasjok greenstone belt, northern Norway, Barnes and

Often (1990) concluded that the Ti-rich nature of the Norwegian rocks is unlikely to be a result of (a) post-magmatic alteration, (b) crystal-liquid fractionation, (c) crustal contamination or (d) lower degrees of melting. These possibilities for the Jeesiörova rocks are briefly considered below.

First, it is possible that elevated abundances of some HFSE, such as Ti, Zr, Hf could result from the loss of other elements or addition of HFSE during some stage of alteration. However, the elements Ti, Zr and Hf are among the least mobile elements during alteration of komatites (e.g., Arndt, 1994), and there are strong negative correlations on plots of MgO versus $TiO_2$ (see Hanski et al., 2001), Zr and Hf in the Jeesiörova rocks. This strongly suggests that Ti abundances were not significantly affected during secondary alteration.

Second, precipitation of some phases in which Ti is incompatible (e.g., olivine, clinopyroxene) could potentially lead to high concentrations of Ti in differentiated magmas. Based on petrographic observations and positive correlations of whole-rock MgO with Ni, Cr (Appendix 1) and S concentrations (E. Hanski, unpubl. data), it is likely that olivine, chromite and sulfide were the only early co-precipitating phases in these rocks. Simple mass-balance calculations, using Cr concentrations in the chromites (Table 3.1) and whole rocks (Hanski et al., 2001), suggest that chromites and sulfides constitute only a minor fraction of the whole rocks (<1 wt.%), and their crystallization could not have affected Ti abundances. Olivine, the only major fractionating phase in these rocks, cannot contribute to higher Ti concentrations of the Jeesiörova komatiites at a given MgO content of the Al-

undepleted and Al-depleted komatiites. Consequently, crystal-liquid fractionation cannot be responsible for the elevated abundances of Ti in these rocks.

The Jeesiörova parental magmas are also unlikely to have suffered a large degree of contamination by old continental crustal materials. The LREE-depleted nature and [143]Nd-enriched initial isotopic composition of the Jeesiörova rocks ($\varepsilon_{Nd}$ ~+4) is consistent with their derivation from a source similar to the contemporaneous depleted model mantle (DePaolo, 1981), suggesting that these komatiites were not significantly crustally contaminated by typical continental crustal materials.

Finally, the enrichment in Ti in the Jeesiörova komatiites is also probably not a result of lower degrees of partial melting of the mantle source than for the Munro or Barberton type rocks. Higher Ti abundances in magmatic rocks as a function of degrees of partial melting are normally accompanied by corresponding increase in LREE/MREE ratios. For example, elevated Ti abundance in picrites from both Hawaii and Finnish Lapland are accompanied by corresponding increases in Ce/Sm ratios (Fig. 3.10). No such correlation is observed for the Jeesiörova komatiites, and instead, the komatiite samples with the most elevated Ti concentrations (and also highest Ti/Ti*) are the most LREE-depleted. Consequently, it is difficult to envision a melting scenario in which the Ti-rich Jeesiörova rocks could have been produced from an LREE-depleted mantle source, similar to that for the Munro komatiites, due solely to lower degrees of melting. It is more likely that either the mantle source for the Jeesiörova komatiites had higher relative Ti and other trace element concentrations, and/or the primary Jeesiörova magmas underwent subsequent
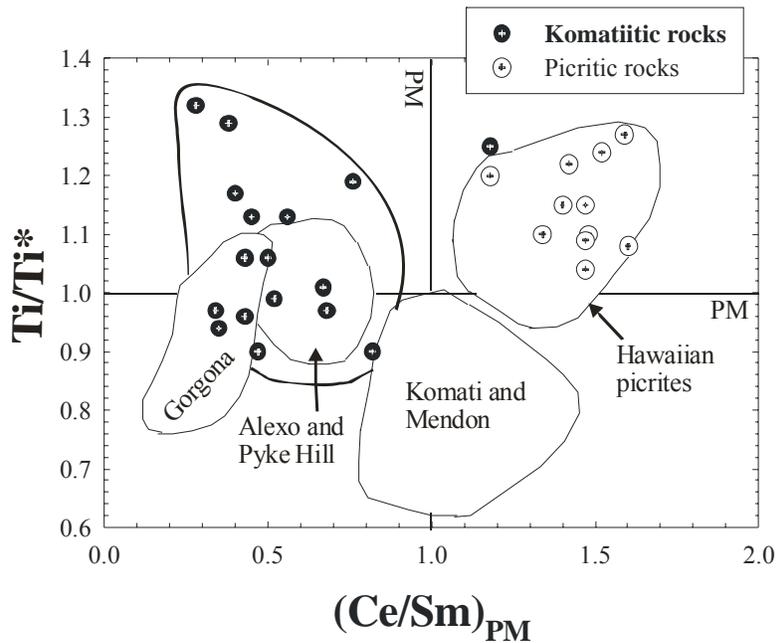
**Fig. 3.10.** Plot of primitive mantle (PM)-normalized Ce/Sm ratios versus Ti/Ti* in the whole rocks of selected suites of magmatic rocks. Data sources are as in Fig. 1. Also plotted for reference are picritic rocks in the Finnish Lapland (Hanski et al., 2001). The fields of the Gorgona ultramafic rocks (MgO > 11 wt.%) and the Hawaiian picrites are drawn after Révillon et al. (2000) and Norman and Garcia (1999), respectively. The fields of Gorgona, Alexo and Pyke Hill, and Komati and Mendon exclude one outlier from each of their respective datasets. The thick solid line, excluding one outlier, defines the field for Jeesiörova komatiitic rocks of this study. Note that the Finnish komatiites and those from Gorgona and the Abitibi greenstone belt (Alexo and Pyke Hill) have similar degrees of LREE-depletion [(Ce/Sm)$_{PM}$ ratios]. Also note that, in contrast to the picritic rocks from Hawaii and the Finnish Lapland, the higher positive Ti anomalies in the Jeesiörova komatiites are not accompanied by corresponding increases in (Ce/Sm)$_{PM}$ ratios.

selective enrichment in these elements *en route* to the surface. These possibilities are discussed below.

### 3.6.4. Consideration of alternative petrogenetic processes

The high Ti concentrations of the Jeesiörova komatiites could have potentially resulted from selective assimilation of Ti-rich phases by a komatiitic primary magma with normal concentrations of Ti and similarly incompatible elements during ascent of the magma through the lithosphere. The elevated Ti and Zr abundances in the Jeesiörova komatiites are coupled with slightly suprachondritic Zr/Hf ratios (typically 42-46 relative to the chondritic value of 36; McDonough and Sun, 1995). Moreover, the rocks show a broad positive correlation between Ti/Ti* and Zr/Zr*, and the samples that have the highest values of Ti/Ti* also typically have the largest positive Zr anomalies (Zr/Zr* up to 1.7; Fig. 3.9A). Some Ti-rich minerals (e.g., rutile, armalcolite, loveringite) produced by metasomatism within lithospheric mantle, as sampled by peridotite xenoliths extracted from sub-continental lithospheric mantle (SCLM), commonly show high abundances of HFSE and also suprachondritic Zr/Hf ratios (up to 58; Kalfoun et al., 2002). The very low modal abundances (40-200 ppm) of these minerals can account for >50% of HFSE budgets in some whole-rock peridotite xenoliths (Kalfoun et al., 2002). Ti-rich metasomatic mineral assemblages (rutile, ilmenite, armalcolite) have also been documented in harzburgitic oceanic mantle xenoliths from the Kerguelen Islands that are likely to have crystallized at temperatures of ~1200°C, consistent with the relatively low melting temperatures for these minerals (Grégoire et al., 2000).

The possibility of selective assimilation of Ti-rich phases by low-Ti primary melts in the generation of Ti-enriched Jeesiörova ultramafic magmas is consistent with some experimental studies. For example, the dissolution rate experiments of Wagner and Grove (1997) suggest that Ti-rich oxide minerals, such as ilmenite, dissolve ~ 3 times faster than clinopyroxene in a typical mineral assemblage in the lunar mantle. They inferred that some high-Ti lunar magmas were produced from low-Ti primitive magmas via assimilation of ilmenite-rich assemblages at shallow levels. Similarly, high-pressure and high-temperature melting experiments on terrestrial picritic basalt compositions suggest that near-solidus melts produced from armalcolite- (± ilmenite)-bearing peridotites have very high $TiO_2$ contents ($\geq$20 wt.%; Xirouchakis et al., 2001), consistent with preferential non-modal melting of Ti-rich phases.

It might also be expected that significant interaction of parental melts with SCLM would lead to a reduction in the initial $^{187}Os/^{188}Os$ of the magmas. This is because it is commonly observed that SCLM has depleted $^{187}Os/^{188}Os$ relative to contemporaneous convective upper mantle as a result of prior Re depletion (Walker et al., 1989). For example, combined Os-Nd isotope characteristics have been used to support up to ~50% contribution of lithospheric components in the generation of ~190 Ma Karoo picrites (Ellam et al., 1992). This interpretation was based on the correspondence of the Karoo picrites on an Os-Nd isotope diagram with the calculated mixing array plotting between the assumed plume (both high $\gamma_{Os}$ and $\varepsilon_{Nd}$) and SCLM (depleted $\gamma_{Os}$ and low $\varepsilon_{Nd}$) end members. Another manifestation of such a process is the ~2.7 Ga Al-depleted picritic rocks from Boston Creek (Abitibi

greenstone belt) with strongly depleted initial Os isotopic composition ($\gamma_{Os}$= -3.8±0.5; Walker and Stone, 2001). The chondritic Os isotopes, combined with the depleted mantle-like Nd isotopic composition of the Jeesiörova rocks, on the other hand, agues against bulk mixing of large proportions of these components, as a mixing array rather than uniform Nd-Os isotopic compositions for these rocks would be expected.

The uniform chondritic initial Os isotopic composition of these rocks may suggest that either (a) Ti-rich lithospheric minerals were not involved, (b) insufficient time between the metasomatic event(s) that produced the Ti-rich mineral assemblages and the melting of the metasomatic minerals precluded significant enrichment or depletion in $^{187}$Os relative to that of the contemporaneous lithospheric mantle, or (c) Os concentrations in the putative Ti-rich mineral assemblages were significantly lower than in the primitive Jeesiörova magmas. Consistent with the last possibility, the Ti-rich phases (picroilmenite) in alkaline ultramafic magmas from Norseman-Wiluna belt, Western Australia have very low concentrations of Os (0.02-0.03 ng/g; Graham et al., 2002) that are 2 orders of magnitude lower than those in whole-rock Jeesiörova komatiites (Table 3.2). In the absence of Os concentrations and isotopic compositions of Ti-rich metasomatized mineral assemblages in xenoliths from representative SCLM that the Jeesiörova magmas have traversed, the likelihood of the last two possibilities, however, cannot yet be evaluated.

Alternatively, the high concentrations of Ti and similarly incompatible elements, combined with their radiogenic initial Nd isotopic composition ($\varepsilon_{Nd}$ ~+4: Hanski et al., 2001) and LREE-depleted nature may have resulted from enrichment of the mantle source by basaltic melt or incorporation of young recycled mafic oceanic

crust (similar to MORB) into the mantle source for these rocks. This possibility is also consistent with the higher average abundance of most incompatible elements of the Jeesiörova komatiites relative to typical Al-undepleted and Al-depleted komatiites. Furthermore, enrichment of peridotite source by mafic melt leads to increase in Re concentrations, so this process could account for higher relative Re concentrations in these komatiites. The high Re/Os ratios of the mantle source, over time, would potentially lead to growth of suprachondritic $^{187}Os/^{188}Os$. Therefore, the chondritic initial $^{187}Os/^{188}Os$ of the Jeesiörova rocks suggests that mafic enrichment could not have occurred more than about 200 Ma prior to komatiite production (see Walker et al., 1991).

Prior mafic melt enrichment, however, is not consistent with all aspects of the Jeesiörova komatiites. For example, the presence of uniform negative Nb anomalies in the Jeesiörova komatiites (Figs. 3.3 and 3.8B) cannot be readily reconciled with the model of trace element enrichement via addition of basaltic melt or recycled oceanic crust to their mantle source. Present-day MORB does not have negative Nb anomalies, and, therefore, the possibility of recycling of oceanic crust would require that the primary Jeesiörova asthenospheric melt possessed negative Nb anomalies to begin with, a possibility for which there are no known analogs.

## 3.7. CONCLUSIONS

The Jeesiörova komatiites have subchondritic $Al_2O_3/TiO_2$ ratios and HREE-depletion ($Gd/Yb_{CN}>1$), similar to those typically observed in Al-depleted komatiites. We have demonstrated that the subchondritic $Al_2O_3/TiO_2$ ratios in the Jeesiörova rocks are not a result of depletion in Al, rather due to high concentrations of Ti at a

given MgO content relative to both Al-undepleted and Al-depleted komatiites. The Jeesiörova rocks also have overall high concentrations of incompatible elements relative to the latter two types of komatiites. These rocks thus represent a chemically distinct type of komatiite.

The whole rock major and trace element characteristics (e.g., absence of depletion in Al corresponding to HREE-depletion), and redox state (~FMQ) derived from chemical composition of chromite are not consistent with either of the two petrogenetic models suggested for the Al-depleted rocks, majorite fractionation in the deep mantle or subduction-related hydrous melting.

The high relative Ti and similarly incompatible element concentrations in these rocks may suggest [1] preferential melting of Ti-rich metasomatized mineral assemblage in the lithospheric mantle or [2] contamination of primary asthenospheric melt by LREE-depleted young oceanic crust. The characteristic negative Nb anomalies in Jeesiörova rocks, however, are not consistent with any of these models.

**Acknowledgements**

his editorial handling, incisive comments and helpful suggestions. This work was supported by NSF Grant 9909197 and is gratefully acknowledged.

# CHAPTER 4: Geochemical evidence for anhydrous melting for the origin of komatiites at Dundonald Beach, Ontario, Canada

**Abstract**

The major and trace elements of whole rocks, and chemical compositions of primary igneous minerals (chromite and clinopyroxene) were examined for a suite of cumulate and spinifex-textured komatiitic flows from the Dundonald Beach area in the Abitibi greenstone belt, Ontario, Canada, in order to evaluate their possible origin through subduction-related hydrous melting. These komatiites and komatiitic basalts have near-chondritic $Al_2O_3/TiO_2$ ratios (21-26 versus ~22) and chondrite-normalized unfractionated heavy rare-earth element (HREE) pattern ($Gd/Yb_{CN}$ ~1), similar to those in the Al-undepleted komatiites from the spatially associated Alexo and Munro Townships. Unlike crustally contaminated komatiites from elsewhere, the degrees of LREE depletion and the absence of significant negative Nb anomalies in the Dundonald rocks ($Nb/La_{CN}$ ~ 0.8-1) are similar to those of komatiites from Alexo and Munro Townships, also of the Abitibi greenstone belt, that have unradiogenic Pb and radiogenic Nd isotopic compositions. This suggests that the Dundonald parental magma underwent minimal or no crustal contamination.

On a plot of Wo contents [Ca/(Ca+Mg+Fe$^{2+}$)] versus Mg# [Mg/(Mg+Fe$^{2+}$)] of preserved clinopyroxenes, the Dundonald rocks cluster between the fields for those

produced in an experimental study of Al-depleted komatiites under anhydrous and H$_2$O-saturated conditions. Thus, the clinopyroxene compositions of Dundonald rocks provide evidence neither against nor in favor of a hydrous nature of the Dundonald parental magmas. However, the strong positive correlation between Ce/Yb$_{CN}$ and H$_2$O/Yb ratios, that is observed in N-MORB and Hawaiian plume-related rocks, amy indicate a low H$_2$O content (<0.04 wt.%) for the Dundonald rocks. Additionally, chromites in the Dundonald komatiites have significantly lower Cr#, at a given Mg#, than chromites in modern arc-related rocks, such as Phanerozoic boninites, suggesting a relatively less refractory mantle source for the Dundonald komatiites.

Compositional homogeneity of the Al-undepleted komatiitic rocks of the Kidd-Munro assemblage, extending over an area of ~180 x 12 Km$^2$, contrast with major compositional heterogeneity manifested over short distances for island arc lavas. Combined, these geochemical characteristics of komatiitic rocks from the Kidd-Munro assemblage suggest their derivation from an essentially anhydrous, non-arc oceanic mantle.

**4.1. INTRODUCTION**

There are currently two contrasting petrogenetic models for the generation of komatiites. According to the widely accepted plume-based model, komatiites are products of high degrees of partial melting (30-40%) of ascending mantle plumes. In the plume model, the Al-depleted komatiites (with subchondritic Al$_2$O$_3$/TiO$_2$ ratio of ~6-12), such as those in the early Archean Barberton Mountainland greenstone belt, are generated via melting of essentially anhydrous mantle where majorite garnet is either a residual phase after melting or it separates from the ascending magma in the

deep mantle (> 14 GPa; e.g., Kato et al., 1988; Ohtani et al., 1989; Herzberg, 1992; McDonough and Ireland, 1993). Consistent with this model, Al-undepleted komatiites (with chondritic $Al_2O_3/TiO_2$ ratio of ~20), such as those from the Alexo and Pyke Hill areas in the late Archean Abitibi greenstone belt, Canada are likely to be produced as a result of partial melting of a mantle source in the shallow mantle (< 14 GPa) (Arndt, 1986; Campbell et al., 1989). This model of komatiite petrogenesis has been subsequently challenged based on experimental studies of Al-depleted komatiites under anhydrous and $H_2O$-saturated conditions (Parman et al., 1997). The experimental studies of Parman et al. (1997) have demonstrated that the clinopyroxene produced under anhydrous versus $H_2O$-saturated conditions have distinctly different compositions, and the compositions of natural clinopyroxene from the Al-depleted komatiites from the Komati Formation of the Barberton Mountainland plot within the field of clinopyroxene produced under experimental $H_2O$-saturated conditions. These observations, combined with some geochemical similarities between Al-depleted komatiites and those for modern arc-related rocks, such as Phanerozoic boninites, were used to suggest a subduction-related hydrous melting origin for Al-depleted komatiites (Parman et al., 1997; Parman et al., 2003). Attempts have also been made to suggest a subduction origin for Al-undepleted komatiites from other greenstone belts, such as Abitibi greenstone belt (Grove et al., 1999; Kerrich et al., 1998; Grove and Parman, 2004). Here we examine the major and trace elemement characteristics of a suite of Al-undepleted komatiites from Dundonald Beach in the Abitibi greenstone belt and the chemical compositions of their primary igneous minerals (chromite and clinopyroxene). The geochemical

characteristics of the Dundonald rocks are compared with stratigraphically-equivalent Al-undepleted komatiites from spatially associated Alexo and Munro Townships, part of the same Kidd-Munro volcanic assemblage, in order to evaluate the possibility of a subduction-related, hydrous melting origin for Al-undepleted komatiites.

## 4.2. GEOLOGICAL SETTING

"Dundonald Beach" is locally referred to a glacially-exposed outcrop of volcano-sedimentary rocks that covers approximately 150 x 60 $m^2$ area in the SW part of the Dundonald Township, northern Ontario (Davis, 1999). These rocks are part of the 2710-2719 Ma "Kidd-Munro assemblage" of ultramafic, mafic and felsic volcanic rocks, exposed over an area of 180 x 12 $km^2$ that extends from the Kidd-Creek area in the west to the Ontario-Quebec border in the east (Jackson and Fyon, 1991; Barnes et al., 1983; Barnes, 1985; Barnes and Naldrett, 1987; Nunes and Pyke, 1980; Barrie et al., 1999; Bleeker et al., 1999; Ayer et al., 2002). The volcanic rocks in the Dundonald Beach area include volumetrically dominant basalts (~75%) with relatively minor komatiitic rocks (~10%), calc-alkaline basalts to rhyolites (~10%), and differentiated volcanics (~5 %: Barrie, 1999; Fig. 4.1).

The Dundonald Beach komatiites and komatiitc basalts have been the subject of several recent studies (e.g., Davis 1997, 1999; Houlé et al., 2002; Cas et al., 2003). According to these and other previous studies, the volcano-sedimentary succession in this area is divided into three members (Fig. 4.1). *Member IA* is comprised of several thin, undifferentiated, non-cumulate sills of komatiitic basalt, porphyritic komatiitic basalt, komatiitic pyroxenite and intercalated graphitic argillaceous metasedimentary
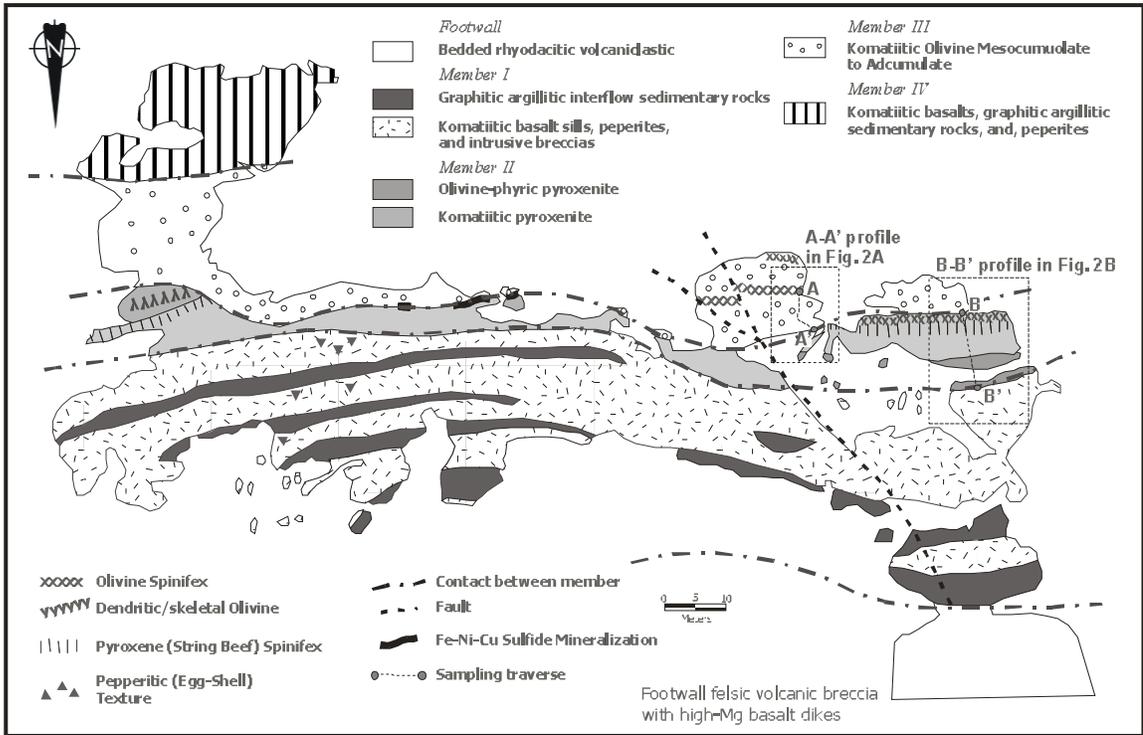
**Figure 4.1.** Geological map of the Dundonald Beach area showing major rock types.

rocks (Davis 1997, 1999). *Member IB* consists of a differentiated, non-cumulate komatiitic pyroxenite flow exhibiting a lower olivine-clinopyroxene cumulate zone, a thick parallel acicular ("string-beef") pyroxene spinifex-textured zone, a thin randomly platy olivine spinifex-textured zone, and a very thin, very fine-grained, upper "chilled" margin (Davis 1999). *Member IC* is comprised of multiple differentiated cumulate komatiite flows/sills with thick lower olivine mesocumulate zones and thin upper olivine spinifex-textured zones (Davis 1997, 1999, Houlé et al., 2002). Fe-Ni-Cu sulfide mineralization is present at the base of several of the komatiitic peridotites. One relatively rare structure, called peperite (or "egg-shell") that is commonly found in the graphitic argillites underlying the komatiitic basalts are interpreted as resulting from intrusion of the komatiitic magmas into the unconsolidated, water-saturated sediments (Houlé et al., 2002; Cas et al., 2003). Thus, although most komatiites in the Kidd-Munro assemblage are interpreted as lava flows (e.g., Arndt et al., 1977; Arndt, 1986; Lahaye and Arndt, 1996), the Dundonald komatiites show evidence for shallow-level intrusions (Arndt et al., in press).

The Dundonald Beach rocks are exposed on the southern limb of a large anticlinal fold, and strike roughly east-west and dip steeply to the south (Davis, 1999). A shear zone runs roughly parallel to the contact between the komatiites and the underlying felsic volcanic rocks. The Dundonald Beach rocks have been metamorphosed to regional lower greenschist facies (Jolly, 1982), and are locally faulted and/or sheared, but primary structures and igneous textures are generally well preserved.

All whole-rock samples examined here were collected from two complete surface flows. One flow consists of a basal olivine-bearing cumulate zone and an overlying platy and random spinifex-textured zone (from *Member IC*; labelled Section A-A' in Fig 4.1). The detailed section of this flow including sample locations is shown in Fig. 4.2. The second unit is komatiitic basalt, composed of a basal olivine-clinopyroxene cumulate zone, pyroxene spinifex, olivine spinifex and an upper chilled margin (from *Member IB*). This flow is labelled Section B-B' in Fig. 4.1, and the detailed section, including sample locations is shown in Fig. 4.2.

## 4.3. Analytical techniques

### 4.3.1. Major and Trace elements

The major element data were obtained by wavelength-dispersive X-ray fluorescence spectrometry (WD-XRFS) of fused glass disks at the University of Western Ontario. The concentrations of Ni, Cu, Co, Cr, V and Zn were determined by WD-XRFS of pressed powder pellets. Other trace elements, including rare-earth elements (REE) and highly incompatible lithophile elements, were determined by inductively-coupled plasma mass spectrometry (ICP-MS) at the Ontario Geoscience Laboratories following a 10-day, mixed-acid, closed-beaker digestion using the method of Tomlinson et al. (1999). Comparison of routine sample replicates indicates that major elements (>1 wt.%) are precise to within 2% of the amount present, minor elements (1-0.1 wt.%) to within 5% of the amount present, and trace elements (<0.1 wt.%) to within 5-10% of the amount present. Furthermore, a comparison of data obtained for trace elements analyzed by the Ontario Geosciences Laboratories (e.g., Sproule et al., 2002) with samples from the same outcrops from different studies (e.g.,
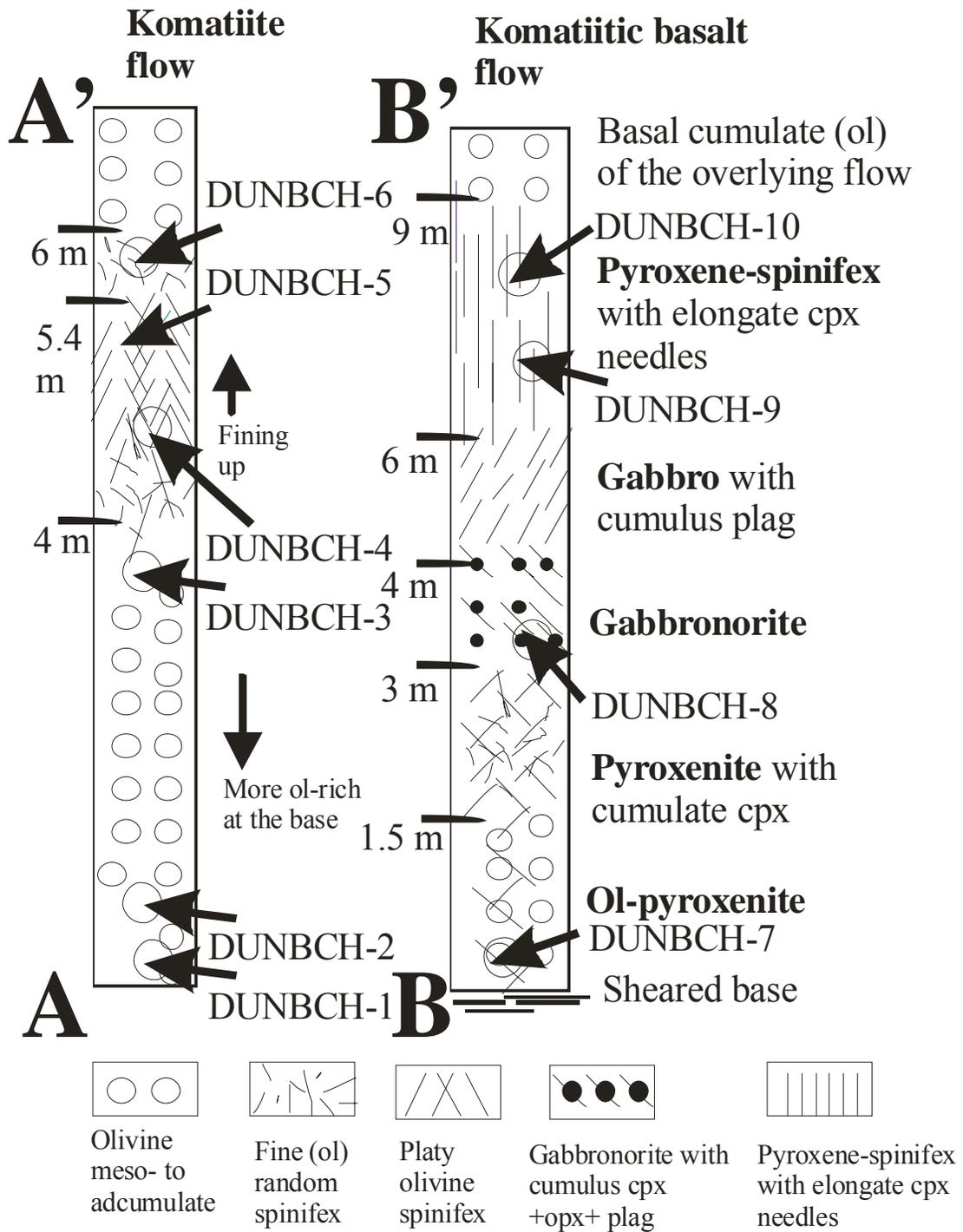
**Figure 4.2.** Stratigraphic section of (A) the komatiite and (B) komatiitic basalt units sampled in this study.

Arndt and Nesbitt, 1982; Xie et al., 1993; Fan and Kerrich, 1997; this study) yield comparable results. The whole-rock major element oxides and trace element data are presented in Table 4.1.

*4.3.2. Microprobe analyses*

The chemical composition data of olivine and chromite were obtained using wavelength dispersive spectrometry (WDS) with a JEOL-8900 Superprobe at the University of Maryland. Both chromite and clinopyroxene were analyzed with a 15 kV accelerating potential. A beam current of 50 nA with 1 $\mu$ beam diameter was used for chromite analyses, whereas the beam current and beam diameter for clinopyroxene analyses were 20 nA and 5 $\mu$, respectively. The peak counting time for clinopyroxene and chromite analyses was 10 s for most elements, and a counting time of 20 s was allowed for Si, Ni and Co. External reproducibility was monitored via analyses of synthetic standards routinely used in the laboratory. Finally, the EPMA data were corrected using ZAF procedure. The composition data for chromite and clinopyroxene are presented in Tables 4.2 and 4.3, respectively.

## 4.4. RESULTS

The Dundonald komatiites and komaiitc basalts have nearly-chondritic $Al_2O_3/TiO_2$ ratios (21-26 versus ~22; McDonough and Sun, 1995) and chondrite-normalized unfractionated HREE pattern ($Gd/Yb_{CN}$ = 0.9-1.1; Table 4.1). These characteristics are similar to those in Al-undepleted komatiites from Alexo and Pyke Hill (e.g., Lahaye and Arndt, 1996; Fan and Kerrich, 1997; Fig. 4.3), and are generally consistent with those observed in Al-undepletd komatiites from elsewhere

**Table 4.1.** Whole-rock major, trace and rare-earth element data for Dundonald Beach suite of komatiitic rocks. All major oxides are recalculated on 100% volatile-free basis (n.d. = not determined; - = below detection limits).

| Samples | Komatiites | | | | | | Komatiitic basalts | |
|---|---|---|---|---|---|---|---|---|
| | DUNBCH -1 | DUNBCH -2 | DUNBCH -3 | DUNBCH -4 | DUNBCH -5 | DUNBCH -6 | DUNBCH -7 | DUNBCH -8 |
| Texture | | | | | | | | |
| Major oxides (wt.%) | | | | | | | | |
| $SiO_2$ | 44.1 | 44.3 | 44.1 | 43.9 | 44.1 | 45.1 | 50.3 | 50.5 |
| $TiO_2$ | 0.14 | 0.14 | 0.15 | 0.46 | 0.43 | 0.38 | 0.55 | 0.64 |
| $Al_2O_3$ | 3.3 | 3.5 | 3.4 | 11.1 | 9.5 | 8.4 | 11.7 | 14.6 |
| $Fe_2O_3^*$ | 9.6 | 8.5 | 9.4 | 10.7 | 12.9 | 11.7 | 11.6 | 12.3 |
| MnO | 0.10 | 0.12 | 0.13 | 0.24 | 0.20 | 0.17 | 0.22 | 0.18 |
| MgO | 42.3 | 42.9 | 42.2 | 21.2 | 22.7 | 25.2 | 12.6 | 8.4 |
| CaO | 0.16 | 0.14 | 0.29 | 12.09 | 9.78 | 8.63 | 11.23 | 10.20 |
| $Na_2O$ | 0.00 | 0.00 | 0.00 | 0.00 | 0.00 | 0.00 | 0.97 | 2.06 |
| $K_2O$ | 0.00 | 0.00 | 0.01 | 0.00 | 0.00 | 0.00 | 0.75 | 1.06 |
| $P_2O_5$ | 0.01 | 0.01 | 0.01 | 0.03 | 0.02 | 0.03 | 0.04 | 0.05 |
| $Cr_2O_3$ | 0.31 | 0.29 | 0.31 | 0.29 | 0.40 | 0.42 | 0.16 | 0.05 |
| LOI | 12.45 | 12.75 | 12.35 | 4.84 | 5.57 | 6.29 | 2.26 | 1.92 |
| Mg#[1] | 0.90 | 0.91 | 0.90 | 0.80 | 0.78 | 0.81 | 0.68 | 0.58 |
| $Al_2O_3/TiO_2$ | 24 | 26 | 23 | 24 | 22 | 22 | 21 | 23 |
| $CaO/Al_2O_3$ | 0.05 | 0.04 | 0.08 | 1.1 | 1.0 | 1.0 | 0.96 | 0.70 |
| Trace elements (ppm) | | | | | | | | |
| Cu | n.d. | n.d. | n.d. | 27 | 24 | 30 | 52 | 68 |
| Zn | 30 | 33 | 36 | 72 | 81 | 69 | 75 | 84 |
| Ni | 2844 | 2659 | 2688 | 829 | 765 | 1082 | 118 | 70 |
| Cr | 1528 | 1546 | 1621 | 1823 | 2782 | 2585 | 1022 | 303 |
| V | 61 | 54 | 63 | 171 | 162 | 144 | 225 | 249 |
| Zr | 7.6 | 6.8 | 8.3 | 25.4 | 23.4 | 19.4 | 32.4 | 37.3 |
| Nb | n.d. | n.d. | n.d. | 0.6 | 0.6 | 0.4 | 1 | 1.2 |
| Y | 2.9 | 2.8 | 3.3 | 11.8 | 10.1 | 8.4 | 14.1 | 16.1 |
| Sr | 4.4 | 3.3 | 5.2 | 3.6 | 4.1 | 3.5 | 87.4 | 139.8 |
| Rb | 1.57 | 1.83 | 2.09 | 0.59 | 1.36 | 1.87 | 22.38 | 34.22 |
| Cs | 0.72 | 0.79 | 0.91 | 0.41 | 0.72 | 1.04 | 0.45 | 0.40 |
| Ba | n.d. | n.d. | n.d. | 12 | n.d. | n.d. | 92 | 91 |
| U | 0.02 | 0.01 | 0.01 | 0.02 | 0.02 | 0.02 | 0.04 | 0.05 |
| Co | 101 | 103 | 96 | 77 | 85 | 90 | 56 | 47 |
| Ta | n.d. | n.d. | n.d. | 0.19 | 0.21 | 0.20 | 0.22 | 0.23 |
| Hf | 0.2 | 0.2 | 0.2 | 0.7 | 0.7 | 0.6 | 0.9 | 1 |
| Rare-earth elements (ppm) | | | | | | | | |
| La | 0.31 | 0.25 | 0.22 | 0.73 | 0.64 | 0.51 | 1.27 | 1.49 |
| Ce | 0.58 | 0.54 | 0.64 | 2.20 | 1.86 | 1.54 | 3.52 | 4.18 |
| Pr | 0.12 | 0.11 | 0.11 | 0.40 | 0.36 | 0.31 | 0.60 | 0.71 |
| Nd | 0.70 | 0.76 | 0.68 | 2.35 | 2.00 | 1.71 | 3.26 | 3.88 |
| Sm | 0.31 | 0.28 | 0.24 | 1.03 | 0.98 | 0.68 | 1.26 | 1.58 |
| Eu | 0.12 | 0.14 | 0.14 | 0.53 | 0.25 | 0.19 | 0.51 | 0.55 |
| Gd | 0.41 | 0.40 | 0.45 | 1.48 | 1.37 | 1.12 | 1.96 | 2.20 |
| Tb | 0.08 | 0.07 | 0.08 | 0.28 | 0.27 | 0.22 | 0.35 | 0.40 |
| Dy | 0.53 | 0.49 | 0.53 | 1.96 | 1.78 | 1.38 | 2.47 | 2.68 |
| Ho | 0.11 | 0.11 | 0.11 | 0.44 | 0.41 | 0.34 | 0.53 | 0.58 |
| Er | 0.34 | 0.34 | 0.37 | 1.32 | 1.25 | 0.98 | 1.57 | 1.69 |
| Tm | 0.05 | 0.05 | 0.06 | 0.19 | 0.17 | 0.15 | 0.26 | 0.29 |
| Yb | 0.36 | 0.32 | 0.37 | 1.16 | 1.16 | 0.95 | 1.52 | 1.68 |
| Lu | 0.05 | 0.06 | 0.06 | 0.19 | 0.18 | 0.14 | 0.25 | 0.27 |
| ΣREE | 4.09 | 3.92 | 4.07 | 14.26 | 12.67 | 10.21 | 19.33 | 22.18 |
| Ratios | | | | | | | | |
| $(La/Sm)_{CN}$ | 0.62 | 0.56 | 0.57 | 0.44 | 0.41 | 0.47 | 0.63 | 0.59 |
| $(Ce/Yb)_{CN}$ | 0.42 | 0.44 | 0.45 | 0.50 | 0.42 | 0.43 | 0.61 | 0.65 |
| $(Gd/Yb)_{CN}$ | 0.9 | 1.0 | 1.0 | 1.0 | 1.0 | 1.0 | 1.0 | 1.1 |
| $(Nb/La)_{CN}$ | - | - | - | 0.81 | 0.93 | 0.77 | 0.78 | 0.80 |

**Table 4.1** (continued)

| Samples | Komatiitic basalts | | | | | | |
|---|---|---|---|---|---|---|---|
| | DUNBCH -9 | DUNBCH -10 | DUNBCH -11 | DUNBCH -12 | DUNBCH -13 | DUNBCH -14 | DUNBCH -15 |
| Texture | | | | | | | |
| Major oxides (wt.%) | | | | | | | |
| $SiO_2$ | 47.8 | 47.9 | 44.0 | 44.2 | 49.2 | 48.7 | 49.2 |
| $TiO_2$ | 0.56 | 0.56 | 0.26 | 0.28 | 0.44 | 0.56 | 0.56 |
| $Al_2O_3$ | 12.7 | 12.0 | 6.4 | 6.4 | 10.2 | 13.7 | 13.3 |
| $Fe_2O_3^*$ | 12.9 | 12.6 | 12.5 | 12.9 | 12.0 | 11.9 | 11.1 |
| MnO | 0.22 | 0.21 | 0.18 | 0.18 | 0.22 | 0.21 | 0.20 |
| MgO | 12.5 | 12.2 | 30.9 | 30.5 | 14.7 | 9.2 | 12.0 |
| CaO | 11.61 | 13.65 | 5.12 | 5.13 | 11.62 | 13.47 | 11.33 |
| $Na_2O$ | 0.36 | 0.01 | 0.02 | 0.02 | 0.73 | 0.15 | 0.38 |
| $K_2O$ | 1.10 | 0.74 | 0.00 | 0.00 | 0.74 | 1.93 | 1.89 |
| $P_2O_5$ | 0.04 | 0.04 | 0.02 | 0.02 | 0.03 | 0.04 | 0.03 |
| $Cr_2O_3$ | 0.12 | 0.10 | 0.61 | 0.40 | 0.20 | 0.06 | 0.07 |
| LOI | 2.98 | 2.72 | 7.39 | 6.77 | 2.38 | 2.66 | 3.09 |
| Mg#[1] | 0.66 | 0.66 | 0.83 | 0.82 | 0.71 | 0.60 | 0.68 |
| $Al_2O_3/TiO_2$ | 23 | 22 | 25 | 23 | 23 | 24 | 24 |
| $CaO/Al_2O_3$ | 0.91 | 1.1 | 0.80 | 0.81 | 1.1 | 0.98 | 0.85 |
| Trace elements (ppm) | | | | | | | |
| Cu | 67 | 57 | 17 | 16 | 44 | 69 | 21 |
| Zn | 76 | 95 | 60 | 64 | 65 | 66 | 77 |
| Ni | 199 | 178 | 1412 | 1344 | 223 | 115 | 119 |
| Cr | 888 | 708 | 2936 | 1662 | 1139 | 327 | 400 |
| V | 211 | 210 | 99 | 102 | 212 | 210 | 219 |
| Zr | 43 | 43 | 24 | 25 | 34 | 41 | 37 |
| Nb | 5 | 4 | 4 | 3 | 3 | 4 | 4 |
| Y | 18 | 19 | 12 | 12 | 17 | 18 | 18 |
| Sr | 84 | 53 | 13 | 13 | 77 | 91 | 108 |
| Rb | 13 | 5 | 7 | 7 | 25 | 8 | 15 |
| Cs | 0.67 | 0.43 | 1.02 | 0.79 | 0.73 | 0.52 | 0.73 |
| Ba | 90 | 5 | 14 | n.d. | 197 | 28 | 71 |
| U | 0.04 | 0.04 | 0.02 | 0.03 | 0.03 | 0.04 | 0.03 |
| Co | 60 | 61 | 117 | 121 | 67 | 56 | 56 |
| Ta | 0.22 | 0.23 | n.d. | 0.18 | 0.19 | 0.20 | 0.21 |
| Hf | 0.9 | 1 | 0.3 | 0.5 | 0.6 | 0.9 | 0.9 |
| Rare-earth elements (ppm) | | | | | | | |
| La | 5.32 | 5.4 | 1.69 | 1.73 | 3 | 4.09 | 5.78 |
| Ce | 5.63 | 5.99 | 1.96 | 2.02 | 3.39 | 4.55 | 6.38 |
| Pr | 6.55 | 6.96 | 2.42 | 2.4 | 4.02 | 5.85 | 6.98 |
| Nd | 7.09 | 7.53 | 2.67 | 3.17 | 4.55 | 7.05 | 8.10 |
| Sm | 7.97 | 8.72 | 4.12 | 4.05 | 6.35 | 8.18 | 9.19 |
| Eu | 8.53 | 9.7 | 3.64 | 3.87 | 7.85 | 9.02 | 11.4 |
| Gd | 9.16 | 9.82 | 4.29 | 4.65 | 7.55 | 9.66 | 9.49 |
| Tb | 9.22 | 9.89 | 4.27 | 4.68 | 7.12 | 9.78 | 10.08 |
| Dy | 9.62 | 9.84 | 4.36 | 4.46 | 7.63 | 9.97 | 10.16 |
| Ho | 9.65 | 9.84 | 4.18 | 4.25 | 7.91 | 9.69 | 9.85 |
| Er | 9.62 | 9.83 | 3.73 | 4.98 | 7.94 | 10.3 | 9.97 |
| Tm | 9.88 | 10.24 | 4.09 | 5.14 | 7.29 | 10.12 | 9.88 |
| Yb | 8.88 | 9.32 | 4.72 | 4.72 | 7.39 | 9.07 | 9.13 |
| Lu | 9.80 | 9.55 | 4.43 | 5 | 8.01 | 9.80 | 9.47 |
| ΣREE | 18.72 | 19.70 | 7.74 | 8.37 | 13.53 | 18.10 | 20.46 |
| Ratios | | | | | | | |
| $(La/Sm)_{CN}$ | 0.67 | 0.62 | 0.41 | 0.43 | 0.47 | 0.50 | 0.63 |
| $(Ce/Yb)_{CN}$ | 0.63 | 0.64 | 0.41 | 0.43 | 0.46 | 0.50 | 0.70 |
| $(Gd/Yb)_{CN}$ | 1.0 | 1.1 | 0.9 | 1.0 | 1.0 | 1.1 | 1.0 |
| $(Nb/La)_{CN}$ | 0.78 | 0.77 | 0.74 | 0.96 | 0.83 | 0.81 | 0.72 |

**Table 4.2** Representative microprobe analyses of chromites from the Dundonald Beach komatiites. All analyses are average of N analyses obtained from the cores of equant grains.

| Sample | DUNBCH-2 | | DUNBCH-4 | DUNBCH-5 | | DUNBCH-6 | | DUNBCH-9 | |
| --- | --- | --- | --- | --- | --- | --- | --- | --- | --- |
| | Grain-1 | Grain-2 | | Grain-1 | Grain-2 | Grain-1 | Grain-2 | Grain-1 | Grain-2 |
| $SiO_2$ | 0.06 | 0.05 | 0.06 | 0.06 | 0.06 | 0.08 | 0.06 | 0.06 | 0.04 |
| $TiO_2$ | 0.31 | 0.26 | 0.38 | 0.35 | 0.43 | 0.34 | 0.34 | 0.42 | 0.44 |
| $Al_2O_3$ | 13.49 | 13.01 | 14.85 | 14.56 | 16.09 | 14.04 | 13.85 | 14.88 | 14.9 |
| $Cr_2O_3$ | 55.10 | 55.81 | 49.45 | 51.48 | 47.33 | 52.27 | 52.54 | 49.67 | 50.06 |
| $Fe_2O_3$ | 3.75 | 3.67 | 4.04 | 5.01 | 5.37 | 4.79 | 4.80 | 5.67 | 5.38 |
| FeO | 10.23 | 10.47 | 20.74 | 13.33 | 18.51 | 13.05 | 12.48 | 14.55 | 14.75 |
| MnO | 0.17 | 0.16 | 0.24 | 0.19 | 0.23 | 0.18 | 0.21 | 0.19 | 0.19 |
| MgO | 15.26 | 15.1 | 8.48 | 13.33 | 10.03 | 13.43 | 13.75 | 12.48 | 12.4 |
| CaO | 0.00 | 0.00 | 0.05 | 0.01 | 0.04 | 0.00 | 0.01 | 0.02 | 0.02 |
| CoO | 0.05 | 0.04 | 0.07 | 0.05 | 0.06 | 0.06 | 0.05 | 0.07 | 0.06 |
| NiO | 0.18 | 0.20 | 0.08 | 0.13 | 0.13 | 0.15 | 0.14 | 0.10 | 0.10 |
| Total | 98.60 | 98.77 | 98.44 | 98.50 | 98.28 | 98.39 | 98.23 | 98.11 | 98.34 |
| N | 5 | 5 | 5 | 3 | 3 | 4 | 5 | 3 | 6 |
| Mg# | 0.73 | 0.72 | 0.42 | 0.64 | 0.49 | 0.65 | 0.66 | 0.60 | 0.60 |
| Cr# | 0.73 | 0.74 | 0.69 | 0.70 | 0.66 | 0.71 | 0.72 | 0.69 | 0.69 |
| $Fe^{3+}$# | 0.05 | 0.04 | 0.05 | 0.06 | 0.07 | 0.06 | 0.06 | 0.07 | 0.07 |
| $Fe^{3+}/\Sigma Fe$ | 0.25 | 0.32 | 0.21 | 0.34 | 0.28 | 0.33 | 0.34 | 0.34 | 0.33 |

**Table 4.2 (continued**)

| Sample | DUNBCH-10 | | DUNBCH-11 | | DUNBCH-12 | |
|---|---|---|---|---|---|---|
| | Grain-1 | Grain-2 | Grain-1 | Grain-2 | Grain-1 | Grain-2 |
| $SiO_2$ | 0.06 | 0.06 | 0.05 | 0.07 | 0.06 | 0.05 |
| $TiO_2$ | 0.45 | 0.50 | 0.50 | 0.32 | 0.41 | 0.47 |
| $Al_2O_3$ | 14.88 | 15.52 | 16.26 | 12.65 | 14.49 | 16.01 |
| $Cr_2O_3$ | 48.57 | 47.01 | 46.52 | 51.18 | 48.39 | 48.87 |
| $Fe_2O_3$ | 5.88 | 6.65 | 5.75 | 5.21 | 5.62 | 5.46 |
| FeO | 17.68 | 17.44 | 20.74 | 19.92 | 20.73 | 14.58 |
| MnO | 0.20 | 0.21 | 0.24 | 0.25 | 0.23 | 0.22 |
| MgO | 10.49 | 10.68 | 8.74 | 8.86 | 8.51 | 12.64 |
| CaO | 0.13 | 0.16 | 0.00 | 0.02 | 0.03 | 0.01 |
| CoO | 0.06 | 0.07 | 0.18 | 0.07 | 0.08 | 0.06 |
| NiO | 0.09 | 0.13 | 0.11 | 0.06 | 0.09 | 0.14 |
| Total | 98.49 | 98.43 | 99.09 | 98.61 | 98.64 | 98.51 |
| N | 4 | 3 | 5 | 3 | 5 | 4 |
| Mg# | 0.51 | 0.52 | 0.43 | 0.44 | 0.42 | 0.61 |
| Cr# | 0.69 | 0.67 | 0.66 | 0.73 | 0.69 | 0.67 |
| $Fe^{3+}$# | 0.07 | 0.08 | 0.07 | 0.07 | 0.07 | 0.07 |
| $Fe^{3+}/\Sigma Fe$ | 0.23 | 0.34 | 0.27 | 0.26 | 0.27 | 0.34 |

**Table 4.3** Representative microprobe analyses of clinopyroxenes from the Dundonald Beach komatiites. All analyses are averages of N analyses.

| Sample | DUNBCH-7 | | | DUNBCH-13 | | DUNBCH-14 | | | |
|---|---|---|---|---|---|---|---|---|---|
| | Grain-1 | Grain-2 | Grain-3 | Grain-1 | Grain-2 | Grain-1 | Grain-2 | Grain-3 | Grain-4 |
| $SiO_2$ | 52.10 | 52.23 | 52.15 | 53.51 | 62.35 | 51.32 | 51.64 | 50.51 | 51.47 |
| $TiO_2$ | 0.15 | 0.17 | 0.17 | 0.13 | 0.09 | 0.42 | 0.32 | 0.44 | 0.19 |
| $Al_2O_3$ | 3.42 | 3.40 | 3.05 | 2.97 | 2.46 | 2.70 | 2.96 | 2.95 | 3.23 |
| $Cr_2O_3$ | 0.73 | 0.51 | 0.46 | 0.49 | 0.07 | 0.03 | 0.03 | 0.02 | 0.47 |
| FeO* | 6.46 | 6.32 | 7.73 | 6.99 | 8.82 | 14.64 | 12.72 | 17.68 | 6.80 |
| MnO | 0.28 | 0.25 | 0.31 | 0.26 | 0.26 | 0.42 | 0.36 | 0.48 | 0.20 |
| MgO | 17.97 | 18.50 | 17.78 | 17.80 | 13.03 | 13.24 | 14.90 | 12.28 | 17.87 |
| CaO | 16.90 | 16.66 | 16.56 | 18.31 | 12.08 | 17.63 | 17.27 | 15.74 | 18.46 |
| $Na_2O$ | 0.13 | 0.12 | 0.11 | 0.13 | 0.11 | 0.17 | 0.17 | 0.17 | 0.14 |
| Total | 98.14 | 98.16 | 98.32 | 100.59 | 99.27 | 100.57 | 100.37 | 100.27 | 98.83 |
| N | 3 | 5 | 3 | 4 | 3 | 4 | 5 | 4 | 5 |
| Wo | 36.0 | 35.2 | 35.0 | 37.7 | 32.6 | 37.1 | 36.0 | 33.8 | 38.0 |
| En | 53.3 | 54.4 | 52.3 | 51.0 | 48.9 | 38.8 | 43.3 | 36.6 | 51.1 |
| Fs | 10.7 | 10.4 | 12.7 | 11.2 | 18.6 | 24.1 | 20.7 | 29.6 | 10.9 |
| Mg# | 83.2 | 83.9 | 80.4 | 81.9 | 72.5 | 61.7 | 67.6 | 55.3 | 82.4 |

**Table 4.3** (continued)

| Sample | DUNBCH-15 | |
|---|---|---|
| | Grain-1 | Grain-2 |
| $SiO_2$ | 52.01 | 51.87 |
| $TiO_2$ | 0.23 | 0.20 |
| $Al_2O_3$ | 4.76 | 3.30 |
| $Cr_2O_3$ | 0.56 | 0.38 |
| FeO* | 6.97 | 7.52 |
| MnO | 0.32 | 0.19 |
| MgO | 16.74 | 18.17 |
| CaO | 18.92 | 17.97 |
| $Na_2O$ | 0.17 | 0.11 |
| Total | 100.68 | 99.71 |
| N | 5 | 5 |
| Wo | 39.7 | 36.6 |
| Fs | 48.9 | 51.5 |
| En | 11.4 | 11.9 |
| Mg# | 81.1 | 81.2 |
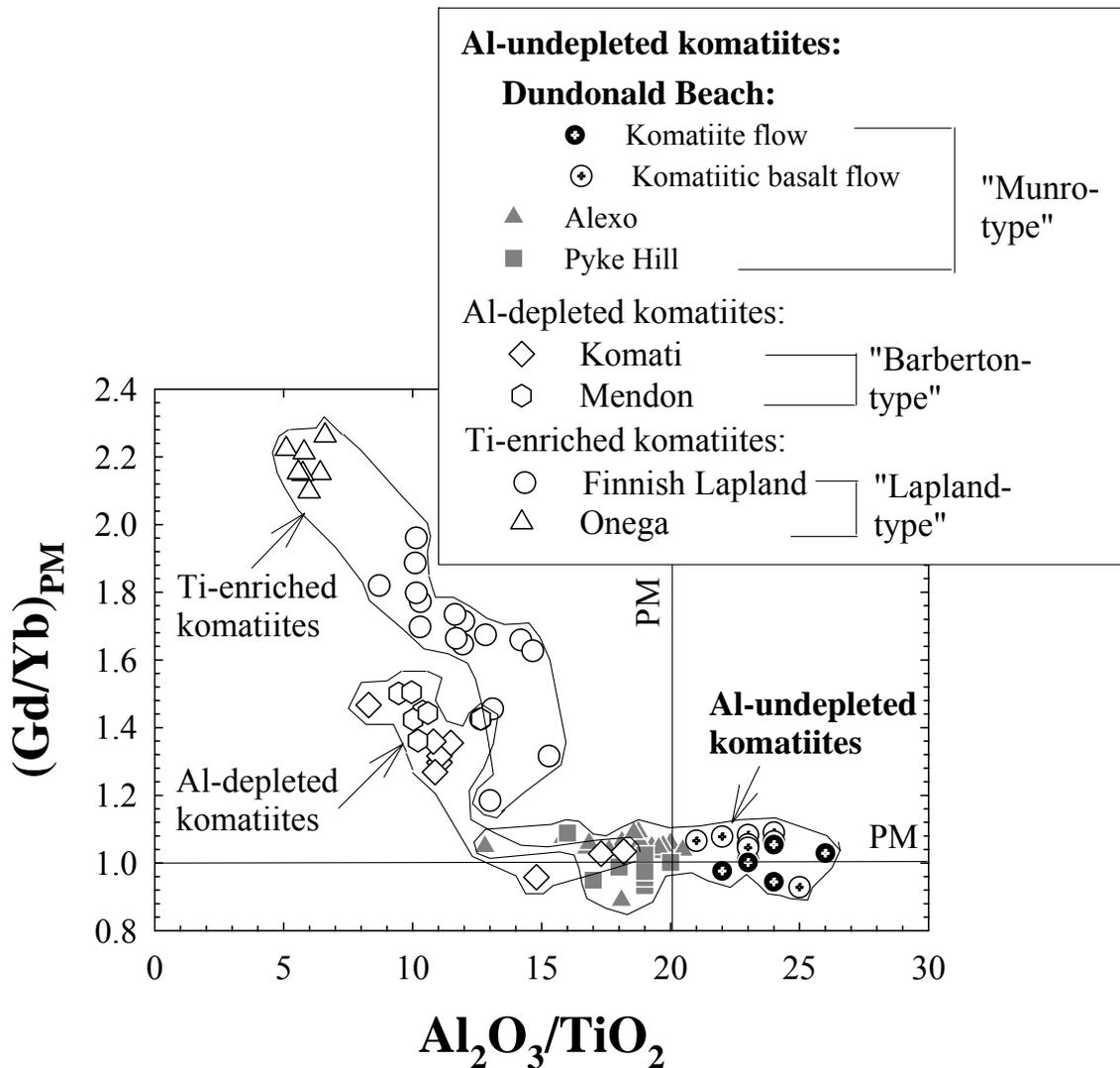
**Figure 4.3.** Plot of $Al_2O_3/TiO_2$ versus chondrite-normalized (CN) Gd/Yb ratios for the Dundonald komatiites and komatiitic basalts. Also shown for reference, these ratios for Al-undepleted komatites from the Alexo (Lahye and Arndt, 1996) and Pyke Hill (Fan and Kerrich, 1997) localities in the Abitibi greenstone belt, Canada, Al-depleted komatiites from Komati (Lahaye et al., 1995; Parman et al., 2003) and Mendon (Lahaye et al., 1995) formations in the Barberton Mountainland, S. Africa, and Ti-enriched komatiites from the Onega plateau (Puchtel et al., 1998) and the Finnish Lapland (Hanski et al., 2001).

(Nesbitt et al., 1979; Lahaye et al., 1995; Sproule et al., 2002). Also, the Dundonald rocks are moderately LREE-depleted (La/Sm$_{CN}$ = 0.41-0.67; Ce/Yb$_{CN}$ = 0.42-0.70; Table 1; Fig. 4.4). The total REE concentrations ($\Sigma$REE = 3.9-22.2 ppm) are comparable to those in komatiites from Alexo and Pyke Hill at given MgO contents (e.g., Lahaye and Arndt, 1996; Fan and Kerrich, 1997). There is a strong negative correlation between Mg# (0.60-0.91: Table 4.1) and $\Sigma$REE. Also, the Dundonald komatiites show consistent LREE-depletion, and flat MREE and HREE patterns (e.g., Gd/Yb$_{CN}$ ~ 1: Table 4.1).

## 4.5. DISCUSSION

The Dundonald Beach komatiites have undergone variable degrees of hydrothermal alteration and greenschist facies metamorphism. Also, these rocks were intruded into graphitic argillites, and thus the possibility of crustal contamination for the parental magmas must be evaluated. We discuss below the influence of alteration, crustal contamination and metamorphism on the geochemical characteristics of the emplaced Dundonald lavas and the mineral composition of chromites.

### 4.5.1. Identification of the least-mobile elements

Previous studies have demonstrated the applicability of olivine-control trends in identifying the least-mobile elements in a given suite of rocks (e.g., Arndt et al., 1989; Lahaye and Arndt, 1996). This is possible because olivine is the dominant fractionating phase in komatiites, and accordingly, linear trends with negative slopes are normally observed on plots of MgO versus the least-mobile incompatible major element oxides and trace elements (e.g., Al$_2$O$_3$, TiO$_2$, Zr, Sm). Deviations from such olivine-controlled fractionation-accumulation trends are commonly ascribed to post-
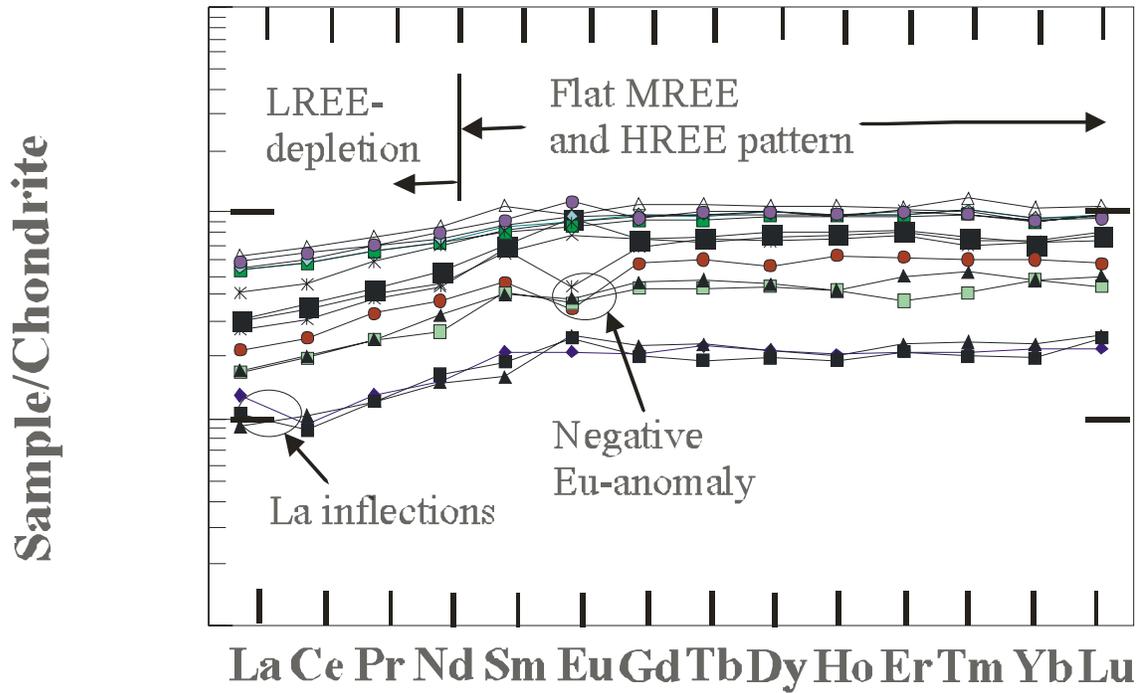
**Figure 4.4.** Chondrite-normalized REE pattern of the whole-rock Dundonald komatiites and komatiitic basalts. These rocks show uniform LREE-depletion and flat MREE and HREE patterns. The negative Eu anomalies and La-inflections in some samples are most likely due to secondary alteration. The normalizing values for chondrites are from McDonough and Sun (1995).

magmatic mobility of the respective elements. Using the same criterion for the Dundonald komatiites suggests that major elements, such as Si, Na, K and Ca, and minor elements, such as Ba, Rb, Sr, U and Pb show significant mobility due to post-crystallization alteration. The concentrations of these elements are, therefore, excluded hereafter from further discussion of geochemical characteristics of these rocks. In contrast, the effects of alteration in Dundonald rocks are minor on some major element oxides, such as $Al_2O_3$ and $TiO_2$ (Fig. 4.5). Using the same olivine-control criterion suggests that the transitional elements, such as V, Cr, Co, Ni, Cu and Zn, and other trace elements including high field strength elements (HFSE), such as Zr and Hf, (Fig. 4.5) have remained relatively immobile on the whole-rock scale. Also, on a chondrite-normalized REE plot, these rocks show very consistent LREE-depletion and flat MREE and HREE patterns among all the samples, suggesting very limited mobility of REE in these rocks (Fig. 4.4). The slightly negative Eu anomalies in three samples of our suite may have been caused by hydrothermal alteration, similar to, for example, those observed in spinifex-textured komatiites from Anderson's Flow in Belingwe, Zimbabwe (e.g., Zhou, 1994) and komatiitic rocks from the Sula Mountain greenstone belt in the West African Craton (Rollinson, 1999). Similarly, the minor La inflections in a different set of three samples of Dundonald rocks may also be a result of alteration (Fig. 4.4).

## 4.5.2. Evaluation of crustal contamination

The most compelling evidence for crustal contamination in a suite of komatiites is provided by a combination of abundance patterns of lithophile elements, such as enrichments in LREE and negative Nb anomalies, (e.g., Jochum et al., 1991;
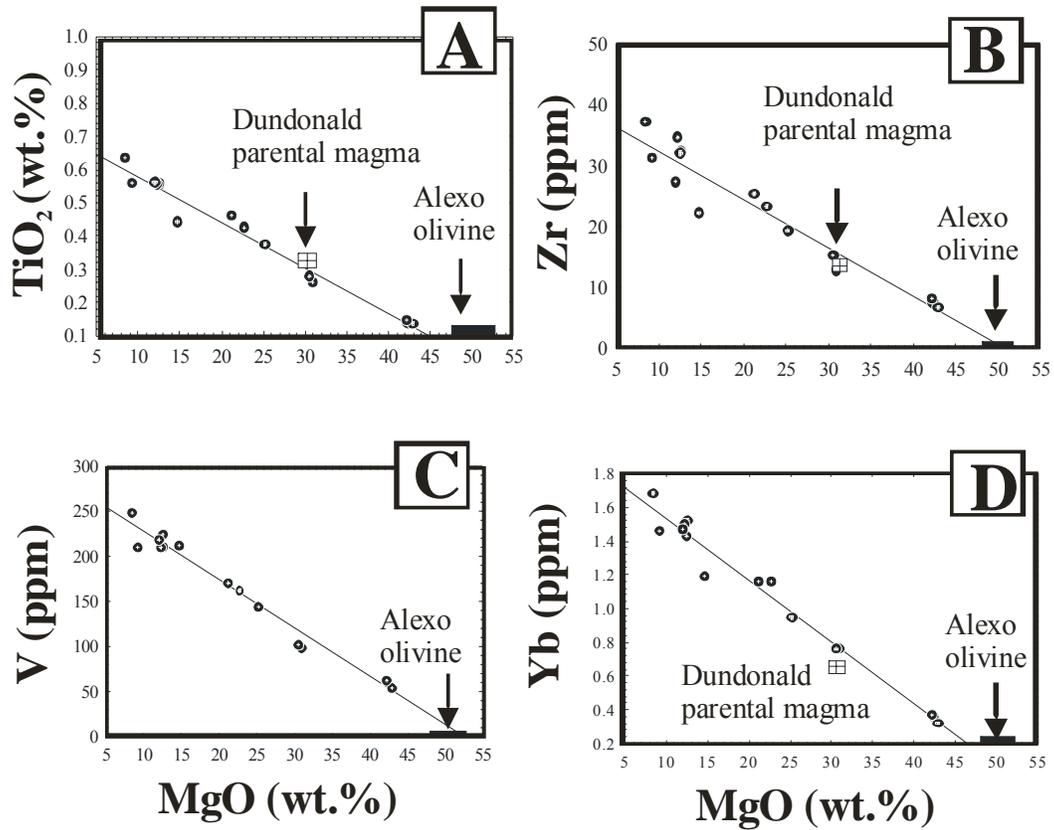
**Fig. 4.5.** Variation diagrams of MgO (wt.% anhydrous) versus (A) TiO$_2$ (wt.%), (B) Zr (ppm), (C) V (ppm) and (D) Yb (ppm) in the whole-rock Dundonald komatiites and komatiitic basalts.

Lesher and Arndt, 1995; Perring et al., 1996) and their key lithophile element isotope systematics (e.g., unradiogenic Nd- and radiogenic Pb-isotopic compositions; Chauvel et al., 1985; Puchtel et al., 1996). The Nd or Pb isotopic compositions of the present suite of samples have not yet been determined. Nevertheless, the degrees of LREE-depletion and Nb anomalies in the Dundonald rocks are compared with those reported for other Precambrian komatiites from North Caribou, NW Superior Province (Hollings and Kerrich, 1999) and Vetreny Belt, Russia (Puchtel et al., 1996) that show strong evidence for crustal contamination (Fig. 4.6). Unlike crustally contaminated komatiites from the NW Superior Province and the Vetreny Belt, the Dundonald rocks plot within the field of uncontaminated Alexo rocks. Also, on a chondrite-normalized plot of La/Sm versus Ce/Sm, the degree of LREE-depletion in the Dundonald rocks is within the range of those for uncontaminated Alexo (Lahaye and Arndt, 1996) and Pyke Hill (Fan and Kerrich, 1997) komatiites. Thus, the uniform LREE-depleted patterns of the Dundonald komatiitic rocks (Fig. 4.4) suggest their derivation from a LREE-depleted mantle source with minimal or no subsequent crustal contamination.

### 4.5.3. Effects of alteration and metamorphism on the chromite compositions

Several lines of evidence suggest that the chromites in the Dundonald rocks have retained their primary magmatic mineral-chemical compositions:

[1] The chromite microphenocrysts in these rocks are typically euhedral crystals with sharp grain boundaries and do not show ubiquitous magnetite rims.

[2] The Dundonald rocks were metamorphosed to regional lower greenschist facies conditions (Jackson and Fyon, 1982; Davis, 1999). Metamorphosed chromites
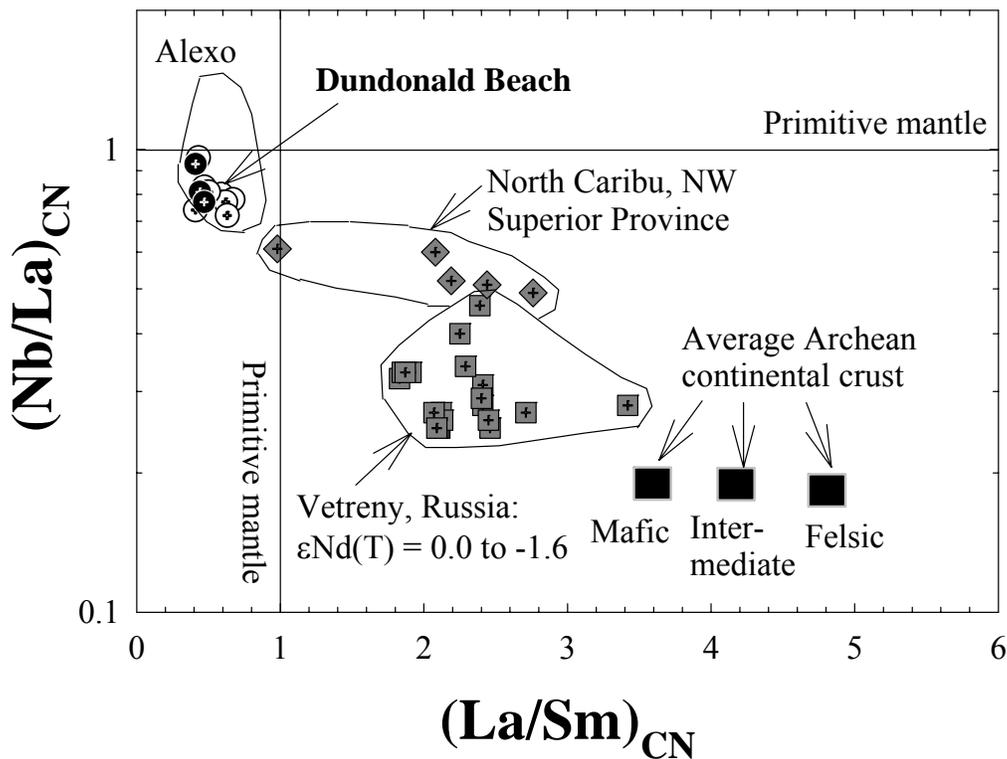
**Figure 4.6.** Chondrite (McDonough and Sun, 1995)-normalized (CN) Nb/La versus La/Sm ratios for the Dundonald komatiites and komatiitic basalts are compared with those for the crustally contaminated komatiitic rocks from North Caribu, NW Superior Province (Hollings and Kerrich, 1999) and the Vetreny Belt, Russia (Puchtel et al., 1996). Also shown for comparison is the field of stratigraphically-equivalent komatiites from Alexo for which Nd and Pb isotopic compositions are strongly indicative of an absence of significant crustal contamination (Dupré et al., 1984; Lahye and Arndt, 1996). For reference, the average compositions of Archean mafic, intermediate and felsic crusts are also plotted (Rudnick and Fountain, 1995). Note that the Dundonald rocks plot within the field of Alexo komatiites consistent with absence of significant crustal contamination.

commonly show more iron-rich compositions relative to their precursors in igneous protoliths as a result of resetting of primary magmatic Fe-Mg exchange equilibria during chemical interactions with silicates and carbonates (Barnes, 2000). The chromite compositions in the Dundonald rocks plot within the field of chromites in komatiites from elsewhere that have undergone greenschist facies metamorphism (not shown), yet are likely to be in equilibrium with primary olivines at high igneous temperatures (see Barnes, 2000).

[3] Alteration of primary chromites in komatiites typically involves oxidation and formation of magnetite rims around Cr-rich cores. The oxidation increases $Fe^{3+}$ in the trivalent cation site and consequently leads to an increase in $Fe^{3+}/Fe^{2+}$. The chromites in these rocks show limited variability in $Fe^{3+}/\Sigma Fe$ (0.21-0.34; Table 4.2). Also, on an Al-Cr-$Fe^{3+}$ ternary cation plot, it can be shown that the chromites have quite uniform proportions of trivalent cations, consistent with an absence of significant post-magmatic secondary alteration.

## 4.5.4. Hydrous versus anhydrous nature of mantle source for Dundonald komatiites

Recent crystallization experiments on Al-depleted komatiite compositions have shown that clinopyroxenes produced under $H_2O$-saturated compared with anhydrous conditions have distinctly different chemical compositions (Parman et al., 1997). For example, clinopyroxenes crystallized under 200 MPa, $H_2O$-saturated conditions have a significantly higher wollastonite content [Wo = Ca/(Ca+Mg+Fe)] at a given Mg# [Mg# = Mg/(Mg+$Fe^{2+}$)] than that of clinopyroxene produced at 0.1 MPa, under anhydrous conditions (Fig. 4.7). It was demonstrated that, on a plot of
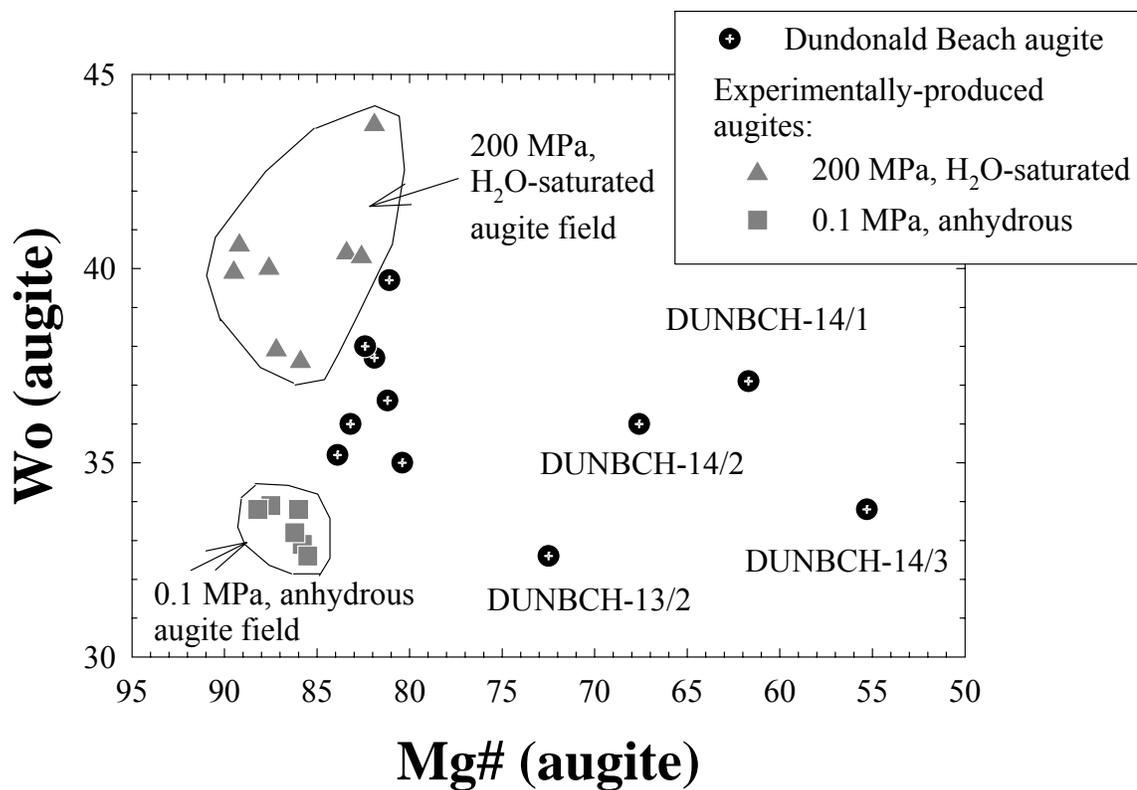
**Figure 4.7**. Plot of Wo contents [Ca/(Ca+Mg+Fe$^{2+}$)] versus Mg# [Mg/(Mg+Fe), mole%] for the core compositions of clinopyroxenes in the Dundonald rocks. Also shown for reference are the fields of clinopyroxene produced in 200 MPa H$_2$O-saturated and 0.1 MPa anhydours experiments (Parman et al., 1997).

Mg# versus Wo content of augite, the compositions of cores of preserved clinopyroxenes from natural, Al-depleted komatiites from the Barberton Mountainland, S. Africa plot within the field for experimentally produced augite under $H_2O$-saturated conditions (Parman et al., 1997). These two observations were used to support a subduction-related hydrous melting origin for the Al-depleted komatiites (Parman et al., 1997; Grove et al., 1999).

None of the analyzed compositions of core of preserved clinopyroxenes in the Al-undepleted Dundonald Beach komatiitic basalt flow (Table 4.3) plots within either the hydrous or anhydrous fields for experimentally produced clinopyroxene for Al-depleted komatiites (Fig. 4.7). This suggests the following two non-exclusive possibilities. First, bulk composition (Al-depleted versus Al-undepleted) of the parental magma may have an additional influence on the Wo contents of the crystallized clinopyroxene at a given Mg#, so that the experimental results obtained for the Al-depleted rocks have only limited applicability in deciphering the $H_2O$ contents of the fractionating magma for the Al-undepleted Dundonald komatiites. Second, most of the Dundonald clinopyroxenes have Wo contents that are intermediate between those corresponding to anhydrous and hydrous starting compositions. It has not yet been demonstrated whether or not the Wo contents of augite continuously increase as a function of increasing $H_2O$ contents of the experimental starting materials. The unconstrained impact of bulk composition and variable $H_2O$ content implies that the significance of the intermediate Wo contents for the Dundonald rocks is currently not decipherable.

117

In addition to high Wo contents of clinopyroxenes, some whole-rock trace element characteristics of the Al-depleted Barberton rocks were shown by Parman et al. (1997) to be similar to those in modern arc-related rocks, such as Phanerozoic boninites. For example, the similarity in co-variations of Ti/Zr with La/Sm ratios in boninites and those in Al-depleted komatiites were used to support a subduction-related hydrous melting origin for the latter (Parman et al., 2003). The co-variations in Ti/Zr and La/Sm ratios in the Dundonald Beach komatitic rocks are very similar to those for Al-undepleted komatiites from the Kidd-Munro assemblage (e.g., Alexo and Pyke Hill areas) that have previously been shown to be different from the Phanerozoic boninites (see Fig. 3.6). Also, chromites from the Dundonald Beach komatiitic rocks have significantly lower Cr# [Cr/(Cr+Al)] at a given Mg# than chromites from boninites (Fig. 4.8). Lower Cr#'s are also observed in Al-undepleted komatiites from Pyke Hill (Arndt, 1977), Gorgona island (Echeverria, 1980), and Belingwe, Zimbabwe (Zhou and Kerrich, 1992), and Ti-rich komatiites from the Finnish Lapland (Gangopadhyay et al., 2004), suggesting that magmas parental to the Al-undepleted and Ti-enriched komatiites have lower Cr contents than those for boninites, consistent with a more refractory source for the latter.

The relatively low Cr contents of chromites in Al-undepleted komatiites are in contrast to the high Cr contents of their olivine. For example, the Al-undepleted komatiites in the Kidd-Munro assemblage from the Munro Township have olivine with Cr contents up to ~2300 ppm (Pyke et al., 1973). Experimental studies suggest that ultramafic rocks with olivine containing > 2000 ppm Cr must have crystallized at temperatures exceeding 1500ºC under appropriate redox states (Murck and Campbell,
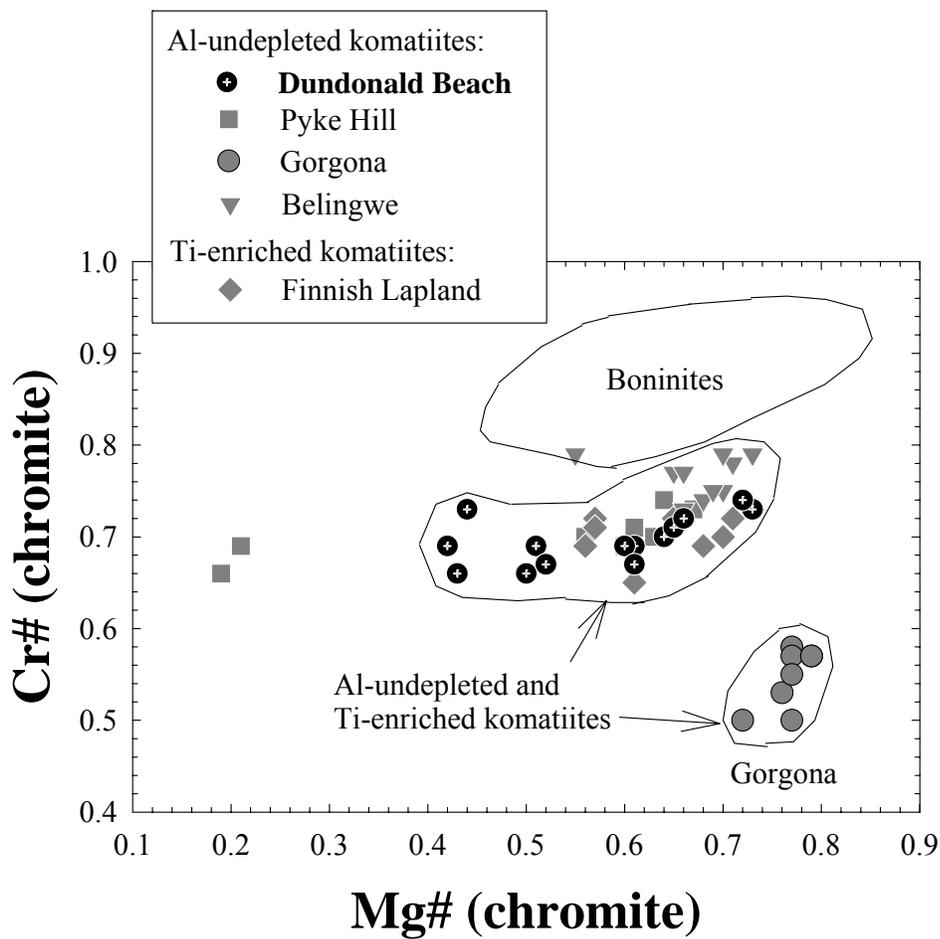
**Figure 4.8**. Plot of Cr# [Cr/(Cr+Al)] versus Mg# [Mg/(Mg+Fe)] for chromites from

the Dundonald komatiites. Also shown comparison is the field for boninites (Brown

and Jenner, 1989; Coish, 1989) and Al-undepleted komatiites from Pyke Hill (Arndt,

1977), Gorgona (Echeverria, 1980) and Belingwe (Zhou and Kerrich, 1992), and Ti-

enriched komatiites from the Finnish Lapland (Gangopadhyay et al., in revision).

1986; Li et al., 1995). Such high temperatures of crystallization for the Al-undepleted komatiites are in contrast to temperatures of ~1250ºC of crystallization, that have been estimated for crystallization of olivine in boninites (see Campbell, 2001). Thus, chromite compositions in the Dundonald komatiites are most consistent with high temperature crystalllization, which is in contrast to a low-temperature, hydrous melting origin in a supra-subduction zone setting.

The uniform LREE depletion, and flat MREE and HREE patterns of the Dundonald komatiitic rocks indicate their derivation from depleted mantle source. The Nb/Y versus Zr/Y ratios of the komatiitic basalts generally plot within the field for plume-related Icelandic basalts, whereas the komatiites plot within the field for N-MORB (Fitton et al., 1997; Fig. 4.9). The compilation of a large dataset for N-MORB and Icelandic basalts showed that the parallel array of high field-strength elements (HFSE) on a discrimination diagram (Fig. 4.9) reflects their differences in mantle source characteristics and that these variations are not functions of degrees of melting, depletion of source due to prior melt extraction, crustal contamination or secondary alteration (Fitton et al., 1997). If true for the mantle source(s) for the Dundonald rocks, their HFSE systematics, combined with the REE pattern (Fig. 4.9) suggest that the incompatible element distribution patterns of these lavas indicate their derivation from sources similar to those of N-MORB and plume related basalts.

The uniform LREE-depletion, combined with unfractionated MREE and HREE patterns of the Dundonald rocks are also in contrast to the typical LREE enrichments and concave-up REE patterns observed in arc-related highly magnesian
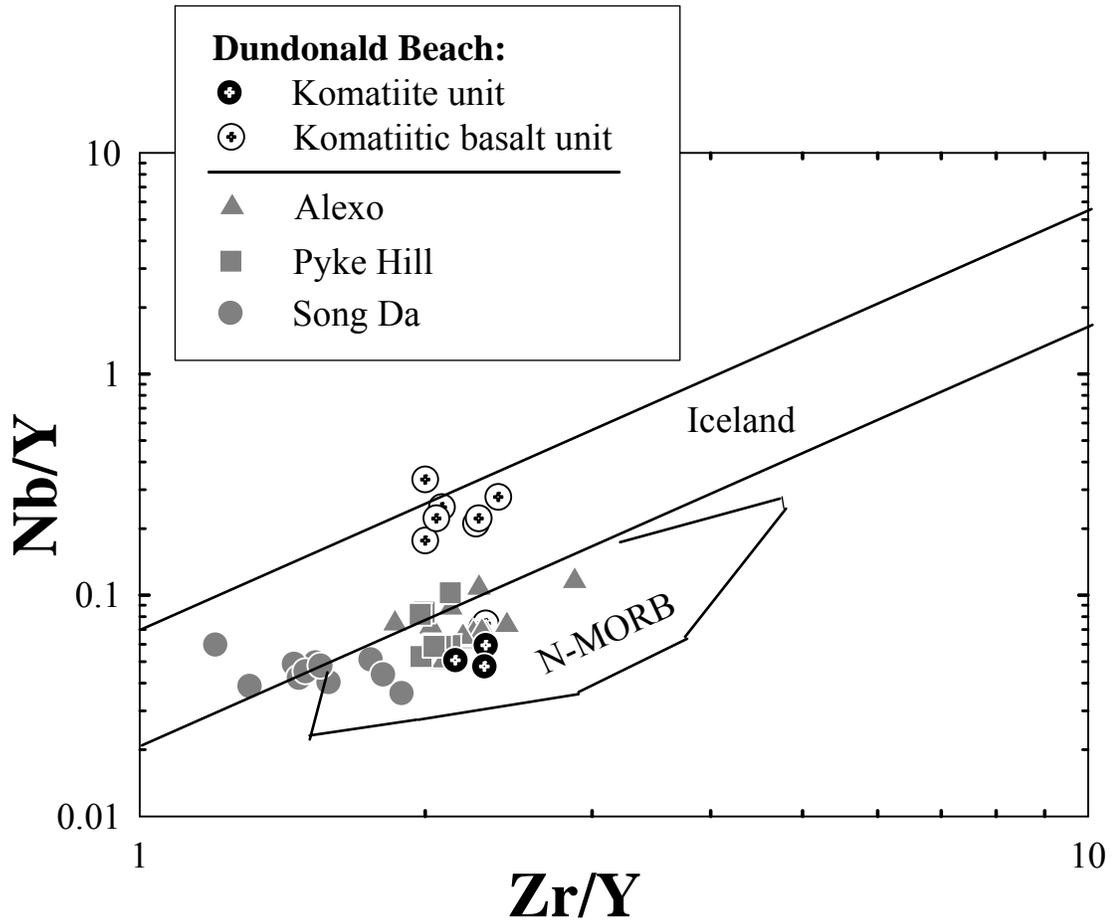
**Figure 4.9.** Plot of the Nb/Y-Zr/Y systematics of the Dundonald komatiites and komatiitic basalts. For comparison, Al-undepleted komatiites from Alexo and Pyke Hill, and Song Da, Vietnam are also plotted. Data sources for Alexo and Pyke Hill rocks are as in Fig. 3.1. Additional data for Song Da are from Hanski et al. (2004). The field for plume-related Iceland rocks and N-MORB (normal mid oceanic ridge basalts) are from Fitton et al. (1997).

rocks, such as boninites (e.g., Hickey and Frey, 1982). Thus, the similarity of the HFSE/REE patterns of the Dundonald rocks with those for N-MORB and plume-related basalts rather than subduction-related rocks, as discussed above, can be utilized as a basis to place empirical constraints on the $H_2O$ contents of the mantle source(s) for the Dundonald rocks. This is possible because previous studies have shown that $H_2O$ behaves as an incompatible element, similar to La and Ce, during melting of mantle sources for MORB and oceanic basalts (Michael, 1995; Danyushevsky et al., 2000; Dixon and Clague, 2001). The similar degree of incompatibility of $H_2O$ and, for example, Ce in submarine basaltic glasses sampled away from subduction zones is manifested by a strong positive correlation between their $(Ce/Yb)_{CN}$ and $H_2O/Yb$ ratios, as shown in Fig. 4.10. Using this correlation, the entire range of $(Ce/Yb)_{CN}$ ratios for the Dundonald komatiites and komatiitic basalts (0.41-0.70) yield $H_2O/Yb$ ratios of ~200-400 that correspond to very low $H_2O$ contents of $\leq 0.04$ wt.% (Fig. 4.10). Similarly, using this $(Ce/Yb)_{CN}$ versus $H_2O/Yb$ correlation, Hanski et al. (2004) estimated $H_2O$ contents of $\leq 0.03$ wt.% of the mantle sources for the Permo-Triassic Al-undepleted komatiites from Song Da, Vietnam. These essentially anhydrous mantle sources for the Al-undepleted komatiitic rocks are not consistent with typical high estimates of $H_2O$ in subduction-related mafic-ultramafic rocks (e.g., Kyser et al., 1986; Sobolev and Chaussidon, 1996; Kamenetsky et al., 2002). We conclude that the major and trace element characteristics of the whole rocks and the chemical composition of chromite and clinopyroxene in the Dundonald komatiites are most consistent with the anhydrous nature and high temperature of parental magmas generated in a within-plate setting.
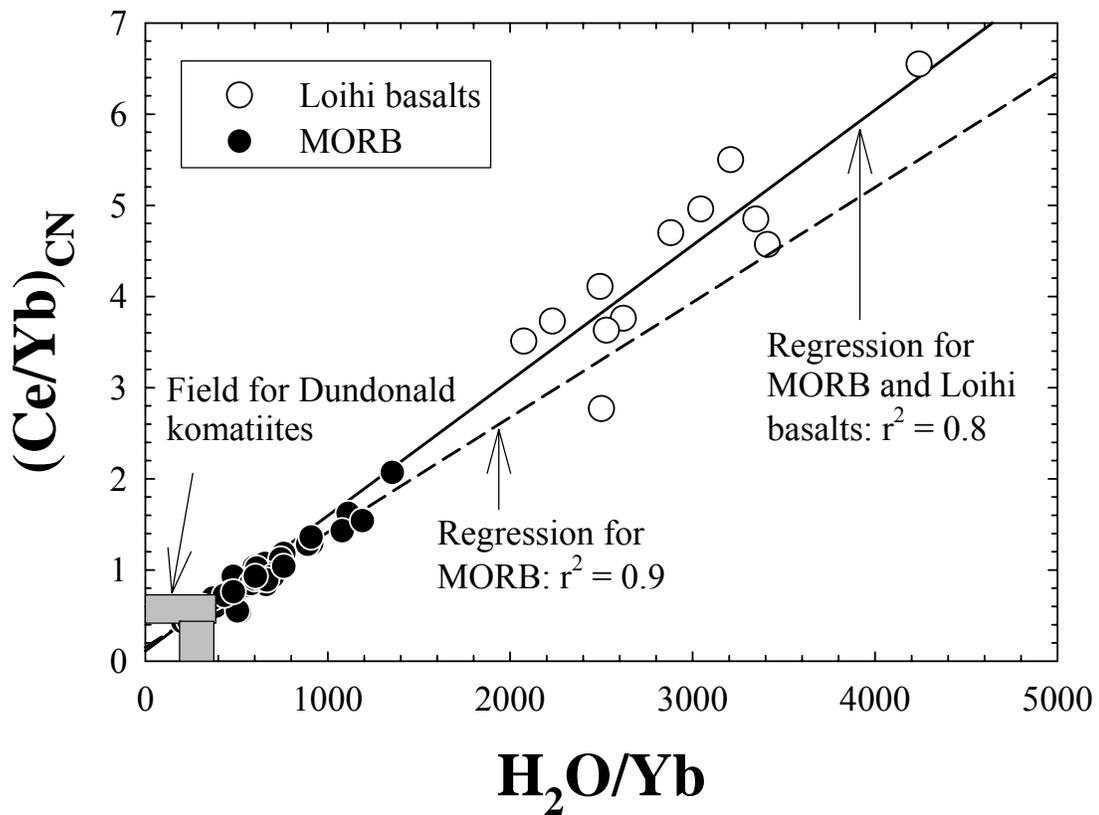
**Figure 4.10**. Plot of chondrite-normalized Ce/Yb (Ce/Yb$_{CN}$) versus H$_2$O/Yb ratios for MORB (Danyushevsky et al., 2000) and Loihi basalts (Dixon and Clague, 2001). Note that the total range in Ce/Yb$_{CN}$ ratios for Dundonald komatiites (grey horizontal field) yield a narrow range of H$_2$O/Yb ratios (maximum of 400), corresponding to maximum H$_2$O contents of $\leq 0.4$ wt.%.

**4.6. CONCLUSIONS**

The geochemical characteristics of the whole rocks and primary igneous minerals (chromite and clinopyroxene) of the Al-undepleted komatiitic rocks at the Dundonald Beach, that are part of the spatially extensive Kidd-Munro volcanic assemblage in the Abitibi greenstone belt, Canada are consistent with their derivation from an essentially anhydrous mantle source. For example, the Dundonald clinopyroxenes, at a given Mg#, have Wo contents, that are intermediate between those experimentally produced from Al-depleted komatiites under anhydrous and $H_2O$-saturated conditions, thus providing no clear evidence for either hydrous or anhydrous melting origin for the Dundonald rocks. We suggest that the influence of variable $H_2O$ contents on the clinopyroxene compositions of different chemical types of komatiites should be further explored via additional melting experiments.

The uniform LREE-depletion, unfractioned HREE pattern and absence of HFSE anomaly in the Dundonald komatiites contrast with concanve-up REE pattern and characteristic HFSE anomaly, that are commonly observed in modern arc-related lavas. Moreover, similar incompatibilities between Ce (or La) and $H_2O$ during mantle melting, that have been reported for MORB and Hawaiian basalts implies an essentially anhydrous mantle source for the Dundonald komatiites.

# CHAPTER 5: Re-Os systematics of komatiites and komatiitic basalts at Dundonald Beach, Ontario, Canada: Evidence for a complex alteration history and implications of a late-Archean chondritic mantle source

**Abstract**

Re-Os concentrations and isotopic compositions have been examined in one komatiite unit and two komatiitic basalt units at Dundonald Beach, which is part of the spatially-extensive 2.7 Ga Kidd-Munro volcanic assemblage in the Abitibi greenstone belt, Ontario, Canada. The komatiitic rocks in this locality record at least three episodes of alteration of Re-Os elemental and isotope systematics. First, an average of 40% and as much as 75% Re was lost due to shallow degassing during eruption and/or hydrothermal leaching during or immediately after the emplacement of these intrusive units. Second, the Re-Os isotope systematics of the rocks with $^{187}Re/^{188}Os$ ratios >1 were reset at ~2.5 Ga, most likely due to a regional metamorphic event. Finally, there is evidence for relatively recent gain and loss of Re.

The variations in Os concentrations in the Dundonald komatiites yield a relative bulk distribution coefficient for Os ($D_{Os}^{solid/liquid}$) of 2-4, consistent with those obtained for stratigraphically-equivalent komatiites in the nearby Alexo area and in Munro Township. This suggests that Os was moderately compatible during crystal-liquid fractionation of the parental magma to the Kidd-Munro komatiitic rocks. Furthermore, whole-rock samples and chromite separates with low $^{187}Re/^{188}Os$ ratios

(<1) yield a precise chondritic average initial $^{187}Os/^{188}Os$ ratio of 0.1083 ± 0.0006 ($\gamma_{Os}$ = 0.0 ± 0.6). The chondritic initial Os isotopic composition of the mantle source for the Dundonald rocks is consistent with that determined for komatiites in the Alexo area and in Munro Township.

Our Os isotope results for the Dundonald komatiitic rocks, combined with those in the Alexo and Pyke Hill areas suggest that the mantle source region for the Kidd-Munro volcanic assemblage had evolved along a long-term chondritic Os isotopic trajectory until their eruption at ~2.7 Ga. The chondritic initial Os isotopic composition of the Kidd-Munro komatiites is indistinguishable from that of the projected contemporaneous convective upper mantle. The uniform chondritic Os isotopic composition for the ~2.7 Ga mantle source for the Kidd-Munro komatiites contrasts with the typical large-scale Os isotopic heterogeneity in the mantle sources for ca. 89 Ma komatiites from the Gorgona Island, and present-day ocean island basalts or arc-related lavas. This suggests a significantly more homogeneous mantle source in the Archean compared to the present-day mantle.

## 5.1. INTRODUCTION

Petrographic and geochemical studies have shown that Precambrian komatiites have undergone variable degrees of weathering, hydrothermal alteration and metamorphism (e.g., Beswick, 1982; Jolly, 1982; Arndt et al., 1989; Arndt and Lesher, 1992; Lesher and Arndt, 1995; Lahaye and Arndt, 1996; Rollinson, 1999; Hanski et al., 2001). The effects of these secondary processes in some suites are manifested by open-system behavior of Re-Os elemental and isotope systematics of whole rocks, which, in some cases, yield inaccurate ages and large uncertainties in

calculated initial $^{187}Os/^{188}Os$ ratios of the emplaced lavas (e.g., Walker and Nisbet, 2002; Gangopadhyay et al., in revision). Thus, some of the previous Os isotopic studies of Precambrian komatiites, for which the crystallization ages were known from other radiogenic isotope systematics (e.g., Sm-Nd, Pb-Pb), have relied on Os-rich, relatively well-preserved primary igneous minerals (e.g., olivine and chromite) in order to determine initial Os isotopic compositions of host lavas (e.g., Walker and Nisbet, 2002; Gangopadhyay et al., in revision). The nature and causes of open-system behavior in the Re-Os system of whole rock komatiite samples, however, have not been well documented. In this paper, we report the Re-Os concentrations and isotopic compositions of whole rocks and chromite separates from a suite of ca. 2.7-Ga komatiites and komatiitic basalts in the Dundonald Beach area in the Abitibi greenstone belt, Ontario, Canada. We quantitatively estimate early losses of Re in our suite of samples through comparison between measured Re concentrations and those recalculated from correlation with the similarly incompatible, yet relatively immobile major element Al, as observed in stratigraphically-equivalent, least-altered komatiites in the Alexo and Pyke Hill areas. Finally, based on our Os isotopic results for the Dundonald rocks and those previously obtained for komatiites from elsewhere, we suggest the factors that should be considered when selecting komatiite samples for future Re-Os isotopic studies.

Another objective of this study was to determine the initial Os isotopic composition of the ~2.7-Ga mantle sources for these rocks. Compilation of the global database for high-precision initial Os isotopic compositions of ultramafic rocks suggests that during the early and mid Archean, the mantle sources for these rocks

had generally chondritic $^{187}Os/^{188}Os$ (Bennett et al., 2002; Wilson et al., 2003). However, Os isotopic heterogeneities in the terrestrial mantle are clearly resolved by the end of the Archean. For example, although the ~2.7 Ga mantle sources for komatiites in the Alexo area of Dundonald Township and in Munro Township ~50 km to the east had essentially chondritic initial Os isotopic compositions (Gangopadhyay and Walker, 2003; Shirey, 1997; Puchtel et al., 2004a), ferropicrites of similar age in Boston Township, part of the 2723-2720 Ma Stoughton-Roquemaure assemblage of the Abitibi greenstone belt, were derived from a source with a subchondritic initial $^{187}Os/^{188}Os$ ratio ($\gamma_{Os}$ = -3.8 ± 0.8: Walker and Stone, 2001). Also, nearly contemporaneous mantle sources for ultramafic flows at Kostomuksha, Russia (Puchtel et al., 2001a), and Belingwe, Zimbabwe (Walker and Nisbet, 2002) show significant positive deviations from the projected chondritic Os isotope evolution trajectory. Thus, by the late Archean, portions of the mantle evidently developed significant Os isotopic heterogeneities, yet the spatial scales of these heterogeneities are largely unknown. The komatiitic rocks at Dundonald Beach therefore also provide an additional point of comparison to other komatiites in the Abitibi Greenstone Belt.

## 5.2. SAMPLES

The samples examined here were collected from the Dundonald Beach outcrop, a mechanically- and hydraulically-stripped area covering approximately 150m x 60m, that is located in the SW part of Dundonald Township in northern Ontario (Houlé et al., 2002). The geochemical characteristics of the komatiites and associated magmatic Ni-Cu-PGE deposits and volcanogenic massive Cu-Zn sulfide

deposits in the Dundonald Township have been reported by previous studies (e.g., Naldrett and Mason, 1968; Muir and Comba, 1979; Barnes et al., 1983; Barnes, 1985; Barnes and Naldrett, 1987; Davis, 1997, 1999; Barrie et al., 1999). The U-Pb zircon age of a dacite unit that is presumably near coeval with the komatiites in the Dundonald Township is 2717.3 ± 1.2 Ma (Barrie et al., 1999). This age is in excellent agreement with U-Pb zircon ages (2717.7 ± 1.1 Ma) for the bimodal komatiite and rhyolite volcanic rocks in the Kidd Creek area 40 km west of Dundonald Township (Bleeker et al., 1999). The Dundonald Beach komatiites are stratigraphically equivalent to those exposed in the Alexo area and in Munro Township ~50 km to the east, and are part of the spatially extensive (~180 km x 12 km) Kidd-Munro volcanic assemblage, which ranges in age from 2719 to 2710 Ma (e.g., Nunes and Pyke, 1980; Corfu and Noble, 1992; Bleeker et al., 1999; Ayer et al., 2002). The volcanic assemblage of Dundonald Township includes volumetrically dominant basalts (~75%) with relatively minor komatiitic rocks (~10%), calc-alkaline basalts to rhyolites (~10%) and tholeiitic rhyolites (~5%: Barrie, 1999). Though relatively minor, the abundance of komatiitic rocks in this assemblage exceeds all other assemblages in the Abitibi greenstone belt.

The whole rock samples examined here were collected from three complete surface units, which were originally interpreted to be extrusive (e.g., Muir and Comba, 1979), but which Arndt et al. (in press) have shown to be intrusive. Samples DUNBCH-1 through DUNBCH-6 were collected from one single (~10 m-thick) komatiite unit, which is one of several differentiated cumulate komatiite units with thick lower olivine mesocumulate zones and thin upper olivine spinifex-textured

zones (Davis, 1997; 1999). Samples DUNBCH-7 through DUNBCH-10 were collected from a single komatiitic basalt unit (Unit I). This ~9m-thick unit consists of a lower olivine-clinopyroxene-(orthopyroxene) cumulate zone, a thick parallel acicular ("string-beef") pyroxene spinifex-textured zone, a thin random platy olivine spinifex-textured zone, and a very thin, very fine-grained, upper "chilled" margin (Davis 1997, 1999). Samples DUNBCH-11 through DUNBCH-15 were collected from another single komatiitic basalt unit (Unit II). This ~25m thick unit is composed of a basal peridotite, an overlying unit of peridotite with postcumulus pyroxene oikocrysts, an overlying unit of skeletal-textured pyroxenite, and an uppermost random pyroxene spinifex unit. The komatiites and komatiitic basalts in the Dundonald Beach area have been metamorphosed to lowermost greenschist facies and are locally faulted and/or sheared, but primary structures and textures are well preserved. All of the interstitial glass has been converted to chlorite, most sulfides have been recrystallized, most of the olivine has been pseudomorphed by serpentine and magnetite, and some of the pyroxene has been pseudomorphed by chlorite. However, some of the olivine, much of the pyroxene, and most of the chromite has been preserved (Davis, 1997, 1999; Arndt et al., in press).

## 5.3. SAMPLE PREPARATION AND ANALYTICAL METHODS

The whole rock samples were crushed into mm-sized pieces using a ceramic jaw crusher. The freshest pieces were cleaned with Milli-Q™ water in an ultrasonic bath for ½ h and were subsequently dried in an oven at 60°C for ~ 1 hour. These pieces were then ground using an agate mill. The powders were carefully mixed and

homogenized and separate aliquots of the same whole rock powder were used for analysis of major and minor elements and Re-Os isotopes.

Chromite separates were obtained by crushing whole rock samples using a ceramic jaw crusher, followed by separation of the ferromagnetic (magnetite) fraction using a hand magnet. The residual, least-ferromagnetic fraction was ground to sub-millimeter grain size using a conventional ceramic mill and a least-magnetic fraction was separated using a Frantz™ magnetic separator with appropriate current settings. Finally, the chromite fraction was purified using heavy liquids.

The major element data (Table 5.1) were obtained by wavelength-dispersive X-ray fluorescence spectrometry (WD-XRFS) of fused glass disks at the University of Western Ontario (Dr. C. Wu, analyst). Nickel and Cr concentrations were determined by WD-XRFS of pressed powder pellets. Comparison of routine sample replicates indicate that major elements (>1 wt.%) are precise to within ±2% and that minor elements (Ni, Cr) are precise within ±5% of the amount present.

Chemical separations of Re and Os and analysis of Re-Os isotopes were performed at the University of Maryland by the senior author. The chemical separation procedures for Re and Os employed in this study have followed previously published work (Shirey and Walker, 1995; Cohen and Waters, 1996). The analytical blanks for Re and Os were 7.6 ± 1.7 pg and 2.5 ± 1.0 pg (n = 4), respectively, and are negligible (<0.5%) compared to their concentrations in most whole rock samples. The Re blank contribution, however, was substantial (>6%) for some chromites. The isotopic compositions of the blanks were natural for Re and had $^{187}Os/^{188}Os$ of 0.313

**Table 5.1.** Whole rock major and selected trace element data for Dundonald Beach suite of komatiitic rocks. All major element oxides are recalculated on 100% volatile-free basis.

| Samples | Komatiite unit | | | | | | Komatiitic basalt unit I | |
|---|---|---|---|---|---|---|---|---|
| | DUNBCH-1 | DUNBCH-2 | DUNBCH-3 | DUNBCH-4 | DUNBCH-5 | DUNBCH-6 | DUNBCH-7 | DUNBCH-8 |
| Major oxides (wt.%) | | | | | | | | |
| $SiO_2$ | 44.1 | 44.3 | 44.1 | 43.9 | 44.1 | 45.1 | 50.3 | 50.5 |
| $TiO_2$ | 0.14 | 0.14 | 0.15 | 0.46 | 0.43 | 0.38 | 0.55 | 0.64 |
| $Al_2O_3$ | 3.3 | 3.5 | 3.4 | 11.1 | 9.5 | 8.4 | 11.7 | 14.6 |
| $Fe_2O_3{}^*$ | 9.6 | 8.5 | 9.4 | 10.7 | 12.9 | 11.7 | 11.6 | 12.3 |
| MnO | 0.10 | 0.12 | 0.13 | 0.24 | 0.20 | 0.17 | 0.22 | 0.18 |
| MgO | 42.3 | 42.9 | 42.2 | 21.2 | 22.7 | 25.2 | 12.6 | 8.4 |
| CaO | 0.16 | 0.14 | 0.29 | 12.09 | 9.78 | 8.63 | 11.23 | 10.20 |
| $Na_2O$ | -* | - | - | - | - | - | 0.97 | 2.06 |
| $K_2O$ | - | - | 0.01 | - | - | - | 0.75 | 1.06 |
| $P_2O_5$ | - | 0.01 | 0.01 | 0.03 | 0.02 | 0.03 | 0.04 | 0.05 |
| $Cr_2O_3$ | 0.31 | 0.29 | 0.31 | 0.29 | 0.40 | 0.42 | 0.16 | 0.05 |
| LOI | 12.45 | 12.75 | 12.35 | 4.84 | 5.57 | 6.29 | 2.26 | 1.92 |
| Mg#[1] | 0.90 | 0.91 | 0.90 | 0.80 | 0.78 | 0.81 | 0.68 | 0.58 |
| $Al_2O_3/TiO_2$ | 24 | 26 | 23 | 24 | 22 | 22 | 21 | 23 |
| $CaO/Al_2O_3$ | 0.05 | 0.04 | 0.08 | 1.1 | 1.0 | 1.0 | 0.96 | 0.70 |
| Ni (ppm) | 2844 | 2659 | 2688 | 829 | 765 | 1082 | 118 | 70 |
| Cr (ppm) | 1528 | 1546 | 1621 | 1823 | 2782 | 2585 | 1022 | 303 |

**Table 5.1** (continued)

| Samples | Komatiitic basalt unit I | | Komatiitic basalt unit II | | | | |
|---|---|---|---|---|---|---|---|
| | DUNBCH-9 | DUNBCH-10 | DUNBCH-11 | DUNBCH-12 | DUNBCH-13 | DUNBCH-14 | DUNBCH-15 |
| Major oxides (wt.%) | | | | | | | |
| $SiO_2$ | 47.8 | 47.9 | 44.0 | 44.2 | 49.2 | 48.7 | 49.2 |
| $TiO_2$ | 0.56 | 0.56 | 0.26 | 0.28 | 0.44 | 0.56 | 0.56 |
| $Al_2O_3$ | 12.7 | 12.0 | 6.4 | 6.4 | 10.2 | 13.7 | 13.3 |
| $Fe_2O_3{}^*$ | 12.9 | 12.6 | 12.5 | 12.9 | 12.0 | 11.9 | 11.1 |
| MnO | 0.22 | 0.21 | 0.18 | 0.18 | 0.22 | 0.21 | 0.20 |
| MgO | 12.5 | 12.2 | 30.9 | 30.5 | 14.7 | 9.2 | 12.0 |
| CaO | 11.61 | 13.65 | 5.12 | 5.13 | 11.62 | 13.47 | 11.33 |
| $Na_2O$ | 0.36 | 0.01 | 0.02 | 0.02 | 0.73 | 0.15 | 0.38 |
| $K_2O$ | 1.10 | 0.74 | 0.00 | 0.00 | 0.74 | 1.93 | 1.89 |
| $P_2O_5$ | 0.04 | 0.04 | 0.02 | 0.02 | 0.03 | 0.04 | 0.03 |
| $Cr_2O_3$ | 0.12 | 0.10 | 0.61 | 0.40 | 0.20 | 0.06 | 0.07 |
| LOI | 2.98 | 2.72 | 7.39 | 6.77 | 2.38 | 2.66 | 3.09 |
| Mg#[1] | 0.66 | 0.66 | 0.83 | 0.82 | 0.71 | 0.60 | 0.68 |
| $Al_2O_3/TiO_2$ | 23 | 22 | 25 | 23 | 23 | 24 | 24 |
| $CaO/Al_2O_3$ | 0.91 | 1.1 | 0.80 | 0.81 | 1.1 | 0.98 | 0.85 |
| Ni (ppm) | 199 | 178 | 1412 | 1344 | 223 | 115 | 119 |
| Cr | 888 | 708 | 2936 | 1662 | 1139 | 327 | 400 |

*- = below detection limits.

133

± 0.037 (n = 4). All data were blank corrected. The uncertainties in the compositions of the blanks are reflected in the respective uncertainties for the isotopic and concentrations reported in Table 5.2. The external reproducibilities on standard analyses for Os and Re were typically better than ±0.1 and ±0.3%, respectively.

Osmium isotopic compositions were analyzed by negative thermal ionization mass spectrometry (Creaser et al., 1991; Völkening et al., 1991) using the procedures discussed in Walker et al. (1994) and Morgan et al. (1995). Samples with high Os abundances were analyzed with Faraday cups in static analytical mode using a VG Sector 54 mass spectrometer, whereas those with relatively low abundances of Os were analyzed with an electron multiplier in dynamic mode using a 12" radius NBS mass spectrometer.

The concentrations of Re were determined using a Nu Plasma multi-collector inductively-coupled plasma mass spectrometer (MC-ICP-MS) using a static mode and either Faraday cup or electron multiplier detectors (Belshaw et al., 1998). The sample solution (in 2% $HNO_3$) was introduced to an Ar plasma using an Aridus® desolvating nebulizer. The instrumental fractionation of $^{185}Re/^{187}Re$ for the samples was monitored and corrected via interspersed analyses of standards of comparable Re concentrations.

## 5.4. RESULTS

The Dundonald komatiites and komatiitic basalts show strong olivine control on $Al_2O_3$ and $TiO_2$ fractionation-accumulation trends (Fig. 5.1). These rocks have near-chondritic $Al_2O_3/TiO_2$ ratios (21-26 vs. chondritic ratio of ~22: McDonough and Sun, 1995), unfractionated chondrite-normalized heavy rare earth element (HREE)

**Table 5.2.** Rhenium and Os concentration and isotope data for the whole rock komatiites and komatiitic basalts, and chromite separates

| Samples | Re (ppb) | Os (ppb) | $^{187}Re/^{188}Os^{1}$ | $^{187}Os/^{188}Os^{1}$ | $\gamma_{Os}(2.7Ga)^{2}$ | Model age (Ga) |
|---|---|---|---|---|---|---|
| Samples from komatiite unit with $^{187}Re/^{188}Os < 1$: | | | | | | |
| DUNBCH-1 | 0.3237 | 3.384 | 0.4610 | 0.1306 | +0.8±0.5 | |
| **DUNBCH-1A**[*] | 0.4391 | 6.392 | 0.3308 | 0.1231 | -0.6±0.4 | |
| **DUNBCH-1B** | 0.5367 | 7.038 | 0.3673 | 0.1250 | -0.4±0.4 | |
| DUNBCH-2 | 0.1771 | 4.093 | 0.2082 | 0.1171 | -0.9±0.4 | |
| Dupl.** | 0.1439 | 3.715 | 0.1863 | 0.1169 | -0.1±0.4 | |
| **DUNBCH-2A** | 0.2830 | 9.610 | 0.1417 | 0.1158 | +0.7±0.4 | |
| **DUNBCH-2B** | 0.3393 | 9.825 | 0.1662 | 0.1156 | -0.5±0.4 | |
| DUNBCH-3 | 0.1684 | 4.252 | 0.1906 | 0.1198 | +2.3±0.4 | |
| Dupl. | 0.1070 | 3.797 | 0.1356 | 0.1155 | +0.6±0.3 | |
| DUNBCH-13 (KBU[3]) | 0.4021 | 2.438 | 0.7963 | 0.1441 | -0.9±0.6 | |
| | | | | | | |
| Samples from komatiite and komatiitic basalt units with $^{187}Re/^{188}Os > 1$: | | | | | | |
| DUNBCH-4 | 0.6125 | 0.3794 | 8.102 | 0.4473 | -30.1 | 2.4 |
| Dupl. | 0.1912 | 0.3260 | 2.940 | 0.4378 | +179 | 6.9 |
| DUNBCH-5 | 0.5431 | 0.8623 | 3.082 | 0.2466 | -3.0 | 2.6 |
| Dupl. | 0.3262 | 0.7522 | 2.123 | 0.2516 | +42.1 | 4.2 |
| DUNBCH-6 | 0.3618 | 0.5870 | 3.014 | 0.2394 | -6.8 | 2.5 |
| Dupl. | 0.4348 | 0.6479 | 3.280 | 0.2383 | -19.0 | 2.3 |
| DUNBCH-7 | 0.7267 | 1.025 | 3.475 | 0.2624 | -5.0 | 2.6 |
| DUNBCH-8 | 0.7406 | 0.3204 | 11.86 | 0.6282 | -22.1 | 2.6 |
| DUNBCH-9 | 0.4886 | 0.4239 | 5.701 | 0.3310 | -35.8 | 2.3 |
| Dupl. | 0.6024 | 0.6132 | 4.848 | 0.3126 | -16.8 | 2.5 |
| DUNBCH-10 | 0.4457 | 0.4354 | 5.057 | 0.3224 | -16.6 | 2.5 |
| DUNBCH-11 | 0.2535 | 0.3980 | 3.108 | 0.2244 | -24.5 | 2.1 |
| DUNBCH-12 | 0.2799 | 0.4415 | 3.096 | 0.2295 | -19.4 | 2.2 |
| DUNBCH-14 | 0.5507 | 0.3881 | 7.054 | 0.3724 | -54.8 | 2.2 |
| DUNBCH-15 | 0.3842 | 0.7376 | 2.540 | 0.2209 | -3.8 | 2.6 |

[*]Bold faced sample numbers represent chromite separates from the corresponding whole rock sample.

** Dupl. = Duplicate analyses of separate powder splits.

[1]The total analytical uncertainties are ±0.5% for $^{187}Re/^{188}Os$ and ±0.3% for $^{187}Os/^{188}Os$ (2σ%) for both whole rock and chromite separates.

[2]$\gamma_{Os}$ is calculated at the assumed age of 2.715 Ga for the crystallization of these rocks. This age is based on U-Pb zircon ages of the volcanics associated with the stratigraphically-equivalent rocks from Alexo and Pyke Hill (Ayer et al., 2002). The chondritic $^{187}Os/^{188}Os$ at 2.7 Ga is calculated to be 0.1084, based on average $^{187}Re/^{188}Os$ ratio of chondrites and initial $^{187}Os/^{188}Os$ (T= 4.558 Ga) for early solar system materials (IIIA irons) of 0.40186 and 0.09531, respectively (Shirey and Walker, 1998). The decay constant (λ) used here is 1.666 x $10^{-11}$ year$^{-1}$ (Smoliar et al., 1996).

[3]KBU = komatiitic basalt unit; rest of the samples are from komatiite unit.
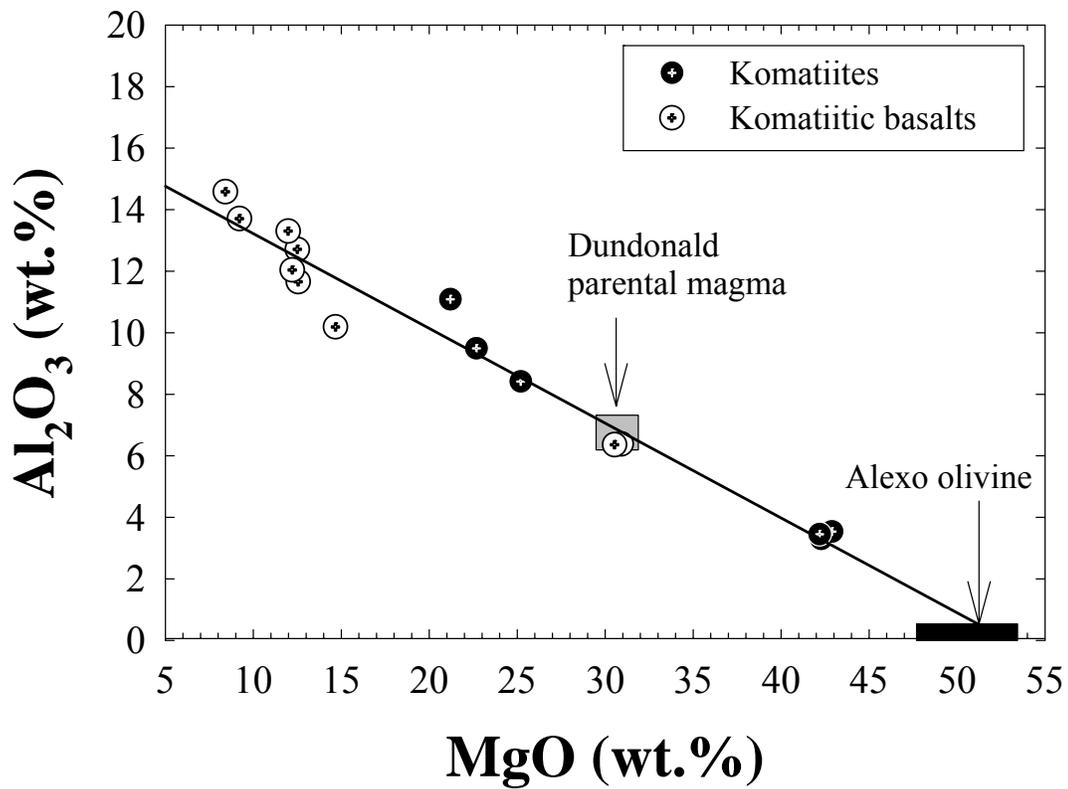
**Fig. 5.1.** Plot of MgO versus $Al_2O_3$ (wt.%, volatile-free) of the Dundonald komatiites and komatiitic basalts. The Dundonald parental magma composition is plotted after Barnes (1985).

patterns (Gd/Yb$_{CN}$ ~ 0.9-1.1) similar to Al-undepleted komatiites at Alexo and Pyke Hill (e.g., Lahaye and Arndt, 1996; Fan and Kerrich, 1997) and to Al-undepleted komatiites worldwide (e.g., Nesbitt et al., 1979; Lahaye et al., 1995; Sproule et al., 2002).

There is a broad positive correlation between MgO and Os concentrations in the whole rock samples from the komatiite unit (Fig. 5.2A). A similar positive correlation is also observed in the komatiitic basalt unit. Two samples of cumulate and spinifex rocks from the komatiitic basalt unit (DUNBCH-11 and DUNBCH-12), however, do not plot on this trend. The trends for the komatiite and komatiitic basalt units are roughly parallel, but the komatiitic basalts have higher Os concentrations at a given MgO content (Fig. 5.2A). An analogous offset is also observed on a plot of MgO versus Ir concentrations for komatiites from Pyke Hill, komatiitic basalts from Fred's flow, and tholeiitic basalts from Theo's flow in Munro Township (Crocket and MacRae, 1986). The olivine cumulate rocks (~43 wt.% MgO: Table 5.1) have the highest Os concentrations (up to ~ 4.3 ppb). The Os concentrations in the more fractionated rocks (Os ~ 0.3-0.9 ppb with MgO = 20-30 wt.%) overlap with those of the komatiitic basalts (Os ~ 0.3-1.0 ppb with MgO < 15 wt.%). One komatiitic basalt sample (DUNBCH-13) has an unusually high Os concentration of ~2.4 ppb for its MgO content (14.7 wt.%; Table 1; Fig. 5.2A).

There is an overall increase in Re concentration with decreasing MgO content in the whole rocks over the entire komatiite and komatiitic basalt fractionation sequence (Fig. 5.2B). The olivine cumulate, spinifex and komatiitic basalt samples,
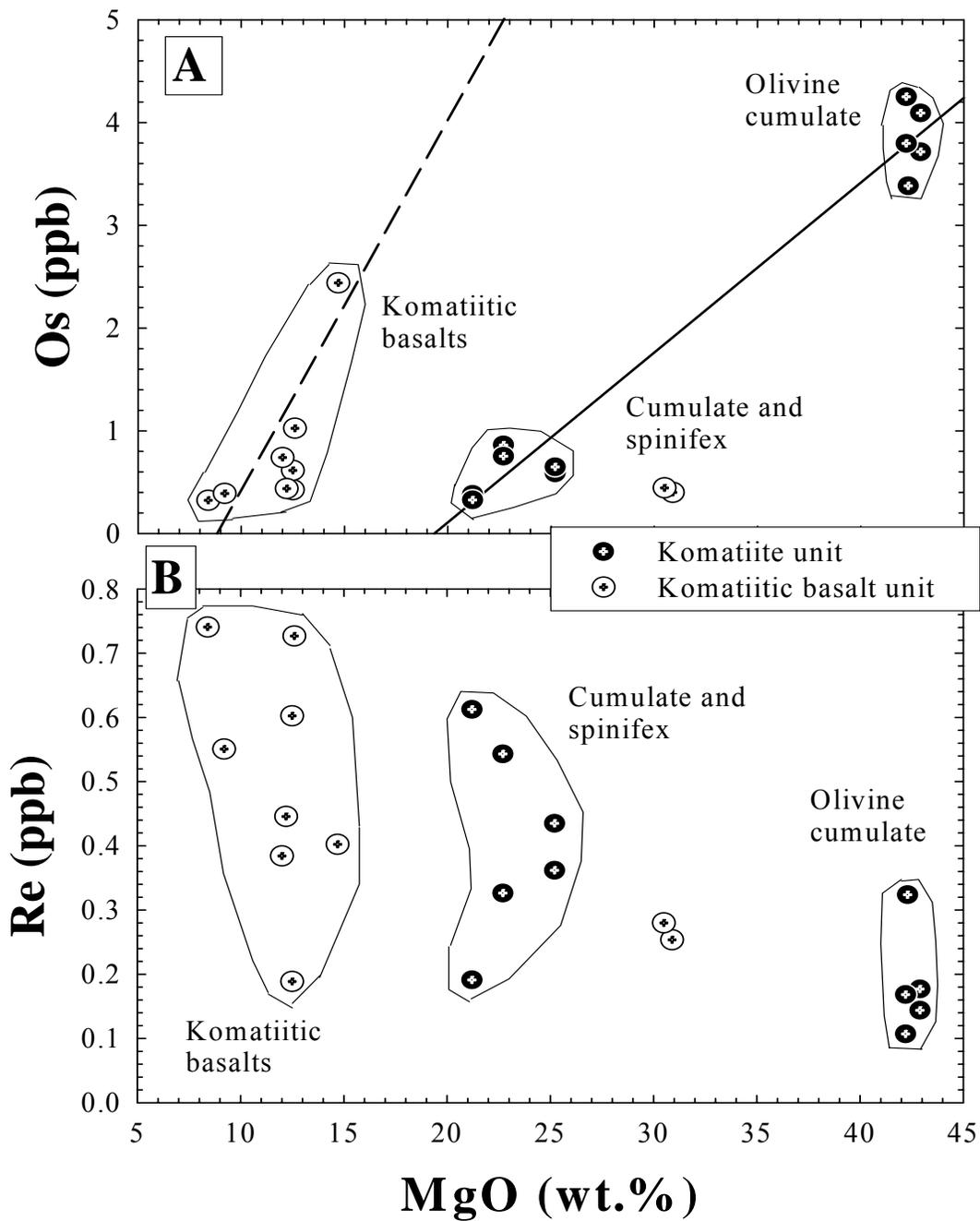
**Fig. 5.2.** Plot of whole rock MgO (wt.%, volatile-free) versus Os and Re concentrations (ppb) in the Dundonald komatiites and komatiitic basalts. The solid line is the best-fit regression for Re concentrations.

however, when considered separately, show large scatter in Re concentrations even within narrow ranges of MgO contents.

Whole rock samples with $^{187}Re/^{188}Os > 1$ (DUNBCH-4 through DUNBCH-15, except DUNBCH-13) show highly variable calculated initial $^{187}Os/^{188}Os$ isotopic ratios ($\gamma_{Os}$ at 2.715 Ga varying between approximately -55 and +179: Table 5.2). Some of the variability is due to error magnifications in the calculated initial $^{187}Os/^{188}Os$ ratios resulting from the relatively high Re/Os (Walker et al., 1994). Nonetheless, most of the whole rock samples plot below a 2.715 Ga chondritic reference isochron (Fig. 5.3A). The variable initial Os isotopic compositions cannot be due to heterogeneity in the mantle source because most non-isochronous samples yield unrealisitically low initial $\gamma_{Os}$ (< -16). Furthermore, such a large initial Os isotopic variation would not be initially present in a single cooling unit. When four samples with extreme values of calculated initial $\gamma_{Os}$ (DUNBCH-4/Dupl., DUNBCH-5/Dupl., DUNBCH-9 and DUNBCH-14) are eliminated from the regression calculation of the Re-Os isotope results, the remaining 21 points yield a model 3 isochron age (Ludwig, 1998) of 2517 ± 61 Ma and an initial $^{187}Os/^{188}Os$ ratio of 0.1079 ± 0.0041 (Fig. 3A). This regression has high MSWD value of 83 and large uncertainty for the initial Os isotopic composition calculated at 2517 Ma ($\gamma_{Os} = 0.0 \pm$ 4.1). This age is ~200 Ma younger than the probable crystallization age of the rocks. The initial Os isotopic composition obtained from this linear correlation, therefore, cannot be taken as that of the mantle source for the rocks.

The initial $^{187}Os/^{188}Os$ ratio of the mantle source for the Dundonald komatiites was instead determined by regressing the calculated initial $^{187}Os/^{188}Os$ ratios (at 2.715
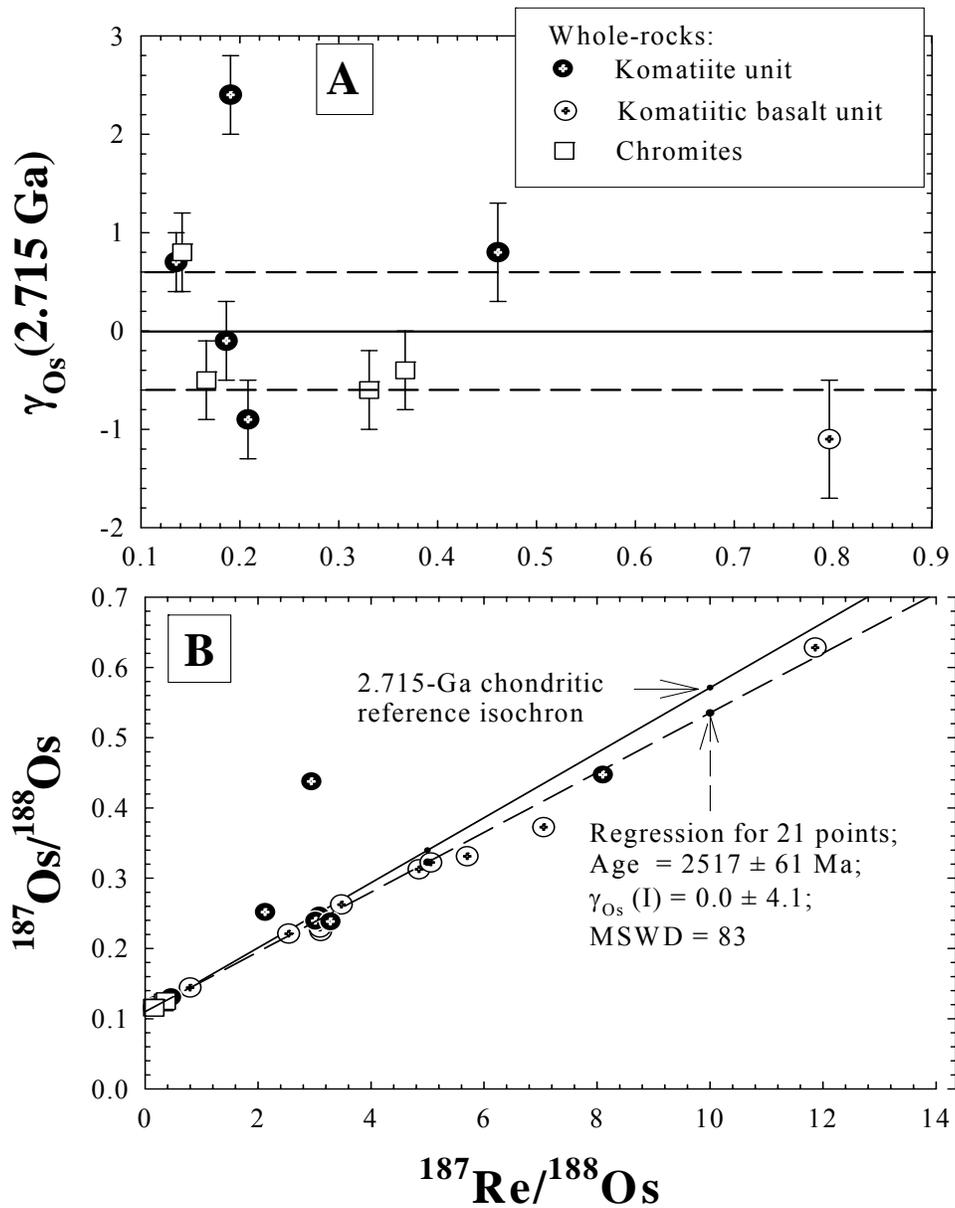
**Fig. 5.3. (A)** Plot of calculated initial $\gamma_{Os}$ at 2.715 Ga versus $^{187}Re/^{188}Os$ ratios (<1)

for the whole rock Dundonald komatiites and chromite separates. Note that,

excluding one outlier of whole rock, all of these samples define a narrow range of

initial $\gamma_{Os}$ of 0.0±0.6. **(B)** Plot of $^{187}Os/^{188}Os$ versus $^{187}Re/^{188}Os$ ratios of all the whole

rocks and chromite separates examined in this study. Also shown for comparison is a

2.7 Ga chondritic reference isochron.

Ga) of several cumulate rocks (DUNBCH-1, DUNBCH-2, DUNBCH-3), a komatiitic basalt (DUNBCH -13), and the chromite separates (Fig. 5.3B). These samples are appropriate for determining initial $^{187}Os/^{188}Os$ because they all have high Os concentrations and low $^{187}Re/^{188}Os$ ratios (<1), and are therefore less susceptible to isotopic resetting. The low Re/Os ratios also result in modest corrections for age and limited sensitivity to Re gain or loss and Os loss. With one outlier eliminated from the regression, the weighted average initial $^{187}Os/^{188}Os$ ratio of 0.1083 ± 0.0006 (2σ) corresponds to an initial $\gamma_{Os}$ = 0.0 ± 0.6 (Fig. 5.3A). This indicates that the Os isotopic composition of the mantle source for the Dundonald komatiites was essentially chondritic, indistinguishable from the initial ratios determined for the sources of the Alexo and Pyke Hill komatiites (Gangopadhyay and Walker, 2003; Shirey, 1997; Puchtel et al., 2004a).

## 5.5. DISCUSSION

### 5.5.1. Calculation of primary Re concentrations in the emplaced lavas

In previous studies of Alexo and Pyke Hill komatiites, the preservation of Re-Os isotope systematics of the emplaced lavas was demonstrated via the generation of isochrons that yielded precise ages, consistent with those obtained from Sm-Nd and Pb-Pb isotope systematics (Gangopadhyay and Walker, 2003; Puchtel et al., 2004a). The closed-system behavior of the elemental Re abundances in these rocks is manifested by a strong linear correlation between whole rock $Al_2O_3$ and Re concentrations (Fig. 5.4). This suggests that Re in the komatiites from Alexo and Pyke Hill was similarly incompatible during the differentiation of their respective parental magmas. In contrast to the Alexo and Pyke Hill rocks, the Dundonald Beach
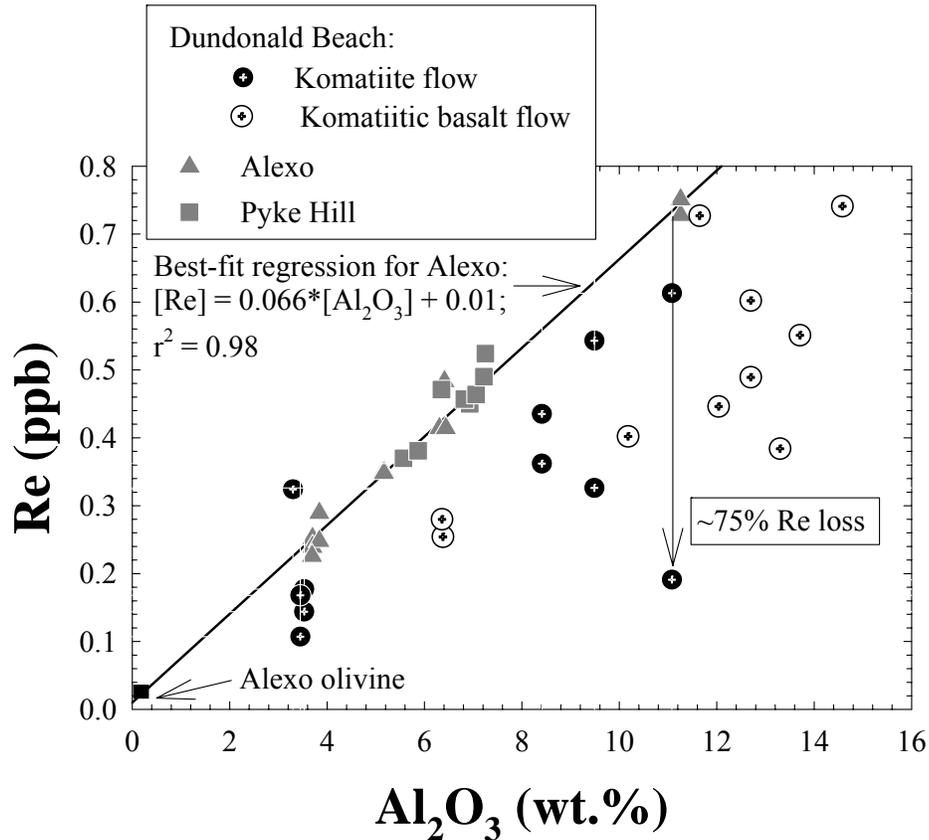
**Fig. 5.4.** Plot of whole rock Re and $Al_2O_3$ concentrations in the Dundonald rocks (present study) and those for the Alexo and Pyke Hill komatites that were shown to define a magmatic Re-Os isochron, consistent with minimal Re mobility (Gangopadhyay and Walker, 2003; Puchtel et al., 2004a). The best-fit $Al_2O_3$-Re regression for Alexo rocks projects back to the field for Alexo olivine (Lahaye et al., 2001; Puchtel et al., 2004a). The Pyke Hill rocks (excluding two outliers that were interpreted to have suffered Re loss during or soon after emplacement; Puchtel et al., 2004a) also plot on the $Al_2O_3$-Re correlation line for Alexo komatiites. Note that virtually all Dundonald rocks plot below the regression, suggesting large percentages of Re loss.

komatiites and komatiitic basalts show a large degree of scatter on a plot of $Al_2O_3$ versus Re concentrations (Fig. 5.4). Given that the Al concentrations in the same set of samples of Dundonald rocks show a strong olivine control (Fig. 5.1A), the large scatter is most likely due to mobility of Re rather than Al. For this reason, we calculated the Re concentrations in the Dundonald komatiites based on the regression for $Al_2O_3$-Re concentrations in the Alexo komatiites. Gangopadhyay and Walker (2003) reported a linear correlation between $Al_2O_3$ versus Re concentrations in the Alexo komatiites of $[Re] = 0.066*[Al_2O_3] + 0.01$ ($r^2 = 0.98$). This equation and the $Al_2O_3$ contents of each Dundonald rock were used to correct each Al-Re sample pair. Because Re and Al have similar incompatibilities, yet the latter is less mobile, a similar method is commonly used in altered peridotites in order to calculate initial $^{187}Os/^{188}Os$ ratios (Reisberg and Lorand, 1995; Rudnick and Lee, 2002 and references therein). Also, Lahaye and Arndt (1996) followed a similar method for Alexo komatiites, where whole rock concentrations of $Al_2O_3$ were used to evaluate the mobility of other incompatible trace elements (including REE).

The $Al_2O_3$-Re regression for the whole rock Alexo komatiites projects back to the field of olivine (Lahaye et al., 2001; Puchtel et al., 2004a), suggestive of a primary magmatic correlation for the Alexo rocks (Fig. 5.4). It cannot be demonstrated, however, whether or not the Dundonald emplaced lavas also had the same $Al_2O_3$-Re linear correlation as Alexo rocks, as opposed to one with a steeper or gentler slope. Nonetheless, given that both Alexo and Pyke Hill komatiites have nearly identical Re/Al ratios, and the Dundonald rocks were presumably derived from chemically very similar parental magmas, it is justifiable to assume that the

Dundonald emplaced lavas also probably crystallized with an Al-Re correlation similar to those for Alexo and Pyke Hill komatiites. Using this assumption, all of our samples except DUNBCH-1, which plots above the trend, appear to have lost variable amounts of Re. Average estimated Re loss is ~40%, but some samples may have lost as much as ~75% Re. The amount of Re loss was as great in the Al-Re-rich, olivine-poor (non-cumulate) samples as in the Al-Re-poor, olivine rich (cumulate) samples.

**5.5.2. Constraints on the timing of open-system behavior of Re-Os systematics**

The Dundonald komatiitic rocks show evidence for at least three episodes of alteration of Re-Os elemental and isotope systematics of the emplaced lavas. Possible mechanisms for these alteration events and their relative timing are discussed below.

The whole rock komatiites and komatiitic basalts with $^{187}Re/^{188}Os > 1$ generally plot below the 2.7 Ga chondritic reference isochron, suggesting either post-crystallization Re gain and/or Os loss. The positive correlation between MgO and Os concentrations in the Dundonald komatiites and komatiitic basalts is common among komatiites (e.g., Walker et al., 1999; Hanski et al., 2004; Puchtel et al., 2004b). Also, our empirical estimate of bulk distribution coefficients of Os during the differentiation of Dundonald lavas ($D_{Os}^{solid/liquid}$) is well within the range of previous determinations for least-altered Alexo and Pyke Hill rocks. Combined, these observations suggest that Os was relatively immobile during the alteration of Dundonald rocks, so the isotopic systematics are most consistent with Re *gain* subsequent to crystallization. However, the Re concentrations in the whole rock samples generally plot below the presumed magmatic Al-Re correlation, suggesting Re *loss* from most samples (Fig. 5.4). The high percentages of Re losses indicated by

the Al-Re plot (Fig. 5.4) and the more modest (maximum of ~6%) addition of Re indicated by the Os isotopic data (Fig. 5.3) require at least two episodes of Re mobility, a larger one at an early stage that would not significantly affect the Re-Os isotope system, and a smaller one at a later stage that modestly affected the Os isotopic systematics.

The variably large Re losses appear to have occurred at or soon after the time of eruption of Dundonald lavas. One mechanism that could potentially be responsible is volatility-related Re loss (e.g., Bennett et al., 2000; Lassiter, 2003), which is consistent with the relatively large amounts of vesicles in these units, the large amount of associated peperites, and the evidence for emplacement into unconsolidated graphitic sediments (Davis, 1999; Houlé et al., 2002). The calculated Re loss in whole rocks is as much as 75% relative to their presumed concentrations in the emplaced lavas. The putative Re losses from the Dundonald rocks are similar in magnitude to losses estimated for Hawaiian lavas that were inferred to have occurred from subaerial or shallow-water flows (Lassiter, 2003), suggesting that this process also occurs when magmas are emplaced into relatively deep-water, graphitic, sulfidic sediments. This mode of emplacement contrasts with Alexo and Pyke Hill where vesicular pillowed komatiitic basalts, hyaloclastite breccias, polyhedral jointing, and O isotope data all suggest a shallow subaqueous environment of eruption (e.g., Arndt et al., 1977; Beaty and Taylor, 1982).

Another potential cause of large degrees of Re loss is hydrothermal leaching of Re immediately after emplacement. For example, Re and Os-rich sulfide phases are commonly oxidized during hydrothermal alteration of abyssal peridotites and may

cause mobility of Re (see Roy-Barman and Allègre, 1994). Also, interactions between komatiites and hydrothermal fluids may produce high contents of halogen salts (e.g., Cl and Br: Appel, 1997) that can be removed by circulating seawater or hydrothermal solution. Rhenium, and also likely Os, is highly soluble in Cl-rich hydrothermal solutions (Xiong and Wood, 1999), and can therefore be potentially leached from the komatiites during their hydrothermal alteration.

From the above discussion, it is apparent that the high percentages of Re losses in the Dundonald rocks were largely coeval with their crystallization. This would have had no significant effect on the Os isotope systematics, so the resetting of Os isotope systematics must have occurred subsequently.

The age of the dominant alteration event that disturbed the Re-Os isotope systematics for the Dundonald rocks likely occurred at ~2.4-2.5 Ga, consistent with both the Os model ages for most samples with high Re/Os ratios (Table 5.2) and the errorchron results (Fig. 5.3B). This age may reflect the time of a regional metamorphic event for the Kidd-Munro komatiitic rocks. The Alexo, Pyke Hill, and Dundonald komatiitic rocks have all been regionally metamorphosed to lower greenschist facies (e.g., Jolly, 1982), yet the Re-Os systematics of Alexo and Pyke Hill rocks do not appear to be affected. The precise ages for metamorphism of the Kidd-Munro rocks are largely unconstrained. For the Pyke Hill komatiites, U-Pb zircon ages are in general agreement with their Pb-Pb isochron ages (e.g., Carignan et al., 1995), which often record the last event of hydrothermal alteration or metamorphic re-equilibrations of Pb isotopes in mafic-ultramafic rocks (e.g., Brévart et al., 1986; Dupré and Arndt, 1990; Frei et al., 2004). In contrast, the Re-Os

errorchron age of 2517 ± 61 Ma obtained for the Dundonald rocks is, within uncertainty, in agreement with the previously reported Pb-Pb isotope results for the komatiitic basalts from Fred's flow and tholeiitic basalts from Theo's flow (2580 ± 20 Ma and 2470 ± 130 Ma, respectively) that crop out near Pyke Hill (Brévart et al., 1986). The Pb-Pb isochron ages for the Fred's and Theo's flows that are ~200 Ma younger than the adjoining Pyke Hill komatiites were also interpreted to reflect a regional metamorphic resetting event (Brévart et al., 1986). Thus, it is possible that the Re-Os isotope systematics of the Dundonald rocks were also reset at ~200 Ma after the crystallization of the emplaced lavas.

Finally, there is also evidence for relatively late-stage, possibly recent mobility of Re in the Dundonald rocks. For example, the two pairs of whole rock samples (DUNBCH-5 and DUNBCH-6) and their corresponding duplicate analyses yield negative slopes for their respective two-point Re-Os isochrons that can best be explained by very recent Re loss or gain. Additionally, another two pairs of whole rocks (DUNBCH-4 and DUNBCH-9) and their duplicate analyses yield significantly younger two-point isochron ages of ~110 Ma and ~1.3 Ga, respectively. The significance of these ages is not obvious, yet the ~1 Ga age for DUNBCH-4 is in agreement with the previously obtained Rb-Sr errorchron age for the Munro komatiites, which was interpreted to reflect a late-stage metamorphic event (Walker et al., 1988).

## 5.5.3. Partitioning behavior of Os during differentiation of komatiitic lavas

On a plot of Os and Ni concentrations, the whole rock Dundonald komatiites and komatiitic basalts define two distinct linear trends with similar slopes (Fig. 5.5).
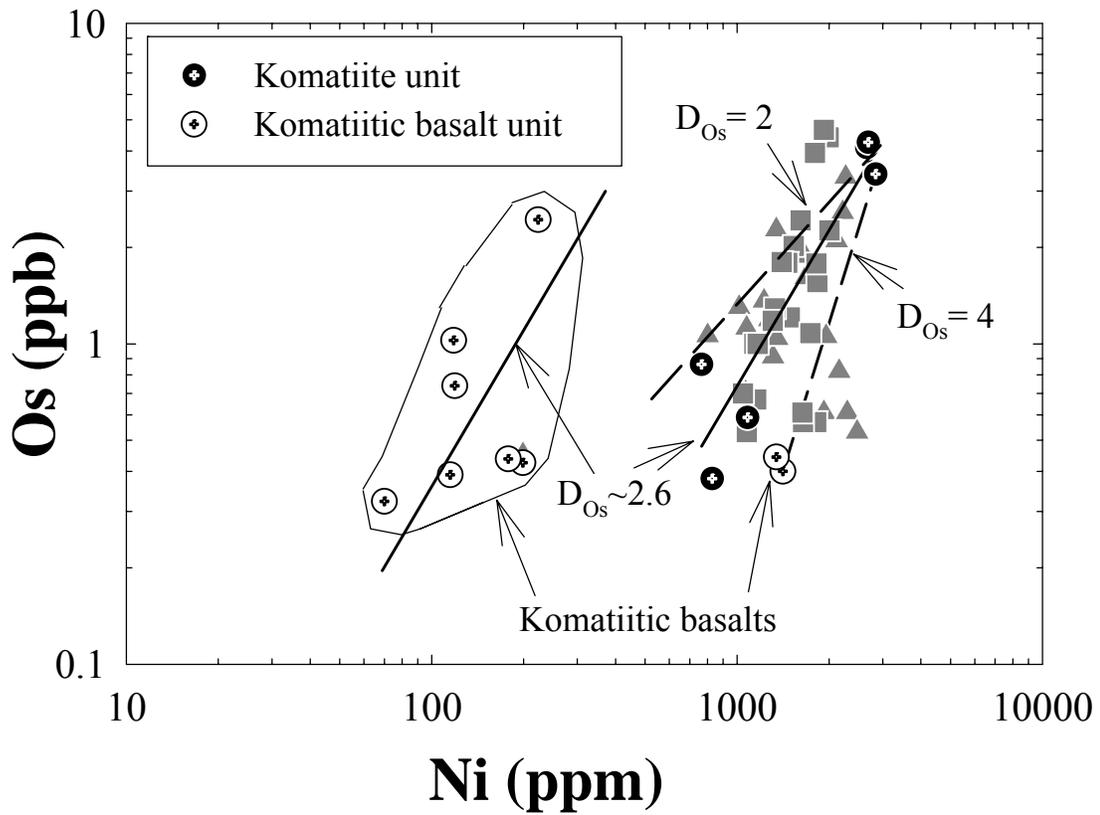
**Fig. 5.5.** Plot of Os and Ni concentrations in the Dundonald rocks are compared with those from Alexo and Pyke Hill in the Abitibi greenstone belt (symbols as in Fig. 5C). The entire range of variations in Ni and Os concentrations in these rocks can be best approximated (shown by two dashed lines) by $D_{Os}^{crystal/liquid} \sim$2-4.

The Dundonald komatiites with high MgO and correspondingly high Ni concentrations plot along a broad linear array together with those from Alexo (Gangopadhyay and Walker, 2003; Puchtel et al., 2004b) and Pyke Hill (A. Gangopadhyay, unpubl. data; Puchtel et al., 2004b). The entire range of Os and Ni concentrations for komatiites from Alexo, Pyke Hill, and Dundonald Beach is best approximated with linear regressions that yield $D_{Os}$ between 2 and 4 (Fig. 5.5). These $D_{Os}$ values are consistent with those independently estimated for komatiites from Alexo and Pyke Hill (1.7-2.8 and 3.8-7.1, respectively: Gangopadhyay and Walker, 2003; Puchtel et al., 2004b) and are in general agreement with the compatibility of IPGEs (Ir, Os, Ru) during mantle melting and magmatic differentiation in mafic-ultramafic system (e.g., Barnes et al., 1985; Brügmann et al., 1987; Lesher and Stone, 1996; Lesher et al., 2001). Combined, these results suggest that Os is moderately to strongly compatible during the differentiation of komatiitic lavas.

A compilation of Cr and MgO data for a variety of ferropicritic, Al-undepleted, Al-depleted ($Al_2O_3/TiO_2$ of ~5-11: Walker and Stone, 2001), and Ti-enriched (e.g., Sproule et al., 2002; Gangopadhyay et al., in revision) ultramafic rocks suggests that olivine crystallizes in komatiitic (*sensu stricto*) magmas, but that chromite and olivine co-precipitate in komatiitic basaltic magmas (Fig. 5.6A). The latter interpretation is consistent with the experimental results of Murck and Campbell (1986) and Thy (1995), and with the empirical observations of Lesher and Stone (1996) and Barnes (1998). Importantly, the same suites of samples that show chromite fractionation/accumulation also show a broad positive correlation between MgO and Os concentrations (Fig. 5.7B). The absence of any significant correlation

**Fig. 5.6.** Plot of whole rock MgO (wt.%, anhydrous) and **(A)** Cr (ppm) and **(B)** Os (ppb) in the Al-undepleted komatiites from Dundonald Beach (this study), Alexo (Gangopadhyay and Walker, 2003), Pyke Hill (Puchtel et al., 2004b) in the Abitibi greenstone belt, Song Da, Vietnam (Hanski et al., 2004), Vetreny, Russia (Puchtel et al., 2001b) and Ti-enriched komatiitic rocks (Gangopahyay et al., in review) and Al-depleted picritic rocks (Walker and Stone, 2001). The shaded rectangle is the estimated parental magma composition for the Dundonald komatiites (Barnes, 1985). The olivine composition is from Arndt, 1986. Note that the low-magnesian komatiitic rocks (MgO < ~25 wt.%) show a strong positive correlation between chromite fractionation (in Fig. 6A) and Os concentrations (in Fig. 5.6B).
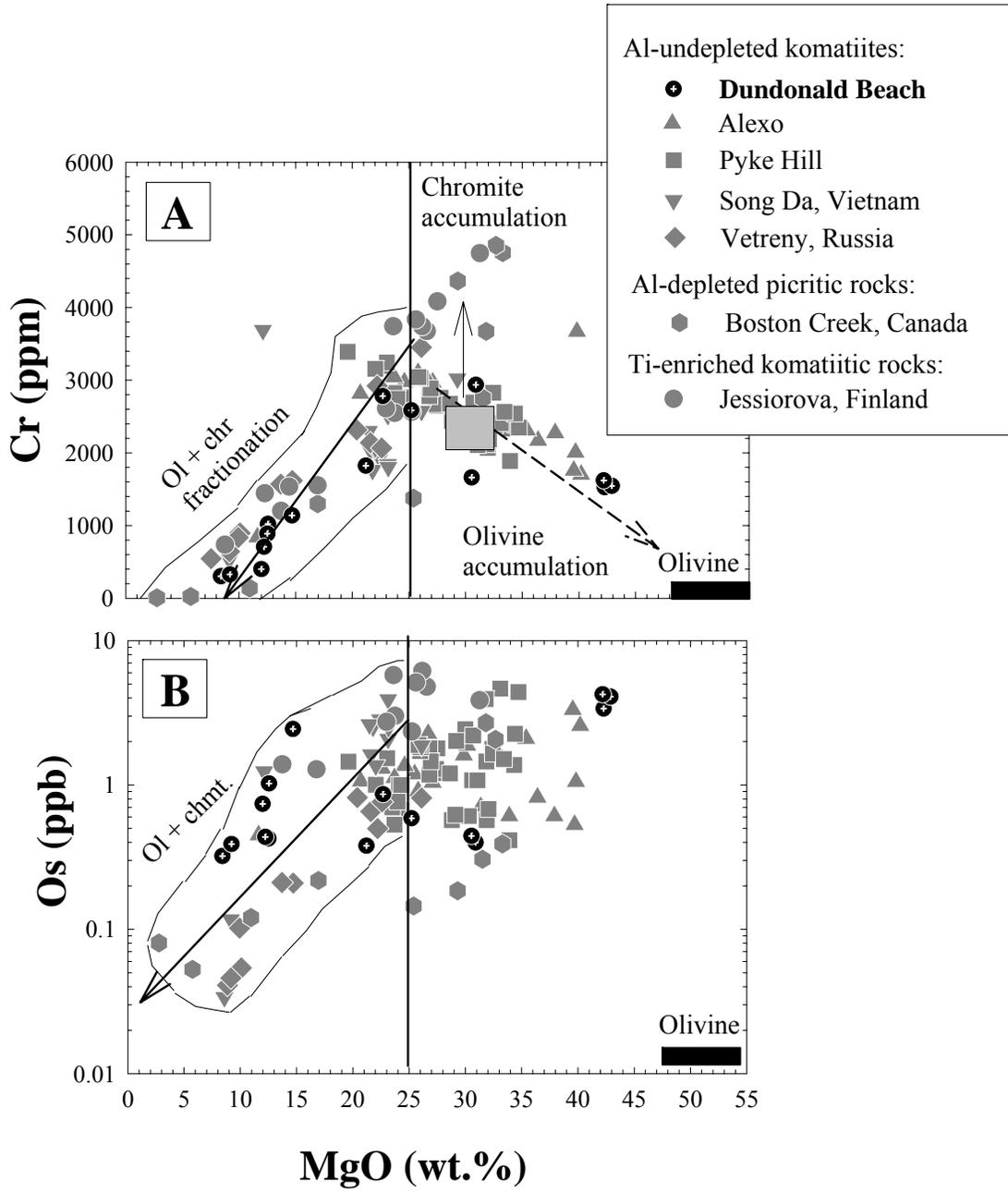
**Fig. 5.6.**

between MgO (at >25 wt.%) and Os concentrations for olivine-only fractionation, combined with a positive correlation between MgO and Os concentrations for olivine+chromite fractionation (see Fig. 5.6B) suggests that chromite and/or co-precipitating trace phase(s) play a significant role in controlling the partitioning behavior of Os during crystallization in komatiitic basalts, but not in most komatiites. Some studies have identified an early fractionating Os-rich trace phase(s) in high-MgO komatiites, but the identity is, as yet, unknown (e.g., see Puchtel et al., 2004b). Nevertheless, the consistent decrease in Os concentrations with chromite fractionation in the different komatiite types is consistent with (a) the experimentally-determined compatibility of IPGE in chromites (Capobianco and Drake, 1990; Righter et al., 2004), (b) preferential partitioning of PGE into sulfide or accessory platinum group minerals (e.g., laurite or alloys) included within chromite crystals (e.g., Sattari et al., 2002; also see Mathez, 1999), (c) direct crystallization of laurite onto the surface of chromite crystals (Bockrath et al., 2004), and (d) up to 2 orders of magnitude higher Os concentrations in chromite separates than in the komatiitic host rocks (Gangopadhyay and Walker, 2003; Gangopadhyay et al., in revision).

### 5.5.4. Factors influencing the selection of samples for Os isotopic studies of Precambrian komatiites

Olivine cumulate portions of komatiite units from Dundonald Beach, although strongly serpentinized, have the highest Os concentrations (Fig. 5.2) and yield uniform chondritic initial Os isotopic compositions that are consistent with those obtained from corresponding chromite separates (Fig. 5.3; Table 5.2). These generally contrast with the significantly lower Os concentrations and highly variable calculated initial $\gamma_{Os}$ in the less magnesian komatiites and komatiitic basalts (Table 5.2).

Combined, these results suggest that Os was dominantly hosted within trace phases (e.g., chromites or Os-rich inclusions within chromites) that were relatively immune to secondary alteration at the whole rock scale of cumulate rocks. Also, the variable calculated initial Os isotopic compositions are limited only to samples with high $^{187}Re/^{188}Os$ ratios (>1). This is largely due to the fact that, for a specific percentage loss or gain of Re, an ancient sample with high initial $^{187}Re/^{188}Os$ ratio yields larger deviation from the true initial Os isotopic composition than one with lower $^{187}Re/^{188}Os$ ratio (Walker et al., 1994).

The Dundonald komatiitic rocks have undergone pervasive hydrothermal alteration, as evidenced by essentially complete serpentinization of olivine and high values of loss on ignition (LOI up to ~13 wt.%; Table 5.1) for the whole rocks. Also, there is a strong positive correlation between the whole rock MgO contents and LOI, suggesting that the rocks with the highest modal abundances of cumulate olivine have undergone the highest degrees of hydration. This is consistent with the near-total serpentinization of olivine in the cumulate rocks. There is, however, no correlation between the calculated Re loss or gain (as discussed above) and LOI in these rocks, indicating that the mobility of Re was not solely caused by hydration of the rocks.

Consistent with the last interpretation, some of the Permo-Triassic komatiitic rocks from Song Da, Vietnam (Hanski et al., 2004) show replacement of olivine by iddingsite and serpentine, and yet record the unaltered Re-Os isotope systematics of the emplaced lavas. Similarly, komatiites from Alexo also show petrographic evidence for extensive serpentinization and oxidation of olivine and devitrification of glass, yet exhibit closed-system Re-Os systematics of the emplaced lavas

(Gangopadhyay and Walker, 2003). Conversely, komatiites from Belingwe, Zimbabwe (e.g., Tony's Flow and Onia's Flow) are among the few Archean komatiites hitherto reported that show well-preserved, polyhedral olivine phenocrysts and microphenocrysts containing fresh glass inclusions (Nisbet et al., 1987). The whole rock Re-Os systematics of these two flows show large-scale open-system behavior (Walker and Nisbet, 2002). Collectively, these observations are consistent with the fact that empirical estimates (Puchtel and Humayun, 2001; Bourton et al., 2002; Bennett et al., 2002) and experimental determinations (Brenan et al., 2003; Righter et al., 2004) suggest that both Re and Os are usually moderately to highly incompatible in olivine in mafic-ultramafic rocks. Olivine is thus unlikely to be the major host for Re and Os in the komatiitic rocks, and accordingly, the replacement processes of olivine, in most cases, were probably not directly responsible for Re and/or Os mobility at the whole rock scale.

Hydrothermal alteration of komatiites, however, can potentially result in mobility of both Re and Os hosted in sulfide phases because the sulfide minerals in komatiites (e.g., pentlandite, pyrrhotite, chalcopyrite, and pyrite) commonly have high concentrations of both Os (up to ~18 ppb: Puchtel and Humayun, 2001) and Re (up to ~270 ppb: Gangopadhyay et al., in revision) in komatiitic rocks. It has been suggested that sulfides are oxidized to sulfates during serpentinization of abyssal peridotites and that this may cause mobility of Os (cf. Roy-Barman and Allegre, 1994). Sulfide minerals are, however, present in typically very low abundances (<1% by weight) in komatiitic rocks that are sampled away from magmatic sulfide ore deposits (e.g., Barnes, 1985). Nevertheless, the Re-Os systematics of sulfide minerals,

154

whenever present in sufficient quantities for mineral separation from magmatic rocks, commonly show open-system behavior (e.g., Luck and Allegre, 1984; Shirey and Walker, 1995; Walker et al., 1997; Gangopadhyay et al., in revision).

Collectively, the above considerations suggest that: [1] olivine cumulate whole rocks and their chromite separates constitute the preferred set of samples for the determination of initial Os isotopic composition of the mantle sources for emplaced Precambrian komatiites; [2] textural preservation may not necessarily serve as a useful guide in selecting Precambrian komatiites for Os isotopic studies; and [3] caution must be taken to avoid sulfide impurities in primary mineral separates (e.g., chromite, olivine) in order to examine the magmatic Re-Os systematics of emplaced komatiitic lavas.

### 5.5.5. Implications of a chondritic initial Os isotopic composition of the Kidd-Munro assemblage

The chondritic initial Os isotopic composition for the mantle source for the Dundonald rocks is consistent with that previously reported for the Alexo and Pyke Hill komatiites (Gangopadhyay and Walker, 2003; Puchtel et al., 2004a). The chondritic initial Os isotopic composition of the Dundonald rocks is also in agreement with the long-term chondritic Os isotopic evolution of the modern terrestrial convecting upper mantle (Snow and Reisberg, 1995; Brandon et al., 2000; Walker et al., 1996; 2002). Furthermore, the initial Os isotopic composition of the ~2.7-Ga mantle source for the Kidd-Munro komatiites, within uncertainties, is indistinguishable from the projected Os isotopic trajectory of the primitive upper mantle (PUM: Meisel et al., 2001). Thus, if the initial $^{187}Os/^{188}Os$ ratios of the Dundonald Beach, Alexo and Pyke Hill komatiites collectively reflect those of a

mantle source for the entire Kidd-Munro volcanic assemblage, their uniformly chondritic initial Os isotopic compositions suggest that this voluminous eruption sampled a mantle source that had no prior history of significant Re-depletion or resolvable [187]Os-enrichments with respect to the projected Os isotopic evolution trajectory for PUM.

The uniform chondritic Os isotopic composition of the ~2.7 Ga mantle source for the Al-undepleted komatiites from Kidd-Munro volcanic assemblage contrasts with the subchondritic Os isotopic composition of the contemporaneous mantle source for the Al-depleted Boston Creek ferropicrites in the 2723-2720 Ma Stoughton-Roquemaure assemblage of the Abitibi greenstone belt ($\gamma_{Os}$ = -3.8 ± 0.8; Walker and Stone, 2001). The subchondritic initial Os isotopic composition of the Boston Creek flows was interpreted to indicate their derivation dominantly from a source [1] that underwent long-term prior depletion in Re, similar to SCLM (sub-continental lithospheric mantle), or [2] from which a Re-rich phase, such as garnet separated a significant time prior to the eruption of the lavas (e.g., $D_{Re}^{garnet/silicate\ melt}$ = 2.7: Righter and Hauri, 1998). Our Os isotopic results for the Dundonald rocks, combined with those for the Alexo ($\gamma_{Os}$ =-0.1 ± 1.0: Gangopadhyay and Walker, 2003) and Pyke Hill ($\gamma_{Os}$ = 0.6 ± 0.2: Puchtel et al., 2004a) komatiites, on the other hand, suggest very limited interaction between the typical mantle sources for these komatiites and the SCLM. The chondritic Os isotopic composition of Al-undepleted komatiites from the Kidd-Munro assemblage is indistinguishable from the normal shallow convective upper mantle.

As for Phanerozoic analogs, the uniform chondritic Os isotopic composition of the Kidd-Munro komatiites is consistent with that recently reported for the Permo-Triassic komatiites from NW Vietnam (Hanski et al., 2004). This suggests that Phanerozoic komatiites, although rare, have tapped mantle sources with uniform chondritic Os isotopic composition similar to those for late-Archean Kidd-Munro komatiites. The uniform chondritic Os isotopic composition of the ~2.7 Ga mantle source for the Kidd-Munro komatiites, however, contrasts with the highly heterogeneous and variably $^{187}$Os-enriched mantle sources for the Mesozoic Gorgona Island komatiites (Walker et al., 1999), present-day ocean island basalts (OIB; $\gamma_{Os}$ up to ~+25: e.g., Hauri and Hart, 1993) and modern arc-related mafic-ultramafic lavas (e.g., Lassiter and Luhr, 2001; Woodland et al., 2002; Alves et al., 2002 and references therein). This suggests a different nature of mantle sources and/or petrogenetic processes for the generation of the Al-undepleted Kidd-Munro komatiites versus those from Gorgona Island, modern ocean island basalts or arc-related rocks.

## 5.6. SUMMARY AND CONCLUSIONS

The Re-Os systematics of the ca. 2.7 Ga komatiites and komatiitic basalts at Dundonald Beach record a complex history of at least three episodes of alteration. First, an average of 40% and as much as 75% of Re was lost from virtually all samples due most likely to volatility-related shallow degassing and/or hydrothermal leaching during or soon after the emplacement of magmas as shallow intrusions into unconsolidated sediments. In the second phase of alteration, the Re-Os isotope systematics of these rocks were reset presumably during a regional metamorphic

event at ca. 2.5 Ga. Finally, some samples with high Re/Os ratios were affected by relatively late-stage, possibly recent mobility of Re.

Despite these multiple stages of alteration, the olivine cumulate whole rock komatiites and their chromite separates, owing to their high Os concentrations and low Re/Os ratios, have preserved the original initial Os isotopic composition of the emplaced magmas. This suggests that olivine cumulate whole rocks and their chromite separates are preferred set of samples for the determination of initial Os isotopic composition of mantle sources for altered Precambrian komatiites. The olivine cumulate whole rocks and corresponding chromite separates in our suite of Dundonald rocks yield a precisely chondritic average initial Os isotopic composition ($\gamma_{Os}$ = 0.0 ± 0.6) for their mantle source. The chondritic initial Os isotopic composition of the Dundonald rocks is consistent with that previously obtained for the stratigraphically-equivalent komatiites from the Alexo and Pyke Hill areas that together belong to the spatially-extensive Kidd-Munro volcanic assemblage in the Abitibi greensonte belt. Combined, these results suggest that the voluminous eruptions of the Kidd-Munro komatiitic rocks sampled mantle source(s), dominated by Os with chondritic isotopic composition.

The uniformly chondritic Os isotopic composition of the mantle source for the Kidd-Munro komatiites is in contrast to the variably radiogenic Os isotopic composition of modern arc-related ultramafic lavas and sub-arc mantle xenoliths (e.g., Woodland et al., 2002; Widom et al., 2003). The contrasting Os isotopic composition of Kidd-Munro komatiites versus modern arc-related mafic-ultramafic rocks suggests that [1] the Kidd-Munro komatiites formed in a non-arc (e.g.,

intraplate: McDonough and Ireland, 1993) setting or [2] the processes responsible for enrichments in radiogenic $^{187}$Os for modern arc-related lavas (e.g., transport of radiogenic Os via Cl-rich hydrous fluid flux into the overlying mantle wedge: Brandon et al., 1996; Widom et al., 2003) were either not operative at all in the mantle source for these komatiites or the processes had only limited efficacy.

**Acknowledgements**

# CHAPTER 6: SUMMARY AND CONCLUSIONS

The major conclusions of this dissertation follow:

## 6.1. Geochemical constraints on the petrogenetic processes for komatiites from Dundonald Beach, Canada and Jeesiörova, Finland

Chromites in the Dundonald komatiites have significantly lower Cr# than Phanerozoic boninites at a given Mg#, suggesting relatively lower Cr concentrations in the magmas parental to the Dundonald komatiites. The relatively lower Cr contents presumed for the magmas parental to the Al-undepleted melts for the Dundonald komatiites, combined with high Cr contents of olivine (~2300 ppm) reported in a previous study of the stratigraphically-equivalent komatiites in Munro Township (Pyke et al., 1973) suggest high temperatures of crystallization ($\geq$1500ºC) for Al-undepleted Kidd-Munro komatiites (Li et al., 1995), consistent with high degrees of melting of an anhydrous mantle source.

In addition to the chemical compositions of chromite in the Kidd-Munro komatiites, several lines of evidence suggest that the Dundonald komatiites were derived from an essentially anhydrous mantle source. First, the uniform LREE-depletion, flat MREE and HREE patterns, combined with Nb/Y-Zr/Y systematics of the Dundonald komatiitic rocks are similar to those for normal mid-oceanic ridge basalts (N-MORB) and ocean island basalts from Iceland (Fitton et al., 1997). These geochemical similarities, combined with the strong positive correlation between Ce/Yb$_{CN}$ and H$_2$O/Yb ratios observed in N-MORB (Danyushevsky et al., 2000) and plume-related Hawaiian basaltic rocks (Dixon and Clague, 2001) were utilized to infer extremely low H$_2$O contents (<0.04 wt.%) for the Dundonald rocks. Thus the

trace element characteristics of the Dundonald komatiites are most consistent with their generation from an anhydrous mantle source that had undergone prior melt extraction. Second, homogeneity in major and trace elements and initial Os isotopic compositions of the Al-undepleted komatiites from the Kidd-Munro assemblage, extending over 180 x 12 $km^2$ area, is in contrast to the ubiquitous radiogenic Os isotopic compositions of arc-related lavas. Moreover, the major and trace element compositions of the Al-undepleted komatiites from the entire Kidd-Munro assemblage are also quite uniform. For example, the uniform LREE-depletion, absence of significant HREE-depletion, and remarkably consistent initial Nd-Os-Pb isotopic compositions of the Kidd-Munro komatiites are usually not observed at such large spatial scales in island arc lavas (e.g., see Campbell, 2001). Combined, these geochemical characteristics of the Kidd-Munro komatiites are consistent with derivation from non-arc, presumably anhydrous, oceanic mantle sources.

The komatiites from the Jeesiörova area in Finnish Lapland have subchondritic $Al_2O_3/TiO_2$ ratios (~10-13) similar to those for the Al-depleted Barberton-type komatiites. The Jeesiörova rocks, however, are distinct in that they are not Al-depleted, and are instead Ti-rich relative to both Al-depleted and Al-undepleted komatiites from elsewhere. The HFSE-HREE characteristics of the Finnish rocks are not consistent with their derivation through either of the two commonly suggested petrogenetic processes for origin of Al-depleted komatiites, namely, majorite fractionation in the deep mantle or hydrous melting in a supra-subduction zone setting. Also, the redox state of the Jeesiörova parental magma (~QFM ± 1.5) is not consistent with derivation from typically oxidized arc mantle.

The high abundance of HFSE (e.g., Ti and Zr) and other similarly incompatible elements in Jeesiörova komatiites, combined with their $^{143}$Nd-enriched nature and uniform LREE-depleted pattern may suggest that [1] the primitive Lapland magmas had assimilated Ti-rich mineral assemblages in the lithospheric mantle *en route* to the surface, or [2] the mantle source for the Jeesiörova komatiites incorporated LREE-depleted recycled mafic oceanic crust (similar to MORB). The uniform negative Nb anomalies in these rocks, however, is not consistent with either of these two possibilities.

## 6.2. The partitioning behavior of Re and Os during melting of mantle source and differentiation of komatiitic lavas

Calculated bulk distribution coefficients ($D^{mantle/melt}$) for Os and Re between the magma parental to the Alexo komatiites and the mantle residue are 2.1 and 0.2, respectively. These D values suggest that Os was slightly compatible, whereas Re was moderately incompatible during the melting of the Alexo mantle source. Similarly, the calculated relative distribution coefficients ($D^{solid/liquid}$) for Os and Re between crystallizing phases and the fractionating liquid during the differentiation of the Alexo lavas are 1.7 and 0.66, respectively. These D values are also consistent with those determined for the stratigraphically-equivalent Dundonald Beach komatiites. These D values suggest that Os was slightly compatible, whereas Re was moderately incompatible in olivine or co-precipitating trace phase(s) (e.g., chromite, laurite) during the fractionation of the magmas parental to the Al-undepleted Kidd-Munro komatiites.

## 6.3. Re-Os systematics of mantle sources of komatiites

The Al-undepleted komatiites from the Alexo area in the Abitibi greenstone belt, Canada demonstrate apparent magmatic behavior of Re-Os elemental and isotope systematics in the whole rocks. The Re-Os isochron of these rocks yields an age of 2762 ± 76 Ma, which is in general agreement with the U-Pb zircon ages of associated felsic units, and Pb-Pb and Sm-Nd isochron ages obtained in a previous study of these lavas. The initial $^{187}Os/^{188}Os$ obtained from the regression (0.1080 ± 0.0012) is chondritic ($\gamma_{Os}$ = -0.1 ± 1.0), and is consistent with that reported for the spatially associated Pyke Hill komatiites (Shirey, 1997; Puchtel et al., 2004a). The chondritic initial Os isotopic composition of the mantle sources for the komatiites from Alexo and Pyke Hill areas are indistinguishable from the projected Os isotopic composition for the convective upper mantle at the ~2.7-Ga. Additionally, the radiogenic initial Nd isotopic composition of Alexo komatiites determined in previous studies ($\varepsilon_{Nd}$ ~ +3.8: Lahaye and Arndt, 1996) is in good agreement with the Nd isotopic composition of the long-term evolution of the LREE-depleted convective upper mantle. Thus, the combined chondritic initial Os isotopic composition and radiogenic initial Nd isotopic composition of the Alexo komatiites suggest their derivation from a mantle source that is indistinguishable from the contemporaneous convective upper mantle.

The ca. 2.05 Ga Ti-rich komatiites from the Jeesiörova area in the Finnish Lapland were derived from a mantle source with chondritic initial Os isotopic composition ($\gamma_{Os}$ = +0.1 ± 0.5). The chondritic initial Os isotopic composition, combined with the depleted mantle-like initial Nd isotopic composition of these rocks

suggest that the parental melts were likely to have been derived from either contemporaneous convective upper mantle or a deep mantle source with similar long-term LREE-depleted characteristics. Furthermore, the chondritic Os isotopic composition of the mantle source for the Finnish Ti-rich komatiites suggests that Re and Os (and, by inference, possibly other highly siderophile elements) were either not significantly fractionated during the process(es) that led to high abundance of of Ti in these rocks, or the process(es) was/were nearly coeval with the generation of the Finnish komatiites. Puchtel et al. (1999) reported a similar uniform chondritic initial Os isotopic composition for the Ti-rich lavas from the Onega plateau in the SE Baltic Shield.

Similar to the Alexo komatiites, as discussed above, the mantle source for the stratigraphically-equivalent komatiites from the Dundonald Beach area also had a precisely chondritic average initial Os isotopic composition ($\gamma_{Os}$ = 0.0 ± 0.6). Thus, the uniform chondritic initial Os isotopic composition of the mantle sources for komatiites from the Alexo, Pyke Hill and Dundonald Beach areas collectively suggest that the voluminous eruption of the Kidd-Munro assemblage at ~2.7 Ga sampled a homogeneous mantle source, with regard to Os isotopes, that had no prior history of significant long-term Re depletion or enrichment in radiogenic $^{187}$Os isotopes relative to chondritic evolution. It is widely believed that the ultimate source of Re and Os in the terrestrial mantle was a chondritic "late veneer" added to the mantle prior to ~3.8 Ga (see chapter 1). The uniform chondritic initial Os isotopic composition of these rocks suggests that the "late veneer" component was well homogenized within the mantle source of these spatially extensive lavas (~ 180 x 12 km$^2$). The uniform

chondritic initial Os isotopic compositions of the Kidd-Munro komatiites contrast with the typically variably radiogenic Os isotopic compositions of Phanerozoic arc-related mafic-ultramafic lavas (e.g., Lassiter and Luhr, 2001; Alves et al., 2002; Woodland et al., 2002).

## 6.4. Implications for the origin and evolution of Os isotopic heterogeneity in the terrestrial mantle

Resolvable Os isotopic heterogeneities have been documented in previous studies of the mantle sources for both modern ocean island basalts (OIBs) and also some ancient mantle reservoirs. For example, late-Archean komatiites from Alexo and Munro Townships (Walker et al., 1988; Shirey, 1997; Gangopadhyay and Walker, 2003) had chondritic initial Os isotopic compositions, whereas nearly contemporaneous mantle sources for ultramafic flows from Boston Creek, Canada (Walker and Stone, 2001), Kostomuksha, Russia (Puchtel et al., 2001a), and Belingwe, Zimbabwe (Walker and Nisbet, 2002), show significant deviations from projected chondritic Os isotopic evolution trajectory (Fig. 6.1). Due to the limited prior number of data for diverse mantle-derived systems, it has not been clear whether (a) the Precambrian mantle was dominantly chondritic, with a few enriched and depleted mantle domains or (b) was characterized by widespread Os isotopic heterogeneities. The Os isotopic results of the Alexo, Dundonald Beach and Jeesiörova komatiites, combined with recent data obtained for older mantle derived system, such as ~3.5-Ga komatiites from the Pilbara region of Western Australia (Bennett et al., 2003) begin to suggest that significant portions of the Precambrian mantle were dominated by Os with chondritic isotopic compositions. This, in turn,
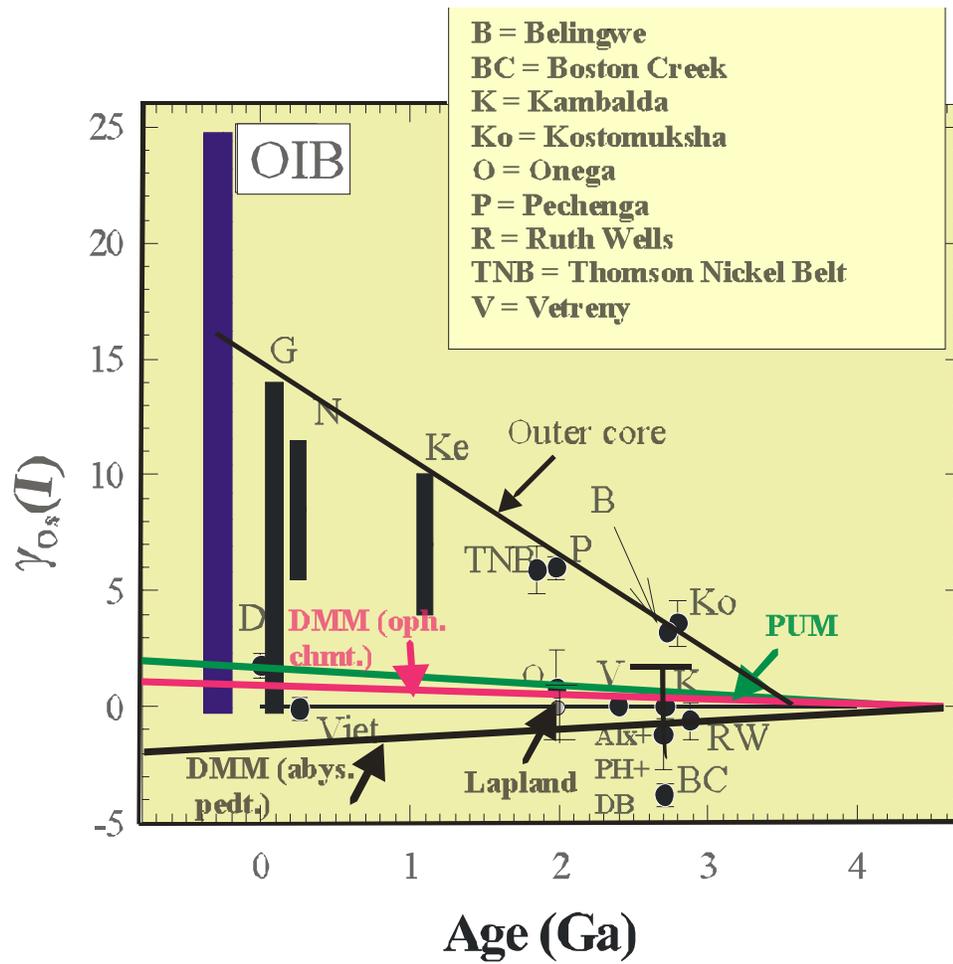
**Fig. 6.1.** Plot of high-precision initial $\gamma_{Os}$ for mafic-ultramafic rocks (determined in this study and those previously reported in the literature; also included some unpublished data) versus geological time (after Gangopadhyay et al., 2004).

suggests that the systems displaying positive or negative deviations from chondritic Os isotopic evolution trajectory are relatively rare and must therefore be attributable to atypical mantle sources. For example, the subchondritic initial Os isotopic composition for the ca. 2.7-Ga Boston Creek flows is the only known occurrence of a long-term Re-depleted mantle source hitherto reported for ancient ultramafic rocks. Walker and Stone (2001) attributed it to the derivation of the Boston Creek rocks from a mantle source, that had undergone long-term Re-depletion, such as SCLM.

The presence of suprachondritic initial Os isotopic compositions of the mantle sources for ultramafic rocks appears in the geologic record at as early as ~2.8 Ga, and is also noted for other late-Archean and early-Proterozoic ultramafic rocks (e.g., Belingwe, Zimbabwe and Pechenga, Russia). Previous studies have attributed such enrichments in radiogenic Os isotopes to core-mantle interaction or crustal recycling in their mantle sources. The scarcity of such [187]Os-enriched Precambrian mantle-derived systems argues against either widespread core-mantle interaction or crustal recycling at the times most komatiites were generated.

# REFERENCES

Allègre, C. J., and Luck, J. M. (1980) Os isotopes as petrogenetic and geological tracers, Earth Planet Sci. Lett., 48, 148-54.

Allègre, C. J. (1982) Genesis of Archean komatiites in a wet ultramafic subducted plate, In: Komatiites, Arndt, N. T. and Nisbet (Eds.), George Allen and Unwin, 495-500.

Allègre, C. J., Birck, J. L., Campas, F. and Courtillot, V. (1999) Age of the Deccan traps using $^{187}Re$-$^{187}Os$ systematics, Earth Planet Sci. Lett., 170: 197-204.

Alves, S., Schiano, P., Capmas, F., and Allègre, C. (2002) Osmium isotope binary mixing arrays in arc volcanism, Earth Planet. Sci. Lett., 198, 355-369.

Appel, P. W. U. (1997) High bromine contents and low Cl/Br ratios in hydrothermally altered Archean komatiitic rocks, West Greenland, Precamb. Res., 177-189.

Arndt, N. T. (1977a) Ultrabasic magmas and high-degree melting of the mantle, Contrib. Mineral. Petrol., 64, 205-221.

Arndt, N. T. (1977a) The separation of magmas from partially molten peridotite. Carnegie. Inst. Wash. Yb., **75**, 555-562.

Arndt, N. T. (1977b) Thick, layered peridotite-gabbro lava flows in Munro Township, Ontario. Carnegie Inst. Washington Yearbk., 14: 2620-2637.

Arndt, N. T., Naldrett, A. J., and Pyke, D. R.1977. Komatiitic and iron-rich tholeiitic lavas from Munro Township, northeast Ontario, J. Petrol., 18: 319-369.

Arndt, N. T. and Nisbet (1982a) (Eds.) Komatiites, George Allen and Unwin.

Arndt, N. T. and Nisbet (1982b) What is a komatiite? In: Komatiites, Arndt, N. T. and Nisbet (Eds.), George Allen and Unwin.

Arndt, N. T., and Nesbitt, R. W. (1982) Geochemistry of Munro township basalts, In: Arndt, N. T., and Nisbet, E. G. (Eds.), Komatiites, George Allen and Unwin, 309-329.

Arndt, N., 1986. Differentiation of komatiite flows. J. Petrol., 27, 2: 279-301.

Arndt, N. T., Teixeria, N. A., and White, W. M. (1989) Bizzare geochemistry of komatiites from the Crixas greenstone belt, Brazil, Contrib., Mineral. Petrol., 101, 187-197.

Arndt, N.T. and Lesher, C.M. (1992) Fractionation of REEs by olivine and the origin of Kambalda komatiites, Western Australia. *Geochim. Cosmochim. Acta* **56**, pp. 4191–4204.

Arndt, N., Ginibre, C., Chauvel, C., Albarede, F., Cheadle, M., Herzberg, C., Jenner, G., Lahaye, Y. (1998) Were komatiites wet? , Geology, 26, 8, 739-742.

Arndt, N.T. and Lesher, C.M. (1992) Fractionation of REEs by olivine and the origin of Kambalda komatiites, Western Australia. *Geochim. Cosmochim. Acta* **56**, pp. 4191–4204.

Arndt, N, T., and Christensen, U. (1992) The Role of Lithospheric Mantle in Continental Flood Volcanism: Thermal and Geochemical Constraints, J. Geophys. Res., 97, 10,967-10,981.

Arndt, N. T. (1994) Archean komatiites, In: Archean Crustal Evolution, Kondie, K. C. (ed.), pp. 11-44, Elsevier, Amsterdam.

Arndt, N. T., Kerr, A. C., and Tarney, J. (1997) Dynamic melting in plume heads: the

formation of Gorgona komatiites and basalts, Earth Planet Sci. Lett., 146, 289-301.

Arndt, N. T., Lesher, C.M., Houlé, M. G., Lewin, E., Lacaze, Y. (2004) Intrusion and crystallization of a spinifex-textured komatiite sill in Dundonald Township, Ontario, J. Petrol. (in press)

Asahara, Y., Ohtani, E., and Suzuki, A. (1998) Melting relations of hydrous and dry mantle compositions and the genesis of komatiites. Geophys. Res. Lett. 25 pp. 2201–2204.

Ayer, J., Amelin, Y., Corfu, F., Kamo, S., Ketchum, J., Kwok, K., Trowell, N. (2002) Evolution of the southern Abitibi greenstone belt based on U-Pb geochronology: autochthonouos volcanic construction followed by plutonism, regional deformation and sedimentation, Precamb. Res., 115, 63-95.

Barnes, S-J., Gorton, M.P., and Naldrett, A.J., (1983) A comparative study of olivine and clinopyroxene flows from Alexo, Abitibi greenstone belt, Ontario, Canada: Contrib. Mineral. Petrol., p. 83, p. 293-308.

Barnes, S-J. (1985) The petrography and geochemistry of komatiite flows from the Abitibi Greenstone Belt and a model for their formation, Lithos, 18, 241-270.

Barnes, S-J., Naldrett, A. J., and Gorton, M., P. (1985) The origin of the fractionation of platinum-group elements in terrestrial magmas, Chem. Geol., 53, 303-323.

Barnes, S-J., and Naldrett, A.J., 1987. Fractionation of the platinum-group elements and gold in some komatiites of the Abitibi greenstone belt, northern Ontario: Economic Geology, v. 82, p. 165-183.

Barnes, Stephen, J. (1998) Chromite in Komatiites, 1. Magmatic Controls on

Crystallization and Composition, J. Petrol., 39, 10, 1689-1720.

Barnes, Stephen J. (2000) Chromites in komatiites, II: Modification during greenschist to mid-amphibolite facies metamorphism, J. Petrol., 41, 3, 387-409.

Barrie, C. T. (1999) The Kidd-Munro Extension Project: Year 3 Report, Unpbl. Report, 263 p.

Barrie, C. T., Corfu, F., Davis, P., Coutts, A. C., and MacEachern, D. (1999) Geochemistry of the Dundonald komatiite-basalt suite and genesis of Dundeal Ni deposit, Abitibi subprovince, Canada, Econ. Geol., 94, 845-866.

Beaty, D. W., and Taylor, H. P. Jr. (1982) The oxygen isotope geochemistry of komatiites: evidence for water-rock interaction, In: Arndt, N. T., and Nisbet, E. G. (Eds.), Komatiites, George Allen and Unwin, 267-280.

Belshaw, N. S., Freedman, P. A., O'Nion, R. K., Frank, M., and Guo, Y. (1998) A new variable dispersion double-focusing plasma mass spectrometer with performance illustrated for Pb isotopes, International J. Mass Spec., 181, 51-58.

Barnes, Sarah-Jane, and Often, M. (1990) Ti-rich komatiites from Northern Norway, Contrib. Mineral. Petrol., 105: 42-54.

Barnes, Stephen, J. (1986) The distribution of chromium among orthopyroxene, spinel and silicate liquid at atmospheric pressure, Geochim. Cosmochim. Acta, 50, 9:1889-1909

Barnes, Stephen, J., and Roeder, P. (2001) The range of spinel compositions in terrestrial mafic and ultramafic rocks, J. Petrol., 42, 12, 2279-2302.

Beaty, D. W., and Taylor, H. P. Jr. (1982) The oxygen isotope geochemistry of komatiites: evidence for water-rock interaction, In: Arndt, N. T., and Nisbet, E. G. (Eds.), Komatiites, George Allen and Unwin, 267-280.

Bennett, V. C., Norman, M. D., Garcia, M. O. (2000) Rhenium and platinum group element abundances correlated with mantle source components in Hawaiian picrites: sulfides in the plume, Earth Planet. Sci. Lett., 183, 513-526.

Bennett, V. C., Nutman, A. P. and Esat, T. M., 2002. Constraints on mantle evolution from $^{187}Os/^{188}Os$ isotopic compositions of Archean ultramafic rocks from southern West Greenland (3.8 Ga) and Western Australia (3.46 Ga). Geochim. Cosmochim. Acta, 66, 14: 2615-2630.

Beswick, A. E. (1982) Some geochemical aspects of alteration and genetic relations in komatiitic suites, In: Arndt, N. T., and Nisbet, E. G. (Eds.), Komatiites, George Allen and Unwin, 281-307.

Bleeker, W., Parrish, R. R., and Sager-Kinsman, A. (1999) High precision U-Pb geochronology of the late Archean Kidd Creek deposit and Kidd Volcanic Complex: Economic Geology Monograph 10, 43-70.

Blichert-Toft, J., Arndt, N. T., and Gruau, **G.** (2004) Hf isotopic measurements on Barberton komatiites: effects of incomplete sample dissolution and importance for primary and secondary magmatic signatures, Chem. Geol., 207, 261-275.

Bockrath, C., Ballahaus, C., and Holzheid, A. (2004) Stabilities of laurite $RuS_2$ and monosulfide liquid solution at magmatic temperature, Chem. Geol., 208, 265-271.

Brandon A., Walker R.J., Morgan J.W., Norman M.D. and Prichard H.M.(1998) Coupled $^{186}$Os and $^{187}$Os evidence for core-mantle interaction. Science 280, 1570-1573.

Brandon A.D., Norman M.D., Walker R.J. and Morgan J.W. (1999) $^{186}$Os-$^{187}$Os systematics of Hawaiian picrites. Earth Planet Sci. Lett. 172, 25-42.

Brandon, A. D., Snow, J. E., Walker, R. J., Morgan, J. W. and Mock., T. D. (2000) $^{190}$Pt-$^{186}$Os and $^{187}$Re-$^{186}$Os systematics of abyssal peridotites, Earth Planet Sci. Lett., 177: 319-335.

Brandon, A. D., Walker, R. J., Puchtel, I. S., Becker, H., Humayun, M., Revillon, S. (2003) $^{186}$Os-$^{187}$Os systematics of Gorgona Island komatiites: implications for early growth of the inner core, Earth Planet Sci. Lett., 206, 411-426.

Brenan, J. M., McDonough, W. F., and Dalpé, C. (2003) Experimental constraints on the partitioning of rhenium and some platinum-group elements between olivine and silicate melt, Earth Planet. Sci. Lett., 212, 135-150.

Brett, R. (1984) Chemical equilibration of the earth's core and upper mantle, Geochim. Cosmochim. Acta, 48, 1183-118.

Brévart, O., Dupré, B., and Allegrè, C. (1986) Lead-lead age of komatiitic lavas and limitations on the structure and evolution of the Precambrian mantle, Earth Planet. Sci. Lett., 77, 293-302.

Brown, A. V. and Jenner, G. A. (1989) Geological setting, petrology and chemistry of Cambrian boninites and low-Ti tholeiite lavas in western Tasmania, In: Boninites, Crawford, A. J. (Ed.), Unwyn Hyman, 232-263.

Brügmann, G. E., Arndt, N. T., Hofmann, A. W. and Tobschall, H. J., 1987. Noble metal abundances in komatiite suites from Alexo, Ontario and Gorgona Island, Columbia, Geochim. Cosmochim. Acta, 51: 2159-2169.

Burton, K. W., Gannoun, A., Birck, J. –L., Allègre, C. J., Schiano, P., Clocchiatti, R., and Alard, O. (2002) The compatibility of rhenium and osmium in natural olivine and their behavior during mantle melting and basalt genesis, Earth Planet. Sci. Lett., 198, 63-76.

Campbell, I. H., Griffiths, R. W., and Hill, R. I. (1989) Melting in an Archean mantle plume: Heads it's basalts, tails it's komatiites, Nature, 339, 697-699.

Campbell, I. H. (2001) Identification of ancient mantle plumes, In: mantle plumes: Their identification through time, Ernst, R. E. and Buchan, K. L. (Eds.), Geol. Soc. Am. Spl. Paper, 352, 5-21.

Canil, D. (1997) Vanadium partitioning and the oxidation state of Archean komatiite magmas, Nature, 389, 842-45.

Canil, D. and Fedortchouk, Y. (2001) Olivine-liquid partitioning of vanadium and other trace elements, with applications to modern and ancient picrites, Can. Min., 39, 319-330.

Capobianco, C. J. and Drake, M. J. (1990) Partitioning of ruthenium, rhodium, and palladium between spinel and silicate melt and implications for platinum group element fractionation trends, Geochim. Cosmochim. Acta, 54, 869-874.

Carignan, J., Machado, N., and Gariepy, C. (1995) U-Pb isotopic geochimstry of komatiites and pyroxenes from the southern Abitibi greenstone belt, Canada, Chem. Geol., 126, 17-27.

Cas, R. A. F., Houlé, M. G., Beresford, S., Lesher, C. M., Fowler, A., Arndt, N. T., Rosengren, N., Thurston, P. (2003) Are spinifex-cumulate textured komatiitic rock units necessarily lavas? Archean examples from Dundonald Beach, Abitibi greenstone belt, Canada, In: Volcanic flows: Observation, experiment and theory, IUGG (abs.).

Chauvel, C., Dupré, B., and Jenner, G. A. (1985) The Sm-Nd age of Kambalda volcanics is 500 Ma too old! Earth Planet. Sci. Lett., 74, 315-324.

Chesley, J. T., Rudnick, R. L., and Lee, C. –T. (1999) Re-Os systematics of mantle xenoliths from the East-African Rift: Age, structure, and history of the Tanzanian craton, Geochim. Cosmochim. Acta, 63, 1203-1216.

Chou, C. -L., 1978. Fractionation of siderophile elements in the earth's upper mantle, Proc. Lunar Planet. Sci. Conf., 9th, 219-230.

Clarke, D. B. (1970) Tertiary basalts of Baffin Bay: Possible primary magma from the mantle, Contrib. Mineral. Petrol., 25, 203-224.

Cohen A. S. and Waters, F. J., 1996. Separation of osmium from geological materials by solvent extraction for analysis by TIMS, Anal. Chim. Acta, 332: 269-275. Corfu, F., 1993. The evolution of the southern Abitibi greenstone belt in light of precise U-Pb geochronology, Econ. Geol., 88:1323-1340.

Coish, R. A. (1989) Boninitic lavas in Appalachian ophiolites: a review, In: Boninites, Crawford, A. J. (Ed.), Unwyn Hyman, 264-287.

Corfu, F., and Noble, S. R. (1992) Genesis of the southern Abitibi greenstone belt, Superior province, Canada: Evidence from zircon Hf isotopipc analyses using a single filament technique, Geochim. Cosmochim. Acta, 56, 2081-2097.

Corgne, A., and Wood, B. J. (2004) Trace element partitioning between majoritic garnet and silicate melt at 25 GPa, Phys. Earth and Planet. Int., 143-144, 407-419.

Creaser, R. A., Papanastassiou, D. A. and Wasserburg, G. J., 1991. Negative thermal ion mass spectrometry of osmium, rhenium and iridium, Geochim. Cosmochim. Acta, 55: 397-401.

Crocket, J. H., and MacRae, W. E. (1986) Platinum-group element distribution in komatiitic and tholeiitic volcanic rocks from Munro Township, Ontario, Econ. Geol., 1242-1251.

Danyushevsky, L. V., Eggins, S. M., Fallon, T. J., Christie, D. M. (2000) $H_2O$ abundance in depleted to moderately enriched mid-ocean ridge magmas; Part I: Incompatible behaviour, implications for mantle storage, and origin of regional variations, J. Petrol., 41, 1329-1364.

Davis, P. C. (1997) Volcanic stratigraphy of the late Archean Kidd-Munro assemblage in Dundonald and Munro Townships and genesis of associated nickel and copper-zinc volcanogenic massive sulfide deposits, Abitibi greenstone belt, Ontario, Canada, Unpubl. M. Sc. Thesis, Univ. of Alabama, Tuscaloosa, 201 pp.

Davis, P. C. (1999) Classic komatiite localities and magmatic Fe-Ni-Cu-(PGE) sulfide deposites of the Abitibi greenstone belt, Ontario-Québec: Guidebook series, 1, Mineral Expl. Res. Centre, Laurentian Univ., 76 p.

DePaolo, D. J., 1981. Neodymium isotopes in the Colorado Front Range and

implications for crust formation and mantle evolution in the Proterozoic, Nature, 291: 193-197.

Dixon, J. E., Clague, D. (2001) Volatiles in basaltic glasses from Loihi Seamount, Hawaii: Evidence for a relatively dry plume component, J. Petrol., 42, 627-654.

Dupre, B., Chauvel, C. and Arndt, N., 1984. Pb and Nd isotopic study of two Archean komatiitic flows from Alexo, Ontario, Geochim. Cosmochim. Acta, 48: 1965-1972.

Dupré, B., and Arndt, N. T. (1990) Pb isotopic compositions of Archean komatiites and sulfides, Chem. Geol., 85, 35-56.

Ebel, D. S. and Naldrett, A. J. (1996) Fractional crystallization of sulfide ore liquids at high temperature, Econ. Geol., 91, 607-621.

Echeverria, L. M. (1980) Tertiary or Mesozoic komatiites from Gorgona Island, Contrib. Mineral. Petrol., 73, 253-266.

Eggins, S. M. (1993) Origin and differentiation of picritic arc magmas, Ambae (Aoba), Vanuatu, Contrib. Mineral. Petrol., 114: 79-100.

Ellam, R. M., Carlson, R. W., and Shirey, S. B. (1992) Evidence from Re-Os isotopes for plume-lithosphere mixing in Karoo flood basalt genesis, Nature, 359, 718-721.

Fan, J. and Kerrich, R., 1997. Geochemical characteristics of aluminum depleted and undepleted komatiites and HREE-enriched low-Ti tholeiites, western Abitibi greenstone belt: A heterogeneous mantle plume-convergent margin environment, Geochim. Cosmochim. Acta., 61, 22: 4723-4744.

Fisk, M. R., and Bence, A. E. (1980) Experimental crystallization of chrome spinel in
FAMOUS basalt 527-1-1, Earth Planet. Sci. Lett., 48, 1 , 111-123.

Fitton, J. G., Saunders, A. D., Norry, M. J. Hardarson, B. S., and Taylor, R. N. (1997)
Thermal and chemical structure of the Icelandic plume, Earth Planet Sci. Lett.,
153, 197-208.

Foster, J. G., Lambert, D. D., Frick, L. R. and Maas, R., 1996. Re-Os isotopic
evidence for genesis of Archean Nickel ores from uncontaminated komatiites,
Nature, 382: 703-706.

Francis, D., 1985. The Baffin Bay lavas and the value of picrites as analogues of
primary magmas, Contrib. Mineral. Petrol. 89: 144-154.

Frei, R., Polat, A., and Meibom, A. (2004) The Hadean upper mantle conundrum:
evidence for source depletion and enrichment from Sm-Nd, Re-Os, and Pb
isotopic compositions in 3.71 Gy boninite-like metabasalts from the Isua
Supracrustal Belt, Greenland, Geochim. Cosmochim. Acta., 68, 7: 1645-1660.

Gangopadhyay, A., and Walker, R. J. (2003) Re-Os systematics of the ca. 2.7-Ga
komatiites from Alexo, Ontario, Canada, Chem. Geol., 196: 147-162.

Gangopadhyay, A., Sproule, R A., Walker, R J. and Lesher, C M. (2004) Re-Os
Abundance and Isotope Systematics of Al-undepleted Komatiites in the Kidd-
Munro Assemblage: Results From Dundonald Beach, Abitibi Greenstone Belt,
Canada, Eos Trans. AGU, 85*(17),* Jt. Assem. Suppl., Abstract V51B-06.

Gangopadhyay, A., and Walker, R. J., Hanski, E., and Solheid, P. Origin of
Paleoproterozoic Ti-enriched komatiitic rocks from Jessiörova, Kittilä
Complex, Finnish Lapland, J. Petrol., (in revision).

Goldstein, S. L., O'Nions, R. K. and Hamilton, P. J., 1984. A Sm-Nd isotopic study of atmospheric dusts and particulates from major river systems, Earth Planet. Sci. Lett., 70: 221-236.

Graham, S., Lambert, D. D., Shee, S. R., and Pearson, N. J. (2002) Juvenile lithospheric mantle enrichment and the formation of alkaline ultramafic magma sources: Re-Os, Lu-Hf and Sm-Nd isotopic systematics of the Norseman melnoites, Western Australia, Chem. Geol., 186, 215-233.

Green, D. H., Nicholls, I.A., Viljoen, M. and Viljoen, R. (1975) Experimental demonstration of the existence of peridotitic liquids in earliest Archean magmatism. Geology, 3, 11–14.

Grégoire, M., Lorand, J. P., O'Reilly, S. Y., and Cottin, J. Y. (2000) Armalcolite-bearing, Ti-rich metasomatic assemblages in harzburgitic xenoliths from the Kerguelen Islands: Implications for the oceanic mantle budget of high-field strength elements, Geochim. cosmochim. Acta, 64, 673-694.

Grove, T. L., Parman, S. W. Dann, J. C. (1999) Conditions of magma generation for Archean komatiites from the Barberton Mountainland, South Africa, in: Y. Fei, C.M. Bertka, B.O. Mysen (Eds.), Mantle Petrology; Field Observations and High-pressure Experimentation; A Tribute to Francis R. (Joe) Boyd, Geochem. Soc. Spec. Publ. 6, 155–167.

Grove, T. L., and Parman, S. W. (2004) Thermal evolution of the Earth as recorded by komatiites, Earth Planet. Sci. Lett., 219, 3-4: 173-187.

Gruau, G., Chauvel, C., Arndt, N. T. and Cornichet, J. (1990) Aluminum depletion in

komatiites and garnet fractionation in the early Archean mantle: Hafnium isotopic constraints, Geochim. Cosmochim. Acta, 54, 3095-3101.

Hanski, E., J., and Smolkin, V. F. (1995) Iron- and LREE-enriched mantle source for early Proterozoic intraplate magmatism as exemplified by the Pechenga ferropicrites, Kola Peninsula, Russia, Lithos, 34, 107-125.

Hanski, E., Huhma, H., Rastas, P., and Kamenetsky, V. S. (2001) The Palaeoproterozoic Komatiite-Picrite Association of Finnish Lapland, J. Petrol., 42, 5, 855-76.

Hanski, E., Walker, R. J., Huhma, H., Polyakov, G. V., Balykin, P. A., Hoa, T. T., Phuong, N. T. (2004) Origin of the Permian-Triassic komatiites, northwestern Vietnam, Contrib. Mineral. Petrol., 147, 453-469.

Hattori, K., and Hart, S. R. (1991) Osmium-isotope ratios of platinum-group minerals associated with ultramafic intrusions: Os-isotopic evolution of the oceanic mantle, Earth Planet Sci. Lett. 107, 499-514.

Hauri, E. H. and Hart, S. R., 1993. Re-Os isotope systematics of HIMU and EMII oceanic island basalts from the south Pacific Ocean, Earth Planet Sci. Lett., 114: 353-371.

Herzberg, C., 1992. Depth and degree of melting of komatiite, J. Geophys. Res., 97: 4521-4540.

Herzberg, C. (1995) Generation of plume magmas through time: an experimental perspective, Chem. Geol., 126, 1-16.

Hickey, R. L., and Frey, F. A. (1982) Geochemical characteristics of boninite series

volcanics: implications for their source, Geochim. cosmochim. Acta, 46, 2099-2115.

Hollings, P., and Kerrich, R. (1999) Trace element systematics of ultramafic and mafic volcanic rocks from the 3 Ga North Caribou greenstone belt, northwestern Superior Province, Precamb. Res., 93, 4: 257-279.

Horan, M.F., Walker, R.J., Fedorenko, V. A. and Czamanske, G. K., 1995. Os and Nd isotopic constraints on the temporal and spatial evolution of Siberian Flood basalt sources, Geochim. Cosmochim. Acta, 59: 5159-5168.

Houlé, M. G., Gibson, H. L., Lesher, C. M., Davis, P. C., and Arndt, N. T. (2002) The role of subvolcanic sills and peperites in facilitating the eruption of Archean komatiitic flows at the Dundonald Beach Ni-Cu-PGE deposit, Northern Ontario, Geol. Soc. Am., Annu. Meeting (abs.).

Jackson, S. L., and Fyon, J. A. (1991) The western Abitibi subprovince in Ontario: Ontario Geol. Surv. Spl. Vol., 4, 405-484.

Jochum, K. P., Arndt, N. T., and Hofmann, A. W. (1991) Nb-Th-la in komatiites and basalts: constraints on komatiite petrogenesis and mantle evolution, Earth Planet. Sci. Lett., 107, 272-289.

Jolly, W. T., 1982. Progressive metamorphism of komatiites and related Archean lavas of the Abitibi area, Canada, In: N. T. Arndt and E. G. Nisbet (Eds.), Komatiites, George Allen & Unwin, London, 245-266.

Jones, J. H., and Drake, M. J. (1986) Geochemical constraints on core formation in the earth, Nature, 322, 221-8.

Kalfoun, F., Ionov, D., and Merlet, C. (2002) HFSE residence and Nb/Ta ratios in

metasomatised, rutile-bearing mantle peridotites, Earth Planet. Sci. Lett., 199: 49-65.

Kamenetsky, V. S., Sobolev, A. V., Eggins, S. E., Crawford, A. J., Arculus, R. J. (2002) Olivine-enriched melt inclusions in chromites from low-Ca boninites, Cape Vogel, Papua New Guinea: evidence for ultramafic primary magma, refractory mantle source and enriched components, Chem. Geol., 183, 287-303.

Kato, T., Ringwood, A. E., and Irifune, T. (1988) Experimental determination of element partitioning between silicate perovskites, garnets and liquids: constraints on early differentiation of the mantle, Earth Planet. Sci. Lett., 89: 123-145.

Kerrich, R., Wyman, D., Fan, J., and Bleeker, W. (1998) Boninite series: low Ti-tholeiite association from the 2.7 Ga Abitibi greenstone belt, Earth Planet Sci. Lett., 164, 303-316.

Kerrich, R. and Xie, Q., 2002. Compositional recycling structure of an Archean super-plume: Nb-Th-U-LREE systematics of Archean komatiites and basalts revisited, Contrib. Mineral Petrol, 142; 476-484.

Kimura, K., Lewis, R. S. and Anders, E., 1974. Distribution of gold and rhenium between nickel-iron and silicate melts: Implications for the abundance of siderophile elements on the earth and moon, Geochim. Cosmochim. Acta, 38: 683-701.

Krill, A. G., Bergh, S., Lindahl, I., Mearns, E. W., Often, M., Olerud, S., Olesen, O., Sandstad, J. S., Siedlecka, A. & Solli, A. (1985). Rb–Sr, U–Pb and Sm–Nd

isotopic dates from Precambrian rocks of Finnmark. Bulletin, Norges Geologiske Undersøkelse 403, 37–54.

Kyser, J. K., Cameron, W. E. and Nisbet, E. G. (1986) Boninite petrogenesis and alteration history: constraints from stable isotope compositions of boninites from Cape Vogel, New Caledonia and Cyprus, Contrib. Mineral. Petrol., 93, 222-236.

Lahaye, Y., Arndt, N., Byerly, G., Chauvel, C., Fourcade, S. and Gruau, G., 1995. The influence of alteration on the trace-element and Nd isotopic compositions of komatiites, Chem. Geol., 126: 43-64.

Lahaye, Y. and Arndt, N., 1996. Alteration of a komatiite flow from Alexo, Ontario, Canada, J. Petrol., 37, 6: 1261-1284.

Lahaye, Y., Barnes, S. -J., Frick, L. R. and Lambert, D. D., 2001. Re-Os isotopic study of komatiitic volcanism and magmatic sulfide formation in the southern Abitibi greenstone belt, Ontario, Canada, Can. Mineral., 39: 473-490.

Lassiter, J. C. (2003) Rhenium volatility in subaerial lavas: constraints from subaerial and submarine portions of the HSDP-2 Mauna Kea drillcore, Earth Planet. Sci. Lett., 214, 311-325.

Lassiter, J. C., and Luhr, J. F. (2001) Osmium abundance and isotope variations in mafic Mexican volcanic rocks: Evidence for crustal contamination and constraints on the geochemical behavior of osmium during partial melting and fractional crystallization, Goechem. Geophys. Geosys., 2, 2000GC000116.

Lee, C. –T. A., Brandon, A. D., and Norman, M. (2003) Vanadium in peridotites as a

proxy for paleo-fO$_2$ during partial melting: Prospects, limitations and implications, Geochim. Cosmochim. Acta, 67, 16: 3045-3064.

Lehtonen, M., Airo, M.-L., Eilu, P., Hanski, E., Kortelainen, V., Lanne, E., Manninen, T., Rastas, P., Räsänen, J. & Virransalo, P. (1998). Kittilän alueen geologia. Lapin vulkaniittiprojektin raportti. Summary: the stratigraphy, petrology and geochemistry of the Kittilä greenstone area, northern Finland. A Report of the Lapland Volcanite Project. Geological Survey of Finland Report of Investigation 140, 144 pp.

Lesher, C. M., and Arndt, N. T. (1995) REE and Nd isotope geochemistry, petrogenesis and volcanic evolution of contaminated komatiites at Kambalda, Western Australia, Lithos, 34, 127-157.

Lesher, C. M., and Stone, W. E. (1996) Exploration geochemistry of komatiites, In: Igneous trace element geochemistry: Applications for massive sulfide exploration, Wyman, D. A. (Ed.) Geol. Assoc. Canada, 153-204.

Lesher, C. M., Burnham, O. M., Keays, R. R., Barnes, S. J., and Hulbert, L. (2001) Trace element geochemistry and petrogenesis of barren and ore-associated komatiites, Can. Mineral., 39, 673-696.

Li, J. P., O'Neil, H. St. C., and Seifert, F. (1995) Subsolidus phase relations in the system MgO-SiO2-Cr-O in equilibrium with metallic Cr, and their significance for the petrochemistry of chromium, J. Petrol., 36, 107-132.

Luck, J. -M., and Allegre, C. J. (1984) [187]Re/[187]Os investigation in sulfide from Cape Smith komatiite, Earth Planet Sci. Lett., 68:205-8.

Luck, J. M. and Allègre, C. J. (1991) Os isotopes in ophiolites,  komatiite, Earth

Planet. Sci. Lett., 107, 406-15.

Ludwig, K . R., 1998. Isoplot/Ex, Version 1.00, A Geochronological Toolkit for
Microsoft Excel. Berkeley Geochronology Center Special Publication No. 1,
43.

Martin, C. E. (1991) Osmium isotopic characteristics of mantle-derived rocks,
Geochim. Cosmochim. Acta, 55, 1421-34.

Mathez, E. A. (1999) On factors controlling the concentrations of platinum group
elements in layered intrusions and chromites, In: Dynamic processes in
magmatic ore deposits and their application in mineral exploration (Eds. R. R.
Keays, C. M. Lesher, P. C. Lightfoot, and C. E. G. Farrow), Geological
Association of Canada, 251-285.

McCulloch M. T. and Bennett, V. C., 1994. Progressive growth of the Earth's
continental crust and depleted mantle: geochemical constraints, Geochim.
Cosmochim. Acta, 58: 4717-4738.

McCuaig, T. C., Kerrich, R., Xie, Q. (1994) Phosphorous and high field strength
element anomalies in Archean high-magnesian magmas as possible indicators
of source mineralogy and depth, Earth Planet Sci. Lett., 124: 221-239.

McDonough, W. F. and Ireland, T. R. (1993) Intraplate origin of komatiites inferred
from trace elements in glass inclusions, Nature, 365: 432-434.

McDonough, W. F. (1995) An explanation for the abundance enigma of the highly
siderophile elements in the earth's mantle, Lunar. Planet. Sci. (abs.), 26, 927-
928.

McDonough, W. F., and Sun, S.-S (1995) The composition of the earth, Chem. Geol.,

120, 223-53.

McDonough, W. F., and Danyuschevsky, L. V. (1995) Water and sulfur contents of melt inclusions from Archean komatiites, Eos Trans., Amer. Geophys. Union, 76, 266.

McDonough, W.F., Eggins, S.M., Sun, S.S. and Campbell, I.H. (1997) The composition of Archean komatiites Seventh annual V.M. Goldschmidt conference. Source: LPI Contribution, Vol. 921, pp. 137-138.

Meisel T., Walker R.J. and Morgan J.W. (1996) The osmium isotopic composition of the Earth's primitive upper mantle. Nature 383, 517-520.

Meisel, T., Walker, R. J., Irving, A. J. and Lorand, J. P., 2001. Os isotopic composition of mantle xenoliths: A global perspective, Geochim. Cosmochim. Acta, 65, 8: 1311-1323.

Meisel, T., Moser J. and Wegscheider W., 2001a. Recognizing heterogeneous distribution of platinum group elements (PGE) in geological materials by means of the Re-Os isotope system, Fresenius J. Anal. Chem. 370: 566-572.

Meisel, T., Walker, R. J., Irving, A. J. and Lorand, J. P., 2001b. Os isotopic composition of mantle xenoliths: A global perspective, Geochim. Cosmochim. Acta, 65, 8: 1311-1323.

Michael, P. (1995) Regionally distinctive sources of depleted MORB: Evidence from trace elements and H2O, Earth Planet. Sci. Lett., 131, 301-320.

Morgan, J. W., 1985. Os isotope constraints on Earth's accretionary history, Nature, 317: 703-705.

Morgan, J. W., 1986. Ultramafic xenoliths: Clues to Earth's late accretionary history,

J. Geophys. Res., 91: 12375-12387.

Morgan, J. W. and Walker, R. J., 1989. Isotopic determinations of rhenium and osmium in meteorites by using fusion, distillation and ion exchange separations, Anal. Chim. Acta, 222: 291-300.

Morgan, J. W., Horan, M. F., Walker, R. J. and Grossman, J. N., 1995. Rhenium-osmium concentration and isotope systematics in group IIAB iron meteorites, Geochim. Cosmochim. Acta, 59: 2331-2344.

Morgan, J. W., Walker, R. J., Brandon, A. D. and Horan, M. F. (2001) Siderophile elements in Earth's upper mantle and lunar breccias: Data synthesis suggests manifestations of the same late influx, Meteor. Planet. Sci., 36: 1257-1275.

Muir, J. E., and Comba, C. D. A. (1979) The Dundonald deposit: an example of volcanic-type nickel-sulphide mineralization. Can. Mineral. 17, 351–360.

Murck, B. W., and Campbell, I. H. (1986) The effects of temperature, oxygen fugacity and melt composition on the behavior of chromium in basic and ultrabasic melts, Geochim. Cosmochim. Acta, 50, 1871-87.

Naldrett, A. J., and Mason, G. D. (1968) Contrasting Archean ultramafic igneous bodies in Dundonald and Clergue township, Ontario. Can. J. Earth Sc., **5**, 111-143.

Nesbitt, R. W., and Sun, S. –S. (1976) Geochemistry of Archean spinifex-textured peridotites and magnesian and low-magnesian tholeiites, Earth Planet. Sci. Lett., 31, 433-453.

Nesbitt, R. W., Sun, S. –S., and Purvis, A. C. (1979) Komatiites: geochemistry and genesis, Canadian Mineralogist, 17, 165-186.

Nesbitt, R. W., Sun, S. –S., and Purvis, A. C. (1979) Komatiites: geochemistry and genesis, Canadian Mineralogist, 17, 165-186.

Nisbet, E. G., N.T. Arndt, M.J. Bickle, W.E. Cameron, C. Chauvel, M. Cheadle, E. Hegner, T.K. Kyser, A. Martin, R. Renner and E. Roedder (1987) Uniquely fresh 2.7 Ga komatiites from the Belingwe greenstone belt, Zimbabwe, Geology, 15, 1147–1150.

Nisbet, E. G., Cheadle, M. J., Arndt, N. T. and Bickle, M. J. (1993) Constraining the potential temperature of Archean mantle: A review of the evidence from komatiites, Lithos, 30: 291-307.

Norman, M. D., and Garcia, M. O. (1999) Primitive magmas and source characteristics of the Hawaiian plume: petrology and geochemistry of shield picrites, Earth Planet. Sci. Lett., 168, 27-44.

Nunes, P. D. and Pyke, D. R., 1980. Geochronology of the Abitibi metavolcanic belt, Timmins area, Ontario – progress report. Ont. Geol. Surv., Misc. Pap., 92: 34-39.

Ohtani, E. (1990) Majorite fractionation and genesis of komatiites in deep mantle, Precam. Res., 48, 195-202.

Olive, V., Ellam, R. M., and Harte, B. (1997) A Re-Os isotope study of ultramafic xenoliths from the Matsoku kimberlite, Earth Planet. Sci. Lett., 150, 129-140.

O'Reilly, S. Y., Griffin, W. L., and Ryan , C. G. (1991) Residence of race elements in metasomatized spinel lherzolite xenoliths: A proton-microprobe study, Contrib. Mineral. Petrol., 109, 98-113.

Parkinson, I. J., and Arculus, R.. J. (1999) The redox state of subduction zones:

insights from arc-peridotites, Chem. Geol., 160, 409-423.

Parman, S.W., Dann, J.C., Grove T.L., and de Wit M.J. (1997) Emplacement conditions of komatiite magmas from the 3.49 Ga Komati Formation, Barberton Greenstone Belt, South Africa. Earth Planet. Sci. Lett. 150, 303–323.

Parman, S. W., Shimizu, N., Grove, T. L., and Dann, J. C. (2003) Constraints on the pre-metamorphic trace element composition of Barberton komatiites from ion probe analyses of preserved clinopyroxene, Contrib. Mineral. Pterol., 144: 383-396.

Perring, C. S., Barnes, S. J., and Hill, R. E. T. (1996) Geochemistry of komatiites from Forrestania, Southern Cross Province, Western Australia: Evidence for crustal contamination, Lithos, 37, 181-197.

Puchtel, I. S., Hofmann, A. W., Mezger, K., Shchipansky, A. A., Kulikov, V. S., and Kulikova, V. V. (1996) Petrology of a 2.41 Ga remarkably fresh komatiitic basalt lava lake in Lion Hills, central Vetreny Belt, Baltic Shield, Contrib. Mineral. Petrol., 124: 273-90.

Puchtel, I. S., Arndt, N. T., Hoffman, A. W., Hasse, K. M., Kröner, A., Kulikov, V. S., Kulikova, V. V., Garbe-Schönberg, C. -D., Nemchin, A., A. (1998) Petrology of mafic lavas within the Onega plateau, central Karelia: evidence for 2.0 Ga plume-related continenetal crustal growth in the Baltic Shield, Contrib. Mineral Petrol., 130:134-153.

Puchtel, I. S., Brügmann, G. E. and Hofmann, A. W., 1999. Precise Re-Os mineral

isochron and Pb-Nd-Os isotope systematics of a mafic-ultramafic sill in the 2.0 Ga Onega plateau (Baltic Shield), Earth Planet Sci. Lett., 170: 447-461.

Puchtel I. S. and Humayun M., 2000. Platinum group elements in Kostomuksha komatiites and basalts: Implications for oceanic crust recycling and core-mantle interaction, Geochim. et Cosmochim. Acta, 64 (24): 4227-4242.

Puchtel, I. S. and Humayun, M. (2001) PGE fractionation in a komatiitic basalt lava lake, Geochim. Cosmochim. Acta, 17, 2979-2993.

Puchtel I. S., Brugmann, G. E. and Hofmann, A. W. (2001a) Os-187-enriched domain in an Archean mantle plume: evidence from 2.8 Ga komatiites of the Kostomuksha greenstone belt, NW Baltic Shield, Earth Planet Sci. Lett., 186 (3-4): 513-526.

Puchtel I. S., Brugmann, G. E., Hofmann, A. W., Kulikov, V. S. and Kulikova, V. V., 2001b. Os isotope systematics of komatiitic basalts from the Vetreny belt, Baltic Shield: Evidence for a chondritic source of the 2.45 Ga plume, Contrib. Mineral. Petrol., 140: 588-599.

Puchtel, I. S., Brandon, A. D., and Humayun, M. (2004a) Precise Pt-Re-Os isotope systematics of the mantle from 2.7 Ga komatiites, Earth Planet. Sci. Lett., 224, 157-174.

Puchtel, I. S., Humayun, M., Campbell, A. J., Sproule, R. A., and Lesher, C. M. (2004b) Platinum group element geochemistry of komatiites from the Alexo and Pyke Hill areas, Ontario, Canada, Geochim. Cosmochim. Acta, 68, 6, 1361-1383.

Pyke, D. R., Naldrett, A. J., and Ecktrand, O. R. (1973) Archean ultramafic flows in

Munro Township, Ontario, Geol. Soc. Am. Bull., 84, 955-978.

Reisberg, L., Zindler, A., Marcantonio, F., White, W. and Wyman, D., 1993. Os isotope systematics in ocean island basalts, Earth Planet. Sci. Lett., 120: 149-167.

Reisberg, L., and Lorand, J. –P. (1995) Longevity of sub-continental mantle lithosphere from osmium isotope systematics in orogenic peridotite massifs, Nature, 376, 159-162.

Révillon, S., Arndt, N. T., Chauvel, C., and Hallot, E. (2000) Geochemical Study of Ultramafic Volcanic and Plutonic Rocks from Gorgona Island, Colombia: the Plumbing System of an Oceanic Plateau, J. Petrol., 41, 7, 1127-1153.

Righter, K., and Hauri, E. (1998) Compatibility of rhenium in garnet during mantle melting and magma genesis, Science, 280, 1737-1741.

Righter, K., Campbell, A. J., Humayun, M., and Hervig, R. L. (2004) Partitioning of Ru, Rh, Pd, Re, Ir, and Au between Cr-bearing spinel, olivine, pyroxene and silicate melts, Geochim. Cosmochim. Acta, 68, 4, 867-880.

Roeder, P. L., and Reynolds, I. (1991) Crystallization of chromite and chromium solubility in basaltic melt, J. Petrol., 32: 909-934.

Rollinson, H. (1999) Petrology and geochemistry of metamorphosed komatiites and basalts from the Sula Mountains greenstone belt, Sierra Leone, Contrib. Mineral. Petrol., 134, 86-101.

Roy-Barman, M. and Allegre, C. J. (1994) $^{187}$Os/$^{186}$Os ratios of mid-ocean ridge basalts and abyssal peridotites, Geochim. Cosmochim. Acta, 58, 22, 5043-5054.

Roy-Barman, M. and Allègre, C. J., 1995. $^{187}$Os/$^{186}$Os in ocean island basalts: Tracing
oceanic crust recycling in the mantle, Earth Planet. Sci. Lett., 154: 331-347.

Rudnick, R. L., and Fountain, D. M. (1995) Nature and composition of the
continental crust: a lower crustal perspective, Rev. Geophys., 33, 267-309.

Rudnick, R. L., and Lee, C. T. (2002) Osmium isotope constraints on tectonic
Evolution of the lithosphere in the southwestern United States, International
Geol. Rev., 44, 501-511.

Sattari, P., Brenan, J. M., Horn, I., and McDonough, W. F. (2002) Experimental
constraints on the sulfide- and chromite-silicate melt partitioning behavior of
rhenium and platinum-group elements, Econ. Geol., 97, 385-398.

Saverikko, M. (1985). The pyroclastic komatiite complex at Sattasvaara in northern
Finland, Bulletin of the Geological Society of Finland 57, 55–87.

Sharma, M., Papanastassiou, D. A. and Wasserburg, G. J. (1997) The concentration
and isotopic composition of osmium in the oceans, Geochim. Cosmochim.
Acta, 3287-3299.

Shimizu K, Komiya T, Hirose K, Shimizu N, Maruyama S (2001) Cr-spinel, an
excellent micro-container for retaining primitive melts - implications for a
hydrous plume origin for komatiites, Earth Planet Sci. Lett., 189 (3-4): 177-
188.

Shirey, S. B. and Walker, R. J., 1995. Carius tube digestion for low-blank rhenium-
osmium analyses, Anal. Chem., 34: 2136-2141.

Shirey, S. B., 1997. Initial Os isotopic composition of Munro Township, Ontario

komatiites revisited: additional evidence for near chondritic, late-Archean convecting mantle beneath the Superior Province, 7th Ann. VM Goldschmidt Conf. LPI Contrib. 921, 193 (abs.).

Shirey, S. B. and Walker, R. J. (1998) The Re-Os isotope system in cosmochemistry and high-temperature geochemistry, Annu. Rev. Earth Planet. Sci., 26: 423-500.

Shore, M., Fowler AD (1999) The origin of spinifex texture in komatiites, Nature, 397 (6721): 691-694.

Smoliar M.I., Walker R.J. and Morgan J.W., 1996. Re-Os ages of group IIA, IIIA, IVA and IVB iron meteorites. Science 271: 1099-1102.

Snow, J. E. and Reisberg, L., 1995. Os isotopic systematics of the MORB mantle: results from altered abyssal peridotites, Earth Planet Sci. Lett., 133: 411-421.

Sobolev, A., and Chaussidon, M. (1996) $H_2O$ concentrations in primary melts from supra-subduction zones and mid-ocean ridges: Implications for $H_2O$ storage and recycling in the mantle, Earth Planet. Sci. Lett., 137, 45-55.

Spadea, P., Espinosa, A., and Orrego, A. (1989) High-Mg extrusive rocks from the Romeral Zone ophiolites in the southwestern Colombian Andes, Chem. Geol., 77, 303-21.

Sproule, R., Lesher, C. M., Ayer, J. A., Thurston, P. C., Herzberg, C. T. (2002) Spatial and temporal variations in the geochemistry of komatiites and komatiitic basalts in the Abitibi greenstone belt, Precamb. Res., 115, 153-86.

Staudigel, H., Plank, T., White, B., Schmincke, H. –U. (1996) Geochemical fluxes

during seafloor alteration of the basaltic upper oceanic crust: DSDP sites 417 and 418. In: Bebout, G. (Ed.), Subduction: Top to Bottom. Am. Geophys. Union.

Stone, W.E., Deloule, E., Larson M.S., and Lesher, C.M. (1997) Evidence for hydrous high-MgO melts in the Precambrian. Geology 25, 143–146.

Sun, S.-S. (1982) Chemical composition and origin of the Earth's primitive mantle, Geochim. Cosmochim. Acta, 46, 179-192.

Sun, S.-S. (1984) Geochemical characteristics of Archean ultramafic and mafic volcanic rocks: implications for mantle composition and evolution, In: Archean Geochemistry, Kröner, A., Hanson, G. N., and Goodwin, A. M. (Eds.), Spinger-Verlag.

Thy, P. (1995) Low-pressure experimental constraints on the evolution of komatiites, J. Petrol., 36, 1529-1548.

Tomlinson, K. Y., Bowins, R., Hechler, J. (1999) Project 95-027: Refinement of hafnium (Hf) and zirconium (Zr) ICP-MS analysis by improvement in the sample digestion procedure, Ont. Geol. Surv. Misc. Pap. 169, 189-194.

Viljoen, M. J., and Viljoen, R. P. (1969a) Evidence for the existence of a mobile extrusive peridotitic magma from the Komati formation of the Onverwacht Group, Sp. Publ. Geol. Soc. S. Afr., 2, 87-112.

Viljoen, M. J., and Viljoen, R. P. (1969b) The geology and geochemistry of the lower ultramafic unit of the Onverwacht Group and a proposed new class of igneous rocks, Sp. Publ. Geol. Soc. S. Afr., 2, 55-85.

Völkening, J., Walczyk, T. and Heumann, K., 1991. Osmium isotope ratio

determinations by negative thermal ionization mass spectrometry, Int. J. Mass Spectr. Ion Proc., 105: 147-159.

Wagner, T. P., and Grove, T. L. (1997) Experimental constraints on the origin of lunar high-Ti ultramafic glasses, Geochim. Cosmochim. Acta, 61, 1315-1327.

Walker R. J., Shirey, S. B. and Stecher, O. (1988) Comparative Re-Os, Sm-Nd and Rb-Sr isotope and trace element systematics for Archean komatiite flows from Munro Township, Abitibi Belt, Ontario, Earth Planet Sci. Lett., 87: 1-12.

Walker, R. J., Carlson, R. W., Shirey, S. B., and Boyd, F. R. (1989) Os, Sr, Nd, and Pb isotope systematics of southern African peridotite xenoliths: implications for the chemical evolution of subcontinental mantle, Geochim. Cosmochim. Acta, 53, 1583-1595.

Walker R.J. , Echeverría L.M., Shirey S.B. and Horan M.F. (1991) Re-Os isotopic constraints on the origin of volcanic rocks, Gorgona Island, Colombia: Os isotopic evidence for ancient heterogeneities in the mantle. Contrib. Mineral. Petrol. 107 , 150-162.

Walker, R. J., Morgan, J. W., Horan, M. F., Czamanske, G. K., Krogstad, E. J., Fedorenko, V. and Kunilov, V. E. (1994) Re-Os isotopic evidence for an enriched-mantle source for the Noril'sk-type ore-bearing intrusion, Siberia, Geochim. Cosmochim. Acta, 58: 4179-4197.

Walker, R. J., Morgan, J. W., Horan, M. F. (1995) [187]Os enrichment in some mantle plume sources: Evidence for core-mantle interaction?, Science, 269, 819-822.

Walker, R. J., Hanski, E., Vuollo, J. and Liipo, J., 1996. The Os isotopic composition

of Proterozoic upper mantle: evidence for chondritic upper mantle from the Outokumpu ophiolite, Finland, Earth Planet Sci. Lett., 141: 161-173.

Walker, R. J., Morgan, J. W., Beary, E., Smoliar, M. I., Czamanske, G. K., Horan, M. F. (1997) Applications of the 190Pt-186Os isotope system to geochemistry and cosmochemistry, Geochim. Cosmochim. Acta, 61, 4799-4808.

Walker, R. J., Morgan, J. W., Hanski, E. J., and Smolkin, V., F. (1997) Re-Os systematics of Early Proterozoic ferropicrites, Pechenga Complex, northwestern Russia: Evidence for ancient [187]Os-enriched plumes, Geochim. Cosmochim. Acta, 61, 15, 3145-60.

Walker, R. J., Storey, M., Kerr, A. C., Tarney, J. and Arndt, N. T. (1999) Implications of Os-187 isotopic heterogeneities in a mantle plume: Evidence from Gorgona Island and Curacao, Geochim. Cosmochim. Acta 63 (5): 713-728.

Walker, R. J. and Stone, W. R. (2001) Os isotopic constraints on the origin of the 2.7 Ga Boston Creek flow, Ontario, Canada, Chem. Geol., 175: 567-579.

Walker, R. J., Prichard, H. M., Ishiwatari, A. and Pimentel, M. (2002) The Os isotopic composition of the convecting upper mantle deduced from ophiolite chromites, Geochim. Cosmochim. Acta, 66, 2: 329-345.

Walker , R. J. and Nisbet, E. (2002) [187]Os isotopic constraints on Archean mantle dynamics. Geochim. Cosmochim. Acta, 66, 18: 3317-3325.

Wilson, A. H. (2003) A new class of silica enriched, highly depleted komatiites in the southern Kaapvaal Craton, South Africa, Precamb. Res., 127, 1-3: 125-141.

Wilson. A. H., Shirey, S. B., and Carlson, R. W. (2003) Archean ultra-depleted

komatiites formed by hydrous melting of cratonic mantle, Nature, 423, 858-861.

Wood, B. J., and Virgo, D. (1989) Upper mantle oxidation state: ferric iron contents of lherzolite spinels by [57]Mössbauer spectroscopy and resultant oxygen fugacities, Geochim. Cosmochim. Acta, 53 1277-1291.

Woodland, S. J., Pearson, D. G., and Thirlwall, M. F. (2002) A platinum group element and Re-Os isotope investigation of siderophile element recycling in subduction zones: Comparison of Grenada, Lesser Antilles arc, and the Izu-Bonin arc, J. Petrol., 43, 1, 171-198.

Xie, Q., Kerrich, R. and Fan, J., 1993. HFSE/REE fractionations recorded in three komatiite-basalt sequences, Archean Abitibi belt: implications for multiple plume sources and depths, Geochim. Cosmochim. Acta, 57: 4111-4118.

Xie, Q., and Kerrich, R. (1994) Silicate-perovskite and majorite signature in komatiites from the Archean Abitibi greenstone belt: Implications for early mantle differentiation and stratification, J. Geophys. Res., 99: 15799-15812.

Xiong, Y., and Wood, S. A. (1999) Experimental determination of the solubility of $ReO_2$ and the dominant oxidation state of rhenium in hydrothermal solutions, Chem. Geol., 158, 245-256.

Xirouchakis, D., Hirschmann, M. M., and Simpson, J. A. (2001) The effect of titanium on the silica content and on mineral-liquid partitioning of mantle-equilibrated melts, Geochim. Cosmochim. Acta, 65, 14: 2201-2217.

Yurimoto, H., and Ohtani, E. (1992) Element partitioning between majorite and

liquid: a secondary ion mass spectrometric study, Geophys. Res. Lett., 19, 1, 17-20.

Zhou, M., and Kerrich, R. (1992) Morphology and composition of chromite in komatiites from the Belingwe greenstone belt, Zimbabwe, Can. Mineral., 30: 303-17.

Zhou, M. F. (1994) PGE distribution in 2.7-Ga layered komatiite flows from the Belingwe greenstone belt, Zimbabwe, Chem. Geol., 118, 155-172.